2011

Computational features and performance-evaluation of discrete/ continuous type discrete-time control systems

Ashley N. Hunt

COMPUTATIONAL FEATURES AND PERFORMANCE-EVALUATION OF DISCRETE/CONTINUOUS TYPE DISCRETE-TIME CONTROL SYSTEMS

by

ASHLEY N. HUNT

A THESIS

Submitted in partial fulfillment of the requirements
for the degree of Master of Science in Engineering
in
The Department of Electrical and Computer Engineering
to
The School of Graduate Studies
of
The University of Alabama in Huntsville

HUNTSVILLE, ALABAMA

2011

In presenting this thesis in partial fulfillment of the requirements for a master's degree from The University of Alabama in Huntsville, I agree that the Library of this University shall make it freely available for inspection. I further agree that permission for extensive copying for scholarly purposes may be granted by my advisor or, in his/her absence, by the Chair of the Department or the Dean of the School of Graduate Studies. It is also understood that due recognition shall be given to me and to The University of Alabama in Huntsville in any scholarly use which may be made of any material in this thesis.

(Student Signature)

10/31/11

(Date)

THESIS APPROVAL FORM

Submitted by Ashley N. Hunt in partial fulfillment of the requirements for the degree of Master of Science in Electrical Engineering and accepted on behalf of the Faculty of the School of Graduate Studies by the thesis committee.

We, the undersigned members of the Graduate Faculty of The University of Alabama in Huntsville, certify that we have advised and/or supervised the candidate on the work described in this thesis. We further certify that we have reviewed the thesis manuscript and approve it in partial fulfillment of the requirements for the degree of Master of Science in Engineering with an option in Electrical Engineering.

Committee Chair	Dr. C.D. Johnson	Oct 28 2011 (Date)
Committee Member	Dr. F.D. Ho	OCT. 28, 2011 (Date)
Committee Member	Dr. K. Howell	Oct 31, 2011 (Date)
Department Chair	Dr. R. Lindquist	11/1/11 (Date)
College Dean	Dr. S. Mahalingam	11/07/11 (Date)
Graduate Dean	Dr. R. Gaede	12/5/11 (Date)

ABSTRACT
The School of Graduate Studies
The University of Alabama in Huntsville

Degree	Master of Science in Engineering
College/Dept.	Engineering / Electrical and Computer Engineering
Name of Candidate	Ashley N. Hunt
Title	Computational Features and Performance-Evaluation of Discrete/Continuous Type Discrete-Time Control Systems

Recently, a new generalization of the traditional zero-order-hold (ZOH) discrete-time control, called Discrete/Continuous (D/C) Control, was developed by C. D. Johnson. D/C-type discrete-time controllers allow the control $u(t)$ to vary continuously across sample-intervals $kT \le t < ((k+1)T)$. In some applications, the use of D/C signals instead of traditional ZOH-type signals can lead to improved control effectiveness and improved system performance due to the unconventional inter-sample behavior of D/C signals.

In this thesis, the structure of the unorthodox dual-kernel convolution matrix, $\overline{BH}(T)$, which arrises in D/C Control Theory is investigated and calculated symbolically for a series of plant models. In addition, the performance of D/C control is evaluated for a series of control-tasks for low-order plant models and compared to the performance of traditional ZOH-type discrete-time control. Several examples are presented to illustrate the results.

Abstract Approval: Committee Chair

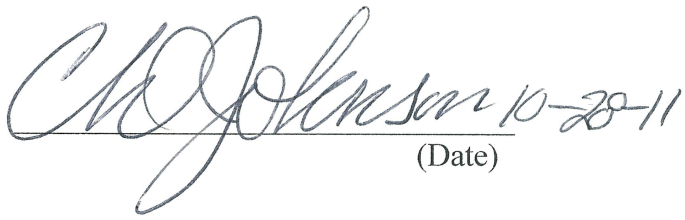

(Date)

Department Chair

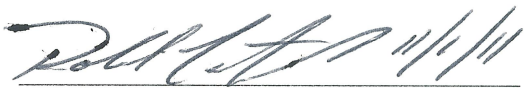

(Date)

Graduate Dean

(Date)

ACKNOWLEDGMENTS

I have been very fortunate to be able to do research in the exciting, new area of Discrete/Continuous Control Theory. My advisor, Dr. C.D. Johnson, has been very patient in guiding me through the understanding of this new generalization of Discrete Control. Dr. Johnson has been beyond generous in suggesting this topic, which he originally developed and has provided so much of the background reference research for. I would like to thank him for all of his time, support, and advice during my long process of thesis-writing. I have learned a great amount from him in the areas of Control Theory, performing scientific research, and proper technical writing. I am sincerely grateful.

I would like to thank my committee members, Dr. F.D. Ho and Dr. K. Howell for their time, patience, and advice with this research.

I would like to thank the Department of Electrical and Computer Engineering at the University of Alabama in Huntsville for supporting me as a teaching assistant during my research.

Finally, I would like to thank my wonderful family: my father Mitchell G. Hunt, my mother Suzanne Hunt, and my brother Mitchell R. Hunt. I could not have had better support and understanding. Without your encouragement, I could have never completed this research. Thank you so much.

TABLE OF CONTENTS

Page

LIST OF FIGURES

Figure Page

LIST OF TABLES

LIST OF SYMBOLS

Symbol	Definition
λ	Eigenvalue
D/C	Discrete/Continuous
ZOH	Zero-Order Hold
LiT	Linear-in-Time
SiT	Sinusoidal-in-Time
PsiT	Pulse-in-Time
EiT	Exponential-in-Time
T	Control Decision / Sampling Period
y	System Output Vector
x	System State Vector
$u_{d/c}$	Discrete-Continuous Control Signal
$\widetilde{K}_{d/c}$	Discrete-Continuous Control Matrix
$\widetilde{K}_{ZOH}$	ZOH Control Matrix
A	State Matrix
B	Control Distribution Matrix
$\widetilde{B}$	ZOH Control Distribution Matrix
v	Dynamic State of Control Vector

$\overline{\overline{BH}}$ ..... Discrete-Continuous Control Convolution Matrix

$\overline{H}$ ..... Dynamic State of Control Distribution Matrix

$\overline{D}$ ..... Dynamic State of Control Distribution Matrix

$\widetilde{A}$ ..... Discretized State Matrix

$\widetilde{A}_{CL}$ ..... Closed-Loop State Matrix

$w(t)$ ..... Disturbance Input

$\hat{x}(kT)$ ..... Discrete-Time Estimated State

$\hat{v}(kT)$ ..... Discrete-Time Estimated Dynamic State of Control

$\widehat{w}(kT)$ ..... Discrete-Time Estimated Disturbance Input

† ..... Moore-Penrose Generalized Inverse

CHAPTER 1

A BRIEF REVIEW OF THE NEW D/C-TYPE DISCRETE-TIME CONTROL THEORY

Control Theory is a branch of engineering that involves analysis and modification of the behavior of dynamical systems, and in particular, measurements of real-time behavior and "smart" real-time changes of the system-inputs to produce more desirable behavior [1],[2]. Continuous control signals are those which are measured and updated continuously, and were commonplace before the widespread use of Discrete-Time (Digital) Control. Presently, Discrete-Time Control is more common, and involves the sampling of continuous signals [3]. The new concept of Discrete/Continuous (D/C)-Type Discrete-Time Control and Signal Theory, originally introduced in [4]-[12], which is a broad generalization of the ubiquitous Zero Order Hold (ZOH)-type discrete-time control, has been explored in recent research [13]-[19] and is of particular interest in those applications involving high performance digital-control.

This interest is motivated by the emerging evidence that a D/C controller is able to better accommodate a wide range of representative tracking-commands and disturbance-inputs, compared-to ZOH, and can achieve unique types of transient-responses the ZOH-type control cannot achieve. In this thesis, the analytical features and

performance capabilities of Discrete-Continuous-Type Discrete-Time Controllers and associated closed-loop system performances are investigated and evaluated for a family of particular cases of practical-importance. The goal of this research is to explore some of the novel performance-capabilities and related mathematical features of the unorthodox matrices involved in the design of D/C Control-algorithms.

1.1 Overview of the Traditional Concept of Discrete-Time Control and ZOH-Signals

The concepts of Discrete-Time Signals and Discrete-Time Control refer to the sampling of continuous signals at discrete points in time $t = kT$, $k = 0,1,2,\ldots$ with T as a finite, known sampling-period, and the control and processing of such signals to form a user-desired result [10]. Traditionally, a so-called zero-order hold (ZOH) procedure, in which control $u(t)$ is constrained to remain a constant between each consecutive pair of signal samples $\{kT,(k+1)T\}$ has been invoked in discrete-time control, where the control-decision about that constant-value $u(kT)$ is updated at each $t = kT$. This traditional form of discrete-time control is discussed in detail in [3],[2].

1.1.1 Continuous-Time Decisions vs. Discrete-Time Decisions

In conventional Continuous-Time control systems, the control-decisions produced by the controller are updated continuously-in-time, by virtue of the continuous stream of real-time sensor/command data provided-to the controller and the continuously acting "control-algorithm," therefore allowing control decisions and updates to be made on a continual basis (at every moment of time t). In discrete-time control, it is understood that control decisions and updates are restricted to occur only at isolated moments of time called the "decision times" [20] (traditionally referred-to as "sample times" in most

textbooks [3]) and only at these times (at every $t = kT$ where T is the user-chosen or system-defined sample period and $k = 0,1,2,\ldots$). The exact state-space representation of the class of Multiple-Input and Multiple-Output (MIMO) continuous linear time-invariant undisturbed dynamical systems utilizing ZOH-type discrete control is typically shown as

$$\dot{x}(t) = Ax(t) + Bu(t) \tag{1.1}$$

$$y(t) = Cx(t) \tag{1.2}$$

$$u(t) = u_{ZOH}(t) = c(kT), \quad kT \le t < (k+1)T. \tag{1.3}$$

A is the state matrix, B is the continuous control distribution matrix, C is the output matrix, and $c(kT)$ is the appropriate constant-value of the ZOH control, updated by the ZOH control-algorithm at each decision/sample time. The ZOH-type of discrete time control has been widely used to characterize discrete time decisions and control time-behavior. In fact, discrete-time control signals have become so synonymous with ZOH-type signals that, in many textbooks, ZOH has been (presumptually) used to define the meaning of the term "Discrete-Time Control." This restricted definition does not allow-for the possibility of more effective "smart" inter-sample time-variations of a discrete-time control-signal. In the more general Discrete-Continuous type of discrete-time control theory introduced in [4], the control may vary in a "smart" manner, across each intersample-interval $kT \le t < (k+1)T,$ according to a predetermined D/C control algorithm (mathematical rule or policy), or remain constant as in ZOH, depending on the D/C control-algorithm's optimal choice among a user/designer selection of D/C "basis functions."

1.1.2 The Traditional ZOH-Paradigm in Discrete-Time Control; Pros and Cons

ZOH is currently the most widely used modern technique in Discrete-Time Control and has been adapted to the LQR family of modern control design-paradigms. While ZOH presents ease of modeling, design and implementation with the D/A converter, discrete-time control, in general, can only guarantee acceptable behavior/compensation at the control-decision times (not between sample periods). As research presented in [9] and the results presented in Chapter 3 show, it is possible to design D/C-type discrete-time controllers to accomplish a given control task with lower system transient amplitude and "arrival time" than with ZOH for systems (plants) above first-order.

It should be mentioned that there exists a classical signal-processing concept known as first-order hold (FOH), a pseudo-generalization of ZOH, in which the ZOH stair-step control-variations are replaced-by a retrofitted linear interpolation of $u(kT)$-values between the two most recent-values to achieve a piecewise-linear signal. Although the FOH model has been discussed in the classical discrete-time control literature, the additional time-delay (phase-lag) it introduces is very undesirable and may even comporimise system stability. For that reason, the traditional FOH and its generalizations are not attractive design options in real-time, high-performance discrete-time control. For those reasons, the traditional FOH and similar "signal-smoothing" algorithms for Discrete-Time Control have little similarity with the relatively new D/C control concept, as developed in [4]-[12] and studied in this thesis, which is not retrofitted and produces no additional phase-lag, and enables significant performance-improvements, rather than deteriorations, compared to ZOH.

1.2 Overview of the New Concept of Discrete/Continuous (D/C)-Type Discrete-Time Control

The idea of Discrete/Continuous Type Discrete-Time control first emerged in a primitive form, in a book-chapter authored by Dr. C.D. Johnson in 1982 [21]. Further development of D/C control was made (in [4]-[12]) to provide a more general and more effective approach to achieving high-performance, real-time Discrete-Time Control than is achievable by the traditional ZOH paradigm. As a broad, natural generalization of ZOH-type discrete-time control, D/C control is unique due to the capability of the D/C control to provide smart/optimal continuous inter-sample real-time variations that classical ZOH-type discrete-time control can not provide. In respect to this, it is important to understand the designer-specified mathematical structure of the class of time-variations of $u_{d/c}(t)$, and the associated real-time D/C algorithm-determined D/C control "weighting-constants," which determine the precise inter-sample variation of $u_{d/c}(t)$ over each sample-interval $kT \le t < (k+1)T$.

1.2.1 Definition of the Generic Mathematical-Structure of a D/C-Type, Discrete-Time Control Input $u_{d/c}(t)$

In D/C Control design, the open-loop, inter-sample time-variations of the control $u_{d/c}(t, kT)$ are the result of careful, strategic control decisions at each smart, real-time adaptive $t = kT$, and embody strategically-weighted, linear combinations of certain, well-defined, user/designer chosen, linearly-independent basis-functions $\{f_i(t)\}_1^m$. The associated constant weighting coefficients C_i, chosen at each $t = kT$, are strategically

updated to optimize closed-loop system performance at each decision/sample time [10]. As in the case of *all* discrete-time control-inputs {ZOH, etc.}, in the case of D/C control-inputs and/or D/C signals, the intersample time-variations are, by definition, constrained to vary in an open-loop manner, i.e., un-coordinated/correlated with system real-time behavior according to a mathematical spline-function of the generic form, [7],

$$u_{d/c_i}(t) = C_{i1}(kT)\,f_{i1}(t-kT) + C_{i2}(kT)\,f_{i2}(t-kT) + \ldots + C_{iMi}(kT)\,f_{iM_i}(t-kT), \qquad (1.4)$$

where $u_{d/c} = \text{col.}\left(u_1(t), u_2(t), u_3(t), \ldots, u_r(t)\right)$ and $\left\{f_i(t)\right\}_1^m$ denotes the user/designer-chosen set of D/C basis-functions chosen to accommodate application specifics or hardware limitations [10]. It is (very) convenient to assume the set of user/designer-chosen basis-functions is a Linear Dynamic (LD) set [12], which means each $f_j(t)$ in (1.4) satisfies a knowable, well-defined, well-behaved, linear, homogeneous, differential-equation. This LD property allows for a wide array of complex, possible time-varying $u_{d/c}(t)$ behavioral capabilities, which enriches diversity of the range of complex waveform/signal-behavior the spline model function (1.4) can provide for control-design capability, by automatically and strategically "choosing" in real-time which subset of function(s) from this basis set and which C_i-values best accomplish the control-task for each real-time control-decision period $kT \le t < (k+1)T$.

Assuming a discrete-time control input $u(t)$ is chosen to be of the D/C type, an associated, valid D/C Control-State $v = \text{col.}\left(v_1, v_2, \ldots, v_s\right)$ and related D/C state-evolution model $\dot{v} = \overline{D}v$ is chosen/developed in the form

$$u(t) = \overline{H}(t)\,v(t), \qquad (1.5)$$

where $\overline{H}$ is a known matrix whose value is defined by the choice of the s-elements of the D/C "control-state". After the user/designer-chosen state variables comprising $v(t)$ are selected, the expression for the associated D/C control-"state evolution equation"

$$\dot{v} = \overline{D}(t)\,v; kT \le T < (k+1)T \tag{1.6}$$

is determined from the set of "s" individual differential equations the (LD) basis – functions $\{f_i(t)\}_1^m$ satisfy [7]. In particular, $\overline{D}$ is typically of a block-diagonal companion form such that the basis-set $\{f_i(t)\}_1^m$ comprises a set of fundamental solutions of the differential equation (1.6) governing $v(t)$, [14].

1.2.2 Beginnings and Motivations for D/C-Type Discrete-Time Signals and Control

The motivation for the D/C-type generalization of discrete-time control arose from the need to achieve improved compensation-of and/or inter-sample accommodation-of uncertain system-inputs, compared to ZOH control. The design of a D/C control algorithm allows for ZOH when ZOH is determined (by the D/C algorithm) to be the best choice of control-behavior at that moment of time [12].

As previously mentioned, D/C signals, and their processing and use for discrete-time control, are all "natural generalizations" of conventional ZOH-type Discrete-Time signals, processing, and control. As discussed below, in many, (if not most) applications, the use of D/C-type signals can lead to improved performance compared-to that obtainable by ZOH, or can provide a variety of real-time performance features not available with ZOH or with any other form of discrete-time control [7],[10].

1.2.3 ZOH-Inclusive Versions of D/C Control

If the user chooses "1" as the only D/C basis function for each $u_i(t)$ component of the vector control $u = \text{col.}(u_1, u_2, \ldots, u_r)$, the generalized, D/C-type Discrete-Time control theory automatically reduces-to (exactly) the conventional ZOH-type discrete-time control theory as a (trivial) special case. Consequently, at each control-decision moment, ZOH is an option for the D/C controller to choose if optimal, at each decision/sample time $t = kT$. In particular, if each $u_i(t)$ has only the one basis-function $f_l(t) = 1$, the control $u_{d/c}(t)$ remains constant over each sample-interval, and then the model (1.5) reduces-to $\overline{H} = I$ and in (1.6), $\overline{D} = [0]$, [4].

1.2.3.1 Technical Benefits of D/C Control Compared-To Traditional ZOH Control

Due to the design of D/C control, which leads to the aforementioned differences in inter-sample behavior between D/C control and traditional ZOH-type discrete-time control, several technical benefits arise. Firstly, due to the ability of the designer to specify the choices of D/C control basis-functions and importantly, the inclusion of ZOH (although optional, is beneficial) a wider variety of real-time control options are available. Since ZOH is included in the design, there is no loss of the capability of ZOH in the resulting control signal. As well, the D/C control time-variations $u_{d/c}(t)$ can be designed as "bumpless" and mathematically "smooth bumpless," which results-in a mathematically-smooth, discrete-time signal $u_{d/c}(t)$ that is absolutely un-obtainable by ZOH-type discrete-time control and may impart less "stress" on the system structure or less wear on physical control-components such as actuators [16], compared to ZOH.

1.2.4 Brief Summary of Basic Elements of D/C Control Theory

The main components of D/C Control theory are presented in the following section. It is assumed that T is constant, however all equations, relations, and models presented here can be generalized to include the time-varying case of $T = T(k)$ [4].

1.2.4.1 D/C Control-Spline Models and State-Models; D/C "Control-State" $v(t)$

The unique and fundamental feature of D/C control $u_{d/c}(t)$ varies in accordance with a strategically-weighted (C_i-values updated in real-time) mathematical spline function of the type (1.4), [4]. That unique feature and the choice of D/C state variables, such as phase-variables, for the dynamic state of control $v(t)$ directly determine the structure of $\overline{D}$ in (1.6) when the basis-set is LD-type.

Several particular LD-type spline models (1.4) were used in this research. They were chosen to encompass simple, representative LD basis functions for comparison and performance evaluation. The sets of basis functions chosen are all ZOH-inclusive versions and consist of what are called [10] Linear-in-Time (LiT), Sinusoidal-in-Time (SiT), Exponential-in-Time (EiT), and Pulse-in-Time (PsiT), types of D/C controls which are defined respectively as

$$\text{LiT:} \quad u_{d/c}(t) \triangleq c_1 + c_2 t, \tag{1.7}$$

$$\text{SiT:} \quad u_{d/c}(t) \triangleq c_1 + c_2 \sin(\omega t) + c_3 \cos(\omega t), \tag{1.8}$$

$$\text{EiT:} \quad u_{d/c}(t) \triangleq c_1 + c_2 e^{\alpha t}, \tag{1.9}$$

$$\text{PsiT:} \quad u_{d/c}(t) \triangleq c_1 + c_2 t e^{\alpha t}. \tag{1.10}$$

1.2.5 Exact D/C-Discretization of the Class of MIMO Linear, Continuous-Time Dynamical Systems

In this thesis, we will consider the class of Linear (linearized) continuous-time dynamical systems modeled by the now-standard linear dynamical system model

$$\dot{x} = A(t)x + B(t)u(t) + F(t)w(t) \tag{1.11}$$

$$y = C(t)x, \tag{1.12}$$

where $A(t)$, $B(t)$, $C(t)$, $F(t)$ are (a priori) known matrices, x is the n-dimensional system (plant) state-vector, u is the r-dimensional vector of (independent) system control inputs, y is the m-dimensional vector of system outputs, and w is the p-dimensional vector of uncontrollable-inputs or "disturbances" [9].

In DAC Theory [20],[22], the uncertain disturbance-inputs are assumed to have "structured-variations" [23] and are modeled as [11],[6]

$$w(t) = H(t)z(t) \tag{1.13}$$

$$\dot{z} = D(t)z + \sigma(t), \tag{1.14}$$

where $H(t)$ and $D(t)$ are known matrices, z is the dynamic state of $w(t)$, and $\sigma(t)$ is a sequence of totally-unknown, time-sparse Dirac-impulses [11].

The exact, discretized state and output equations for the continuous-time model (1.11), (1.12), assuming $u(t)$ in (1.11) is a ZOH-type discrete-time control input, and $w(t) \equiv 0$, was first introduced by Kalman, and generalized to include (1.13), (1.14) in [10] to obtain the DAC/ZOH discretization of (1.11), (1.12) as

$$x\big((k+1)T\big) = \widetilde{A}(\cdot)x(kT) + \widetilde{B}(\cdot)u(kT) + \widetilde{FH}(\cdot)z(kT) \tag{1.15}$$

$$y(kT) = C(kT)\,x(kT), \tag{1.16}$$

where $\widetilde{A}$, $\widetilde{B}$, C are well-known matrices [21]. Matrix $\widetilde{FH}$ is defined by

$$\widetilde{FH}(T) \triangleq \int_{kT}^{(k+1)T} \Phi_A\left((k+1)T,\tau\right)F(\tau)H(\tau)\Phi_D(\tau,kT)\,d\tau, \tag{1.17}$$

where $\Phi_A(\cdot,\cdot)$, $\Phi_D(\cdot,\cdot)$ denote the state-transistion matrix for $A(t)$ and $D(t)$, respectively [21].

The discrete-time, ZOH control $u(kT)$ is commonly derived by pole assignment, LQR, and other well-known methods and in the linear case results-in a linear state-feedback control-law of the form

$$u(kT) = -\widetilde{K}(\cdot)\,x(kT); \widetilde{K}(\cdot) = \text{"gain-matrix"}. \tag{1.18}$$

D/C Theory can be applied to three broad modes of "disturbance-accommodation" tasks using pole-assignment, LQR, etc., and that topic is presented, in detail, in [5],[6].

The new, generalized-form of discrete-time control called "D/C control" is designed in a manner similar to that of Disturbance-Accommodating Controllers [22], so that the control $u_{d/c}(t)$ is of the form $u_{d/c}(t) = \overline{H}(t)\,v(t)$ for each $kT \le t < (k+1)T$, where as explained earlier, $\overline{H}$ is a (known or chosen) matrix relating $u_{d/c}(t)$ to the user-chosen, s-dimension dynamic state v of D/C control. The D/C Control $u_{d/c}(t)$ is selected at each $t = kT$ by the D/C-algorithm's "smart"/optimal choice of the "initial-condition" $v(kT)$ in (1.6) at each $t = kT$.

It was first shown in [4] that the exact discretization process leading-to the ZOH results (1.15)-(1.16) can be applied also to the more general case of D/C-type Discrete-

Time control inputs $u_{d/c}(t)$ with the result that the more-general, exact D/C-discretized state-model that replaces (1.15) is [4]

$$x\big((k+1)T\big) = \widetilde{A}(kT)\,x(kT) + \overline{BH}(kT)\,v(kT) + \widetilde{FH}(kT)\,z(kT), \qquad (1.19)$$

where, as in (1.15), $\widetilde{A}$ is the state transition matrix of A and $\overline{BH}$ is a dual-kernel matric convolution integral comparable-to (1.17), [7] but defined as

$$\overline{BH}(T) \triangleq \int_{kT}^{(k+1)T} \Phi_A\big((k+1)T,\tau\big)B(\tau)\overline{H}(\tau)\Phi_{\overline{D}}(\tau,kT)\,d\tau. \qquad (1.20)$$

1.2.6 Unique Computational Challenges Associated-With the Unorthodox Dual-Kernel, Counterflow "D/C Convolution-Integral" Defining $\overline{BH}(T)$

The computation of the $n \times s$ matrix $\overline{BH}$ defined in (1.20) (and the analogus $\widetilde{FH}$ matrix in (1.17)) involves a unique convolution-integral computation with two independent kernels which evolve in counterflow directions [19]. In general, a dual-kernel, counterflow matric convolution integral of the form (1.20) is very computationally intensive (requiring large amounts of memory) when the matrices A, B, are allowed to vary with time. In those cases, numerical-evaluation of $\overline{BH}$ requires evaluation (a priori) for each value of k [19].

1.2.6.1 Design of the D/C "Control-State" Control-Law; The Linear Case of $v(kT) = \widetilde{K}_{d/c}x(kT)$

The design of the D/C control $u_{d/c}(t) = \overline{H}v(t)$ for $kT \le t < (k+1)T$ where T is constant, k = 0,1,2,… and $\dot{v} = \overline{D}(t)v(t);\ kT \le t < (k+1)T$ is conducted by first choosing the set of D/C basis functions in (1.4). Once this is accomplished, the minimal-

order (N^{th} order) differential equation D that an arbitrarily chosen, constant-weighted linear combination of those basis functions satisfies is determined, [9]. Then a valid set of state-variables $\{v_1 \dots v_N\}$ is user-chosen/assigned for D and the $N \times N$ matrix $\overline{D}$ is chosen such that (1.6) is satisfied. Similarly, once a valid set of state-variables $\{v_1 \dots v_N\}$ is assigned, the $s \times N$ matrix $\overline{H}$ is chosen such that (1.5) is satisfied. In this thesis, the state variables were chosen according to the well-known, popular, phase-variable paradigm for all cases. In addition, the set of independent (LD) basis functions are selected to a unity basis-term $f_1(t) \equiv 1,$ which is always a requirement to enable inclusion of ZOH in the real-time choices of control-variations in a D/C-type control-algorithm.

At each $t = kT,$ the dynamic state $v(kT)$ of D/C control, $u_{d/c}(t),$ is automatically chosen (by the D/C-algorithm) to be a specified function of $x(kT)$ in accordance with state-feedback control principles. In the linear case, that function has the form

$$v(kT) = \widetilde{K}_{d/c}\, x(kT); \widetilde{K}_{d/c} = \text{D/C "gain-matrix".} \tag{1.21}$$

1.2.7 D/C-Controlled, Closed-Loop System Model; The Case of Linear Dynamic Systems

From equation (1.21), the closed-loop, D/C controlled system of (1.19) reduces to

$$x\big((k+1)T\big) = \big(\widetilde{A}_{CL}\big)\, x(kT) + \widetilde{FH}z(kT), \tag{1.22}$$

or, in the idealized case of no disturbance $w(t) \equiv 0,$ (1.22) further reduces-to

$$x\big((k+1)T\big) = \big(\widetilde{A}_{CL}\big)\, x(kT) \tag{1.23}$$

where $\widetilde{A}_{CL}$ is the D/C Closed Loop system matrix, defined as

$$\widetilde{A}_{CL} = \widetilde{A} + \overline{BH}\widetilde{K}_{d/c}. \tag{1.24}$$

If $\widetilde{A}_{CL}$ in (1.24) is viewed as a given/desired-value of $\widetilde{A}_{CL}$ in (1.22), (1.23), the expression (1.24) may be used to design the "unknown" gain-matrix $\widetilde{K}_{d/c}$. The research in this thesis explores that $\widetilde{K}_{d/c}$ design method, and the possibilities of achieving $\det\left(\widetilde{A}_{CL} - \lambda I\right) = 0,$ and (whenever possible) $\widetilde{A}_{CL} = [0]$ by $\widetilde{K}_{d/c}$ design. In general, the spectrum of eigenvalues $\sigma\left(\widetilde{A}_{CL}\right) = \{\lambda_1, \lambda_2, \ldots, \lambda_s\}$ must be designed to achieve closed-loop stability, i.e., $\lambda_i \in$ the unit circle (as with a conventional ZOH-type discrete-time control design). In those cases where there is no value of $\widetilde{K}_{d/c}$ that can make the matrix $\widetilde{A}_{CL}$ equal to the null-matrix, $\widetilde{A}_{CL} = [0],$ designing $\widetilde{K}_{d/c} = \overline{BH}^{\dagger}\left(-\widetilde{A}\right),$ where $\overline{BH}^{\dagger}$ represents the Moore-Penrose Generalized Inverse of $\overline{BH},$ may provide the next best option, and is included in the research explorations here.

1.2.8 Some Computational and Performance-Capability Issues in D/C Control

The evaluation of the novel dual-kernal, counterflow matric convolution integral $\overline{BH}(T)$ in (1.20) can be computationally challenging due to its unorthodox structure. For this reason, the possibility of using symbolic software (Maple ®) to evaluate the exact, symbolic expression for $\overline{BH}(T)$ was explored in this research, the results of which are presented, in detail in Appendix A. Beyond third-order systems (n = 3 in (1.19)), it is particularly difficult to achieve effective symbolic calculations of the discretized system matrices such as $\widetilde{A}$ and $\overline{BH}(T)$. For this reason, beyond third-order systems, numerical

integration methods employing novel, exact matric differential equations for $\overline{\mathrm{BH}}$ have been shown to be a particularly useful way to evaluate $\overline{\mathrm{BH}}(\mathrm{T}),$ and such techniques have been explored in [18].

CHAPTER 2

INVESTIGATION OF COMPUTATION, STRUCTURE AND PROPERTIES OF KEY MATRICES IN D/C CONTROL

The structure of the matrix $\overline{BH}$ in D/C Control is unique, possessing many features of interest, such as the dependency of the rank of $\overline{BH}$ on the sampling-period T. In this chapter, the results of an investigation of effective computation of the $\overline{BH}$ matrix, based-on a family of particular generic cases of practical importance, is presented along with some numerical results on the variation of rank $\overline{BH}$ as a function of the sampling-period T.

2.1 Computation of the D/C "Matrix Convolution-Integral" $\overline{BH}(T)$

The D/C "control state" distribution matrix, $\overline{BH}(T)$ is computed from the defining integral equation, (1.20). In the time-invariant case, the system and control matrices $\left\{A, B, C, \overline{D}, \overline{H}\right\}$ are all constant. In that case, the expression for $\overline{BH}(T)$ simplifies. In particular, the state transition matrix $\widetilde{A}$ then reduces-to

$$\widetilde{A} = \Phi_A(T, \tau) = e^{A(T-\tau)} \tag{2.1}$$

in the convolution integral, (1.20). Moreover, the D/C state-transisition matrix $\Phi_{\overline{D}}(\tau, kT)$ in (1.20) then reduces-to

$$\Phi_{\overline{D}}(\tau, kT) = e^{\overline{D}(\tau - kT)}. \tag{2.2}$$

Finally, to compute $\overline{BH}(T)$, knowledge of the matrix B in the underlying continuous-time plant model (1.11) and selection of the D/C control type and associated matrix $\overline{D}$ in (1.6) must be obtained. The underlying, continuous-time plant matrix A, control distribution matrix B, and output matrix C are obtained from the time-invariant case of the given, continuous time model

$$\dot{x}(t) = Ax(t) + Bu(t) \tag{2.3}$$

$$y = Cx. \tag{2.4}$$

By developing/deriving the linear, homogenous differential equation that the D/C control-type (expressed in the spline-model (1.4) format) satisfies, the dimension and value of $\overline{D}$ is found after a valid set of linearly-independent D/C state variables $v_j(t)$ are chosen, based on the minimal-order differential equation D in Chapter 1. The matrix $\overline{H}$ is defined by expression (1.5) and the underlying relation/definition of $u_{d/c}$ in terms of the state v. With this assortment of "components" determined, the computation of $\overline{BH}(T)$ defined by (1.20) can proceed, in principle.

2.1.1 Example 2-1

As an illustrative example, consider the simple second-order double integrator plant model

$$\ddot{y} = u_{d/c}(t). \tag{2.5}$$

In this Example, we will agree to choose the D/C control type as the Linear-in-Time (LiT) type defined by the following specific case of the spline function of (1.7),

$$u_{d/c}(t) \triangleq c_1(kT) + c_2(kT)(t - kT);\ c_i\left(kT\right) = \text{"smart" constant over each}$$

$$kT \le t < \left(k+1\right)T. \tag{2.6}$$

As a result of the D/C control state v, selected according to phase-variable choice, $\overline{D}$ is determined to be

$$\overline{D} = \begin{bmatrix} 0 & 1 \\ 0 & 0 \end{bmatrix} \tag{2.7}$$

and $\overline{H}$ is determined to be

$$\overline{H} = \begin{bmatrix} 1 & 0 \end{bmatrix}. \tag{2.8}$$

From the $\overline{BH}\left(T\right)$ convolution integral,

$$\overline{BH}\left(T\right) = \int_{kT}^{(k+1)T} e^{A(T-\tau)} B \overline{H} e^{\overline{D}\tau} d\tau = \int_{kT}^{(k+1)T} \underbrace{\begin{bmatrix} 1 & \left(T-\tau\right) \\ 0 & 1 \end{bmatrix}}_{e^{A(T-\tau)}} \underbrace{\begin{bmatrix} 0 \\ 1 \end{bmatrix}}_{B} \underbrace{\begin{bmatrix} 1 & 0 \end{bmatrix}}_{\overline{H}} \underbrace{\begin{bmatrix} 1 & \tau \\ 0 & 1 \end{bmatrix}}_{e^{\overline{D}\tau}} d\tau, \tag{2.9}$$

so that the final expression for $\overline{BH}\left(T\right)$ in the double-integrator case with LiT-type D/C control and the D/C state-variable choices

$$\text{LiT Case; } \ddot{y} = u_{d/c},\ v_1 = u_{d/c},\ v_2 = \dot{u}_{d/c} : \ \overline{BH}\left(T\right) = \begin{bmatrix} \left(\frac{T^2}{2}\right) & \left(\frac{T^3}{6}\right) \\ \left(T\right) & \left(\frac{T^2}{2}\right) \end{bmatrix}. \tag{2.10}$$

When it is possible to successfully use a symbolic calculation software package such as Maple ® to symbolically-compute the convolution integral (1.20) defining the matrix $\overline{BH}\left(T\right)$, the results obtained are considerably more useful, compared to a

numeric-specific result. Human intervention and observation are required however, when using symbolic-computation software, to arrange the final expressions obtained into an orderly, consistent pattern that is user-friendly. In particular, the output formulas obtained by Maple ® software required several stages of aesthetic manipulation of the raw results. Examples of the Maple software code used can be found in Appendix B.

2.2 Structural-Features of $\overline{\mathbf{BH}}$(T)

It is important to observe that by choice of $\{v\}_1^s$ and incorporation/inclusion of ZOH (eg. choose $f_1 \triangleq 1$ in (1.4)) into the D/C generalized Discrete-Time Control, the first column vector of $\overline{BH}(T)$ corresponds to scalar-control ZOH and matches directly to the matrix $\widetilde{B}$ in the ZOH-type state space discretization, (1.15)-(1.16). If the spline model is chosen to be of polynomial-type, and $\{v\}_1^s$ is chosen of the phase-variable type, the subsequent columns of $\overline{BH}(T)$ are structured such that each successive column $n-q-1$ (excluding the first column) is the derivative of the n-q column to the right-hand side. Moreover, the first (left-most) column of $\overline{BH}(T)$ then corresponds to the classical ZOH-related matrix $\widetilde{B}$ in (1.15) when u is a scalar control-input. That is,

$$\overline{BH}(T) = \left[\underbrace{bh^{(1)}}_{ZoH} \;\middle|\; \ldots \middle|\; bh^{(n-q-1)} \middle|\; bh^{(n-q)} \middle| \ldots \middle|\; bh^{(n)} \right]. \tag{2.11}$$

The structure displayed in (2.11) is a direct result of the phase variable choice for v, and is seen throughout the $\overline{BH}$ examples where the D/C spline model (1.4) is of polynomial type used in this thesis and available in Chapter 3 and Appendix A.

In general, the numerical value of the $n \times s$ matrix $\overline{BH}$ is dependent on the chosen value of T and the values associated with the plant and D/C control parameters. It is of particular interest to investigate the dependency of the rank of $\overline{BH}(T)$ on the value of s. Clearly, regardless of the T-value, the rank of $\overline{BH}(T)$ cannot exceed the value $\min.\{n, s\}$, but it turns-out that in D/C control, the value of s, which is the number of linearly independent basis functions included in D/C spline model of (1.4), can easily equal or exceed the value n and that novel result presents the possibility of achieving the never-before possible result in discrete-time control of realizing rank $\overline{BH}(T) = n$ for one or more values of T, even when u is a scalar and $n >> 1$. Even when $\text{rank}\left(\overline{BH}\right) = n$ is not achievable for some T, it is still a fact that the larger the rank of $\overline{BH}$, the more effective the D/C control can be in achieving control tasks that are difficult or impossible to achieve using conventional ZOH-type discrete-time control.

2.3 Some Mathematical Properties of $\overline{\mathbf{BH}}(T)$

Exploration of the mathematical properties of the $\overline{BH}$ matrix entails exploring the ranges and values of T for which $\text{rank}\left(\overline{BH}(T)\right) < n$. Symbolic representations of $\overline{BH}(T)$ are calculated for a variety of plants and D/C control-types in Chapter 3 and Appendix A. The Gram matrix [24] of the row vectors of $\overline{BH}(T)$, form a square matrix,

$$M(T) = \overline{BH}(T)\left(\overline{BH}(T)^T\right). \tag{2.12}$$

This matrix preserves the rank property of $\overline{BH}(T)$ (see Appendix C). Since $M(T)$ preserves the rank of $\overline{BH}$ [1], in taking $\det(M(T))$, an equation dependent on T is achieved which allows detection of $\text{rank}(\overline{BH}) < n$ by determining when $\det(M(T)) = 0$. In each case, T was varied over a suitable range, such that any variances in $\det(M(T))$ were notable. This result was plotted to determine, graphically, the values of T, where $\text{rank}(\overline{BH}(T)) < n$. Knowledge of these areas beforehand, reveals where the never-before achievable "ultimate deadbeat" response discussed in Chapter 4, is not possible.

For the reader's convenience, the following Table 2.1 is provided to display the results in this section in a usable format. Computations and analysis are made according to this table of plants and associated D/C control-types.

[1] The definition of M(T) is chosen by case among $\left\{\left(\overline{BH}^T\overline{BH}\right),\left(\overline{BH}\,\overline{BH}^T\right)\right\}$, such that the resulting M(T) is a square matrix of dimension $\min\{n,s\} \times \min\{n,s\}$. Matrix M(T) is defined in the possible cases of s > n, s < n, and s = n such that $\det(M(T)) = 0$ reveals where rank $\overline{BH} < \min\{n,s\}$.

Table 2.1 Summary of D/C Control Types and Plant Types Investigated for Rank $\overline{BH}(T)$

D/C Control-Type	Plant-Type	
	$\dot{y} + a_1 y = b_1 u = u$ $A = [-a_1] = [-1]$ $B = [b_1] = [1]$	$\ddot{y} + a_2 \dot{y} + a_1 y = b_1 u = u$ $A = \begin{bmatrix} 0 & 1 \\ -a_2 & -a_1 \end{bmatrix}$, where the values of a_1 and a_2 are the result of selection of the eigenvalues of A $B = \begin{bmatrix} 0 \\ b_1 \end{bmatrix} = \begin{bmatrix} 0 \\ 1 \end{bmatrix}$
$u_{d/c} = c_1 + c_2 t$ (LiT)	Case 1. a)	Case 2. a)
$u_{d/c} = c_1 + c_2 e^{\alpha t}$ (EiT)	Case 1. b)	Case 2. b)
$u_{d/c} = c_1 + c_2 \sin(\omega t) + c_3 \cos(\omega t)$ (SiT)	Case 1. c)	Case 2. c)
$u_{d/c} = c_1 + c_2 t e^{\alpha t}$ (PsiT)	Case 1. d)	Case 2. d)

All weighting constants c_i shown in Table 2.1 are understood to mean $c_i = c_i(kT)$, where the "smart" $c_i(kT)$-values are determined at, and only at, the control decision times $t = kT$, $k = 0,1,2,\ldots$. The first-order plant models explored (case 1, a-d) considered the behavior of $\det(M(T))$, and $\text{rank}(\overline{BH}(T))$ for $a_1 = b_1 \neq 0$. Second-order plant models explored (case 2 a-d) considered five combinations of the values $\{a_1, a_2\}$. Those combinations are reflected in the pairs of plant model characteristic-roots (λ_1, λ_2) for the second-order plants of case 2 and are $(\lambda_1, \lambda_2) = (0.5 \pm j0.5)$, $(-0.5 \pm j0.5)$, $(-0.25, -0.5)$, $(0.25, 0.5)$, and $(-0.25, 0.5)$.

In the following explorations of the behavior of $\det\left(M\left(T\right)\right)$, and $\operatorname{rank}\left(\overline{BH}\left(T\right)\right)$, separate calculations were performed to check the value of $\operatorname{rank}\left(\overline{BH}\left(T\right)\right)$ for values of T where $\det\left(M\left(T\right)\right)=0$. The value of $\operatorname{rank}\left(\overline{BH}\left(T\right)\right)$ has been verified to reduce-to unity where stated, rather than zero. While the explorations performed in this Chapter show that $\operatorname{rank}\left(\overline{BH}\left(T\right)\right)=n$ occurs often, knowledge of what values of T for which "sudden drops" in $\operatorname{rank}\left(\overline{BH}\left(T\right)\right)$ occur are useful. It is a possibility that, in general, "sudden drops" in the value of $\operatorname{rank}\left(\overline{BH}\left(T\right)\right)$ could cause unexpected changes in parameter values of the plant model, leading-to unexpected concequences, all of which may not be desirable.

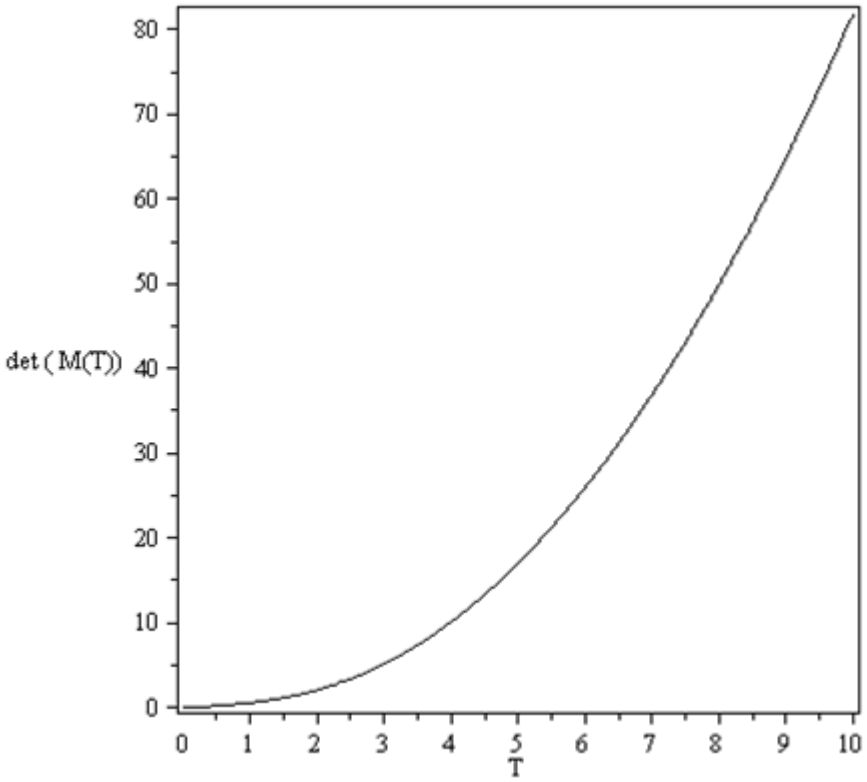

Figure 2.1 Case 1. a) Plot of $\det\left(M\left(T\right)\right)$ corresponding to $\operatorname{rank}\left(\overline{BH}\left(T\right)\right)=1$ for $\det\left(M\left(T\right)\right)\neq 0$ for the First-Order Plant Model $\dot{y}+y=u$ with LiT-Type D/C Control

In Figure 2.1, $\det\left(M\left(T\right)\right)$ shows an exponential-like increase for increasing values of T and does not decrease to zero for any value $T>0$. This behavior is verification of the Theorem [24] which describes the preservation of the rank property of $\overline{BH}\left(T\right)$ in through $M\left(T\right)$. For all $T>0$, $\operatorname{rank}\left(\overline{BH}\left(T\right)\right)=n=1$. Increased robustness of the $\operatorname{rank}\left(\overline{BH}\left(T\right)\right)$ is shown by the increased magnitude of $\det\left(M\left(T\right)\right)$.

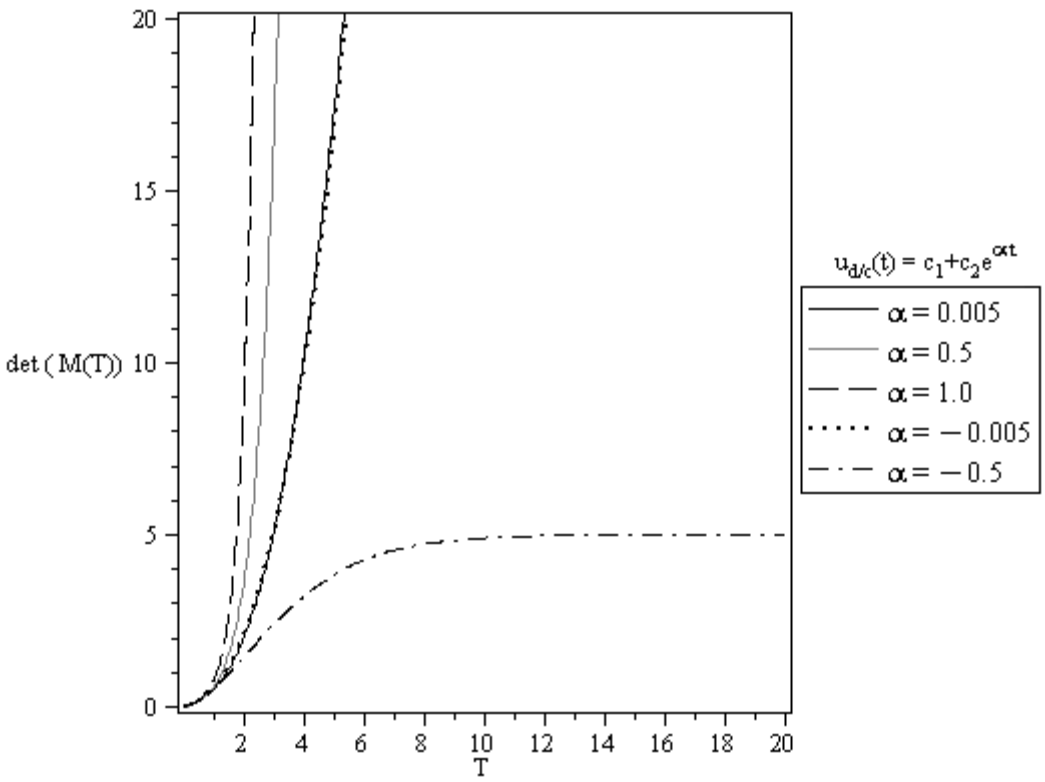

Figure 2.2 Case 1. b) Plot of $\det\left(M\left(T\right)\right)$ corresponding to $\text{rank}\left(\overline{BH}\left(T\right)\right) = 1$ for $\det\left(M\left(T\right)\right) \neq 0$ for the First-Order Plant Model $\dot{y} + y = u$ with EiT-Type D/C Control

When EiT-type D/C control is applied, a value of α is selected. In Figure 2.2, the plot of $\det\left(M\left(T\right)\right)$ is presented for the first-order plant model $\dot{y} + a_1 y = u$ for a selected range of α-values. In this plot, the value of $\det\left(M\left(T\right)\right)$ increases in an exponential-like manner for all values of α except for α = -0.5, where the constant value of $\det\left(M\left(T\right)\right) = 5.0$ is achieved by T = 20. This is evidence that when $\alpha = -0.5$, $\overline{BH}\left(T\right)$ reaches and retains $\text{rank}\left(\overline{BH}\left(T\right)\right) = 1$ for all $T > 0$.

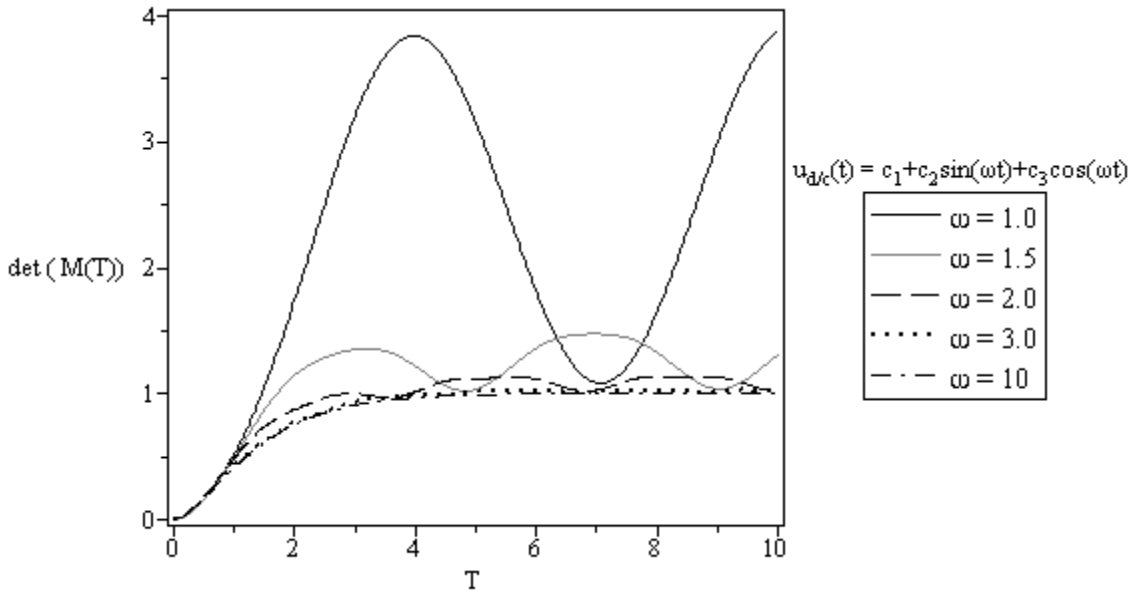

Figure 2.3 Case 1. c) Plot of $\det\left(M(T)\right)$ corresponding to $\operatorname{rank}\left(\overline{BH}(T)\right)=1$ for $\det\left(M(T)\right)\neq 0$ for the First-Order Plant Model $\dot{y}+y=u$ with SiT-Type D/C Control

When SiT-type D/C control is applied, a numerical value of ω is selected. In Figure 2.3, the plot of $\det\left(M(T)\right)$ is presented for the first-order plant model $\dot{y}+y=u$ with a selected range of ω-values > 0. The plot in Figure 2.3 shows that for lower values of ω, larger "hills and valleys" can be seen than for larger values of ω. The value of $\det\left(M(T)\right)$ gradually increases in the range of $0<T\leq 5$ into a steady-state sinusoidal behavior for $T>5$. Since $\det\left(M(T)\right)$ never approaches zero for $T>0$, $\operatorname{rank}\left(\overline{BH}(T)\right)=1$, full rank for all values of $T>0$.

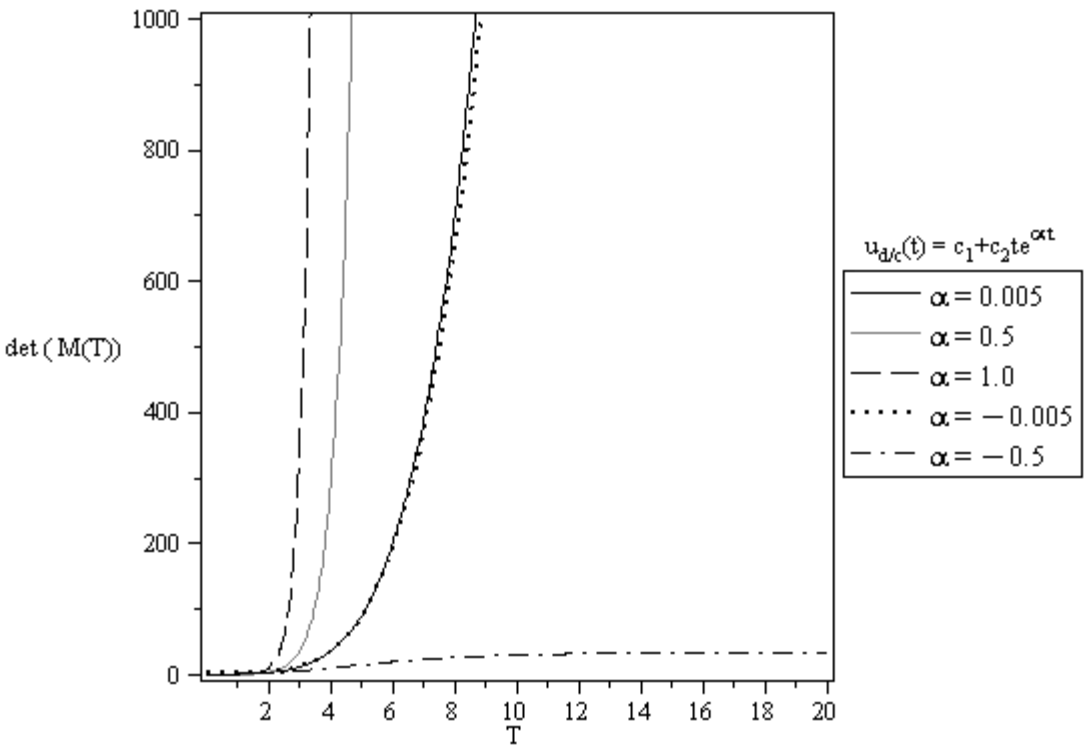

Figure 2.4 Case 1. d) Plot of $\det\left(M\left(T\right)\right)$ corresponding to $\operatorname{rank}\left(\overline{BH}\left(T\right)\right)=1$ for $\det\left(M\left(T\right)\right)\neq 0$ for the First-Order Plant Model $\dot{y}+y=u$ with PsiT-Type D/C Control

When PsiT-type D/C control is applied, a numerical value of α is selected in the same manner as with EiT-type D/C control. In Figure 2.4, the plot of $\det\left(M\left(T\right)\right)$ is presented for the first-order plant model $\dot{y}+y=u$ with a selected range of α. In this plot, the behavior of $\det\left(M\left(T\right)\right)$ exhibits a large exponential-like increase for all cases of α selected, except α = -0.5, where a constant value of 33.0 is achieved by $T=20$. The value of $\det\left(M\left(T\right)\right)>0$ for all $T>0$ shows that $\overline{BH}\left(T\right)$ retains full rank ($\operatorname{rank}\overline{BH}\left(T\right)=1$) for all $T>0$.

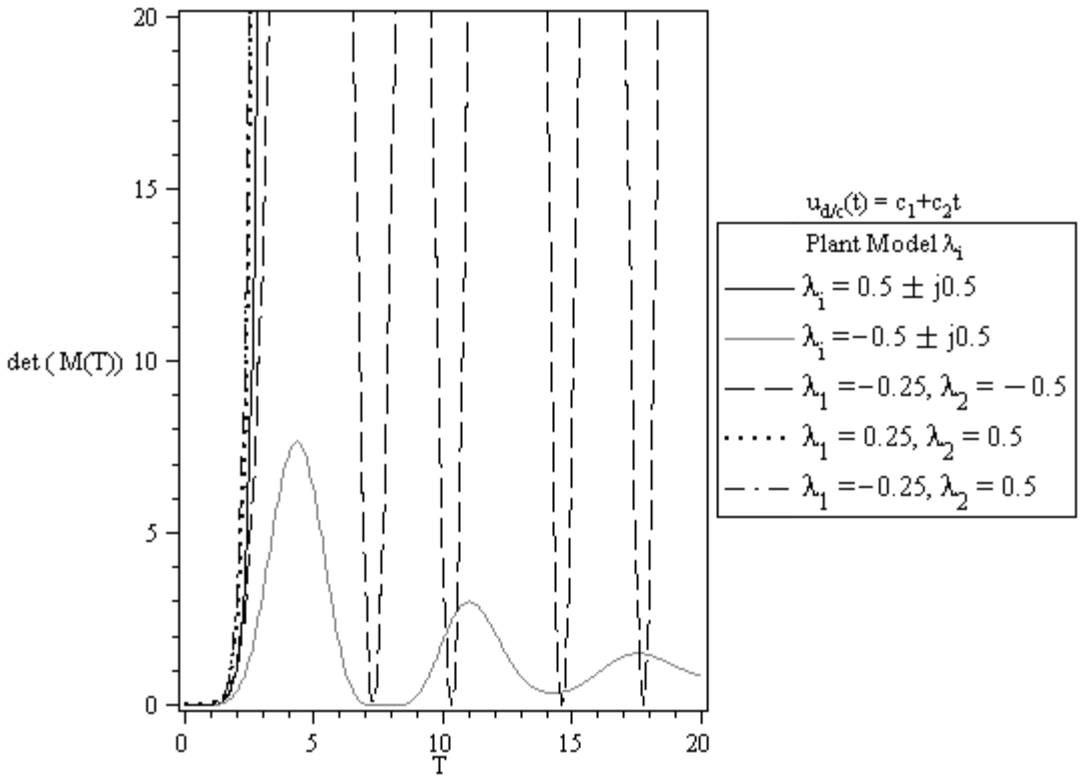

Figure 2.5 Case 2. a) Plot of $\det\left(M(T)\right)$ corresponding to $\text{rank}\left(\overline{BH}(T)\right) = 2$ for $\det\left(M(T)\right) \neq 0$ for Various λ_i in the Second-Order Plant Model $\ddot{y} + a_2\dot{y} + a_1 y = u$ with LiT-Type D/C Control

In Figure 2.5, the plot of $\det\left(M(T)\right)$ is shown for $0 \le T < 15$ for the second-order plant model using LiT-type D/C control where the plant open-loop roots are $\lambda_i = \left(0.5 \pm j0.5\right)$, $\left(0.25, 0.5\right)$, and $\left(-0.25, 0.5\right)$. As can be seen, $\det\left(M(T)\right)$ increases rapidly in an exponential-like manner for increasing values of T. For $\lambda_i = \left(-0.5 \pm j0.5\right)$, $\det\left(M(T)\right)$ decreases to a small value > 0 where $\det\left(M(T)\right) > 0.0150$, for $7 < T < 8.5$, but does not decrease to zero. For $\lambda_i = \left(-0.25, -0.5\right)$, $\det\left(M(T)\right) = 0$ when $T = \left\{7.3130, 10.3480, 14.6305, 21.9567, 25.0852, ...\right\}$. At these values of T, the D/C

control cannot be designed for the unique case of "ultimate deadbeat" response for $\lambda_i = (-0.25, -0.5)$.

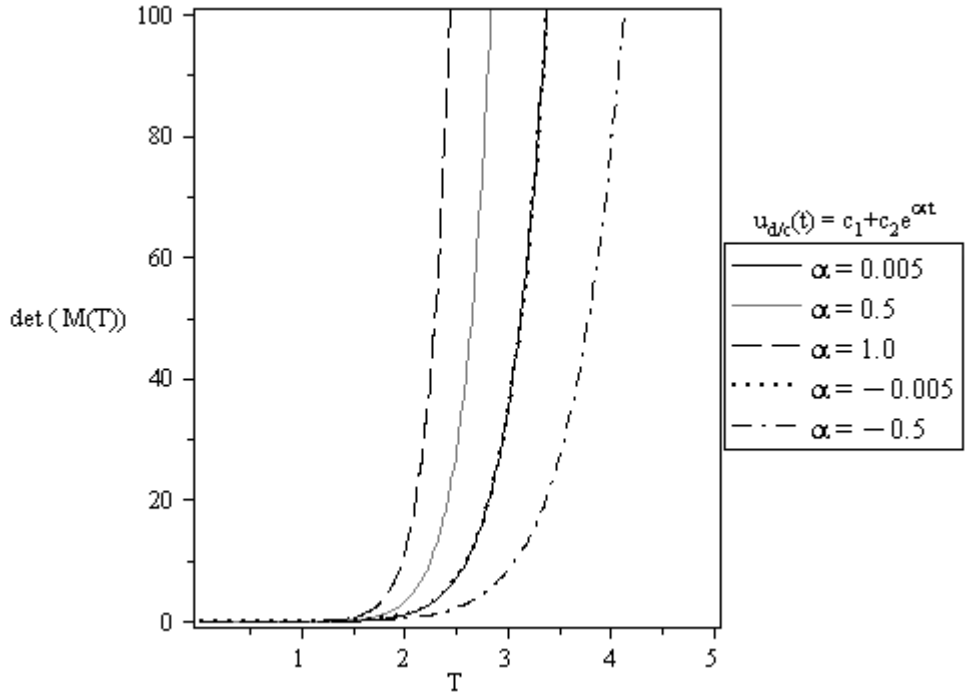

Figure 2.6 Case 2. b) Plot of $\det(M(T))$ corresponding to $\text{rank}(\overline{BH}(T)) = 2$ for $\det(M(T)) \neq 0$ for the Second-Order Plant Model $\ddot{y} + a_2\dot{y} + a_1 y = u$ with $\lambda_i = 0.5 \pm j0.5$ and EiT-Type D/C Control

In Figure 2.6, the plot of $\det(M(T))$ for the second-order plant with $\lambda_i = 0.5 \pm j0.5$ and EiT-type D/C control is shown. The stated-values of λ_i mean that $a_1 = -1,\ a_2 = 0.5$ in the plant model. For all values of α shown, $\det(M(T))$ stays > 0 and grows in value in an exponential-like manner and does not approach zero. This demonstrates the robustness of $\overline{BH}$ to retain full rank, $\text{rank}(\overline{BH}(T)) = 2$.

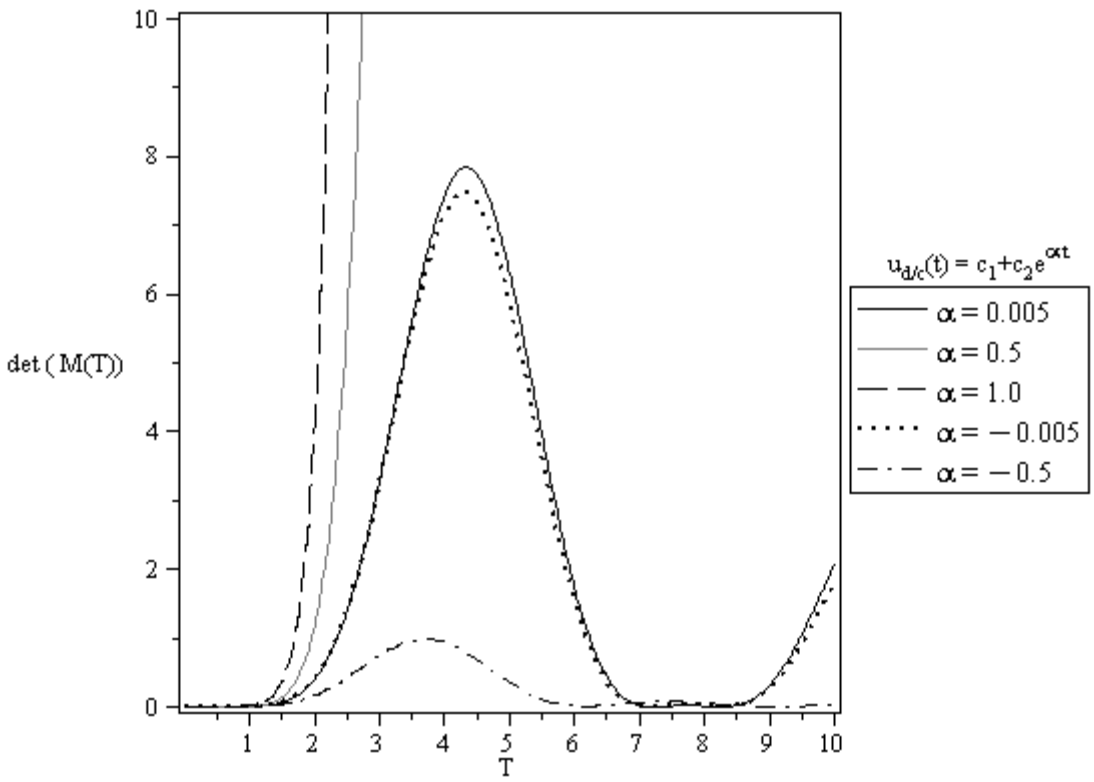

Figure 2.7 Case 2. b) Plot of $\det\left(M(T)\right)$ corresponding to $\text{rank}\left(\overline{BH}(T)\right) = 2$ for $\det\left(M(T)\right) \neq 0$ for the Second-Order Plant Model $\ddot{y} + a_2\dot{y} + a_1 y = u$ with $\lambda_i = -0.5 \pm j0.5$ and EiT-Type D/C Control

In Figure 2.7, the plot of $\det\left(M(T)\right)$ for the second-order plant with $\lambda_i = -0.5 \pm j0.5$ and EiT-type D/C control is shown. The specified values of λ_i correspond-to the plant parameter-values $a_1 = 1,\ a_2 = 0.5$. The value of $\det\left(M(T)\right)$ where α = - 0.5 at T = 6 is zero (5-point decimal precision). The value of $\det\left(M(T)\right)$ where α = 0.005 and α = - 0.005 at T = 7.5 and T = 8.25, is zero (5-point decimal precision). The value of $\det\left(M(T)\right)$ where α = - 0. 5 at T = 9, is zero (5-point decimal precision). Without sufficient decimal precision, $\text{rank}\left(\overline{BH}\right) < n$, which does not allow for the unique D/C case of "ultimate deadbeat" control design.

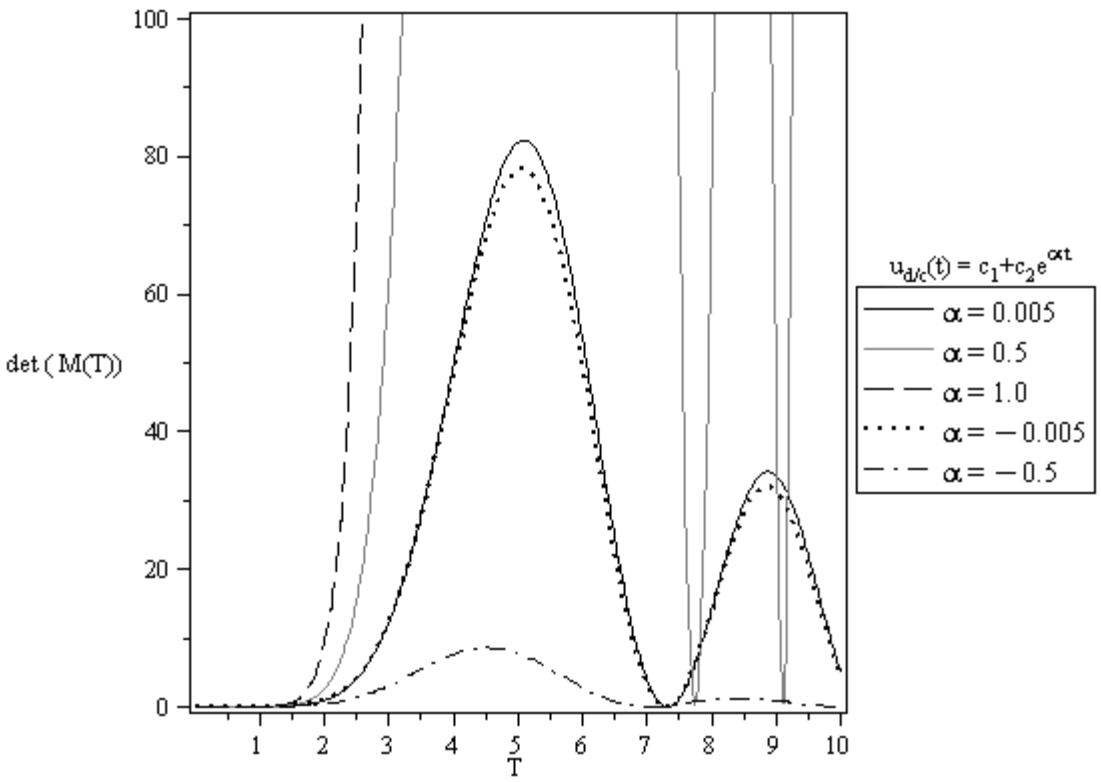

Figure 2.8 Case 2. b) Plot of $\det\left(M(T)\right)$ corresponding to $\operatorname{rank}\left(\overline{BH}(T)\right) = 2$ for $\det\left(M(T)\right) \neq 0$ for the Second-Order Plant Model $\ddot{y} + a_2\dot{y} + a_1 y = u$ with $\lambda_1 = -0.25, \lambda_2 = -0.5$ and EiT-Type D/C Control

In Figure 2.8, the plot of $\det\left(M(T)\right)$ for the second-order plant with $\lambda_1 = -0.25, \lambda_2 = -0.5$ and EiT-type D/C control is shown. The indicated values of λ_i correspond-to the plant parameter values $a_1 = 0.75,\ a_2 = 0.125$. The value of $\det\left(M(T)\right)$ where α = 0.005 and α = - 0.5 at T = 7, is zero (4-point decimal precision). The "hills and valleys" trend continues as T increases, where the determinant value decreases to zero at larger values of T. The value of $\det\left(M(T)\right)$ where α = - 0.5 at T = 10, is zero (4-point decimal precision). Without sufficient decimal precision, the

rank decreases to $\text{rank}\left(\overline{\text{BH}}\right) = 1,$ which does not allow for the unique case of D/C "ultimate deadbeat" design.

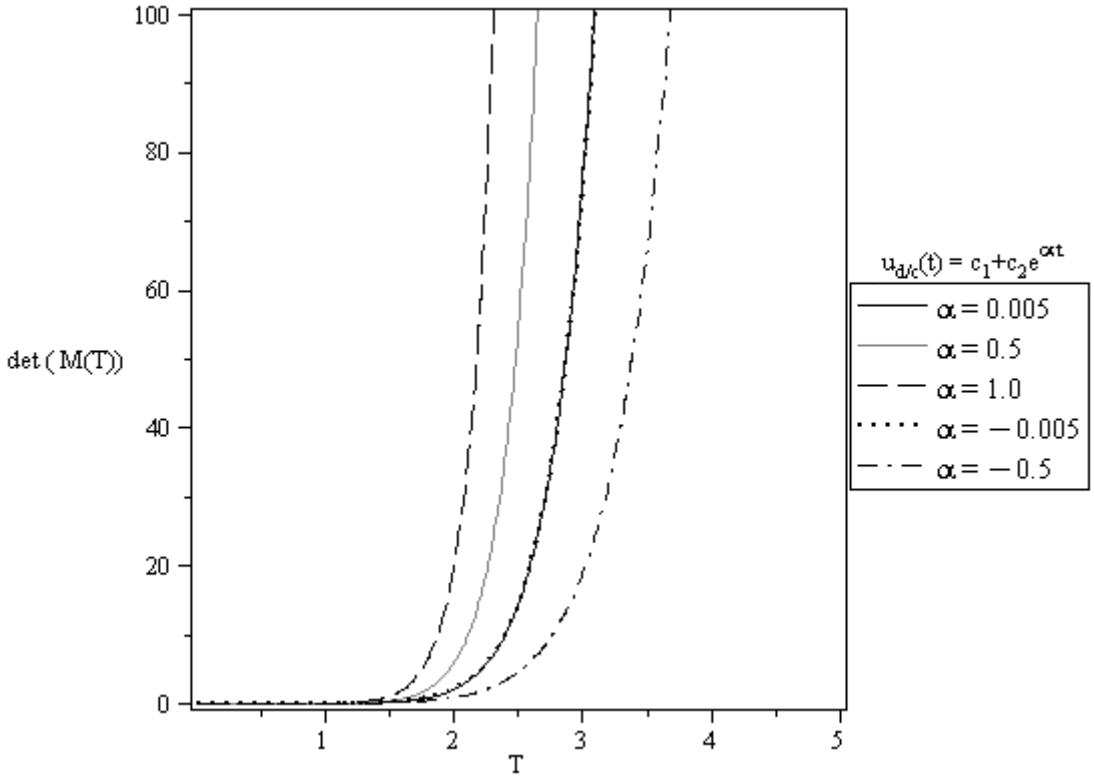

Figure 2.9 Case 2. b) Plot of $\det\left(\text{M}\left(\text{T}\right)\right)$ corresponding to $\text{rank}\left(\overline{\text{BH}}\left(\text{T}\right)\right) = 2$ for $\det\left(\text{M}\left(\text{T}\right)\right) \neq 0$ for the Second-Order Plant Model $\ddot{y} + a_2\dot{y} + a_1 y = u$ with $\lambda_1 = 0.25,\ \lambda_2 = 0.5$ and EiT-Type D/C Control

In Figure 2.9, the plot of $\det\left(\text{M}\left(\text{T}\right)\right)$ for the second-order plant with $\lambda_1 = 0.25,\ \lambda_2 = 0.5$ and EiT-type D/C control is shown. The values of λ_i correspond-to the plant parameter values $a_1 = -0.75,\ a_2 = 0.125.$ For all values of $\alpha,\ \det\left(\text{M}\left(\text{T}\right)\right)$ remains > 0 and increases in value in an exponential-like manner and does not approach zero. This demonstrates the robustness of $\overline{\text{BH}}$ to retain full rank = 2 for all values T > 0.

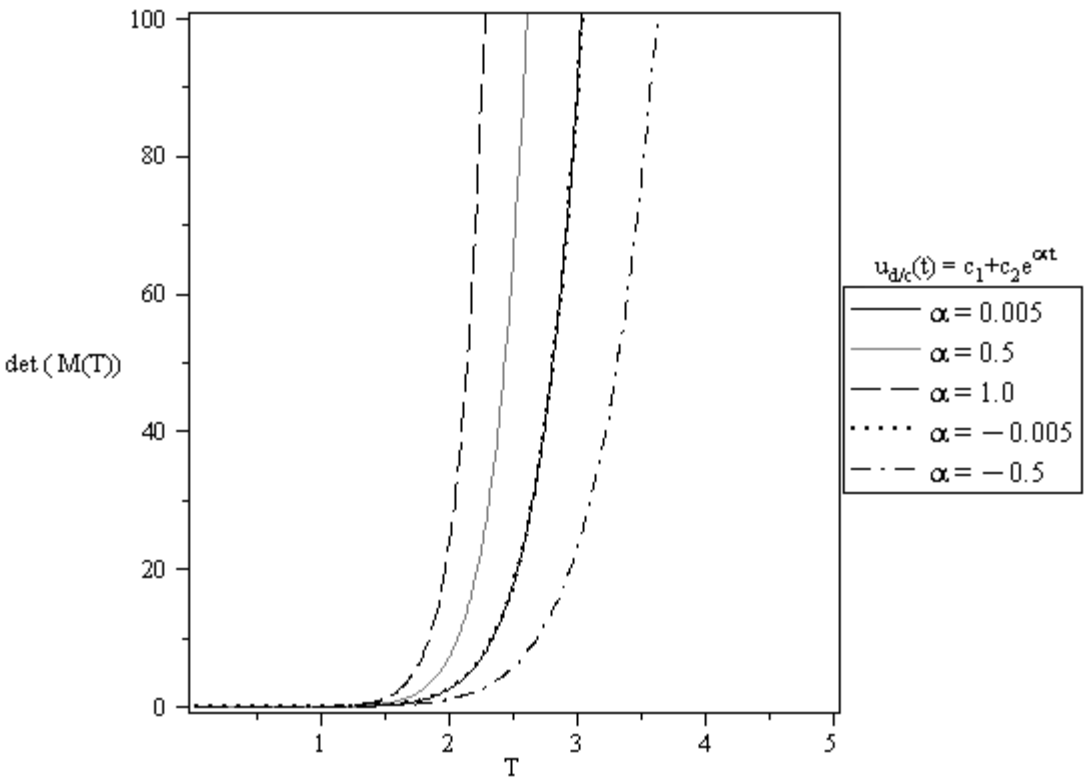

Figure 2.10 Case 2. b) Plot of $\det\left(M\left(T\right)\right)$ corresponding to $\text{rank}\left(\overline{BH}\left(T\right)\right) = 2$ for $\det\left(M\left(T\right)\right) \neq 0$ for the Second-Order Plant Model $\ddot{y} + a_2\dot{y} + a_1 y = u$ with $\lambda_i = -0.25,\ 0.5$ and EiT-Type D/C Control

In Figure 2.10, the plot of $\det\left(M\left(T\right)\right)$ for the second-order plant with $\lambda_1 = -0.25,\ \lambda_2 = 0.5$ and EiT-type D/C control is shown. The values of the λ_i correspond-to $a_1 = -0.25,\ a_2 = -0.125$. The behavior of $\det\left(M\left(T\right)\right)$ is similar to the previous case, such that for all values of α, $\det\left(M\left(T\right)\right)$ grows in an exponential-like manner and does not approach zero. This demonstrates the robustness of $\overline{BH}$ to retain full rank for all $T > 0$.

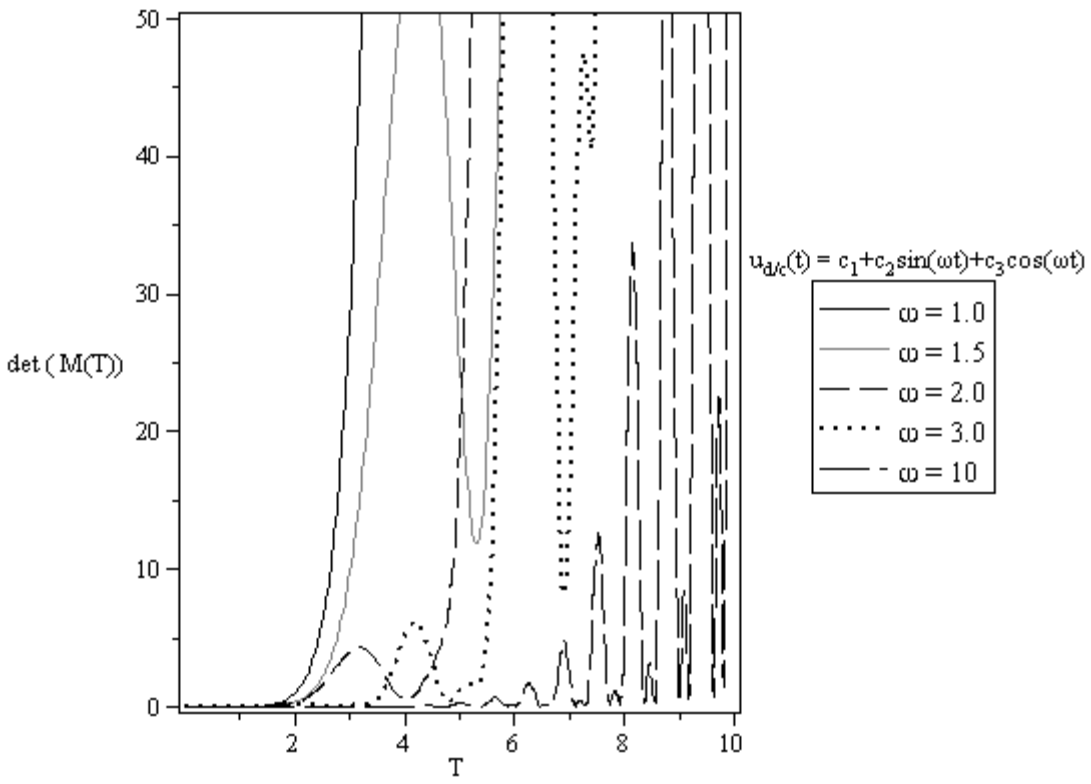

Figure 2.11 Case 2. c) Plot of $\det\left(M\left(T\right)\right)$ corresponding to $\text{rank}\left(\overline{BH}\left(T\right)\right)=2$ for $\det\left(M\left(T\right)\right)\neq 0$ for the Second-Order Plant Model $\ddot{y}+a_2\dot{y}+a_1y=u$ with $\lambda_i=0.5\pm j0.5$, and SiT-Type D/C Control

The plot of $\det\left(M\left(T\right)\right)$ for $\lambda_i=0.5\pm j0.5,$ with SiT-type D/C control is shown in Figure 2.11. The values of the λ_i corresponds-to $a_1=-1,\ a_2=0.5.$ In this case, the plot of $\det\left(M\left(T\right)\right)$ experiences increasing sinusoidal-like behavior, which result in minimum determinant values where, $0<\det\left(M\left(T\right)\right)<0.1$ and are seen visibly on the curve where $\omega=10$. The trend of the local minimum values is an increase. This trend continues for $T>10.$ The value of $\det\left(M\left(T\right)\right)>0\ \ \forall T,$ for $\lambda_i=0.5\pm j0.5,$ in this second-order example.

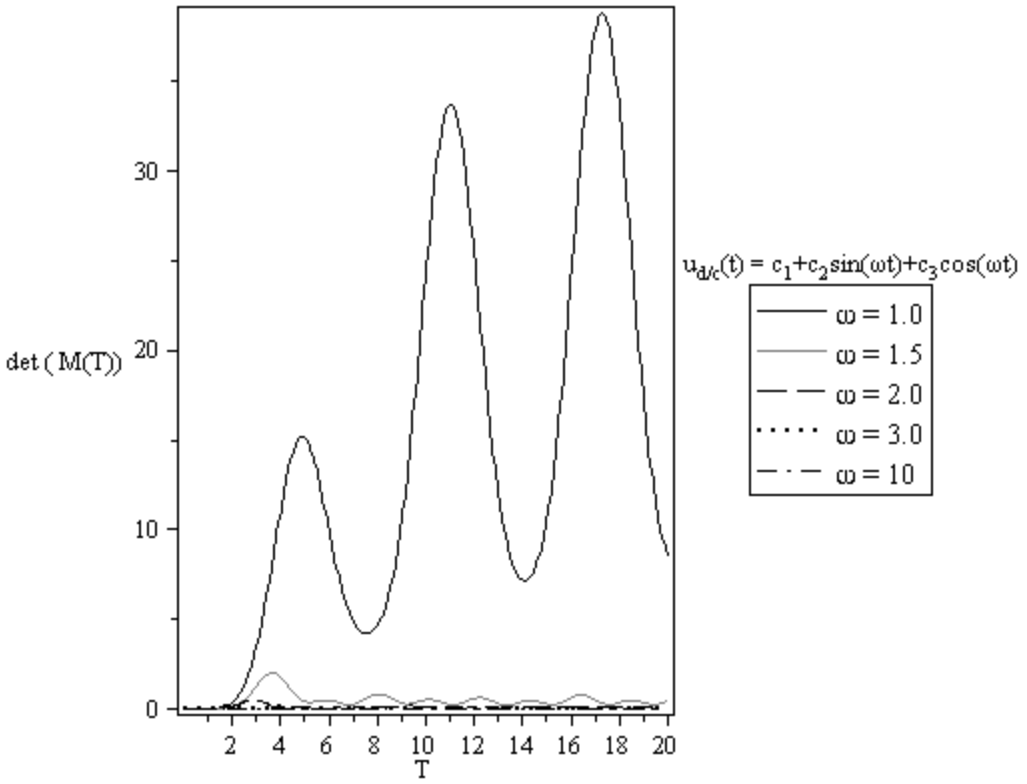

Figure 2.12 Case 2. c) Plot of $\det\left(M\left(T\right)\right)$ corresponding to $\text{rank}\left(\overline{BH}\left(T\right)\right) = 2$ for $\det\left(M\left(T\right)\right) \neq 0$ for the Second-Order Plant Model $\ddot{y} + a_2\dot{y} + a_1 y = u$ with $\lambda_i = -0.5 \pm j0.5$ and SiT-Type D/C Control

The plot of $\det\left(M\left(T\right)\right)$ for the second-order plant model with $\lambda_i = -0.5 \pm j0.5$ and SiT-type D/C control is shown in Figure 2.12. The values of the plant λ_i correspond-to $a_1 = 1,\ a_2 = 0.5$. In this case, the plot of $\det\left(M\left(T\right)\right)$ experiences sinusoidal-like behavior. As might be expected, increased values of ω decrease the value of $\det\left(M\left(T\right)\right)$ and increase the frequency of the sinusoidal-like behavior. For larger values of ω, $\det\left(M\left(T\right)\right) = 0$ (6-point decimal precision), meaning $\text{rank}\left(\overline{BH}\right) < n$ at these minimum values if digit precision > 6 is not possible. Figure 2.13 provides a closer view of $\det\left(M\left(T\right)\right)$ for ω = 10.

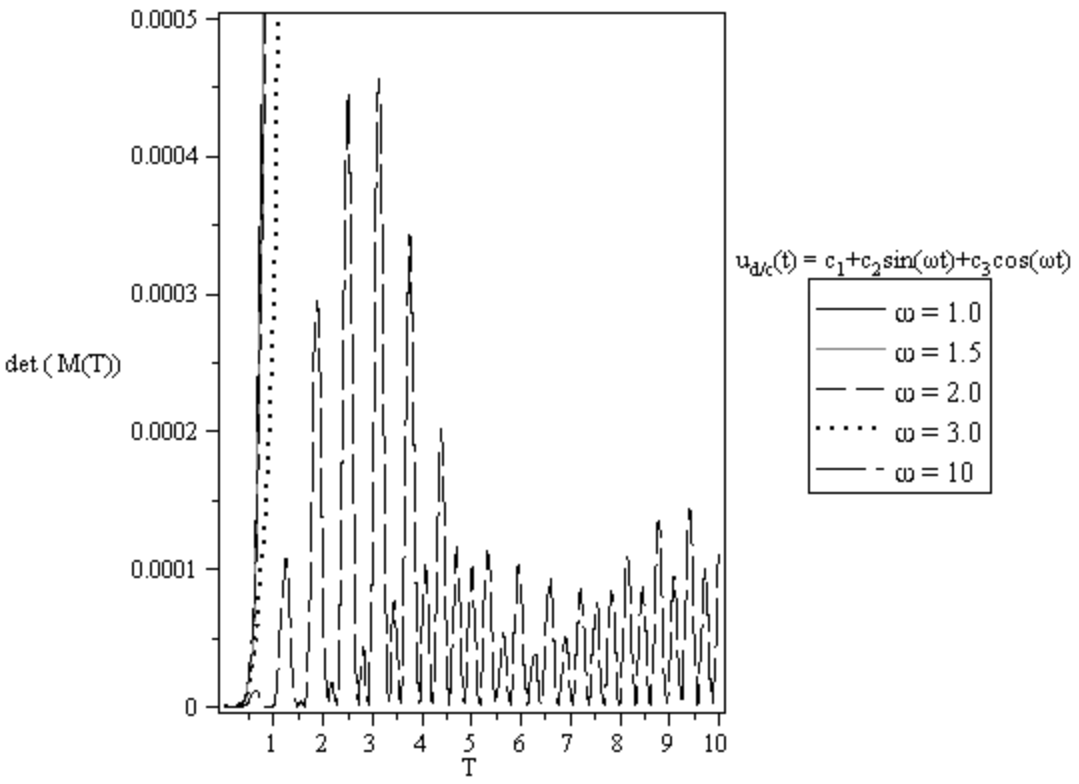

Figure 2.13 Closer Examination of Case 2. b) Shown in Figure 2.12, for $\omega = 10$

Figure 2.13 provides a closer view of the plot of Figure 2.12 for ω = 10. The minimum values of the determinant in the plot of $\det\left(\mathrm{M}\left(\mathrm{T}\right)\right)$ where $\omega = 10$ are zero with 6-point decimal precision.

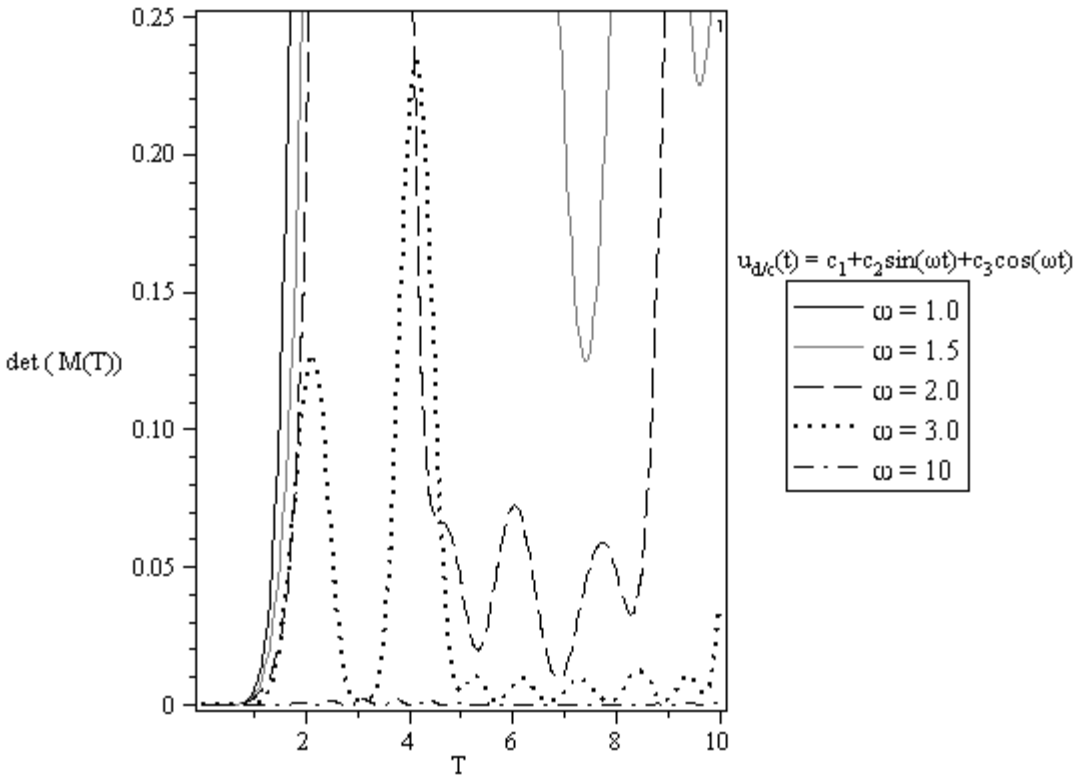

Figure 2.14 Case 2. c) Plot of $\det\left(M\left(T\right)\right)$ corresponding to $\text{rank}\left(\overline{BH}\left(T\right)\right)=2$ for $\det\left(M\left(T\right)\right)\neq 0$ for the Second-Order Plant Model $\ddot{y}+a_2\dot{y}+a_1y=u$ with $\lambda_1=-0.25,\ \lambda_2=-0.5$ and SiT-Type D/C Control

The plot of $\det\left(M\left(T\right)\right)$ for the second-order plant model with $\lambda_1=-0.25,\ \lambda_2=-0.5$ and SiT-type D/C control is shown in Figure 2.14. The value of the plant λ_i corresponds-to $a_1=0.75,\ a_2=0.125$. When $\omega=1.0,$ the plot of $\det\left(M\left(T\right)\right)$ grows in an exponential-like manner until decreasing when $6<T<8$. For this value of $\omega,$ $\det\left(M\left(T\right)\right)$ never approaches zero, which means $\text{rank}\left(\overline{BH}\right)=2$. The plot of $\det\left(M\left(T\right)\right)$ demonstrates sinusoidal-like behavior for $\omega=1.5,2.0,3.0,10$. The minimum of $\det\left(M\left(T\right)\right)$ when is, 0.1 when $\omega=1.5$, 0.005 when $\omega=2.0$, and 0.001

when $\omega = 3.0$. When $\omega = 10$, $\det\left(M\left(T\right)\right) = 0$ with 6-point decimal precision. However, the designer must provide sufficient digit precision for this case if $\omega = 10$ is desired in the design. If such precision cannot be realized, the rank of $\overline{BH}$ reduces to 1, and the unique case of D/C "ultimate deadbeat" design cannot be realized for $\omega = 10$.

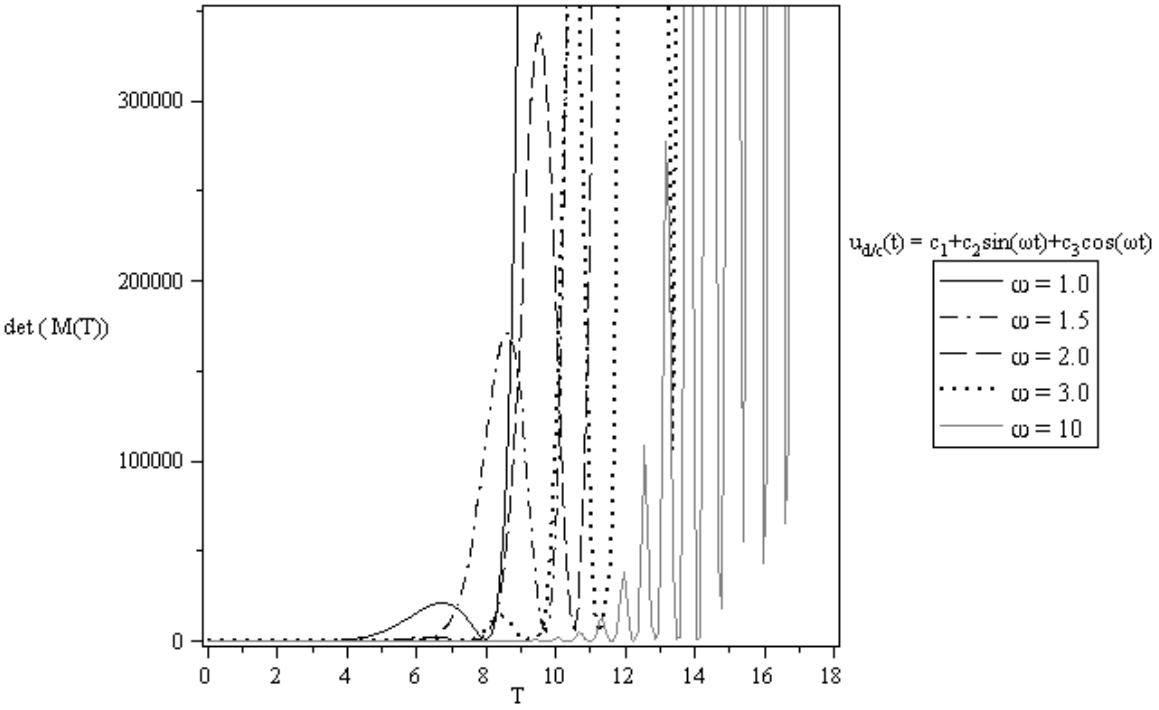

Figure 2.15 Case 2. c) Plot of $\det\left(M\left(T\right)\right)$ corresponding to $\text{rank}\left(\overline{BH}\left(T\right)\right) = 2$ for $\det\left(M\left(T\right)\right) \neq 0$ for the Second-Order Plant Model $\ddot{y} + a_2\dot{y} + a_1 y = u$ with $\lambda_1 = 0.25,\ \lambda_2 = 0.5$ and SiT-Type D/C Control

The plot of $\det\left(M\left(T\right)\right)$ for the second-order plant model with $\lambda_1 = 0.25,\ \lambda_2 = -0.5$ and SiT-type D/C control is shown in Figure 2.15. The value of the plant λ_i corresponds-to $a_1 = -0.75,\ a_2 = 0.125$. For all values of ω, $\det\left(M\left(T\right)\right)$ increases rapidly in an exponential-like manner, with increasing "hills and valleys" for increasing values of ω. Although the plot shows that $\det\left(M\left(T\right)\right)$ for $\omega = 10$ is small by

comparison to the other values of ω, $\det\left(M(T)\right)$ where $\omega = 10$ is approximately 1581.3580 at T = 10. The value of $\det\left(M(T)\right)$ does not approach zero for any value of ω shown, which means that the rank of $\overline{BH}$ remains full rank (= 2).

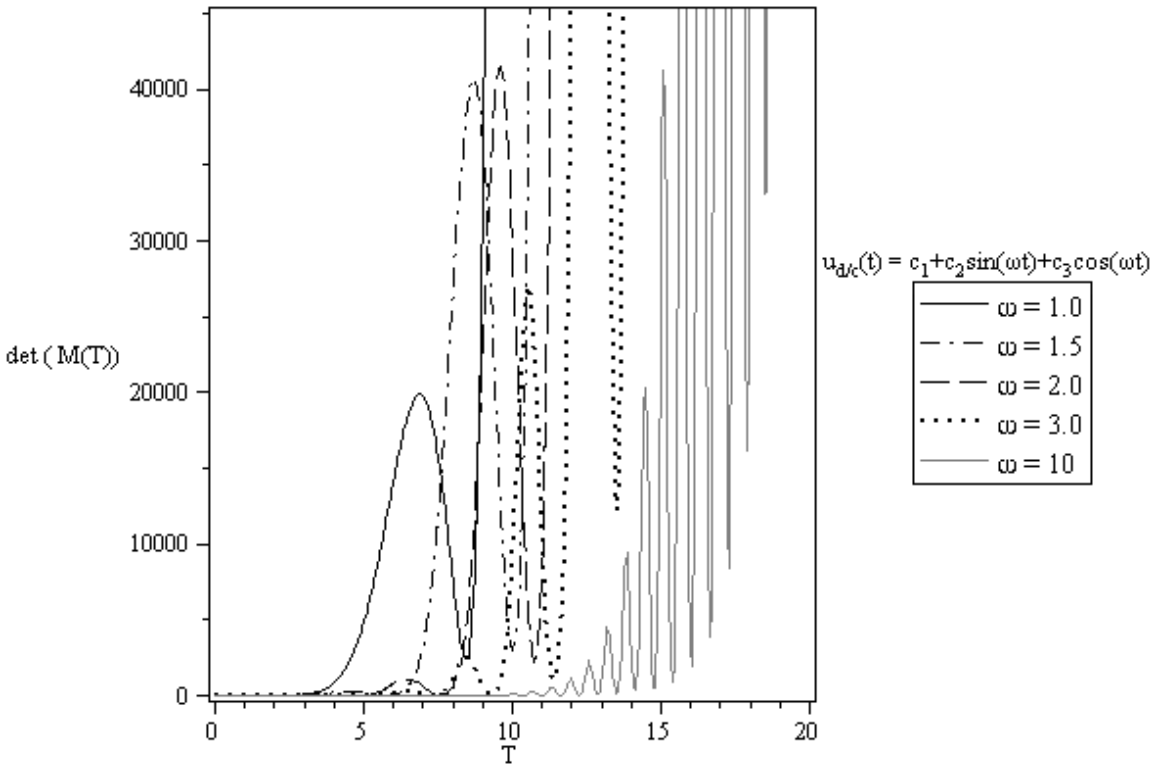

Figure 2.16 Case 2. c) Plot of $\det\left(M(T)\right)$ corresponding to $\text{rank}\left(\overline{BH}(T)\right) = 2$ for $\det\left(M(T)\right) \neq 0$ for the Second-Order Plant Model $\ddot{y} + a_2\dot{y} + a_1 y = u$ with $\lambda_1 = -0.25, \lambda_2 = 0.5$ and SiT-Type D/C Control

The plot of $\det\left(M(T)\right)$ for the second-order plant model with $\lambda_1 = -0.25, \lambda_2 = 0.5$ and SiT-type D/C control is shown in Figure 2.16. The value of the plant λ_i corresponds-to $a_1 = -0.25$, $a_2 = -0.125$. For all values of ω, $\det\left(M(T)\right)$ shows an exponential-like increase with harmonic behavior. Although the plot shows that $\det\left(M(T)\right)$ for $\omega = 10$ is small by comparison to the other values of ω, $\det\left(M(T)\right)$

where $\omega = 10$ is approximately 115.564 at T = 10, and expands to 1.03×10^{10} by T=20. The value of $\det\left(M\left(T\right)\right)$ does not approach zero for any value of ω shown, which means that the rank of $\overline{BH}$ remains full rank (= 2).

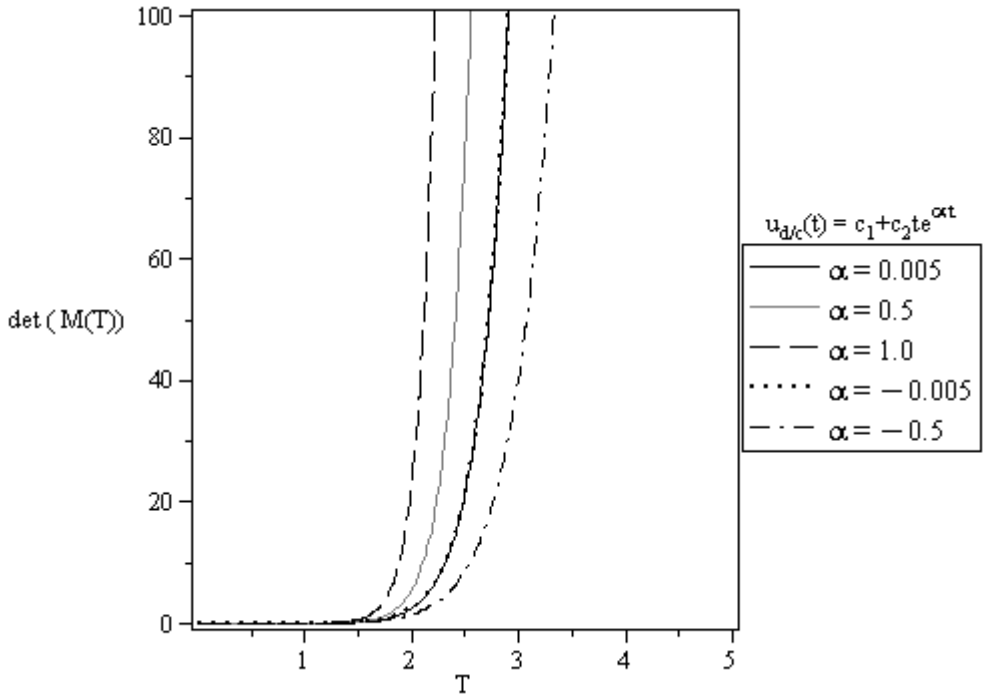

Figure 2.17 Case 2. d) Plot of $\det\left(M\left(T\right)\right)$ corresponding to $\text{rank}\left(\overline{BH}\left(T\right)\right) = 2$ for $\det\left(M\left(T\right)\right) \neq 0$ for the Second-Order Plant Model $\ddot{y} + a_2\dot{y} + a_1 y = u$ with $\lambda_i = 0.5 \pm j0.5$ and PsiT-Type D/C Control

In Figure 2.17, the plot of $\det\left(M\left(T\right)\right)$ for the second-order plant with $\lambda_1 = -0.25, \lambda_2 = 0.5$ and PsiT-type D/C control is shown. The values of λ_i correspond-to $a_1 = -1, \ a_2 = 0.5$. The behavior of $\det\left(M\left(T\right)\right)$ is a pulse-like ($te^{\alpha t}$ -like) expansion. $\det\left(M\left(T\right)\right)$ does not approach zero at any point of T. This demonstrates the robustness of $\overline{BH}$ to retain full rank (= 2).

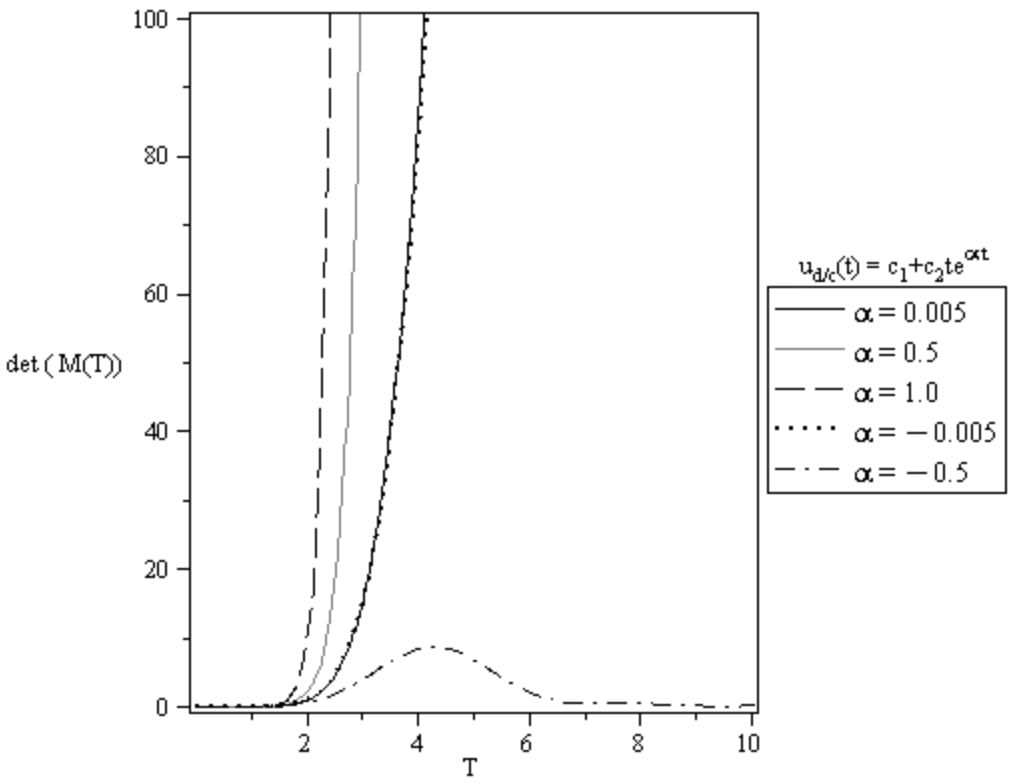

Figure 2.18 Case 2. d) Plot of $\det\left(M\left(T\right)\right)$ corresponding to $\text{rank}\left(\overline{BH}\left(T\right)\right) = 2$ for $\det\left(M\left(T\right)\right) \neq 0$ for the Second-Order Plant Model $\ddot{y} + a_2\dot{y} + a_1 y = u$ with $\lambda_i = -0.5 \pm j0.5$ and PsiT-Type D/C Control

In Figure 2.18, the plot of $\det\left(M\left(T\right)\right)$ for the second-order plant with $\lambda_i = -0.5 \pm j0.5$ and PsiT-type D/C control is shown. The values of λ_i determine that $a_1 = 1,\ a_2 = 0.5$. The behavior of $\det\left(M\left(T\right)\right)$ is an exponential-like increase for all shown values of α except for $\alpha = -0.5$. When $\alpha = -0.5,\ \det\left(M\left(T\right)\right) = 0$ with 3-point decimal precision by T = 10. This decreasing trend continues for larger values of T. The behavior of $\det\left(M\left(T\right)\right)$ for $\alpha = -0.5$ with large values of T (depending upon decimal precision available) do not permit D/C "ultimate deadbeat" design.

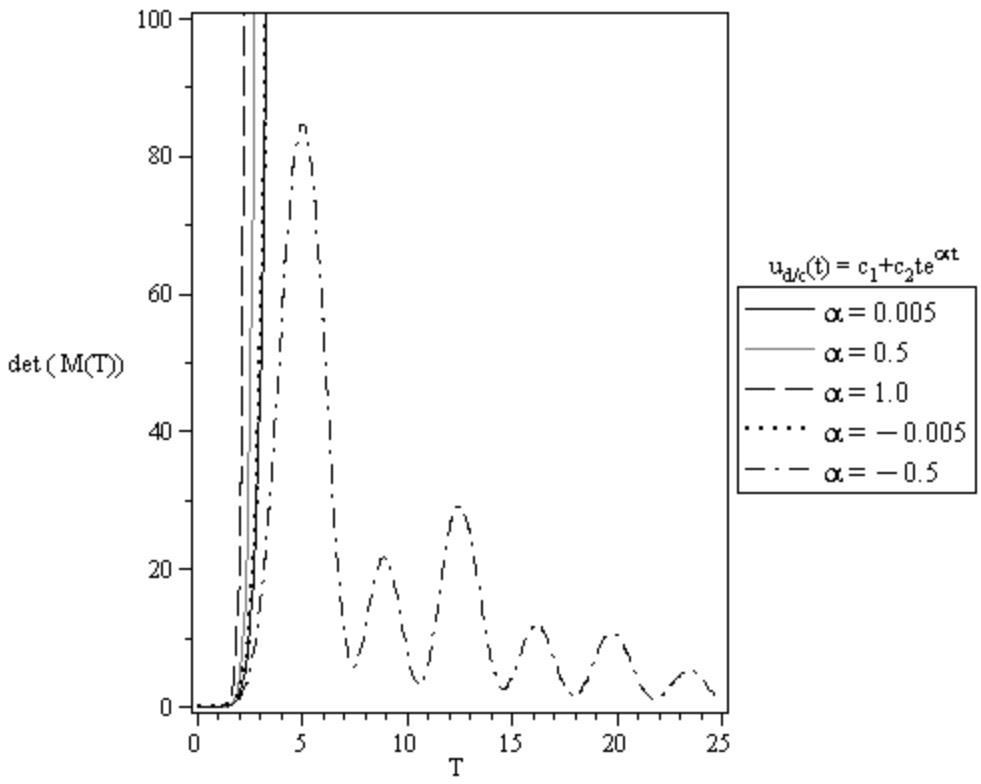

Figure 2.19 Case 2. d) Plot of $\det\left(M\left(T\right)\right)$ corresponding to $\text{rank}\left(\overline{BH}\left(T\right)\right) = 2$ for $\det\left(M\left(T\right)\right) \neq 0$ for the Second-Order Plant Model $\ddot{y} + a_2\dot{y} + a_1 y = u$ with $\lambda_1 = -0.25, \lambda_2 = -0.5$ and PsiT-Type D/C Control

In Figure 2.19, the plot of $\det\left(M\left(T\right)\right)$ for the second-order plant with $\lambda_i = -0.5 \pm j0.5$ and PsiT-type D/C control is shown. The values of the plant λ_i correspond-to $a_1 = 0.75,\ a_2 = 0.125$. The behavior of $\det\left(M\left(T\right)\right)$ is an exponential-like increase for all shown values of α except for $\alpha = -0.5$. When $\alpha = -0.5,\ \det\left(M\left(T\right)\right) = 0$ decreases gradually to zero. Control design with $\alpha = -0.5$ does not permit D/C "ultimate deadbeat" design for very large values of T.

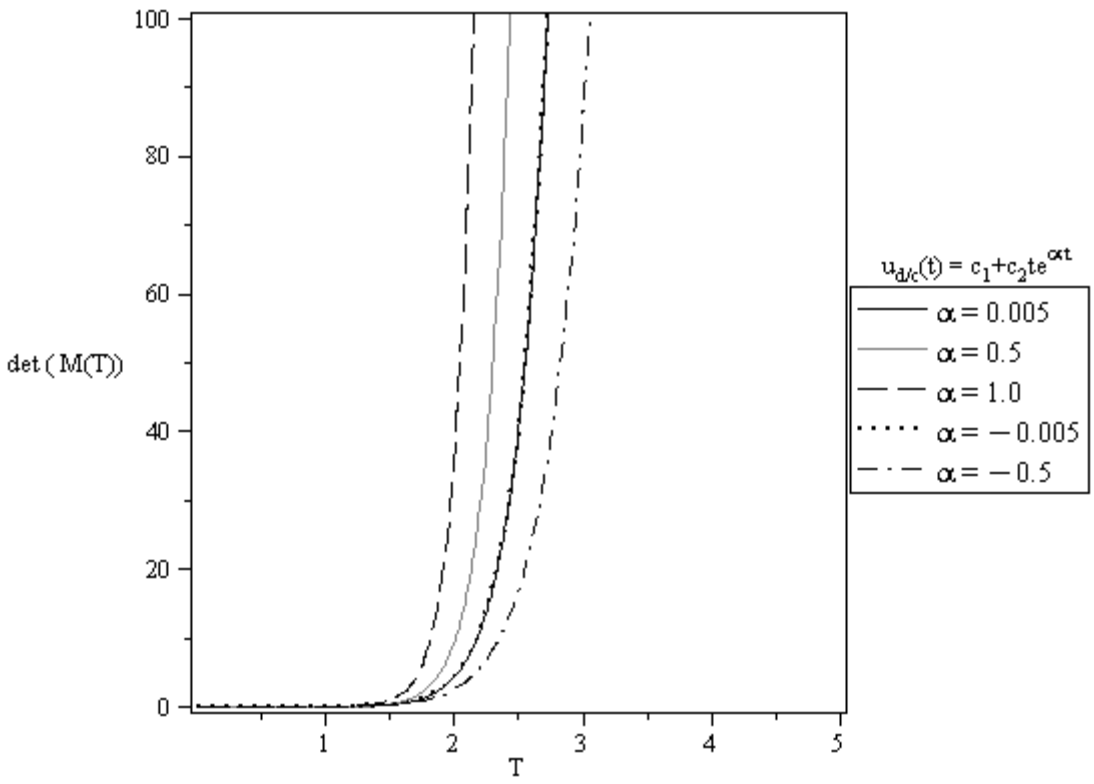

Figure 2.20 Case 2. d) Plot of $\det\left(M\left(T\right)\right)$ corresponding to $\text{rank}\left(\overline{BH}\left(T\right)\right)=2$ for $\det\left(M\left(T\right)\right)\neq 0$ for the Second-Order Plant Model $\ddot{y}+a_2\dot{y}+a_1y=u$ with $\lambda_1=0.25,\ \lambda_2=0.5$ and PsiT-Type D/C Control

In Figure 2.20, the plot of $\det\left(M\left(T\right)\right)$ for the second-order plant with $\lambda_1=-0.25,\ \lambda_2=0.5$ and PsiT-type D/C control is shown. The values of the plant λ_i correspond-to $a_1=-0.75,\ a_2=0.125$. The behavior of $\det\left(M\left(T\right)\right)$ is a pulse-like ($te^{\alpha t}$ -like) expansion. The value of $\det\left(M\left(T\right)\right)$ does not approach zero at any point of T. This demonstrates the robustness of $\overline{BH}$ to retain full rank (= 2).

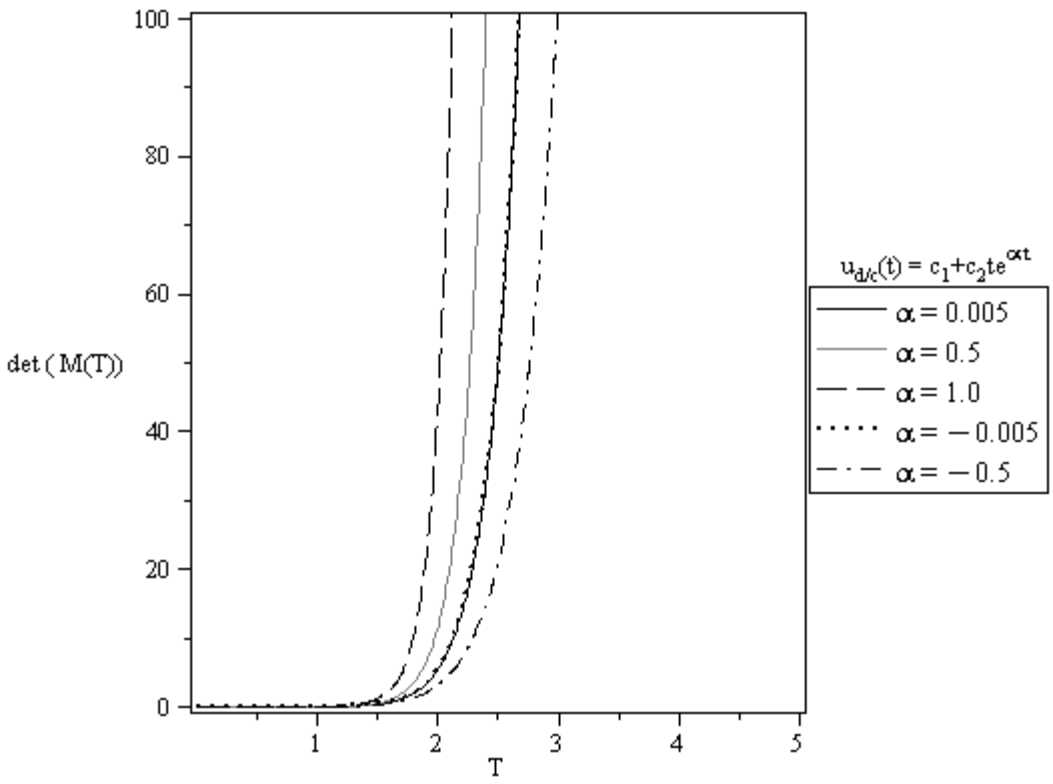

Figure 2.21 Case 2. d) Plot of $\det\left(M\left(T\right)\right)$ corresponding to $\text{rank}\left(\overline{BH}\left(T\right)\right)=2$ for $\det\left(M\left(T\right)\right)\neq 0$ for the Second-Order Plant Model $\ddot{y}+a_2\dot{y}+a_1y=u$ with $\lambda_1=-0.25,\ \lambda_2=0.5$ and PsiT-Type D/C Control

In Figure 2.21, the plot of $\det\left(M\left(T\right)\right)$ for the second-order plant with $\lambda_1=-0.25,\ \lambda_2=0.5$ and PsiT-type D/C control is shown. The values of the plant λ_i correspond-to $a_1=-0.25,\ a_2=-0.125$. The behavior of $\det\left(M\left(T\right)\right)$ is similar to the previous case, such that for all values of α, $\det\left(M\left(T\right)\right)$ expands in a pulse-like ($te^{\alpha t}$ -like) manner and does not approach zero. This demonstrates the robustness of $\overline{BH}$ to retain full rank (= 2).

It should be noted that similar explorations may be performed for third-order cases such as the following generalized third-order plant model,

$$\dddot{y} + a_3\ddot{y} + a_2\dot{y} + a_1 y = b_1 u \tag{2.13}$$

with the system matrices

$$A = \begin{bmatrix} 0 & 1 & 0 \\ 0 & 0 & 1 \\ -a_1 & -a_2 & -a_3 \end{bmatrix}, \tag{2.14}$$

$$B = \begin{bmatrix} 0 \\ 0 \\ 1 \end{bmatrix}. \tag{2.15}$$

Some third-order $\overline{BH}$ calculations appear in Appendix A. Third-order explorations such as those performed for the first-order and second-order plant models of Table 2.1 do not appear here due to symbolic software limitations in the calculation of $\overline{BH}(T)$ for a plant such as that of (2.13), where scalars $\{a_1, a_2, a_3\} \neq 0$, which is the only case where $\det(M(T)) \neq 0$.

2.3.1 Some Mathematical Properties of the Closed-Loop Matrix $\left[\widetilde{A} + \overline{BH}\widetilde{K}_{d/c}\right]$

The closed-loop system matrix for a D/C-type controlled system is

$$\widetilde{A}_{CL} = \left[\widetilde{A} + \overline{BH}\widetilde{K}_{d/c}\right]. \tag{2.16}$$

Control matrix $\widetilde{K}_{d/c}$ is designed to make the closed-loop system matrix $\widetilde{A}_{CL}$ equal to a desired matrix, $\widetilde{A}_m$. For traditional, ZOH-type discrete-time control, the existence of a control matrix, $\widetilde{K}$ is such that

$$\widetilde{A}_m = \left[\widetilde{A} + \widetilde{B}\ \widetilde{K}\right] \tag{2.17}$$

has the necessary and sufficient condition of [9]

$$R_c\left[\widetilde{A}_m - \widetilde{A}\right] \subseteq R_c\left[\widetilde{B}\right], \forall k = 0,1,2,.... \tag{2.18}$$

In the case of D/C-type control, the column range space $R_c\left[\overline{BH}\right]$, may have a larger dimension than the dimension of control vector u, leading to possible control-action enhancement. This feature is thoroughly discussed in [9], where the existence condition for a control matrix $\widetilde{K}_{d/c}$ first appears,

$$R_c\left[\widetilde{A}_m - \widetilde{A}\right] \subseteq R_c\left[\overline{BH}\right], \forall k = 0,1,2,..., \tag{2.19}$$

described in Appendix C. For the remarkable D/C-unique "ultimate deadbeat" response discussed further in Chapter 4, where $\left[\widetilde{A}_{CL}\right] = \left[\widetilde{A}_m\right] = [0]$, the necessary and sufficient existence condition of (2.19) reduces-to

$$R_c[-A] \subseteq R_c\left[\overline{BH}\right], \forall k = 0,1,2,.... \tag{2.20}$$

If the existence condition of (2.19) is satisfied, matrix $\widetilde{K}_{d/c}$ is then designed. Further detail of the existence conditions are given in Appendix C.

CHAPTER 3

EXACT, SYMBOLIC COMPUTATION OF THE D/C CONVOLUTION-MATRIX $\overline{BH}$ FOR SOME COMMON PLANT MODELS AND TYPES OF D/C CONTROL

In this chapter, we compute exact, symbolic expressions for the D/C convolution matrix $\overline{BH}$ using the following types of scalar D/C control.

Table 3.1 D/C Spline Models and Related Control Matrices

Control Type	D/C Spline Model $u_{d/c}(t)$	$\bar{\mathbf{D}}$ (Phase Variables)	$\bar{\mathbf{H}}$ (Phase Variables)
LiT	$c_1 + c_2 t$	$\begin{bmatrix} 0 & 1 \\ 0 & 0 \end{bmatrix}$	$\begin{bmatrix} 1 & 0 \end{bmatrix}$
SiT	$c_1 + c_2 \sin(\omega t) + c_3 \cos(\omega t)$	$\begin{bmatrix} 0 & 1 & 0 \\ 0 & 0 & 1 \\ 0 & -\omega^2 & 0 \end{bmatrix}$	$\begin{bmatrix} 1 & 0 & 0 \end{bmatrix}$
EiT	$c_1 + c_2 e^{\alpha t}$	$\begin{bmatrix} 0 & 1 \\ \alpha & 0 \end{bmatrix}$	$\begin{bmatrix} 1 & 0 \end{bmatrix}$
PsiT	$c_1 + c_2 t e^{\alpha t}$	$\begin{bmatrix} 0 & 1 & 0 \\ 0 & 0 & 1 \\ 0 & -\alpha^2 & 2\alpha \end{bmatrix}$	$\begin{bmatrix} 1 & 0 & 0 \end{bmatrix}$

In addition, we will consider representative plant-examples of the first, second, and third-order type. In each individual example, the elements of the associated $\overline{BH}$ matrix are denoted by bh_{ij} or $bh_{ij,k}$, in order to simplify the presentation-format. An example of the Maple ® computation code can be found in Appendix B.

3.1 First-Order Plant Models (Phase-Variables); $\dot{x} = Ax + Bu_{d/c}(t)$; $n = 1 = r$

Table 3.2 First-Order Plant Models (Phase-Variables)

Case Number	Plant Model	**A**	**B**
1	$\dot{y} + y = u$	$[-1]$	$[1]$
2	$\dot{y} + ay = u$	$[-a]$	$[1]$

3.1.1 First-Order Plant Model; Case 1 with Scalar D/C Control

For the LiT-type D/C control, $\overline{BH}$ is computed symbolically to be

$$\overline{BH} = \left[bh_{11} \quad bh_{12}\right]_{1\times 2}, \tag{3.1}$$

$$bh_{11} \triangleq \left(1 - e^{(-T)}\right), \tag{3.2}$$

$$bh_{12} \triangleq \left(T - 1 + e^{(-T)}\right). \tag{3.3}$$

For the SiT-type D/C control, $\overline{BH}$ is computed to be

$$\overline{BH} = \left[bh_{11} \quad bh_{12} \quad bh_{13}\right]_{1\times 3}, \tag{3.4}$$

$$bh_{11} \triangleq \left(1 - e^{(-T)}\right), \tag{3.5}$$

$$bh_{12} \triangleq \left[\frac{1}{\omega\left(1+\omega^2\right)}\left(\omega e^{(-T)} - \omega\cos\left(\omega T\right) + \sin\left(\omega T\right)\right)\right], \tag{3.6}$$

$$bh_{13} \triangleq \left[\frac{1}{-\omega^2\left(1+\omega^2\right)} \left(\omega^2 \left(e^{(-T)} - 1 \right) + \omega \sin\left(\omega T\right) + \cos\left(\omega T\right) - 1 \right) \right]. \tag{3.7}$$

For the EiT-type D/C control $\overline{BH}$ is computed to be

$$\overline{BH} = \left[bh_{11} \quad bh_{12} \right]_{1\times 2}, \tag{3.8}$$

$$bh_{11} \triangleq \left[\frac{1}{2(\alpha-1)} \left(\left(\sqrt{\alpha}-1\right) e^{\left(\sqrt{\alpha}T\right)} - \left(\sqrt{\alpha}+1\right) e^{\left(-\sqrt{\alpha}T\right)} + 2e^{(-T)} \right) \right], \tag{3.9}$$

$$bh_{12} \triangleq \left[\frac{1}{2\sqrt{\alpha}(\alpha-1)} \left(\left(\sqrt{\alpha}-1\right) e^{\left(\sqrt{\alpha}T\right)} + \left(1+\sqrt{\alpha}\right) e^{\left(-\sqrt{\alpha}T\right)} - 2\sqrt{\alpha} e^{(-T)} \right) \right]. \tag{3.10}$$

For the PsiT control, $\overline{BH}$ is computed to be

$$\overline{BH} = \left[bh_{11} \quad bh_{12} \quad bh_{13} \right]_{1\times 3}, \tag{3.11}$$

$$bh_{11} \triangleq \left(1 - e^{(-T)}\right), \tag{3.12}$$

$$bh_{12} \triangleq \left[\frac{1}{\alpha(1+\alpha)^2} \left(\left(2+3\alpha-\alpha T(1+\alpha)\right) e^{(\alpha T)} - 2(1+\alpha)^2 + \alpha(1+2\alpha) e^{(-T)} \right) \right], \tag{3.13}$$

$$bh_{13} \triangleq \left[\frac{1}{\alpha^2(1+\alpha)^2} \left(\left((1+\alpha)\alpha T - 2\alpha - 1\right) e^{(\alpha T)} + (1+\alpha)^2 - \alpha^2 e^{(-T)} \right) \right]. \tag{3.14}$$

3.1.2 First-Order Plant Model; Case 2 with Scalar D/C Control

For the LiT-type D/C control, $\overline{BH}$ is computed as

$$\overline{BH} = \left[bh_{11} \quad bh_{12} \right]_{1\times 2}, \tag{3.15}$$

$$bh_{11} \triangleq \frac{1}{a}\left(1 - e^{(-aT)}\right), \tag{3.16}$$

$$bh_{12} \triangleq \frac{1}{a^2}\left(e^{(-aT)} - 1 + aT\right). \tag{3.17}$$

For the SiT-type D/C control, $\overline{BH}$ is computed as

$$\overline{BH} = \begin{bmatrix} bh_{11} & bh_{12} & bh_{13} \end{bmatrix}_{1\times 3}, \tag{3.18}$$

$$bh_{11} \triangleq \frac{1}{a}\left(1 - e^{(-aT)}\right), \tag{3.19}$$

$$bh_{12} \triangleq \left[\frac{1}{\omega\left(a^2+\omega^2\right)}\left(\omega e^{(-aT)} - \omega\cos\left(\omega T\right) + a\sin\left(\omega T\right)\right)\right], \tag{3.20}$$

$$bh_{13} \triangleq \left[\frac{-1}{a\omega^2\left(a^2+\omega^2\right)}\left(a^2\cos\left(\omega T\right) + a\omega\sin\left(\omega T\right) + \omega^2 e^{(-aT)} - a^2 - \omega^2\right)\right]. \tag{3.21}$$

For the EiT-type D/C control, $\overline{BH}$ is computed as

$$\overline{BH} = \begin{bmatrix} bh_{11} & bh_{12} \end{bmatrix}_{1\times 2}, \tag{3.22}$$

$$bh_{11} \triangleq \left[\frac{1}{2\left(a^2-\alpha\right)}\left(\left(a-\sqrt{\alpha}\right)e^{\left(\sqrt{\alpha}T\right)} + \left(a+\sqrt{\alpha}\right)e^{\left(-\sqrt{\alpha}T\right)} - 2ae^{(-aT)}\right)\right], \tag{3.23}$$

$$bh_{12} \triangleq \left[\frac{1}{2\sqrt{\alpha}\left(a^2-\alpha\right)}\left(\left(a-\sqrt{\alpha}\right)e^{\left(\sqrt{\alpha}T\right)} - \left(a+\sqrt{\alpha}\right)e^{\left(-\sqrt{\alpha}T\right)} + 2\sqrt{\alpha}e^{(-aT)}\right)\right]. \tag{3.24}$$

For the PsiT-type D/C control, $\overline{BH}$ is computed as

$$\overline{BH} = \begin{bmatrix} bh_{11} & \left(bh_{12,1} + bh_{12,2}\right) & \left(bh_{13,1} + bh_{13,2}\right) \end{bmatrix}_{1\times 3}, \tag{3.25}$$

$$bh_{11} \triangleq \left[\frac{1}{a}\left(1 - e^{(-aT)}\right)\right], \tag{3.26}$$

$$bh_{12,1} \triangleq \left[\frac{1}{\alpha\left(a+\alpha\right)^2}\left(\left(2a+3\alpha\right) + \left(a-\alpha\right)\alpha T\right)e^{(\alpha T)}\right], \tag{3.27}$$

$$bh_{12,2} \triangleq \left[\frac{1}{a\alpha\left(a+\alpha\right)^2}\left(-2\left(a+\alpha\right)^2 + \alpha\left(a+2\alpha\right)e^{(-aT)}\right)\right], \tag{3.28}$$

$$bh_{13,1} \triangleq \left[\frac{1}{\alpha^2 (a+\alpha)^2} \left((\alpha + a)\alpha T + (a - 2\alpha) \right) e^{(\alpha T)} \right], \tag{3.29}$$

$$bh_{13,2} \triangleq \left[\frac{1}{a\alpha^2 (a+\alpha)^2} \left(2a(a+\alpha) + \alpha^2 \left(1 - e^{(-aT)} \right) \right) \right]. \tag{3.30}$$

Symbolic expressions for $\overline{BH}(T)$ considering plants of second and third-order were computed using the D/C control-types of Table 3.1. Due to the cumbersome nature of the equations necessary to express $\overline{BH}$ symbolically, the computations have been continued in Appendix A.

CHAPTER 4

EVALUATION OF PERFORMANCE CAPABILITIES OF REPRESENTATIVE EXAMPLES OF D/C-CONTROLLED, CLOSED-LOOP SYSTEMS

In this chapter, various types of D/C control systems are designed, implemented on representative plant models, and simulated. The closed-loop performance of these D/C control systems is evaluated and compared to the performance obtained by using traditional ZOH-type discrete-time control systems.

4.1 Overview of Results Presented

The design and calculation of the control matrix D/C control-state (linear) feedback-gain matrix $\widetilde{K}_{d/c}$ to accomplish various control tasks and the comparison of the D/C control results to that of ZOH-type discrete-time control results, using simulation exercises are explored in this Chapter. The simulation results pertain to the main classes of control problems: system stabilization where the closed-loop system roots $\{\lambda_i\}_1^N$ are placed at prescribed-locations in the complex-plane; system output driven to and held at a designer-chosen set-point value; and system output driven to a designer-chosen command signal, and disturbance accommodation by real-time observer estimation.

Design methods for the associated D/C control gain-matrix $\widetilde{K}_{d/c}$ are outlined and demonstrated, and simulation results are presented for the best performance case of each control. Comparisons to the performance achieved by traditional ZOH-type Discrete-Time Control are made for each of the aforementioned control tasks.

4.2 Design of $\widetilde{K}_{d/c}$

In modern linear, state-feedback control techniques, the design of the associated feedback control gain-matrix is very important to the application of the control. The existence conditions for $\widetilde{K}_{d/c}$ are given by (2.19) for a desired closed-loop matrix, $\widetilde{A}_{CL} = \widetilde{A}_m$, and by (2.20) for the never-before possible case of $\widetilde{A}_{CL} = [0]$, known as "ultimate deadbeat". The D/C control gain-matrix $\widetilde{K}_{d/c}$ may be designed using two different closed-loop pole assignment techniques: "deadbeat" design, and "ultimate deadbeat" design using the Moore-Penrose Generalized Inverse technique. In the following subsections, each of these techniques is detailed.

4.2.1 $\widetilde{K}_{d/c}$ Design for "Deadbeat" Closed-Loop System Response

Within the field of discrete-time control, the term "deadbeat" system response refers-to the design of $\widetilde{K}_{d/c}$ such that the closed loop system matrix $\widetilde{A}_{CL}$, which is defined as the composite-matrix

$$\widetilde{A}_{CL} = \left[\widetilde{A} + \overline{BH}\widetilde{K}_{d/c} \right], \tag{4.1}$$

has (discrete-time) zero-eigenvalues; $\left\{\tilde{\lambda}_i\right\}_i^n = 0$. While a closed-loop, discrete-time controlled system $\left|\tilde{\lambda}_i\right| < 1$ to ensure system stability [3], placing all $\tilde{\lambda}_i$ of the closed-loop

system at the special-value $\tilde{\lambda}_i = 0$ results-in the system state (or "error-state") being controlled-to zero within a finite-number "NT," N = positive integer ≥ 1, of sample/decision periods T, [3]. It is for this quick, finite-time "zero-state" response, that such a design is desirable.

The closed loop (discrete-time) $\tilde{\lambda}_i$ may all be placed at the common zero value very simply through calculation by setting the roots $\tilde{\lambda}_i$ of the closed-loop, characteristic polynomial. The matrix $\widetilde{A}_{CL}$, and a nonzero eigenvector α corresponding to an eigenvalue $\tilde{\lambda}$, of $\widetilde{A}_{CL}$, obey the relation, [24]

$$\widetilde{A}_{CL}\alpha = \lambda\alpha. \tag{4.2}$$

Equation (4.2) is equivalently expressed as

$$\left(\widetilde{A}_{CL} - \lambda I\right)\alpha = 0. \tag{4.3}$$

This implies that the determinant of (4.3) is zero, forming the characteristic polynomial

$$\det\left[\tilde{\lambda}I - \widetilde{A}_{CL}\right] = \tilde{\lambda}^n = 0, \tag{4.4}$$

where (4.4) leads-to an equation dependent upon the elements of $\widetilde{K}_{d/c}$. Solving for the $\widetilde{K}_{d/c}$ element values yields the desired closed-loop "deadbeat"-performance. By forcing each coefficient of $\tilde{\lambda}$ in (4.4) to become zero, as shown, the rs-elements of $\widetilde{K}_{d/c}$ may be solved-for simultaneously for the resulting values of the elements of $\widetilde{K}_{d/c}$. For $\dim\left(\widetilde{K}_{d/c}\right) = r \times s$, when $rs > n^2$, the designer may specify the values of $\left(rs - n^2\right)$ elements of $\widetilde{K}_{d/c}$ or assign these values according to a predetermined methodology, and calculate the remaining element values. It

is important to note that when $rs > n^2$, in some cases, if the designer specifies the values of one or more elements of $\widetilde{K}_{d/c}$, it is possible that the magnitude of the system output response $y(t)$ overshoot and undershoot may increase, compared to ZOH-type control, due to compensation for these specified $\widetilde{K}_{d/c}$ element values. Such behavior is not typical of D/C control in general.

4.2.2 $\widetilde{K}_{d/c}$ Design for "Ultimate Deadbeat" System Response

A (very) remarkable special case of "deadbeat" system response design is referred-to as "ultimate deadbeat," [10], which consists of designing $\widetilde{K}_{d/c}$ for the never-before achieveable $\widetilde{A}_{CL} = [0]$. This method accomplishes the control task in only one sample period ($T = 1$) [19], a result previously impossible with discrete-time control methods, including traditional ZOH-type discrete-time control beyond n = 1. This result is far superior for an n^{th} order system, as compared-to the "deadbeat" design of accomplishing the control task within $T = n$. This design technique is applicable when dimension $s \geq n$.

Two possible techniques for determining the values of $\widetilde{K}_{d/c}$ such that $\widetilde{A}_{CL} = [0]$ are (i) using the Moore-Penrose Generalized Inverse to minimize the column rank of $\widetilde{A}_{CL}$ and (ii) forming each element of $\widetilde{A}_{CL}$ as an equation dependent on $\widetilde{K}_{d/c}$ and solving this set of equations simultaneously such that $\widetilde{A}_{CL} = [0]$.

The first method for "ultimate deadbeat" design of $\widetilde{K}_{d/c}$ is Moore-Penrose Column Rank Minimization. In this method, the Moore-Penrose Generalized Inverse of $\overline{BH}$ (denoted with †) is used in the calculation of $\widetilde{K}_{d/c}$ is according to

$$\widetilde{K}_{d/c} = \overline{BH}^{\dagger}\left(\widetilde{A}_{CL} - \widetilde{A}\right), \tag{4.5}$$

where $\left[\widetilde{A}_{CL}\right] = \left[\widetilde{A}_{m}\right]$, a desired closed-loop matrix. Additional detail of this calculation technique is given in Appendix C. If $\widetilde{A}_{CL} = [0]$, $\widetilde{K}_{d/c}$ design from (4.5) results in "ultimate deadbeat" response features. If $\widetilde{A}_{CL} = [0]$ cannot be realized, the design of $\widetilde{K}_{d/c}$ by (4.5) results in $\widetilde{A}_{CL}$ with minimized rank, resulting in "deadbeat" performance design.

Another method for solving for the element-values of $\widetilde{K}_{d/c}$ is from

$$\widetilde{A}_{CL} = \left[\widetilde{A} + \overline{BH}\widetilde{K}_{d/c}\right] = \left[\widetilde{A}_{m}\right], \tag{4.6}$$

which forms an equation for each entry of $\widetilde{A}_{CL}$ which can, when the existence conditions of (2.19) are satisfied, be solved for simultaneously for each element $\widetilde{K}_{d/c_{i,j}}$ such that $\widetilde{A}_{CL_{i,j}} = \widetilde{A}_{m_{i,j}}$. If the $\widetilde{K}_{d/c}$ solution to (4.6) is not unique, the designer may specify $\left(rs - n^2\right)$ element values of $\widetilde{K}_{d/c}$ resulting in n^2 total $\widetilde{K}_{d/c}$ elements remaining to be the result of computation. While this design accomplishes the control task within $T = 1$, any designer-chosen values are accommodated by the elements resulting from computation, possibly resulting in higher magnitudes of the system output during the response transient than with traditional ZOH-type control, and is worth further investigation. Such performance "costs" are not typical of D/C-type control. It is extremely difficult for the designer to know the "best" values of $\widetilde{K}_{d/c}$, such that increased magnitude of the system response does not occur. It is for this reason that the Moore-Penrose method of choosing $\widetilde{K}_{d/c}$ elements is preferred. In fact, if the designer chooses element-values of $\widetilde{K}_{d/c}$ to be

equal to the elements of $\widetilde{K}_{d/c}$ obtained by the Moore-Penrose method, the remaining $\widetilde{K}_{d/c}$ elements designed by this method after computation are equal to that of the Moore-Penrose method.

4.3 Some Simulated Examples of D/C Control Design for Particular Cases

Table 3.1 contains the plant models used for the various simulations in this chapter. The plant models are of representative type first-order, second-order, and third-order. The uncontrolled plant models (the case where u = 0) presented in Table 3.1 are stable. In general, the techniques applied here to the stable plants of Table 3.1 may be applied to unstable plants, however, stability and control-task achievement may only be guaranteed at the control decision times, $T = kT,\ k = 1,2,3,...$ as is the case with all discrete-time controllers. Examples of the Simulink simulation models used in this chapter can be found in Appendix F.

Table 4.1 Plant Models for D/C Control Simulated Cases

Order n	Plant Equation	Scalar Values
1	$\dot{y} + ay = u$	$a = 1$
2	$\ddot{y} + a_2\dot{y} + a_1 y = u$	$a_1 = 1,\ a_2 = 3$
3	$\dddot{y} + ay = u$	$a = 1$

4.3.1 Example 1: System Stabilization

The first control task example is to move the closed-loop system λ_i of the plant models shown above in Table 4.1 to drive the output $y(t) \to 0$ in finite-time. For

comparison with the D/C-type control algorithms, the ZOH-control is computed and simulated. In all cases, control decision period $T = 3,$ SiT-type D/C control value $\omega = 1.0,$ and EiT and PsiT-type D/C control value $\alpha = 0.5.$

4.3.1.1 First-Order System Stabilization with ZOH-Type Control

Shown in Figure 4.1-Figure 4.4, the ZOH "ultimate deadbeat" control design for the first-order plant of Table 4.1 may be computed from either (4.4) or (4.5), with the same result, where $\overline{BH} = \widetilde{B}$ and may be calculated from (1.20) with $\overline{D} = [0]$ and $\overline{H} = [1].$ The resulting 1×1 control design matrix is calculated to be

$$\widetilde{K}_{ZOH} = [-0.0524]. \tag{4.7}$$

4.3.1.2 First-Order System Stabilization with LiT-Type D/C Control

The LiT-type D/C "ultimate deadbeat" control design for the first-order plant of Table 4.1 was computed from the Moore-Penrose technique of (4.5), where $\overline{BH}$ is calculated to be (3.1)-(3.3). The detailed calculations can be found in Appendix D. The resulting 1×2 control gain matrix is

$$\widetilde{K}_{d/c} = \begin{bmatrix} -0.0093 \\ -0.0200 \end{bmatrix}. \tag{4.8}$$

This case is simulated in Figure 4.1. For both LiT-type D/C control and ZOH-type control, the control task is achieved with one control decision ($t = kT;\ k = 1$).

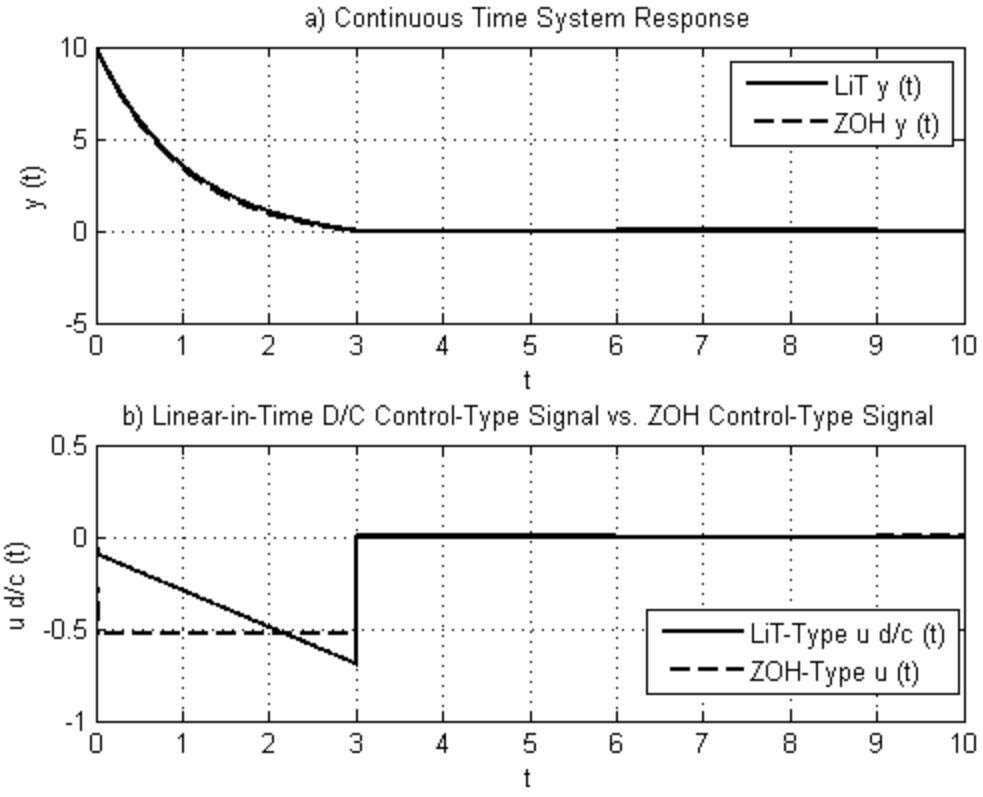

Figure 4.1 System Response and Control Signal for the First-Order Plant Model with LiT-Type D/C Control

4.3.1.3 First-Order System Stabilization with EiT-Type D/C Control

The EiT-type D/C "ultimate deadbeat" control design for the first-order plant of Table 4.1 may be computed from (4.5), where $\overline{BH}$ is calculated from (1.20) and is found in Appendix A. The resulting 1×2 control gain matrix is computed to be

$$\widetilde{K}_{d/c} = \begin{bmatrix} -0.0074 \\ -0.0095 \end{bmatrix}, \tag{4.9}$$

with simulation results shown in Figure 4.2. The control task is achieved by $T = 3$ with one control decision.

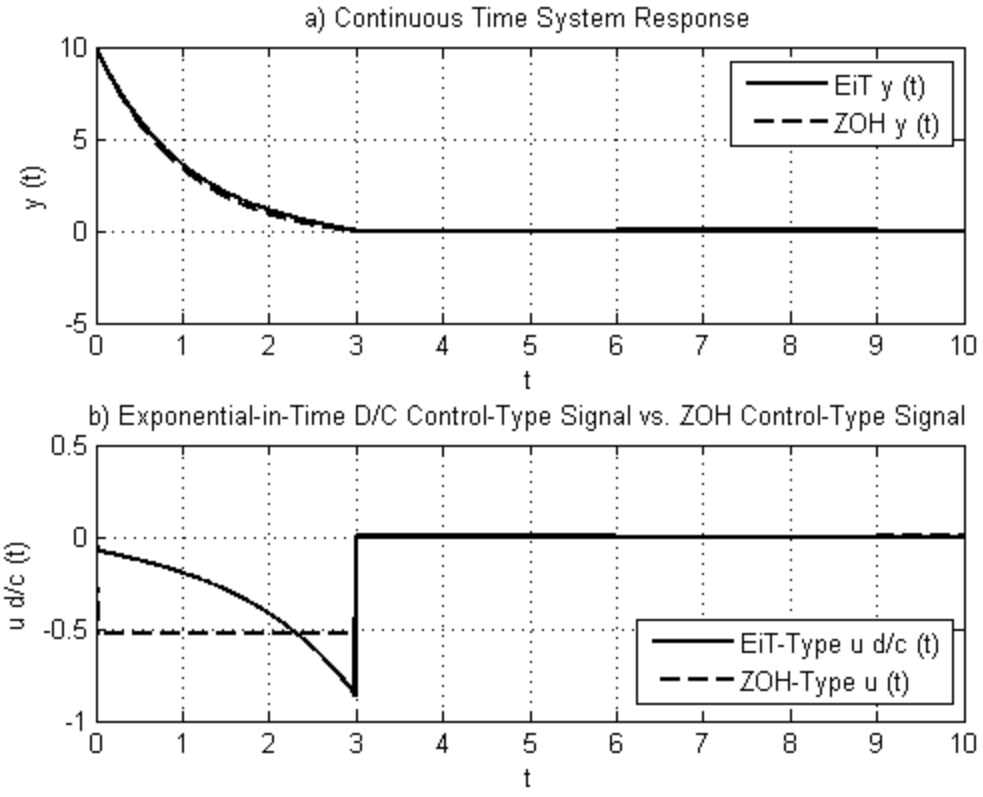

Figure 4.2 System Response and Control Signal for the First-Order Plant Model with EiT-Type D/C Control

4.3.1.4 First-Order System Stabilization with SiT-Type D/C Control

The SiT-type D/C "ultimate deadbeat" control design for the first-order plant of Table 4.1 may be computed from (4.5), where $\overline{\mathrm{BH}}$ is calculated from (1.20) and is found in Appendix A. The resulting 1×2 control gain matrix is computed to be

$$\widetilde{\mathrm{K}}_{\mathrm{d/c}} = \begin{bmatrix} -0.0147 \\ -0.0092 \\ -0.0217 \end{bmatrix}, \tag{4.10}$$

and the simulation results are shown in Figure 4.3. The control task is achieved by $\mathrm{T} = 3$ with one control decision.

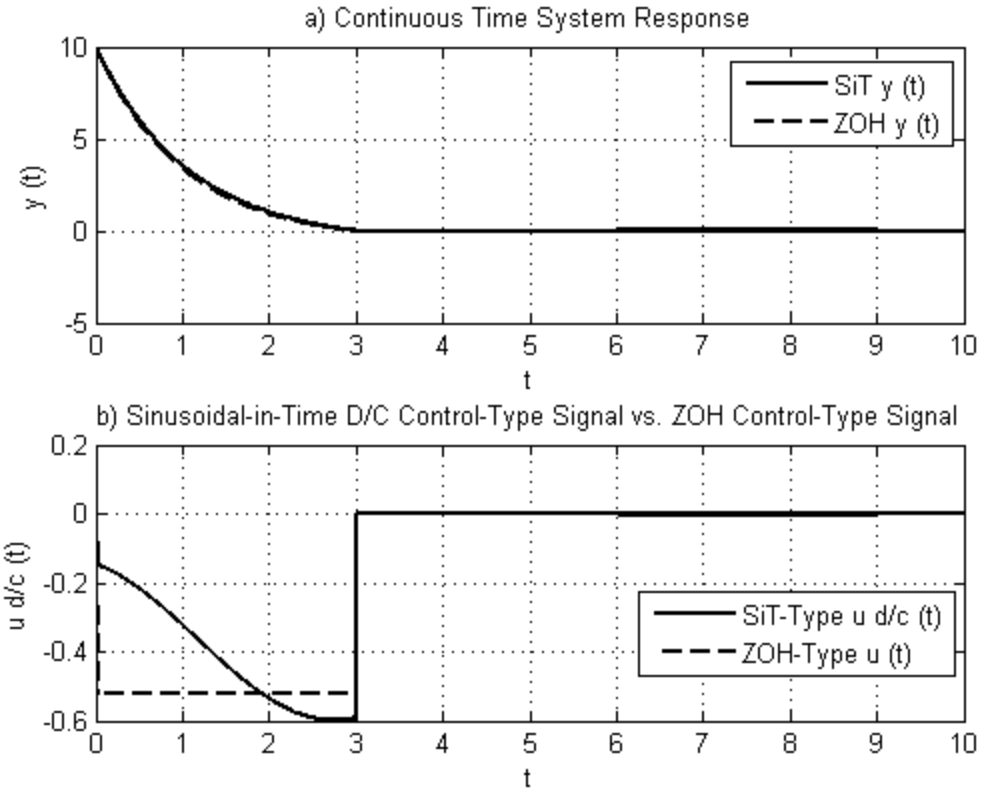

Figure 4.3 System Response and Control Signal for the First-Order Plant Model with SiT-Type D/C Control

4.3.1.5 First-Order System Stabilization with PsiT-Type D/C Control

For the "ultimate deadbeat" PsiT-type D/C control design for the first-order plant of Table 4.1, $\widetilde{K}_{d/c}$ is computed from the Moore-Penrose technique of (4.5) to be

$$\widetilde{K}_{d/c} = \begin{bmatrix} -0.0013 \\ -0.0014 \\ -0.0079 \end{bmatrix}, \tag{4.11}$$

where $\overline{BH}$ is calculated from (1.20) and is found in Appendix A. The simulation results are shown in Figure 4.4. The control task is achieved by $T = 3$ with one control decision.

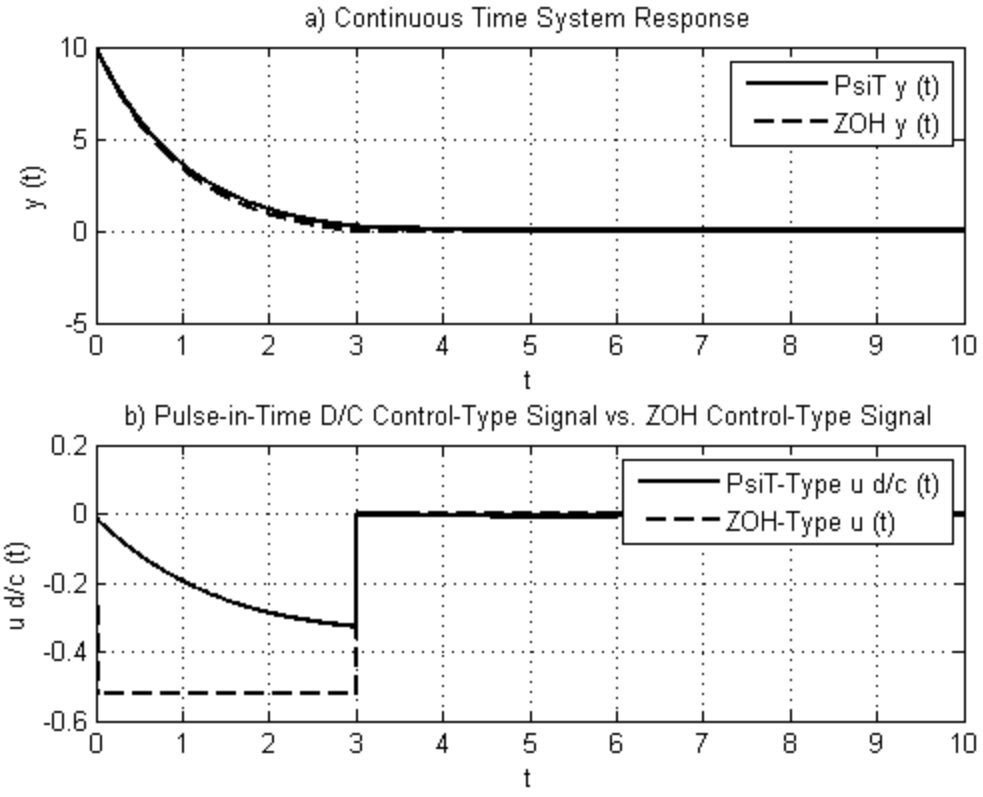

Figure 4.4 System Response and Control Signal for the First-Order Plant Model with PsiT-Type D/C Control

4.3.1.6 Second-Order System Stabilization with ZOH-Type Control

For performance comparisons with D/C control signals, ZOH is computed for the second-order plant model of Table 4.1. For this control-type and plant model combination, the "ultimate deadbeat" design of (4.6) is not possible. From (4.6), calculation for $\widetilde{K}_{ZOH}$ involves solving four linearly independent equations with only two variables available, the elements of 1×2 $\widetilde{K}_{ZOH}$. "Deadbeat" design is possible however. $\widetilde{K}_{ZOH}$ design by the Moore-Penrose method in (4.5) is calculated to be

$$\widetilde{K}_{ZOH} = \begin{bmatrix} -0.5153 & -0.1967 \end{bmatrix}, \tag{4.12}$$

which results in $\widetilde{A}_{CL}$ with $\lambda_1 = 0,$ and $\lambda_2 = -0.0331.$ This indicates that the system response will take at least two control decisions ($T = 2$) to perform the control task. The design of (4.12) is used in the simulation plots of Figure 4.5-Figure 4.11.

4.3.1.7 Second-Order System Stabilization with LiT-Type D/C Control

For the "ultimate deadbeat" LiT-Type D/C control for the second-order plant model of Table 4.1, $\widetilde{K}_{d/c}$ may be computed from either (4.1) or (4.5) to be

$$\widetilde{K}_{d/c} = \begin{bmatrix} -1.4547 & -0.5538 \\ 0.5553 & 0.2111 \end{bmatrix}. \tag{4.13}$$

The simulation results are shown in Figure 4.5.

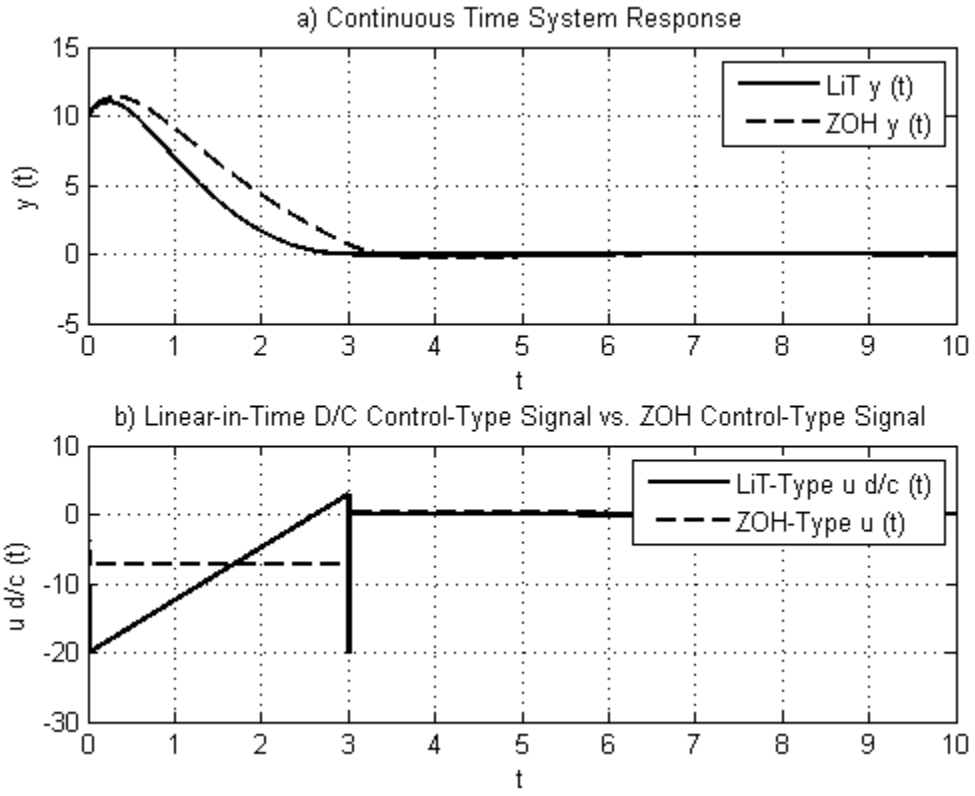

Figure 4.5 System Response and Control Signal for the Second-Order Plant Model with LiT-Type D/C Control

In this simulation, the system response with the ZOH-type control signal results in a higher system output response magnitude before stabilization. The control task of $y(t) \to 0$ is accomplished with one control decision for the D/C control, while two control decisions (two sample periods) are required for the ZOH-type control signal to accomplish this task. The D/C state plots for both the LiT-type D/C controlled system and the ZOH-controlled system are shown in Figure 4.6.

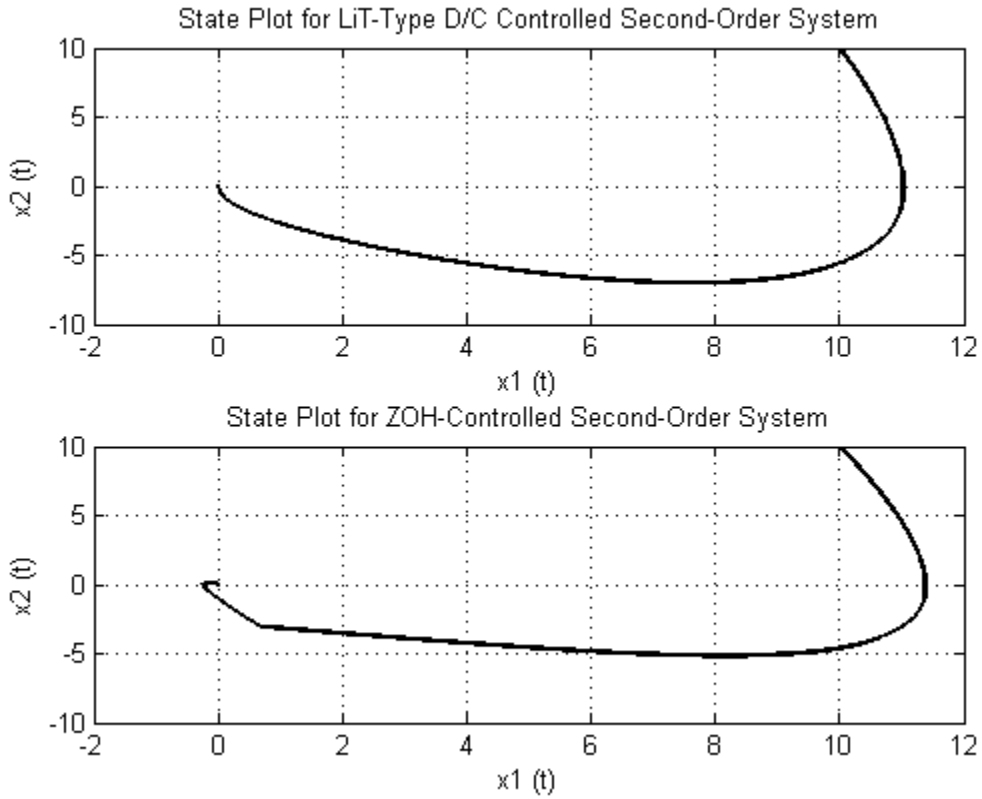

Figure 4.6 State Plot for the Second-Order System with LiT-Type D/C Control

4.3.1.8 Second-Order System Stabilization with EiT-Type D/C Control

For the "ultimate deadbeat" EiT-type D/C control for the second-order plant model of Table 4.1, $\widetilde{K}_{d/c}$ may be computed from either (4.1) or (4.5) to be

$$\widetilde{K}_{d/c} = \begin{bmatrix} -1.9064 & -0.7261 \\ 1.4169 & 0.5394 \end{bmatrix}. \tag{4.14}$$

The simulation results are shown in Figure 4.7. As in the case of LiT-type D/C control, the system response with the ZOH-type control signal results in a 0.5-unit higher system output response magnitude before stabilization than the D/C controlled system output. The control task of $y(t) \to 0$ is accomplished with one control decision for the D/C control, while two control decisions (two sample periods) are required for the ZOH-type control signal to accomplish this task. The D/C state plots for both the EiT-type D/C controlled system and the ZOH-controlled system are shown in Figure 4.8.

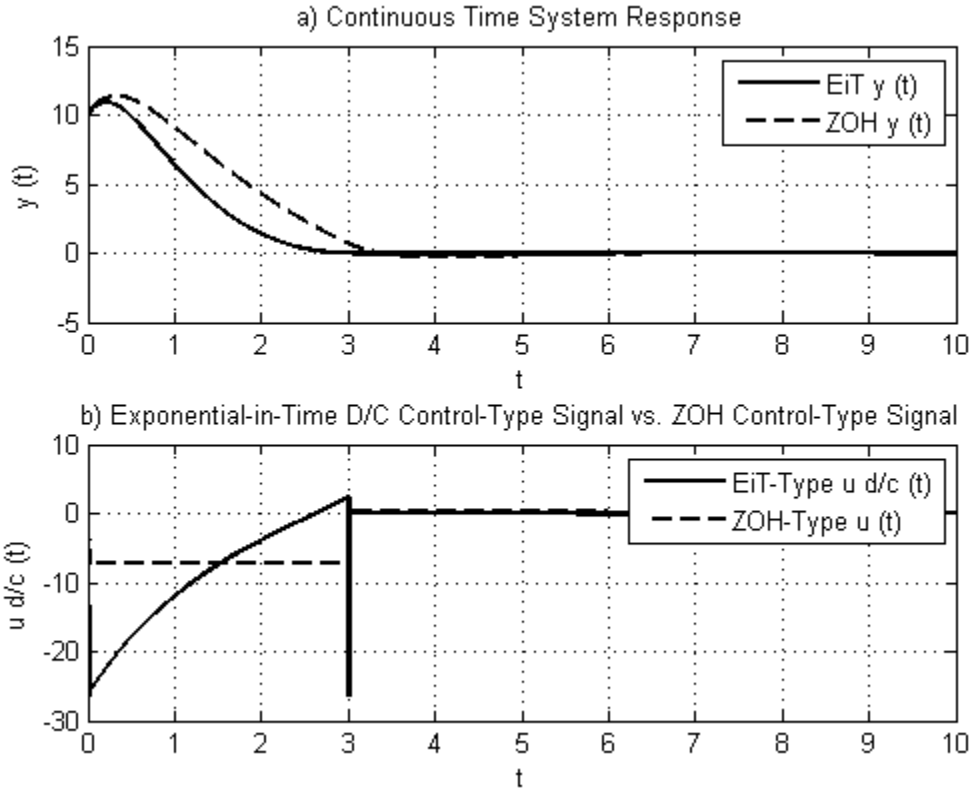

Figure 4.7 System Response and Control Signal for the Second-Order Plant Model with EiT-Type D/C Control

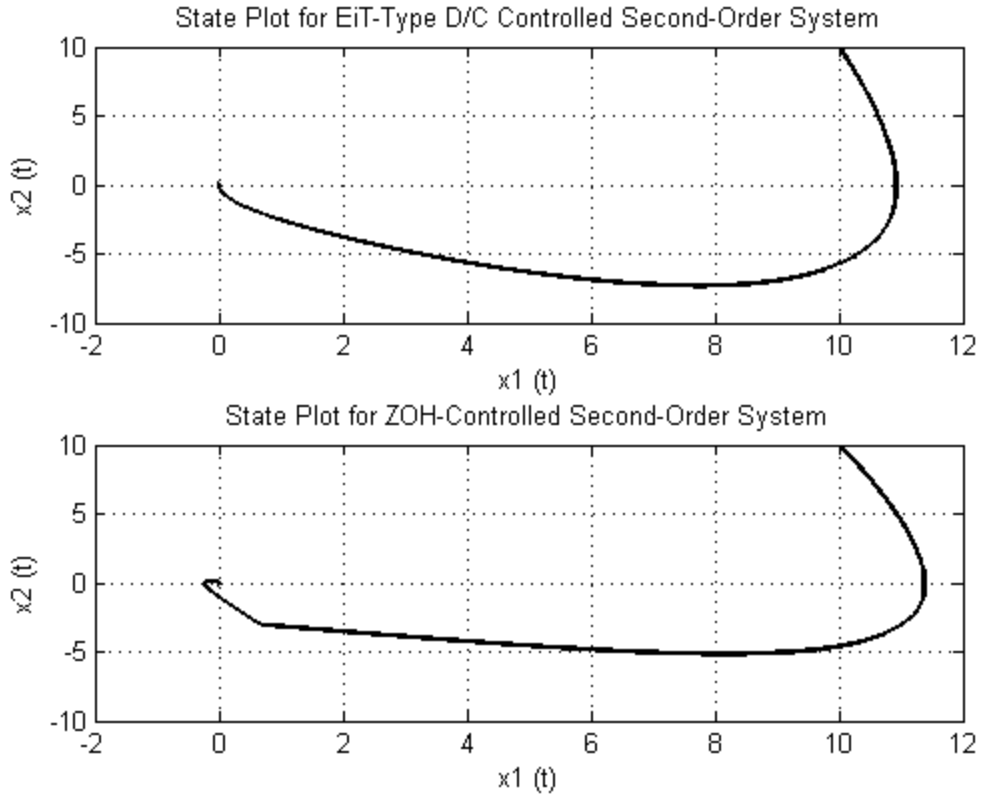

Figure 4.8 State Plot for Second-Order System with EiT-Type D/C Control

4.3.1.9 Second-Order System Stabilization with SiT-Type D/C Control

For the "ultimate deadbeat" SiT-type D/C control for the second-order plant model of Table 4.1, $\widetilde{K}_{d/c}$ may be computed from (4.5) to be

$$\widetilde{K}_{d/c} = \begin{bmatrix} -0.5452 & -0.2076 \\ -0.7338 & -0.2793 \\ 0.4828 & 0.1834 \end{bmatrix}, \tag{4.15}$$

resulting in $\widetilde{A}_{CL} = [0]$. The simulation results are shown in Figure 4.9. As in the previous cases, the system response with the ZOH-type control signal results in a higher system output response magnitude before stabilization than the D/C controlled system. The control task of $y(t) \to 0$ is accomplished with one control decision for the D/C

control, while two control decisions (two sample periods) are required for the ZOH-type control signal to accomplish this task. The D/C state plots for both the SiT-type D/C controlled system and the ZOH-controlled system are shown in Figure 4.10.

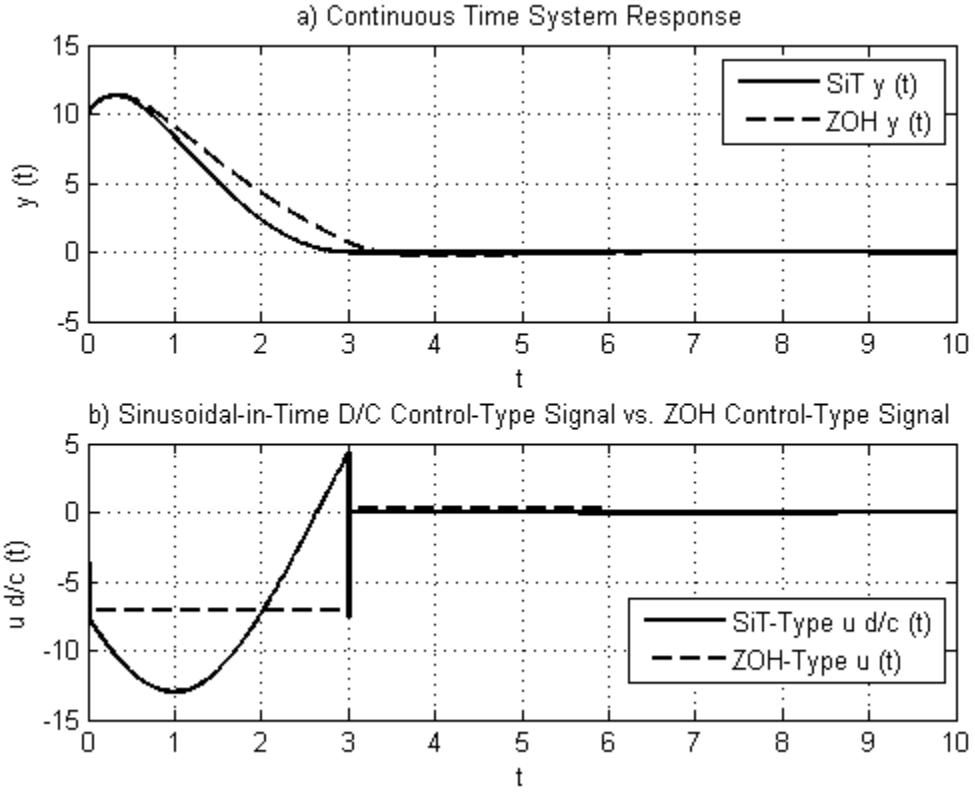

Figure 4.9 System Response and Control Signal for the Second-Order Plant Model with SiT-Type D/C Control

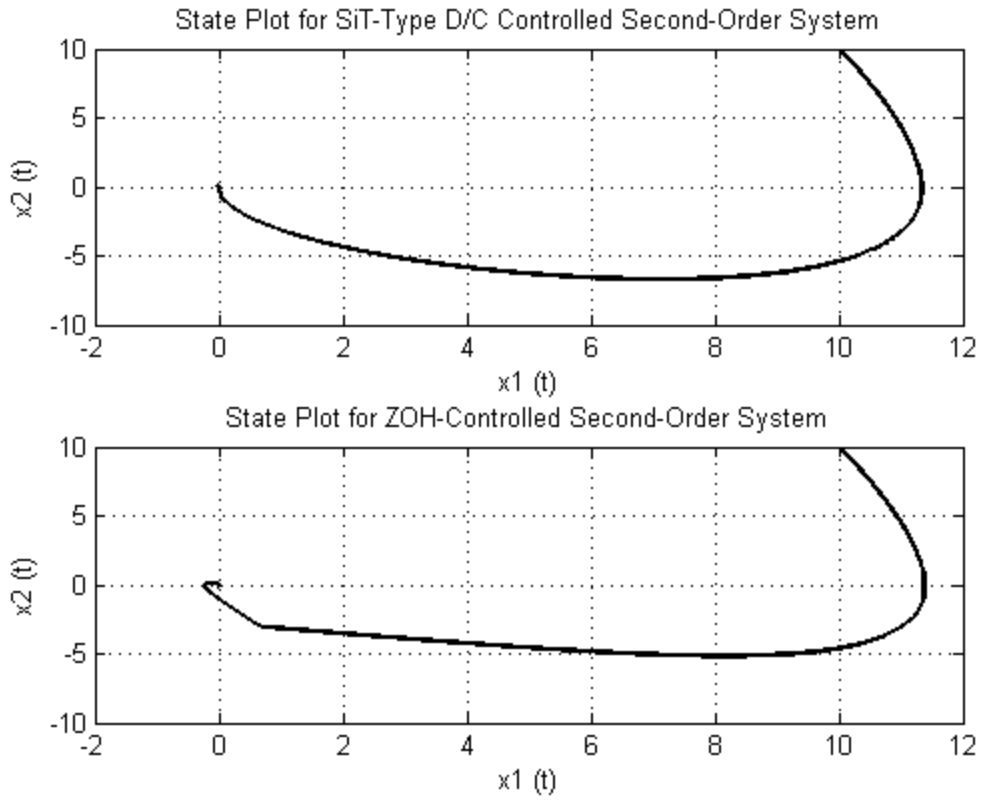

Figure 4.10 State Plot for Second-Order System with SiT-Type D/C Control

4.3.1.10 Second-Order System Stabilization with PsiT-Type D/C Control

For the "ultimate deadbeat" PsiT-type D/C control for the second-order plant model of Table 4.1, $\widetilde{K}_{d/c}$ may be computed from (4.1) to be

$$\widetilde{K}_{d/c} = \begin{bmatrix} -0.4161 & -0.1586 \\ -0.4590 & -0.1749 \\ 0.0945 & 0.0359 \end{bmatrix}, \tag{4.16}$$

resulting in $\widetilde{A}_{CL} = [0]$. The simulation results are shown in Figure 4.11. As in the previous cases, the system response with the ZOH-type control signal results in a higher system output response magnitude before stabilization than the D/C controlled system. The control task of $y(t) \to 0$ is accomplished with one control decision for the D/C

control, while two control decisions (two sample periods) are required for the ZOH-type control signal to accomplish this task. The D/C state plots for both the SiT-type D/C controlled system and the ZOH-controlled system are shown in Figure 4.12.

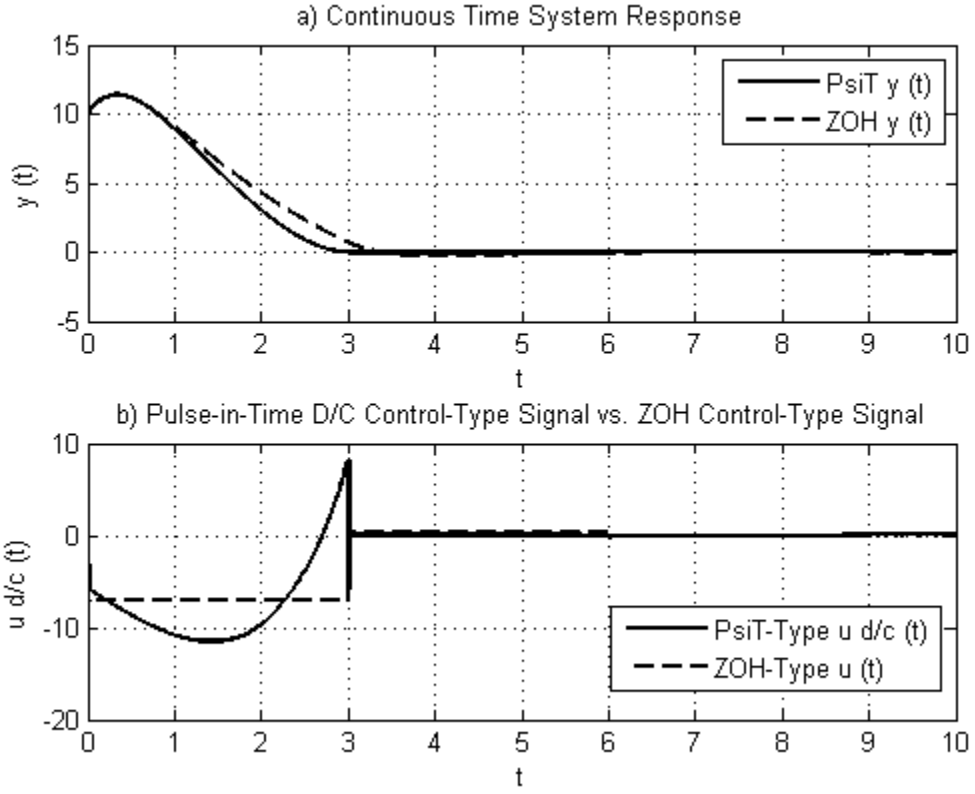

Figure 4.11 System Response and Control Signal for the Second-Order Plant Model with PsiT-Type D/C Control

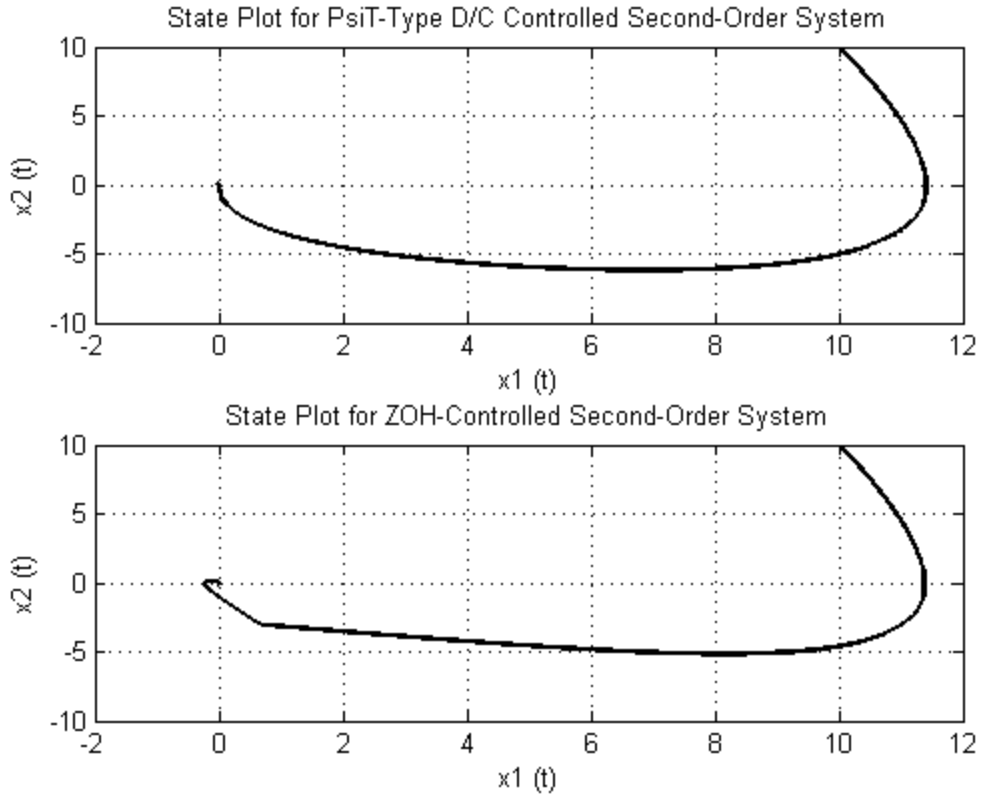

Figure 4.12 State Plot for the Second-Order System with PsiT-Type D/C Control

4.3.1.11 Third-Order System Stabilization with ZOH-Type Control

For performance comparisons with D/C control signals, ZOH is computed for the third-order plant model of Table 4.1. For this control-type and plant model combination, the "ultimate deadbeat" design of is not possible, since this method would involve solving nine linearly independent equations with only three available variables (the elements of $\widetilde{K}_{ZOH}$). "Deadbeat" design is possible, however, $\widetilde{K}_{ZOH}$ design by the Moore-Penrose method of (4.5) is not valid as this results in $\widetilde{A}_{CL}$ $|\lambda_i| > 1,$ which permits instability. The Moore Penrose method calculation results in

$$\widetilde{K}_{ZOH}^{*} = \begin{bmatrix} 0.8182 & 0.3416 & -0.4790 \end{bmatrix}, \tag{4.17}$$

where the $\widetilde{A}_{CL}$ λ_i from the design of (4.17) are $\lambda_i = \{0, -0.0321, -3.8140\}$.

The "deadbeat" design of $\widetilde{K}_{d/c}$ by the method in (4.1) and (4.4) results in

$$\widetilde{K}_{ZOH} = \begin{bmatrix} 0.9634 & 1.5889 & 0.6254 \end{bmatrix}. \tag{4.18}$$

The $\widetilde{A}_{CL}$ $\lambda_i = 0$ from the design of (4.18) and this design is used in the simulations of Figure 4.13-Figure 4.16.

4.3.1.12 Third-Order System Stabilization with LiT-Type D/C Control

$\widetilde{K}_{d/c}$ design for "ultimate deadbeat" response for the third-order plant model of Table 4.1 cannot be performed for LiT-type D/C control, since LiT-type $\widetilde{K}_{d/c}$ contains only six elements, and $\widetilde{A}_{CL} = \begin{bmatrix} 0 \end{bmatrix}$ involves solving nine linearly independent equations simultaneously. "Deadbeat" design of $\widetilde{K}_{d/c}$ is possible with the Moore-Penrose technique. The resulting $\widetilde{K}_{d/c}$ design is computed to be

$$\widetilde{K}_{d/c} = \begin{bmatrix} 0.7321 & -0.8288 & -1.5563 \\ 0.0842 & 1.1448 & 1.0538 \end{bmatrix}. \tag{4.19}$$

Simulation results for this design are shown in Figure 4.13. The control task is achieved with three control decisions ($T = 9$) as designed, for both LiT-type D/C Control and ZOH-type control. The magnitude of the control signal is significantly larger for ZOH. The system output response magnitude for the ZOH-controlled system is also significantly higher than that of the D/C controlled system, by a magnitude of 100. This large difference in the magnitude of the control signals as well as the system output response demonstrates the superiority of the D/C control-action over that of ZOH in this application.

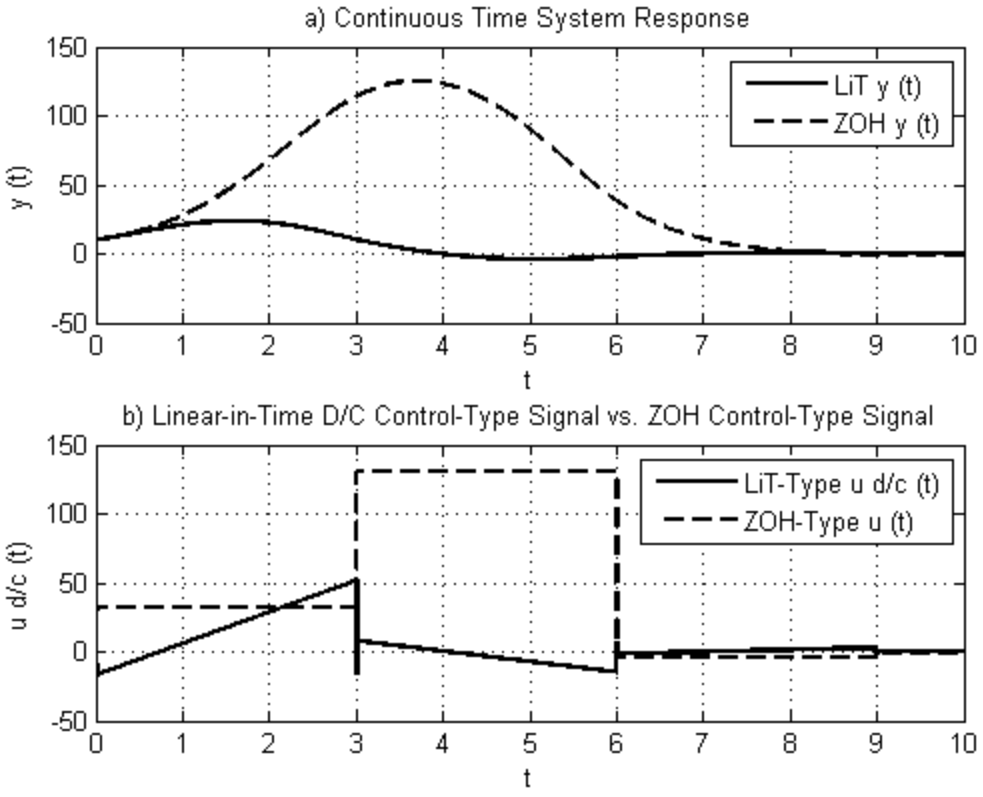

Figure 4.13 System Response and Control Signal for the Third-Order Plant Model with LiT-Type D/C Control

4.3.1.13 Third-Order System Stabilization with EiT-Type D/C Control

As with the previous case of LiT-type D/C control, $\widetilde{K}_{d/c}$ design for "ultimate deadbeat" response for the third-order plant model of Table 4.1 cannot be performed for EiT-type D/C control. This is due to the fact that EiT-type $\widetilde{K}_{d/c}$ contains only six elements, and $\widetilde{A}_{CL} = [0]$ involves solving nine linearly independent equations simultaneously. "Deadbeat" design of $\widetilde{K}_{d/c}$ is possible with the Moore-Penrose technique. The resulting $\widetilde{K}_{d/c}$ design is computed to be

$$\widetilde{K}_{d/c} = \begin{bmatrix} 0.9740 & -0.6976 & -1.6680 \\ -0.4577 & 1.0576 & 1.5090 \end{bmatrix}. \tag{4.20}$$

Simulation results for this design are shown in Figure 4.14. Similar to the previous case of LiT-type D/C control, the control task is achieved with three control decisions ($T = 9$) as designed, for both EiT-type D/C Control and ZOH-type control. The magnitude of the control signal is, again, significantly larger for ZOH. The system output response magnitude for the ZOH-controlled system is also significantly higher than that of the D/C controlled system, by a magnitude of 100. This large difference in the magnitude of the control signals as well as the system output response demonstrates the superiority of the D/C control-action over that of ZOH in this application.

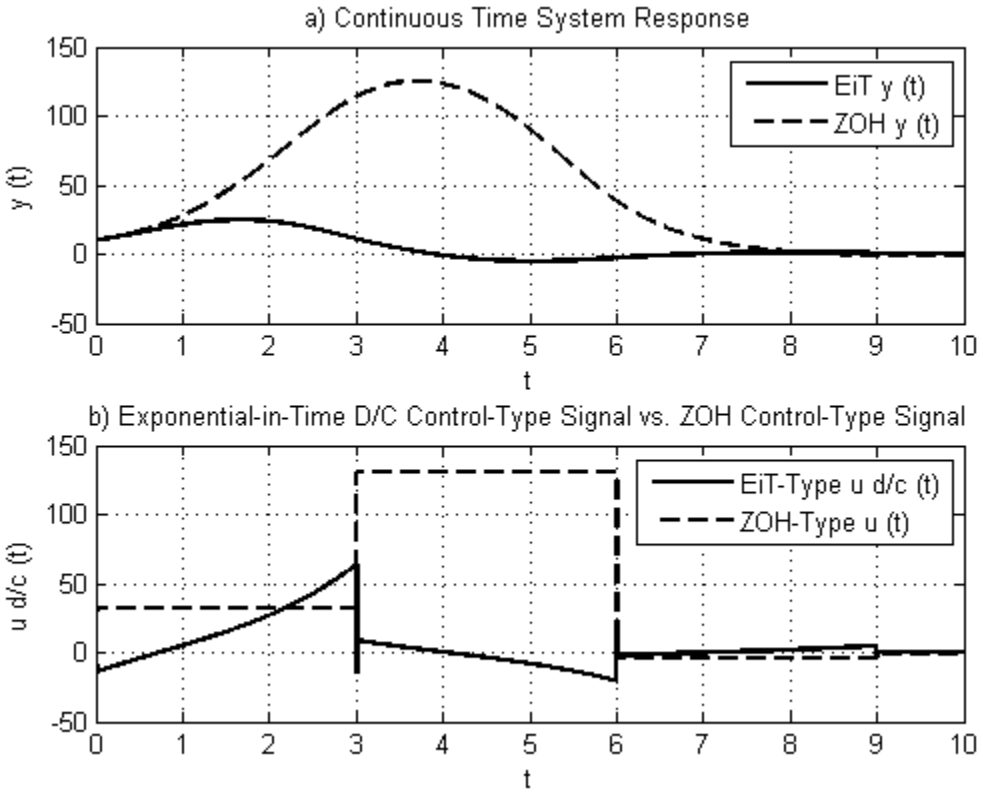

Figure 4.14 System Response and Control Signal for the Third-Order Plant Model with EiT-Type D/C Control

4.3.1.14 Third-Order System Stabilization with SiT-Type D/C Control

For the "ultimate deadbeat" SiT-type D/C control for the third-order plant model of Table 4.1, $\widetilde{K}_{d/c}$ may be computed from (4.1) to be

$$\widetilde{K}_{d/c} = \begin{bmatrix} -1.0343 & -3.4947 & -2.7292 \\ 3.4483 & 5.7801 & 2.8544 \\ -0.7881 & -0.0303 & 0.6132 \end{bmatrix}. \tag{4.21}$$

This results in $\widetilde{A}_{CL} = [0]$. The simulation results are shown in Figure 4.15. The SiT-type D/C control achieves the control task with only one control decision ($T = 3$), while the ZOH-control requires three control decisions ($T = 9$) to achieve the same control task. As in the previous cases, the control signal magnitude and system output response magnitude is significantly greater for the ZOH-type control than for the D/C control. In this case, the magnitude of $y(t)$ is greater for the ZOH-type control by 109 units. Due to the faster control task achievement time and the reduced magnitude of the control signal and system output, D/C shows superiority over the ZOH-type control.

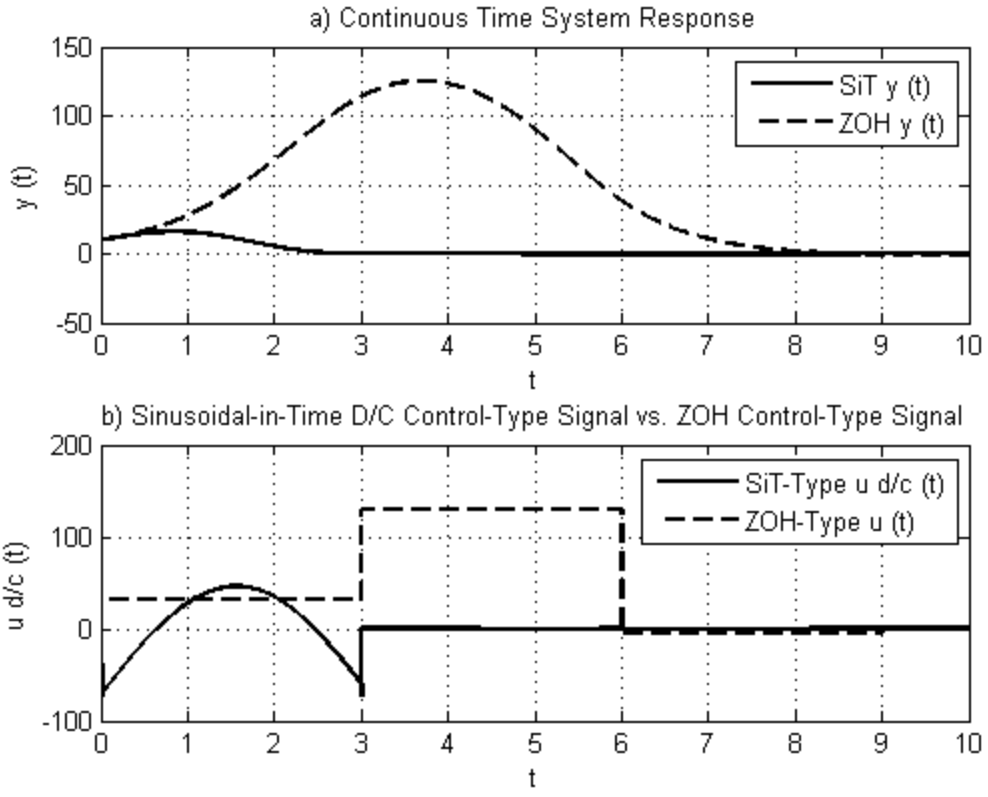

Figure 4.15 System Response and Control Signal for the Third-Order Plant Model with SiT-Type D/C Control

4.3.1.15 Third-Order System Stabilization with PsiT-Type D/C Control

For the "ultimate deadbeat" PsiT-type D/C control for the third-order plant model of Table 4.1, $\widetilde{K}_{d/c}$ may be computed from (4.1) to be

$$\widetilde{K}_{d/c} = \begin{bmatrix} -0.5368 & -2.8700 & -2.5226 \\ 2.0756 & 4.2647 & 2.4882 \\ -0.2789 & -0.2663 & -0.0336 \end{bmatrix}, \tag{4.22}$$

resulting in $\widetilde{A}_{CL} = [0]$. The simulation results are shown in Figure 4.16. Similar to the SiT-type D/C of the previous case, the PsiT-type D/C control achieves the control task with only one control decision ($T = 3$), while the ZOH-control requires three control decisions ($T = 9$) to achieve the same control task. As in the previous cases, the control

signal magnitude and system output response magnitude is significantly greater for the ZOH-type control than for the D/C control. In this case, the magnitude of $y(t)$ is greater for the ZOH-type control by 110 units. Due to the faster control task achievement time and the reduced magnitude of the control signal and system output, D/C shows superiority over the ZOH-type control.

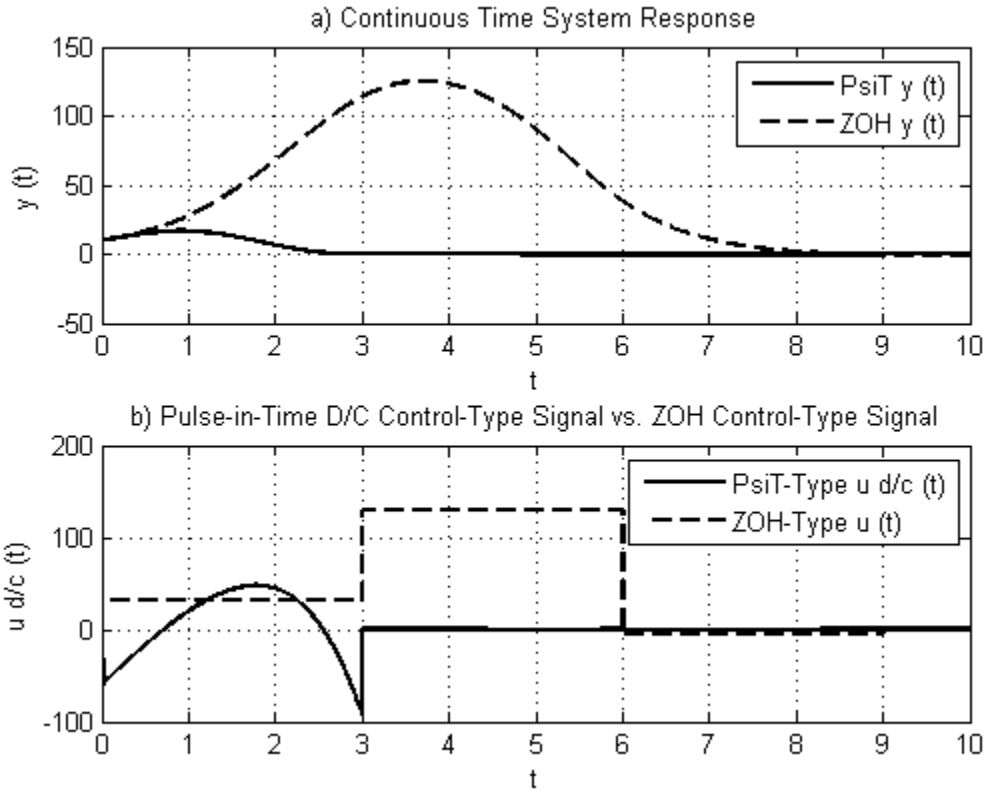

Figure 4.16 System Response and Control Signal for the Third-Order Plant Model with PsiT-Type D/C Control

4.3.2 Example 2: Set-Point Regulation

The set-point regulation control task consists of driving the output $y(t)$ of the plant models shown above in Table 4.1 to a stepwise constant $y_{sp}(t)$ in finite-time. For comparison with the D/C-type control signal performance, the ZOH-control is computed

and simulated. In all cases, set-point $y_{sp}(t) = 5$ for $0 \le T < 8$ and $y_{sp}(t) = 4$ for $8 \le T < 15$. Control decision period $T = 3$, SiT-type D/C control value $\omega = 1.0$, and EiT and PsiT-type D/C control value $\alpha = 0.5$.

4.3.2.1 Set-Point Regulation for a Representative First-Order Plant Model

In this example, $y_{sp}(t)$ represents a step-wise constant-value. The control task is to make $y(t) \to y_{sp}(t)$ for the first-order plant model

$$\dot{y}(t) + ay(t) = u(t) + w(t), \tag{4.23}$$

with user-designed control $u(t)$ and disturbance $w(t)$. System set-point error is defined as

$$e(t) = y_{sp}(t) - y(t). \tag{4.24}$$

The first derivative of the error in (4.24) is

$$\dot{e}(t) = -\dot{y}(t) = ay(t) - u(t) - w(t). \tag{4.25}$$

Control $u(t)$ is designed in the composite form

$$u(t) = u_p(t) + u_{sp}(t) + u_d(t) \tag{4.26}$$

where $u_p(t)$ is designed such that the closed-loop system λ_i are in the desired locations, $u_{sp}(t)$ is designed to make $y(t) \to y_{sp}(t)$, and $u_d(t)$ is designed to accommodate disturbances. Here, we assume that $u_d(t)$ is able to completely accommodate $w(t)$, leaving $u_p(t)$ and $u_{sp}(t)$ to be designed. Control $u_{sp}(t)$ is designed such that

$$u_{sp}(t) = ay_{sp}(t). \tag{4.27}$$

From (4.25) and (4.27), the first derivative of the error with $u_d(t)$ and $u_{sp}(t)$ implemented is

$$\dot{e}(t) = -\dot{y}(t) = -ae(t) - u_p(t). \tag{4.28}$$

Control $u_p(t)$ is then designed with the D/C algorithm

$$u_p(t) = \overline{H}e^{\overline{D}(t-kT)}\widetilde{K}_{d/c}\left(-e(kT)\right). \tag{4.29}$$

Control matrix $\widetilde{K}_{d/c}$ is computed with the Moore-Penrose column rank minimization technique in equations (4.7)-(4.11). The simulation of this algorithm is shown as compared to ZOH-type control for LiT-type D/C control in Figure 4.17, EiT-type D/C control in Figure 4.18, SiT-type D/C control in Figure 4.19, and PsiT-type D/C control in Figure 4.20. In each example, achievement of the set-point value is accomplished with one control decision ($T = 3$). The performance of the D/C-type control signals is equivalent to that of ZOH for the first-order plant model.

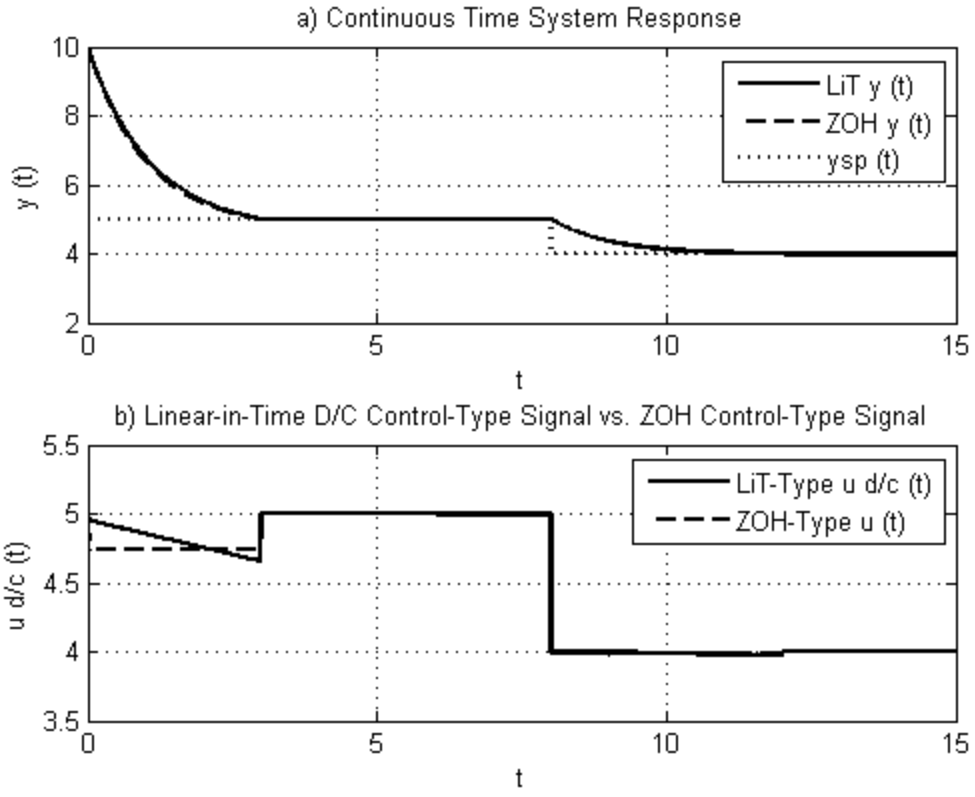

Figure 4.17 Set-Point Regulation for the First-Order System with LiT-Type D/C Control

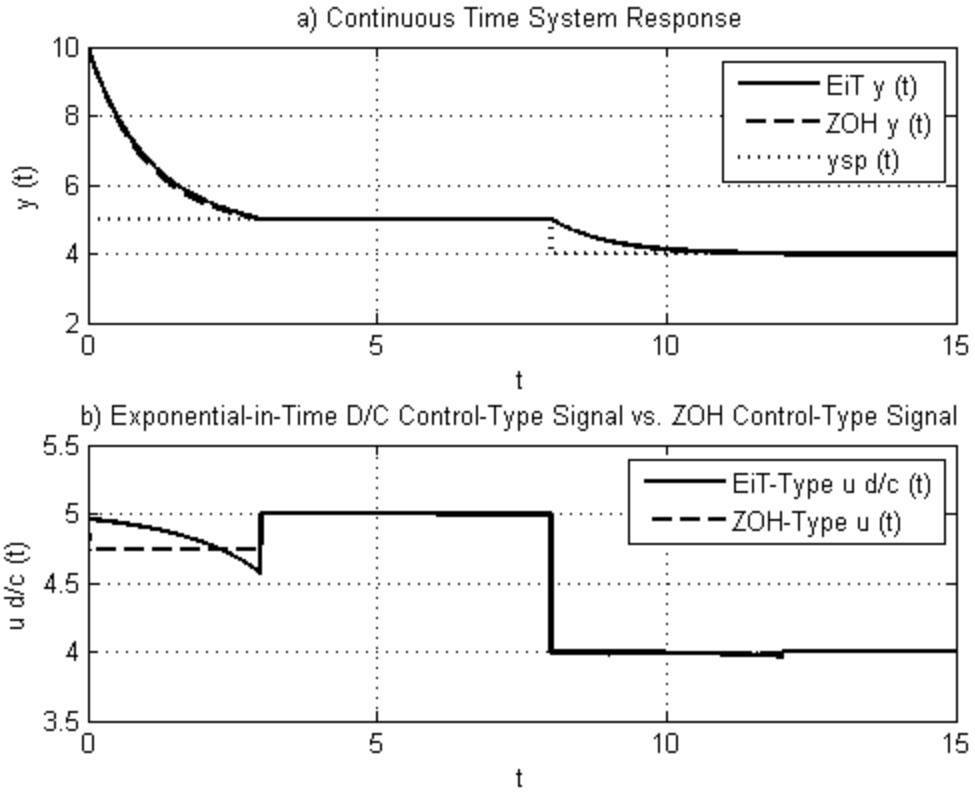

Figure 4.18 Set-Point Regulation for the First-Order System with EiT-Type D/C Control

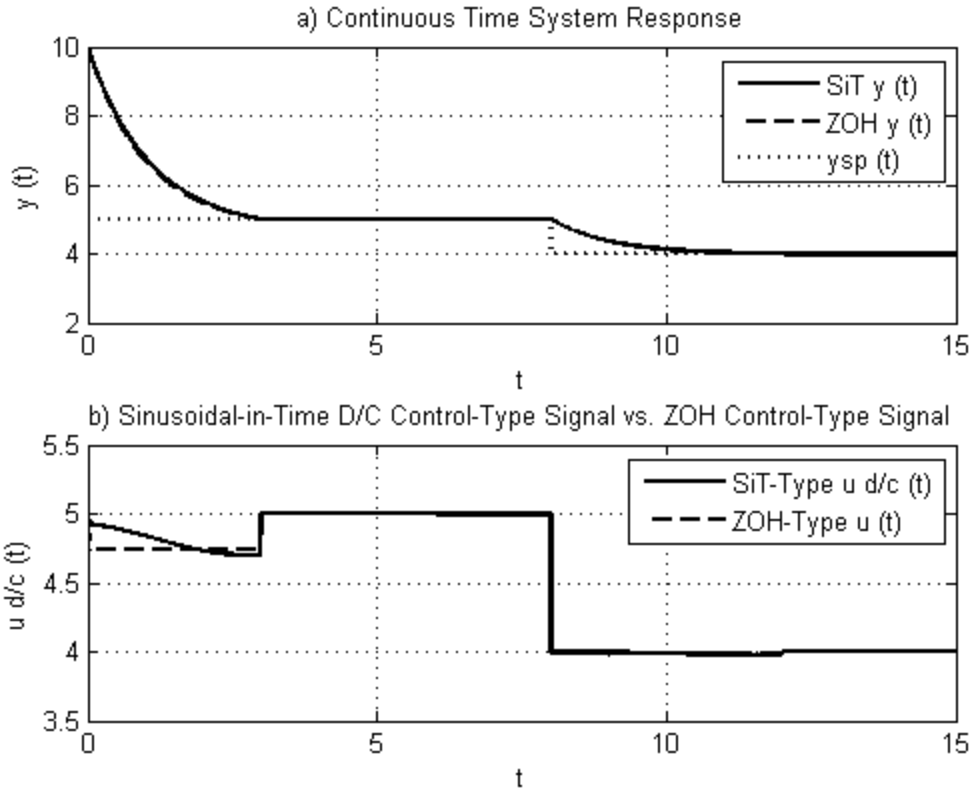

Figure 4.19 Set-Point Regulation for the First-Order System with SiT-Type D/C Control

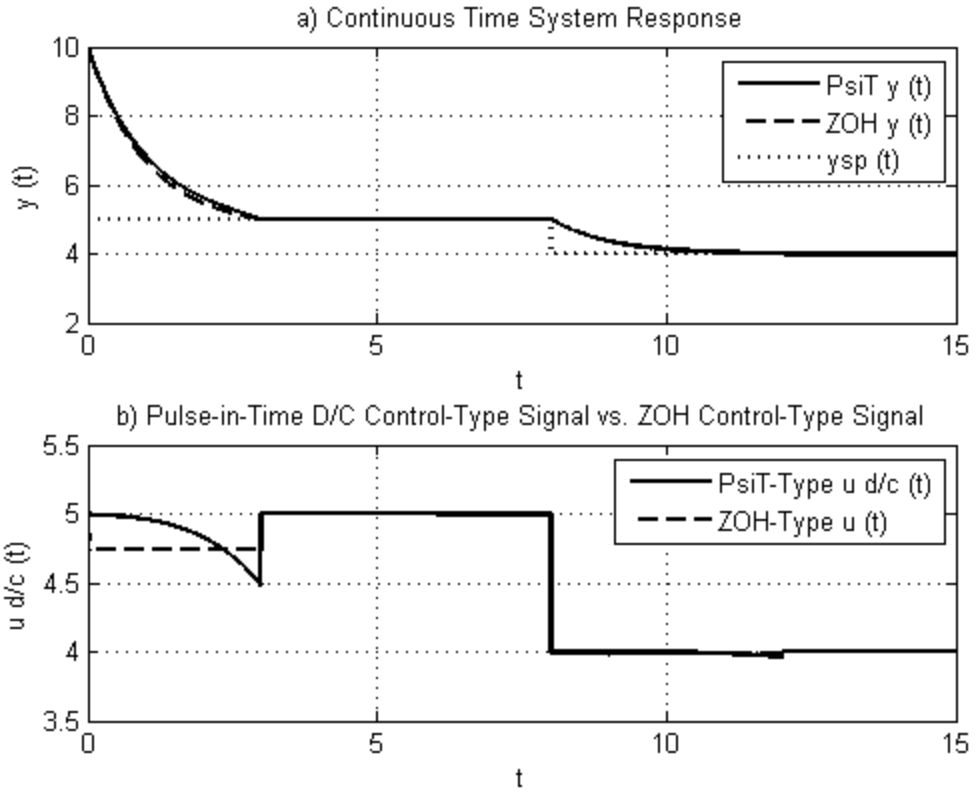

Figure 4.20 Set-Point Regulation for the First-Order System with PsiT-Type D/C Control

4.3.2.2 Set-Point Regulation for a Representative Second-Order Plant Model

For this example, the control task is to make $y(t) \to y_{sp}(t)$ for the second-order plant model

$$\ddot{y}(t) + a_2\dot{y}(t) + a_1 y(t) = u(t) + w(t). \tag{4.30}$$

System set-point error $e(t)$ is defined as in (4.24) and the first and second derivatives of $e(t)$ for the plant model of (4.30) are respectively

$$\dot{e}(t) = -\dot{y}(t), \tag{4.31}$$

$$\ddot{e}(t) = -\ddot{y}(t) = a_2\dot{y}(t) + a_1 y(t) - u(t) - w(t). \tag{4.32}$$

Control $u(t)$ is of the composite form defined in (4.26). It is assumed that $u_d(t)$ is able to completely accommodate $w(t)$. Control $u_{sp}(t)$ is designed for the system model of (4.30) as

$$u_{sp}(t) = a_1 y_{sp}(t). \tag{4.33}$$

From (4.32) and (4.33),

$$\ddot{e}(t) = -a_1 e(t) - a_2 \dot{e}(t) - u_p(t). \tag{4.34}$$

Control $u_p(t)$ is then designed according to the D/C algorithm such that

$$u_p(t) = \overline{H} e^{\overline{D}(t-kT)} \widetilde{K}_{d/c} \begin{bmatrix} -e(kT) \\ -\dot{e}(kT) \end{bmatrix}. \tag{4.35}$$

Control matrices $\widetilde{K}_{ZOH}$ for ZOH and $\widetilde{K}_{d/c}$ for the D/C controls are computed with the Moore-Penrose column rank minimization technique in equations (4.12)-(4.16). The simulation of this algorithm is shown as compared to ZOH-type control for LiT-type D/C control in Figure 4.21, EiT-type D/C control in Figure 4.22, SiT-type D/C control in Figure 4.23, and PsiT-type D/C control in Figure 4.24. In each example, achievement of the set-point value is accomplished with one control decision ($T = 3$) for the D/C control signals whereas the ZOH-type control signals require two control decisions to accomplish this task. The magnitude of the system output $y(t)$ during the control task transient is comparable between ZOH and the D/C-type controls.

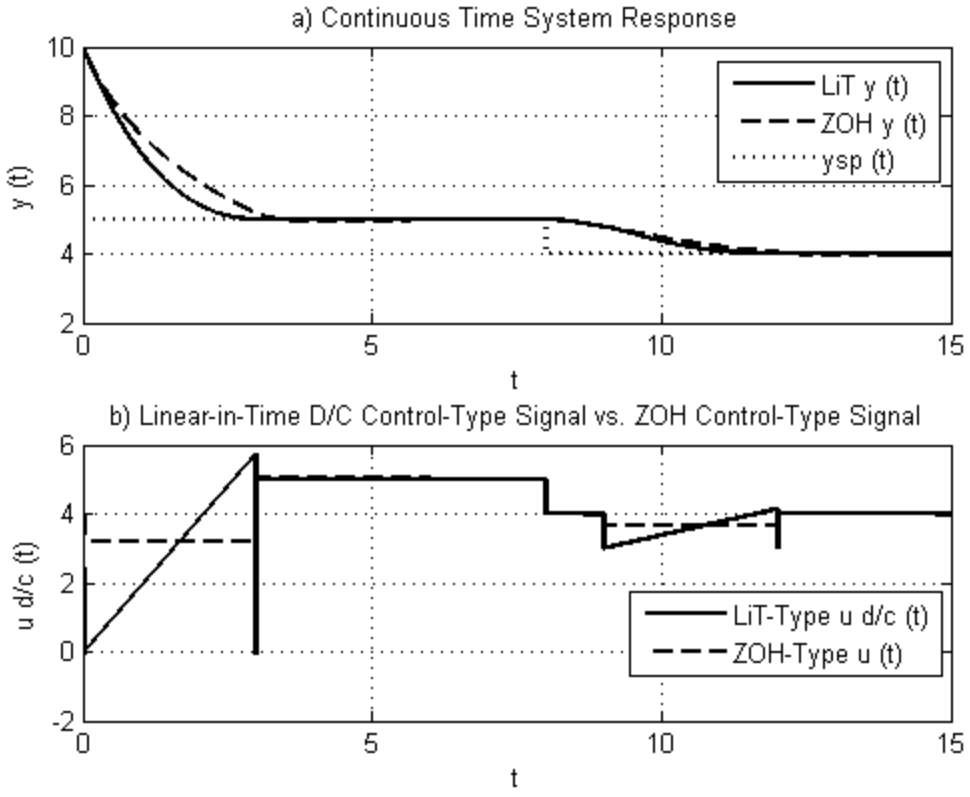

Figure 4.21 Set-Point Regulation for the Second-Order System with LiT-Type D/C Control

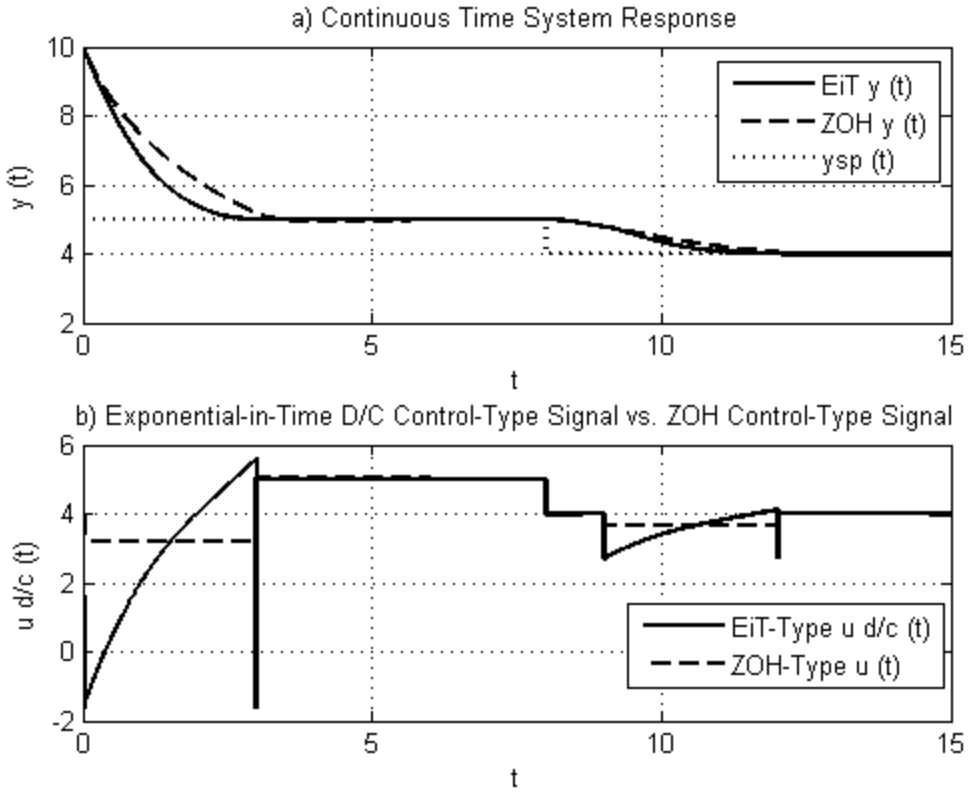

Figure 4.22 Set-Point Regulation for the Second-Order System with EiT-Type D/C Control

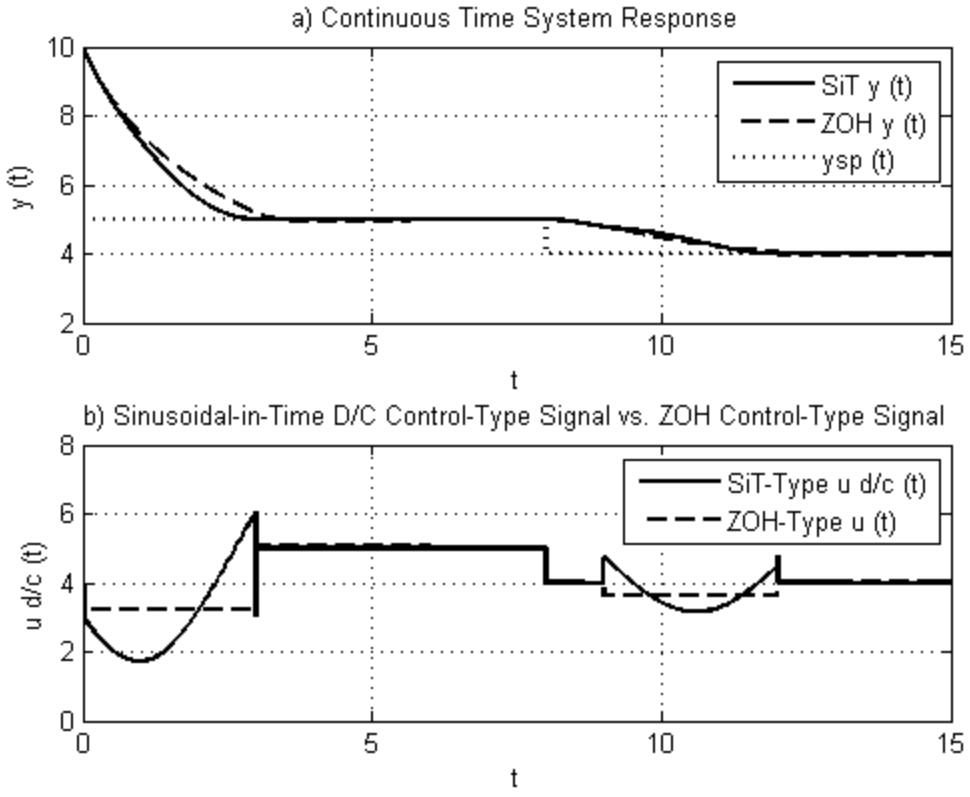

Figure 4.23 Set-Point Regulation for the Second-Order System with SiT-Type D/C Control

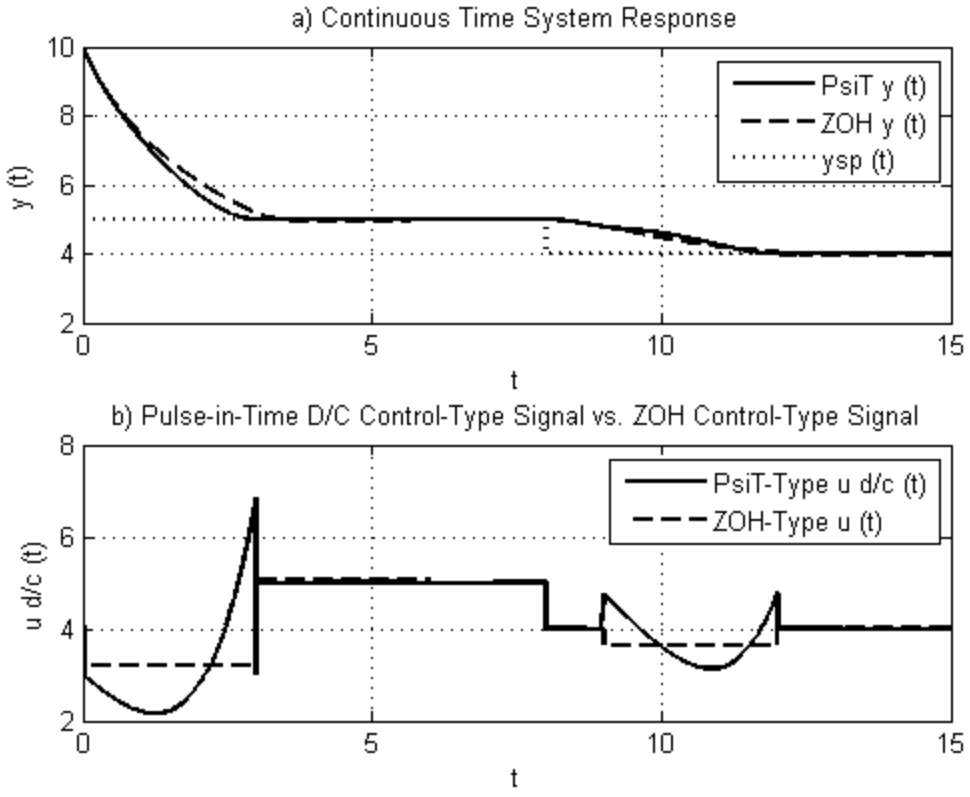

Figure 4.24 Set-Point Regulation for the Second-Order System with PsiT-Type D/C Control

4.3.2.3 Set-Point Regulation for a Representative Third-Order Plant Model

In this example, the control task is to make $y(t) \to y_{sp}(t)$ for the third-order plant model

$$\dddot{y}(t) + a\ddot{y}(t) = u(t) + w(t). \tag{4.36}$$

System set-point error $e(t)$ is defined in (4.24). The first, second, and third derivatives of the error for the system model of (4.36) are respectively

$$\dot{e}(t) = -\dot{y}(t), \tag{4.37}$$

$$\ddot{e}(t) = -\ddot{y}(t), \tag{4.38}$$

$$\dddot{e}(t) = -\dddot{y}(t) = a\ddot{y}(t) - u(t) - w(t). \tag{4.39}$$

Control $u(t)$ defined in the composite form of (4.26), and it is assumed that $u_d(t)$ is able to completely accommodate $w(t)$. Control $u_{sp}(t)$ is designed for the system model of (4.36) to be

$$u_{sp}(t) = ay_{sp}(t). \tag{4.40}$$

From (4.39) and (4.40),

$$\ddot{e}(t) = -ae(t) - u_p(t). \tag{4.41}$$

Control $u_p(t)$ is then designed with the D/C algorithm such that

$$u_p(t) = \overline{He}^{\overline{D}(t-kT)}\widetilde{K}_{d/c}\begin{bmatrix} -e(kT) \\ -\dot{e}(kT) \\ -\ddot{e}(kT) \end{bmatrix}. \tag{4.42}$$

Control matrix $\widetilde{K}_{d/c}$ is computed for the D/C control signals with the Moore-Penrose column rank minimization technique, as in equations (4.19)-(4.22). For the ZOH-control signal, $\widetilde{K}_{ZOH}$ was computed using "deadbeat" design as in (4.18), since the Moore-Penrose technique results do not yield closed-loop system λ_i within the unit circle for the third-order plant model for ZOH (resulting in an unstable closed-loop system) in this particular case. These designs of $\widetilde{K}_{d/c}$ and of $\widetilde{K}_{ZOH}$ are the "best case" of each control-type.

The simulated system responses and D/C control signals are shown as compared to ZOH-controlled system responses and control signals for LiT-type D/C control in Figure 4.25, EiT-type D/C control in Figure 4.26, SiT-type D/C control in Figure 4.27, and PsiT-type D/C control in Figure 4.28. In each example, achievement of the set-point value is accomplished with one control decision ($T = 3$) for the D/C control signals

whereas the ZOH-type control signals require three control decisions ($T = 9$) to accomplish this task. The magnitude of the control signal utilized is also significantly less for the D/C-type controllers than for ZOH-type controllers. The ZOH-controlled system output response $y(t)$ has a greater magnitude during the control task transient by 25 units than for that of the LiT-type and EiT-type D/C controlled systems, and a greater magnitude of 26 units than for that of the SiT-type and PsiT-type D/C controlled systems.

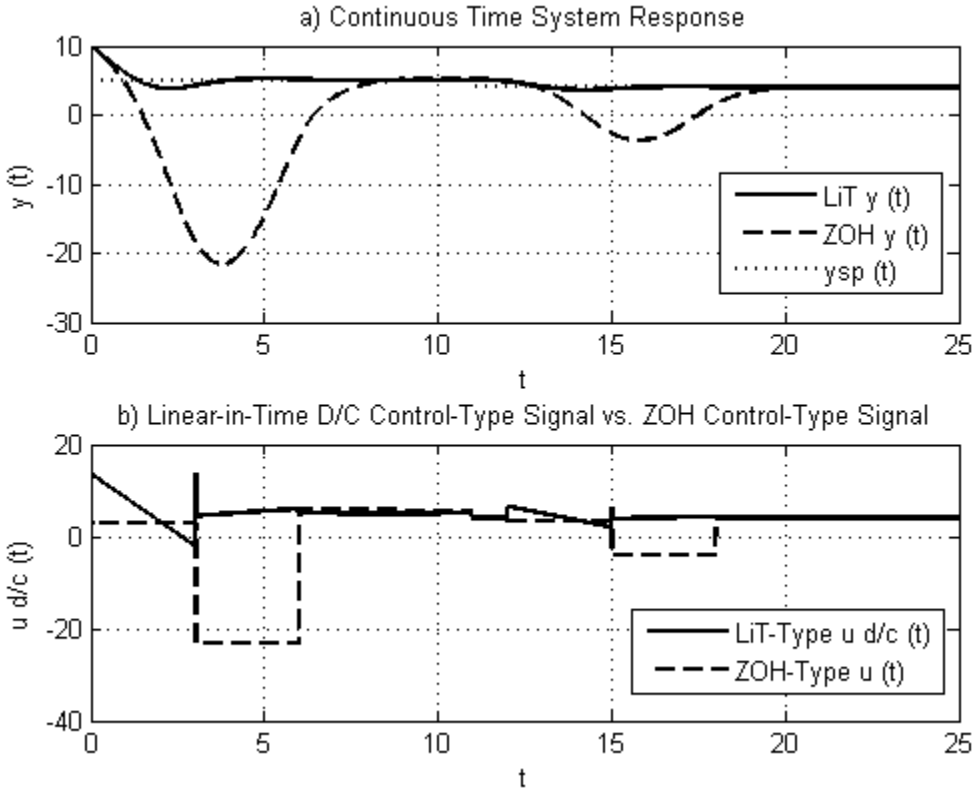

Figure 4.25 Set-Point Regulation for the Third-Order Plant Model with LiT-Type D/C Control

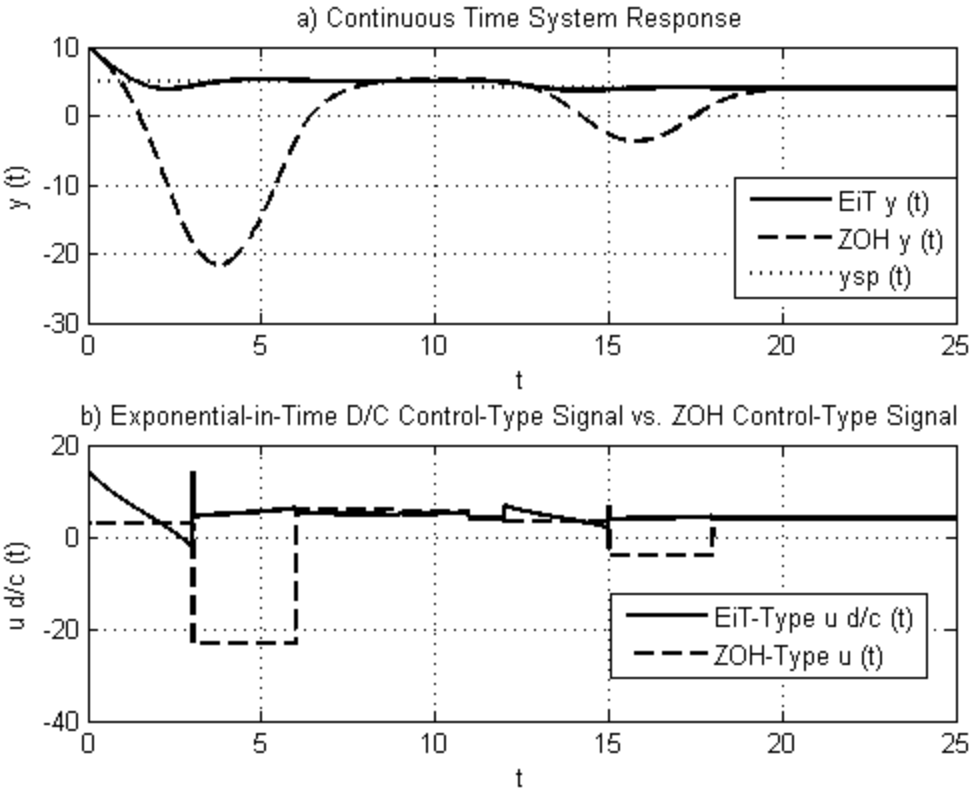

Figure 4.26 Set-Point Regulation for the Third-Order Plant Model with EiT-Type D/C Control

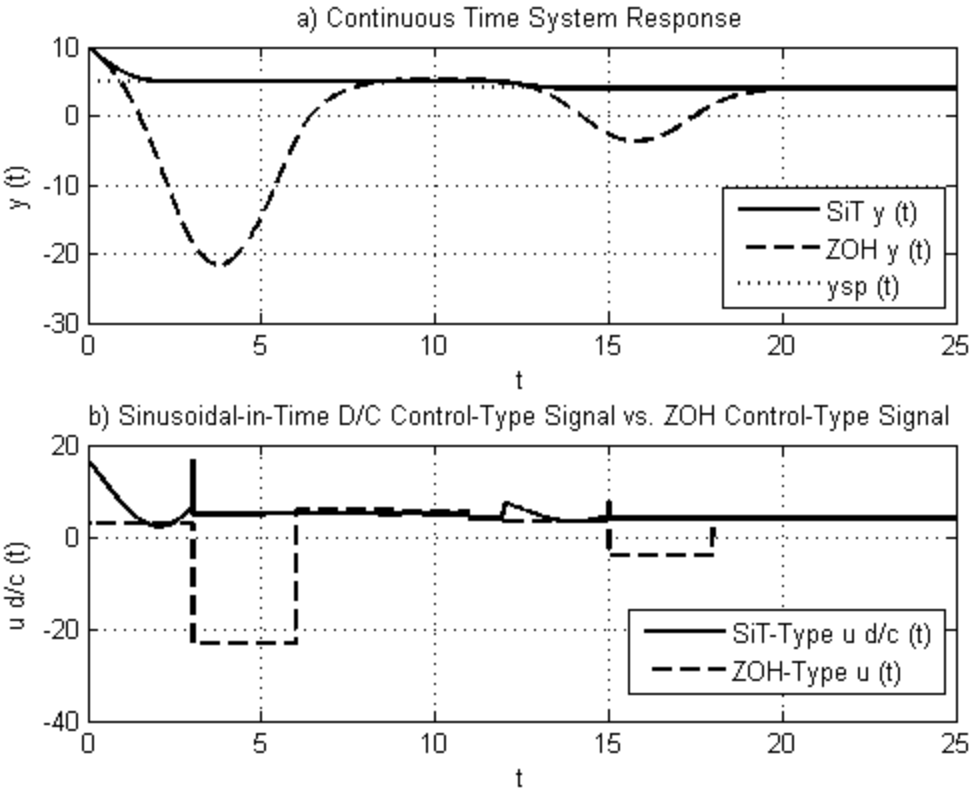

Figure 4.27 Set-Point Regulation for the Third-Order Plant Model with SiT-Type D/C Control

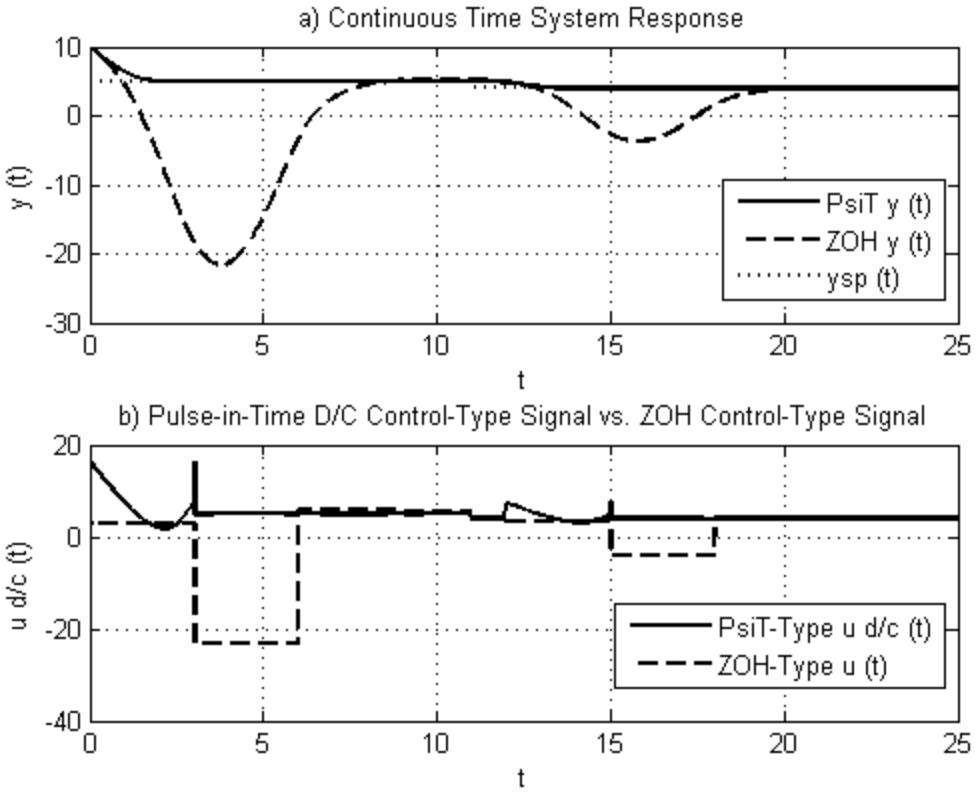

Figure 4.28 Set-Point Regulation for the Third-Order Plant Model with PsiT-Type D/C Control

4.3.3 Example 3: Command Signal-Tracking

The command signal-tracking control task is to drive the output $y(t)$ of the plant models shown in Table 4.1 to a time-varying command signal $y_c(t)$ in finite-time. For comparison with the D/C-type control algorithms, the ZOH-control is computed and simulated. A command signal with a constant and an integral component was used, so that $y_c(t) = 3 + t$ for $0 \le T < 11$ and $y_c(t) = 2 + 3t$ for $11 \le T < 25$. Control decision period $T = 3$, SiT-type D/C control value $\omega = 1.0$, and EiT and PsiT-type D/C control value $\alpha = 0.5$.

4.3.3.1 Command Signal-Tracking for a Representative First-Order Plant Model

In this example, $y_c(t)$ represents a command-signal of the assumed form

$$y_c(t) = c_{c1} + c_{c2}t. \tag{4.43}$$

The control task is to make $y(t) \to y_c(t)$ for the first-order plant model

$$\dot{y} + ay = u(t) + y_c(t) + w(t). \tag{4.44}$$

System signal-tracking error $e(t)$ is defined as

$$e(t) = y_c(t) - y(t), \tag{4.45}$$

and the first derivative for the plant model of (4.44) is

$$\dot{e}(t) = \dot{y}_c(t) - \dot{y}(t) = ay(t) - u(t) - y_c(t) - w(t). \tag{4.46}$$

Control $u(t)$ is designed in the composite form

$$u(t) = u_p(t) + u_c(t) + u_d(t), \tag{4.47}$$

where $u_p(t)$ is designed such that the closed-loop system poles are in the desired locations, $u_c(t)$ is designed to make $y(t) \to y_c(t)$, and $u_d(t)$ is designed to accommodate disturbances. Here, we assume that $u_d(t)$ is able to completely accommodate $w(t)$, leaving $u_p(t)$ and $u_c(t)$ to be designed. Control $u_c(t)$ is designed such that

$$\dot{e}(t) = \dot{y}_c(t) - \dot{y}(t) = ay(t) - u_p(t) - u_c(t) - y_c(t) + \dot{y}_c(t) \tag{4.48}$$

$$u_c(t) = -\dot{y}_c(t) + ay_c(t) \tag{4.49}$$

$$\dot{e}(t) = -ae(t) - u_p(t) \tag{4.50}$$

$$u_p(t) = \overline{H} e^{\overline{D}(t-kT)} \widetilde{K}_{d/c}(-e(t)). \tag{4.51}$$

Control matrices $\widetilde{K}_{ZOH}$ for ZOH and $\widetilde{K}_{d/c}$ for the D/C controls are computed with the Moore-Penrose column rank minimization technique in equations (4.7)-(4.11). The simulated system responses and D/C control signals are shown as compared to ZOH-controlled system responses and control signals for LiT-type D/C control in Figure 4.29, EiT-type D/C control in Figure 4.31, SiT-type D/C control in Figure 4.33, and PsiT-type D/C control in Figure 4.35. In each example, successful tracking of the command signal is accomplished with one control decision ($T = 3$) for both the D/C control signals and the ZOH-type control signals. The system output response $y(t)$ and the magnitude of the control signals are similar. The error, as in (4.45), is given for the LiT-type D/C control in Figure 4.30, the EiT-type D/C control in Figure 4.32, SiT-type D/C control in Figure 4.34, and PsiT-type D/C control in Figure 4.36.

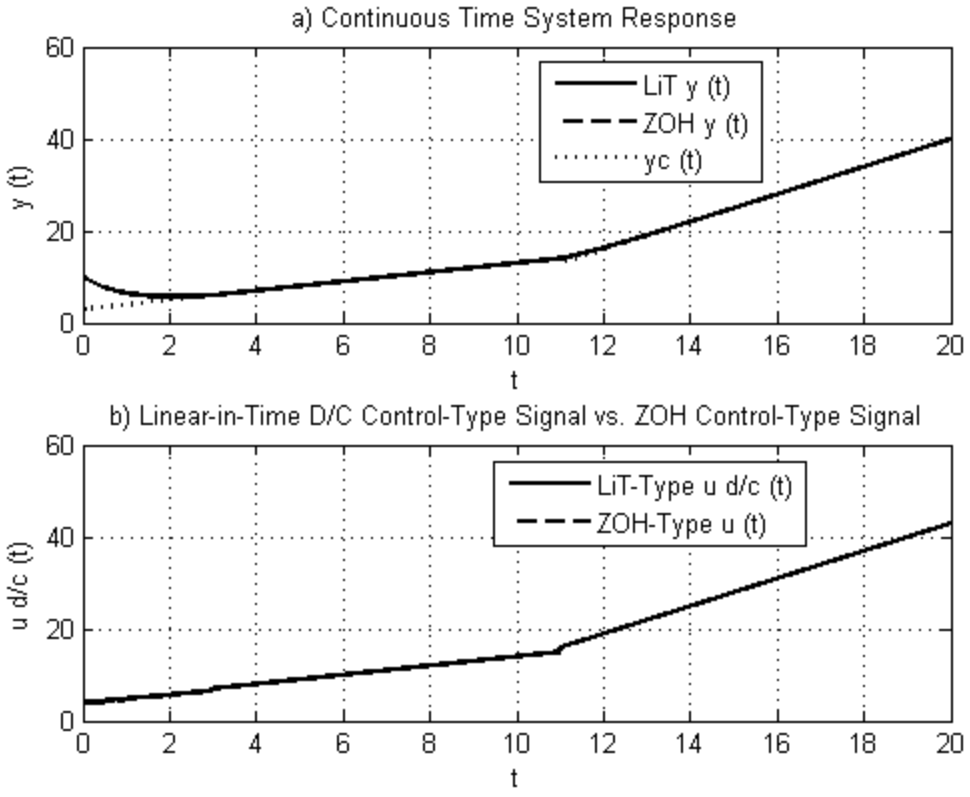

Figure 4.29 Command Signal-Tracking for the First-Order Plant Model with LiT-Type D/C Control

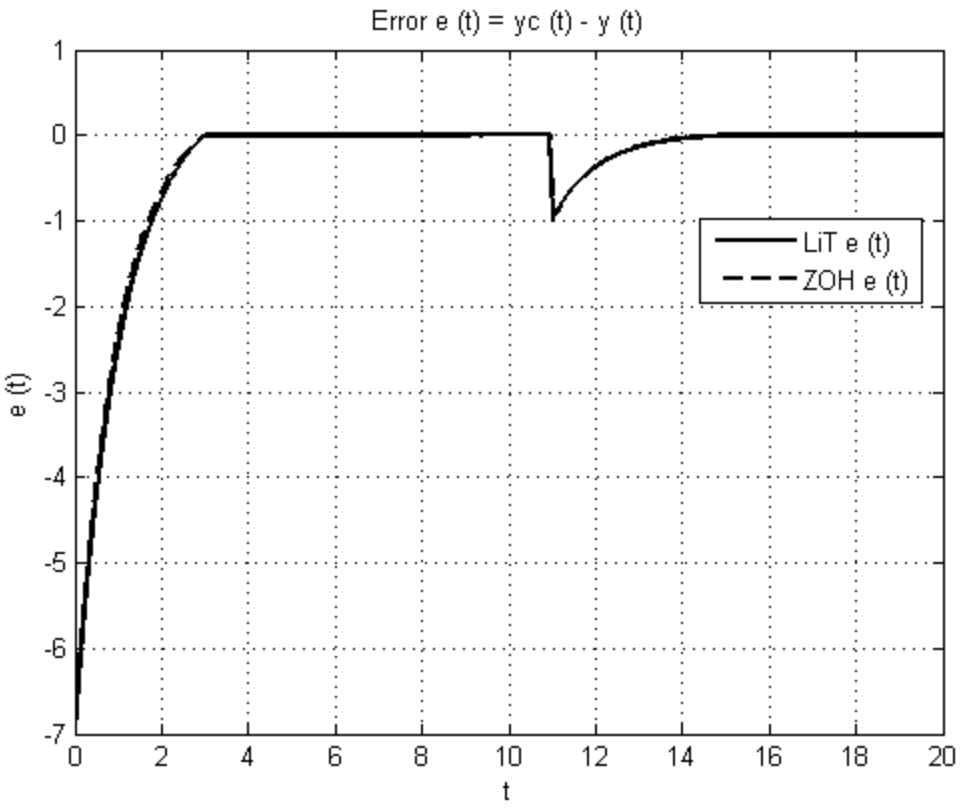

Figure 4.30 Command Signal Error for the First-Order Plant Model with LiT-Type D/C Control

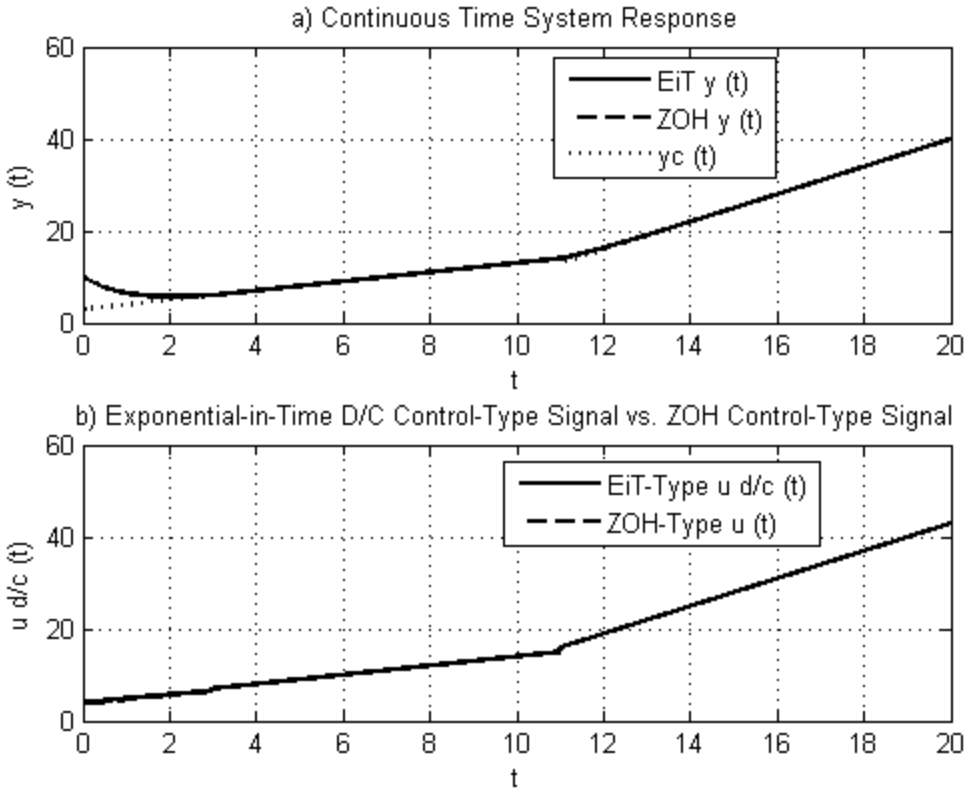

Figure 4.31 Command Signal-Tracking for the First-Order Plant Model with EiT-Type D/C Control

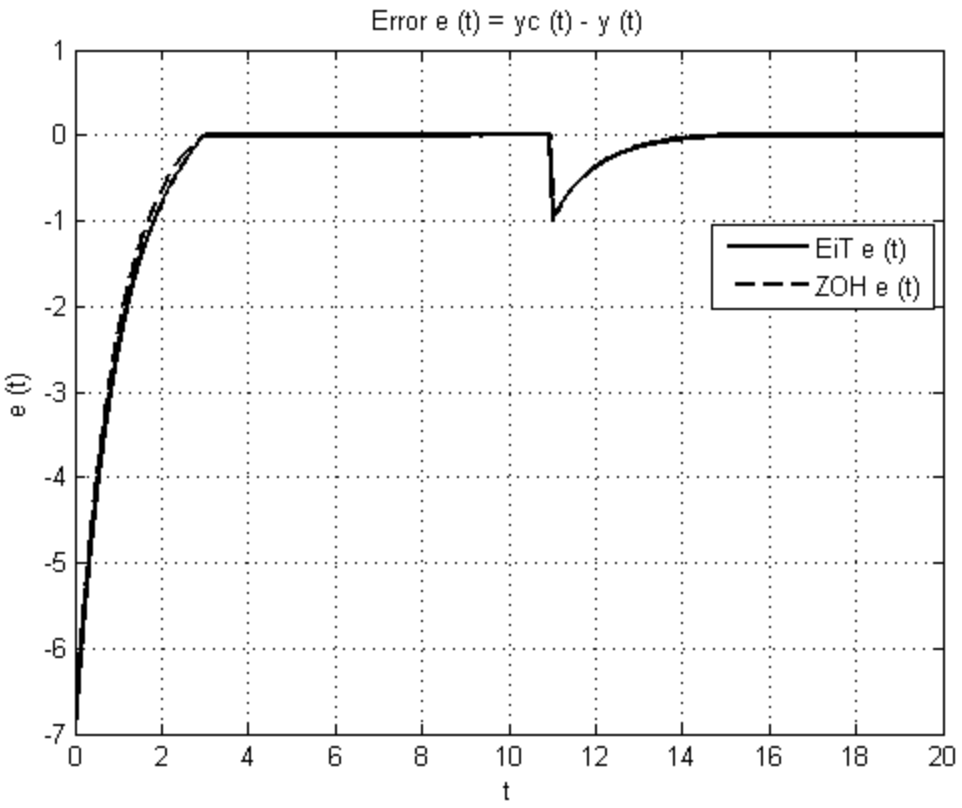

Figure 4.32 Command Signal Error for the First-Order Plant Model with EiT-Type D/C Control

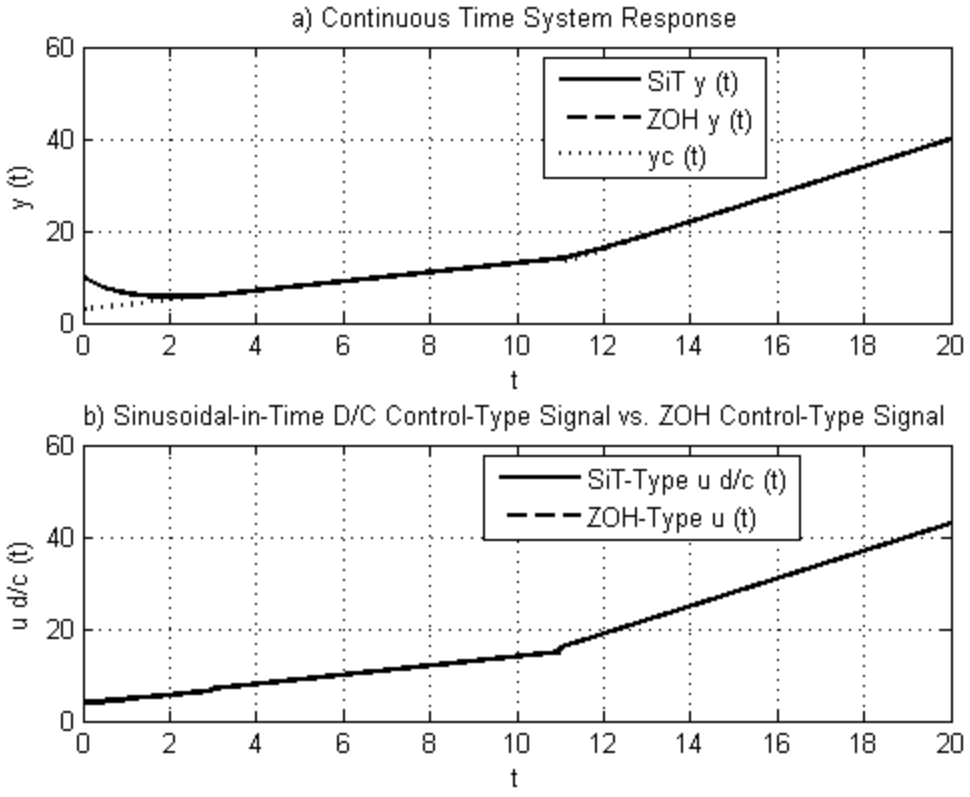

Figure 4.33 Command Signal-Tracking for the First-Order Plant Model with SiT-Type D/C Control

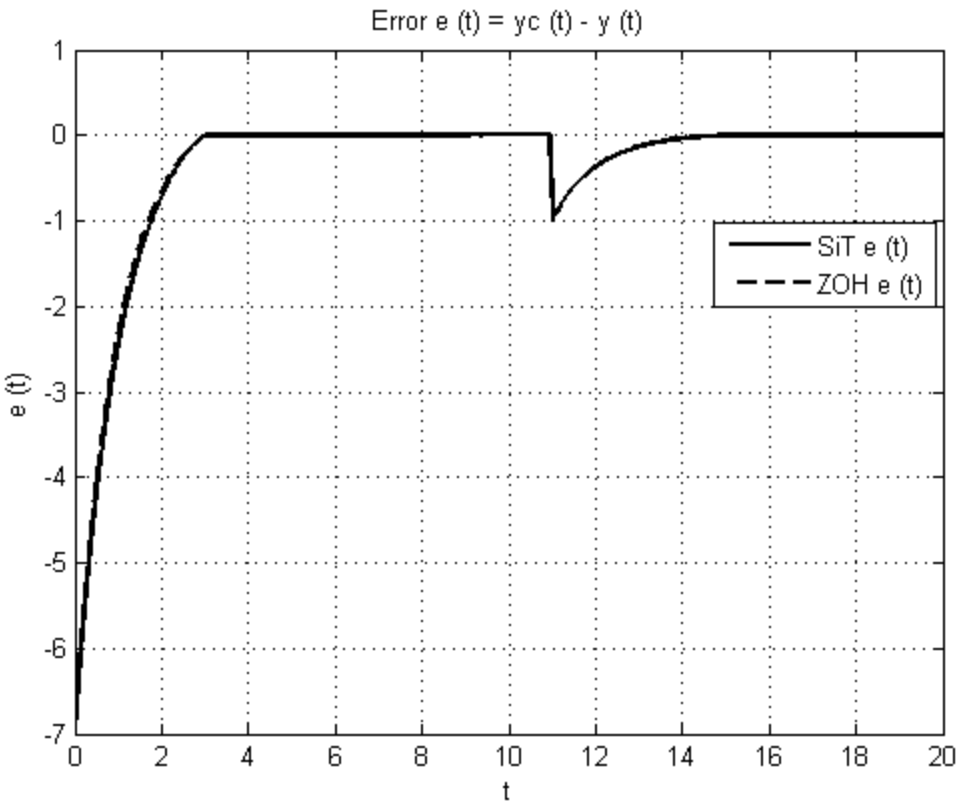

Figure 4.34 Command Signal Error for the First-Order Plant Model with SiT-Type D/C Control

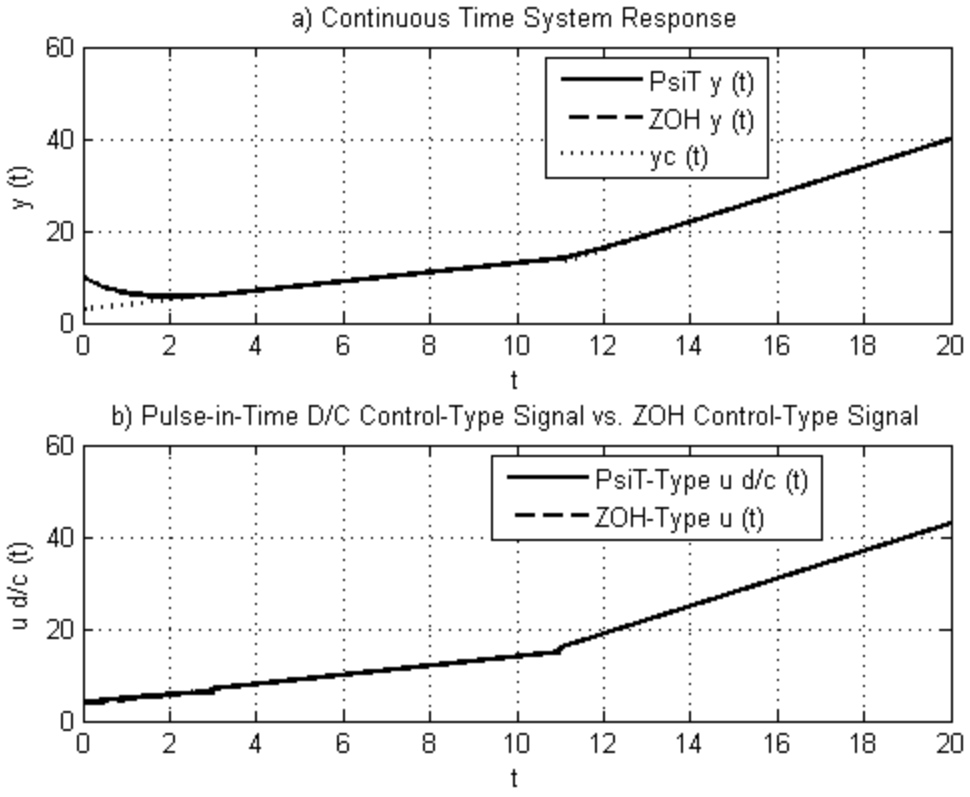

Figure 4.35 Command Signal-Tracking for the First-Order Plant Model with PsiT-Type D/C Control

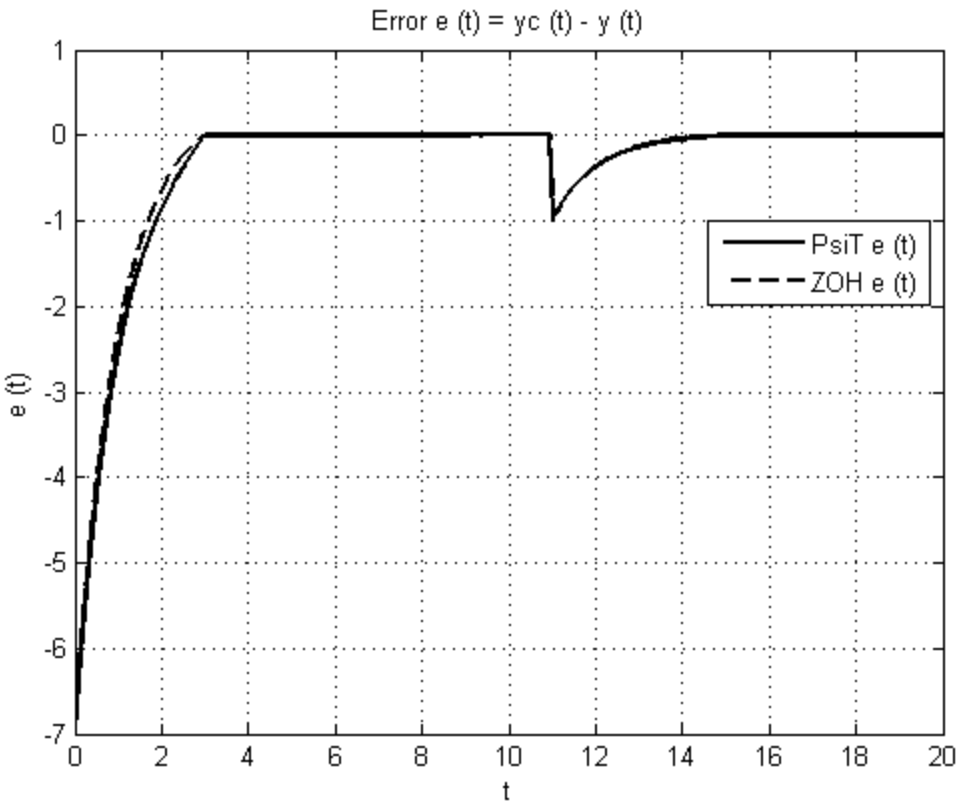

Figure 4.36 Command Signal Error for the First-Order Plant Model with PsiT-Type D/C Control

4.3.3.2 Command Signal-Tracking for a Representative Second-Order Plant Model

In this example, the control task is to make $y(t) \to y_c(t)$ for the second-order model

$$\ddot{y}(t) + a_2\dot{y}(t) + a_1 y(t) = u(t) + w(t), \tag{4.52}$$

where command signal $y_c(t)$ has the form of (4.43). System signal-error $e(t)$ is defined as in (4.45) and the first and second derivatives for the plant model of (4.52) are respectively

$$\dot{e}(t) = \dot{y}_c(t) - \dot{y}(t) \tag{4.53}$$

$$\ddot{e}(t) = -\ddot{y}(t) = a_2\dot{y}(t) + a_1 y(t) - u(t) - w(t). \tag{4.54}$$

Control $u(t)$ is of the composite form defined in (4.47). It is assumed that $u_d(t)$ is able to completely accommodate $w(t)$. Control $u_c(t)$ is designed for the system model of (4.52) as

$$u_c = a_2(\dot{y}_c) + a_1(y_c). \tag{4.55}$$

From (4.54) and (4.55),

$$\ddot{e}(t) = -a_2\dot{e}(t) - a_1 e(t) - u_p(t). \tag{4.56}$$

Control $u_p(t)$ is then designed according to the D/C algorithm such that

$$u_p(t) = \overline{H}e^{\overline{D}(t-kT)}\widetilde{K}_{d/c}\begin{bmatrix} -e(kT) \\ -\dot{e}(kT) \end{bmatrix}. \tag{4.57}$$

Control matrices $\widetilde{K}_{ZOH}$ for ZOH and $\widetilde{K}_{d/c}$ for the D/C controls are computed with the Moore-Penrose column rank minimization technique in equations (4.12)-(4.16). The simulated system responses and D/C control signals for the second-order case are shown as compared to ZOH-controlled system responses and control signals for LiT-type D/C control in Figure 4.37, EiT-type D/C control in Figure 4.39, SiT-type D/C control in Figure 4.41, and PsiT-type D/C control in Figure 4.43. In each example, successful tracking of the command signal is accomplished with one control decision ($T = 3$) for the D/C control signals and two control decisions ($T = 6$) for the ZOH-type control signals. The system output response $y(t)$ differs by 1 unit during the control task transient. The error, as in (4.53), is given for the LiT-type D/C control in Figure 4.38, the EiT-type D/C control in Figure 4.40, SiT-type D/C control in Figure 4.42, and PsiT-type D/C control in Figure 4.44.

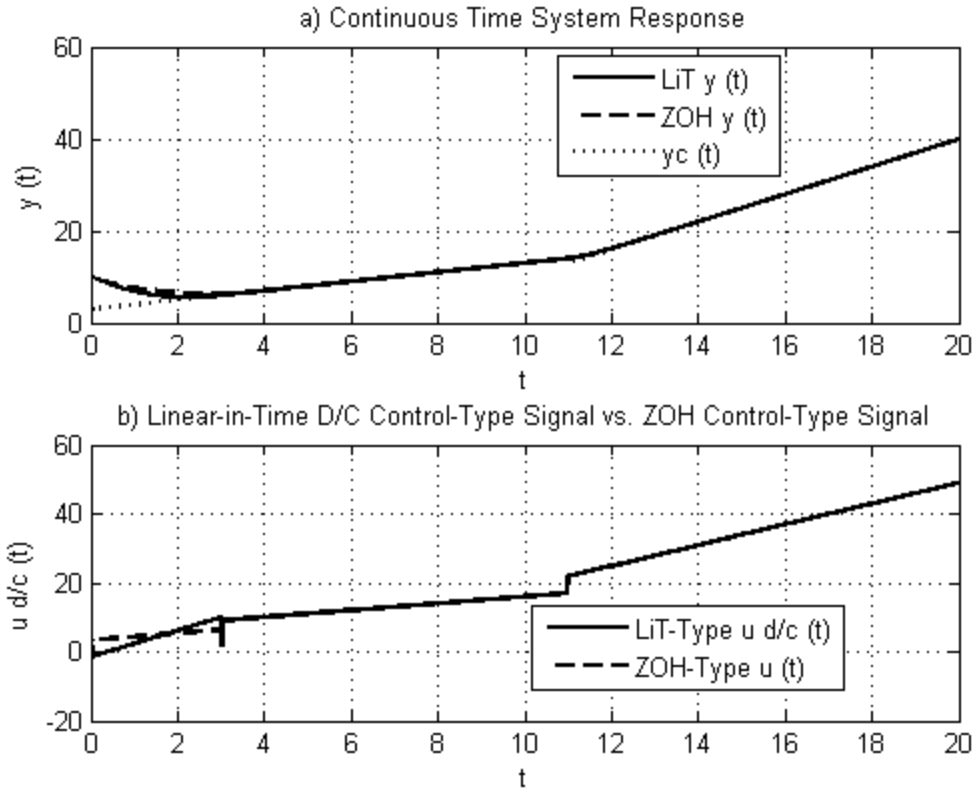

Figure 4.37 Command Signal-Tracking for the Second-Order Plant Model with LiT-Type D/C Control

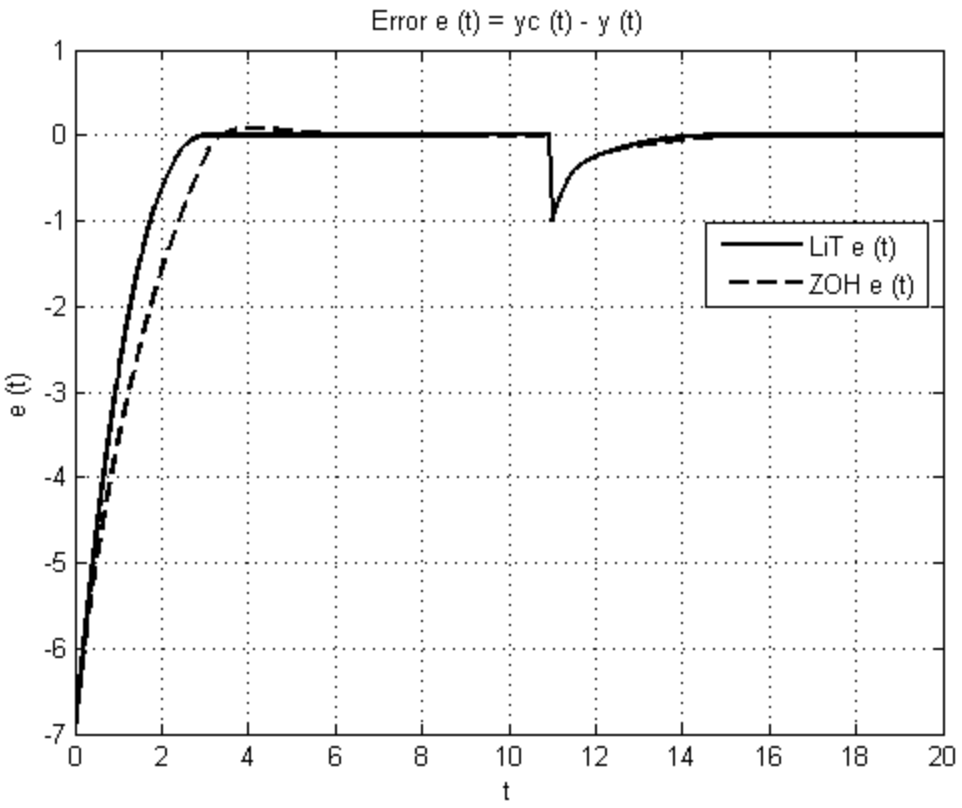

Figure 4.38 Command Signal Error for the Second-Order Plant Model with LiT-Type D/C Control

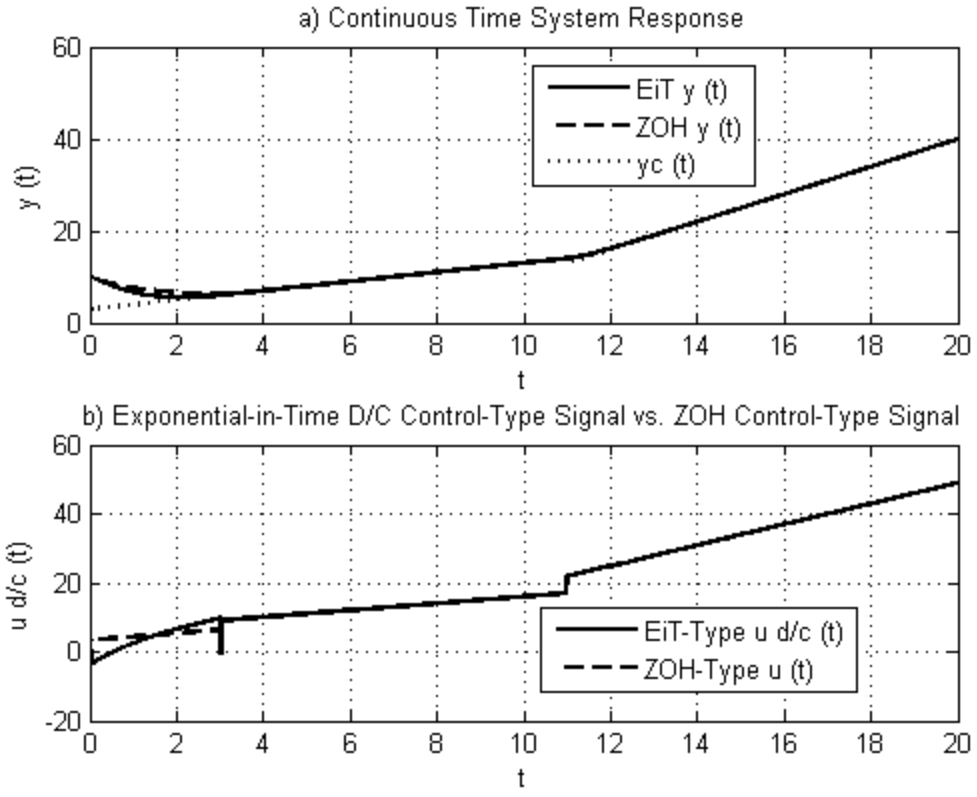

Figure 4.39 Command Signal-Tracking for the Second-Order Plant Model with EiT-Type D/C Control

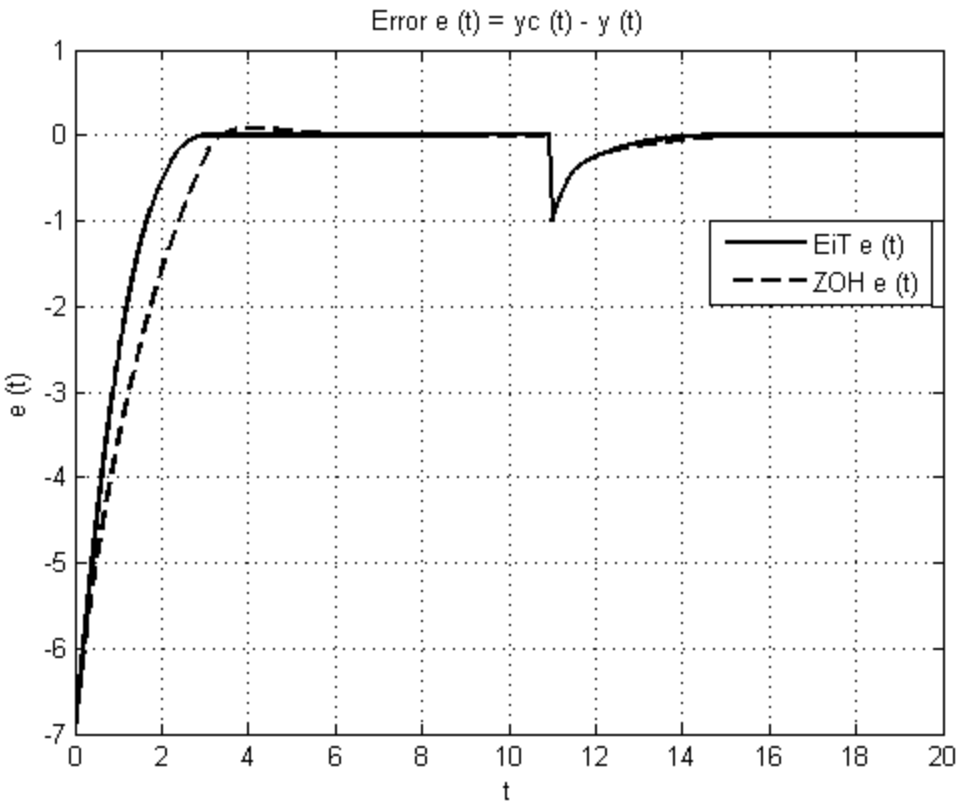

Figure 4.40 Command Signal Error for the Second-Order Plant Model with EiT-Type D/C Control

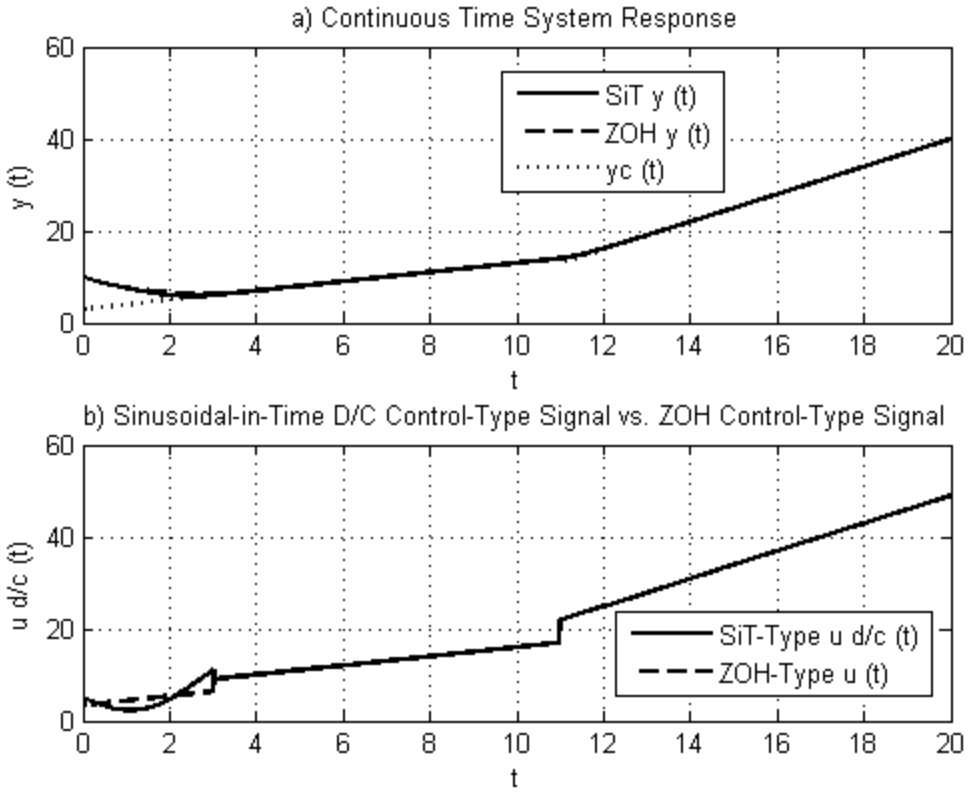

Figure 4.41 Command Signal-Tracking for the Second-Order Plant Model with SiT-Type D/C Control

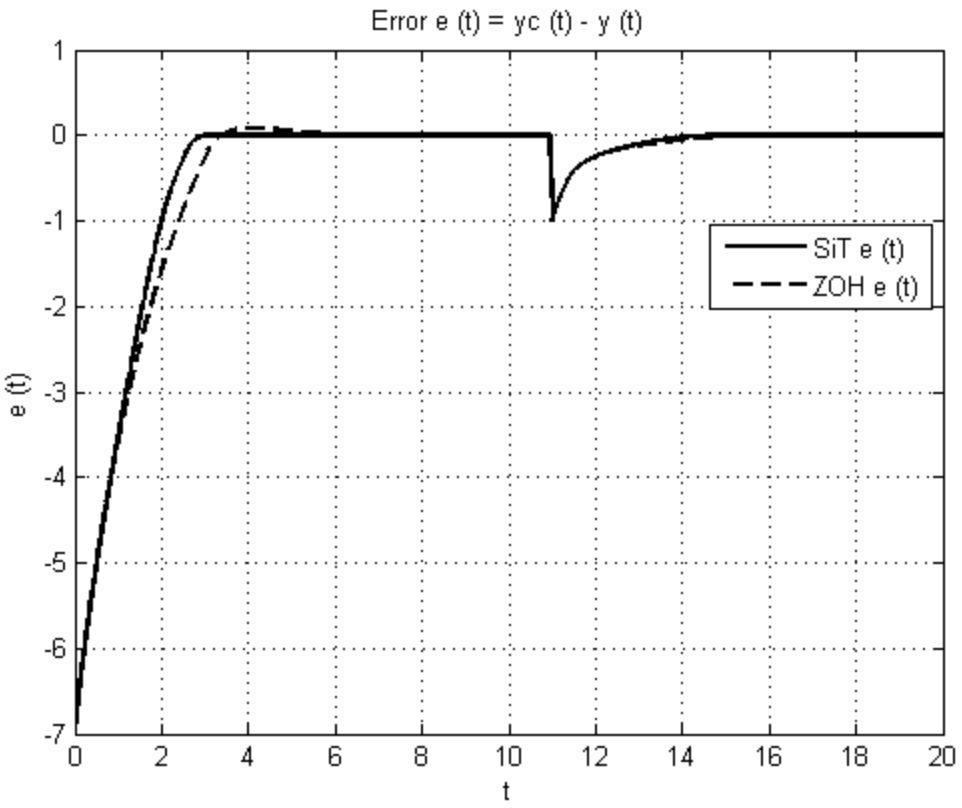

Figure 4.42 Command Signal Error for the Second-Order Plant Model with SiT-Type D/C Control

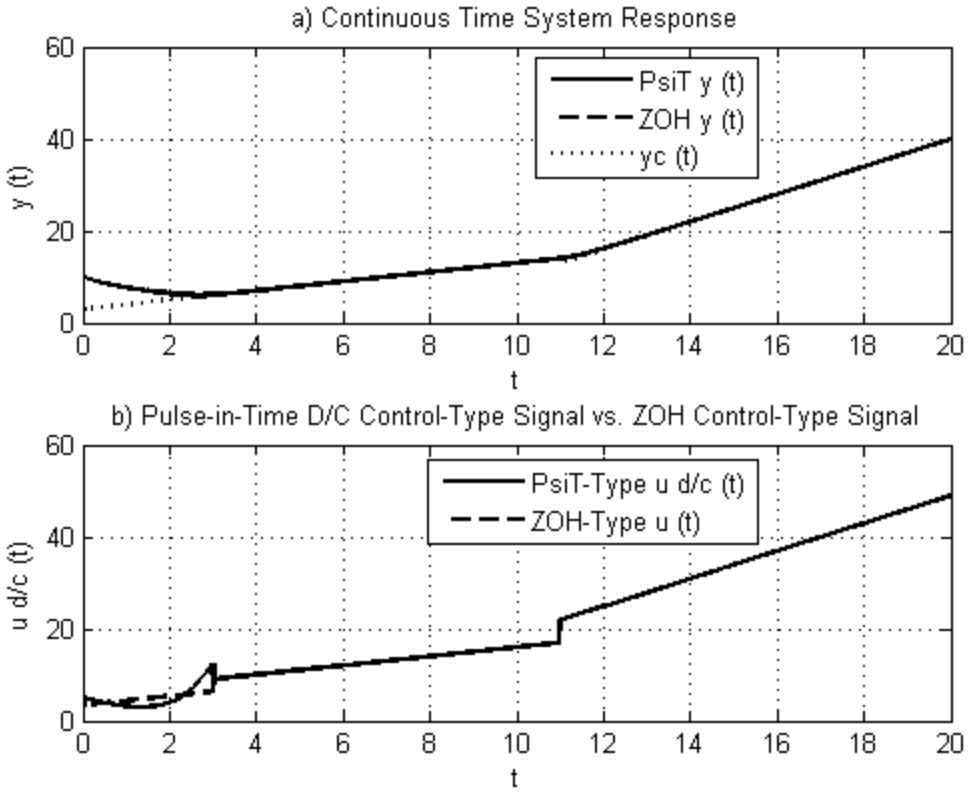

Figure 4.43 Command Signal-Tracking for the Second-Order Plant Model with PsiT-Type D/C Control

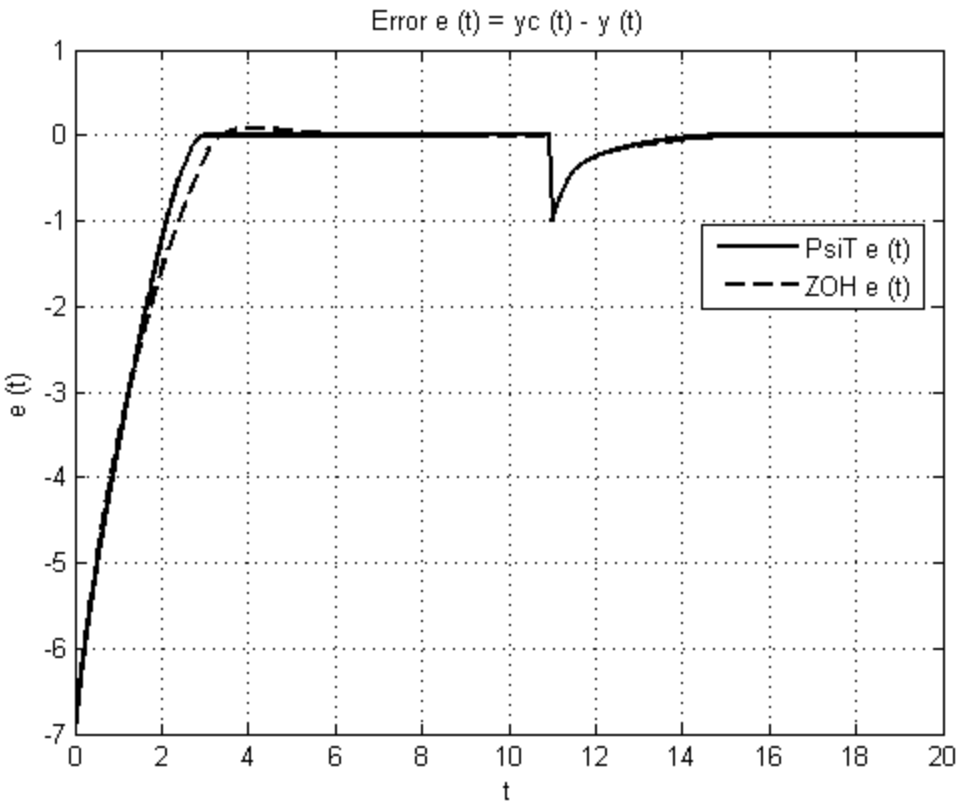

Figure 4.44 Command Signal Error for the Second-Order Plant Model with PsiT-Type D/C Control

4.3.3.3 Command Signal-Tracking for a Representative Third-Order Plant Model

In this example, the control task is to make $y(t) \to y_c(t)$ for the third-order plant model

$$\dddot{y}(t) + a\ddot{y}(t) = u(t) + \dot{y}_c(t) + w(t), \tag{4.58}$$

where command signal $y_c(t)$ has the form of (4.43). System signal-error $e(t)$ is defined as in (4.45) and the first, second, and third derivatives for the plant model of (4.58) are, respectively,

$$\dot{e}(t) = \dot{y}_c(t) - \dot{y}(t) \tag{4.59}$$

$$\ddot{e}(t) = -\ddot{y}(t) \tag{4.60}$$

$$\dddot{e}(t) = -\dddot{y}(t) = a\ddot{y}(t) - \dot{u}(t) - \dot{w}(t). \tag{4.61}$$

Control $u(t)$ defined in the composite form of (4.47), and it is assumed that $u_d(t)$ is able to completely accommodate $w(t)$. Control $u_c(t)$ is designed for the system model of (4.58) to be

$$u_c(t) = a\ddot{y}_c. \tag{4.62}$$

From (4.61) and (4.62),

$$\dddot{e}(t) = -a\ddot{e}(t) - \dot{u}_p(t). \tag{4.63}$$

Control $u_p(t)$ is then designed with the D/C algorithm such that

$$u_p(t) = \overline{H}e^{\overline{D}(t-kT)}\widetilde{K}_{d/c}\begin{bmatrix} -e(kT) \\ -\dot{e}(kT) \\ -\ddot{e}(kT) \end{bmatrix}. \tag{4.64}$$

The control matrix $\widetilde{K}_{d/c}$ is computed for the D/C control signals with the Moore-Penrose column rank minimization technique in (4.19)-(4.22). For the ZOH-control signal, $\widetilde{K}_{ZOH}$ was computed using "deadbeat" design as in (4.18), since the Moore-Penrose technique results do not yield closed-loop system λ_i within the unit circle for the third-order plant model for ZOH (resulting in an unstable closed-loop system) in this particular case. These designs of $\widetilde{K}_{d/c}$ and of $\widetilde{K}_{ZOH}$ are the "best case" of each control-type.

The simulated system responses and D/C control signals for the third-order case are shown as compared to ZOH-controlled system responses and control signals for LiT-type D/C control in Figure 4.45, EiT-type D/C control in Figure 4.47, SiT-type D/C control in Figure 4.49, and PsiT-type D/C control in Figure 4.51. In each example,

successful tracking of the command signal is accomplished with one control decision ($T = 3$) for the D/C control signals and three control decisions ($T = 9$) for the ZOH-type control signals. The error, as in (4.45), is given for the LiT-type D/C control in Figure 4.46, the EiT-type D/C control in Figure 4.48, SiT-type D/C control in Figure 4.50, and PsiT-type D/C control in Figure 4.52. For every type of D/C control signal, the error for the ZOH-controlled system is much greater than the error for the D/C-controlled system.

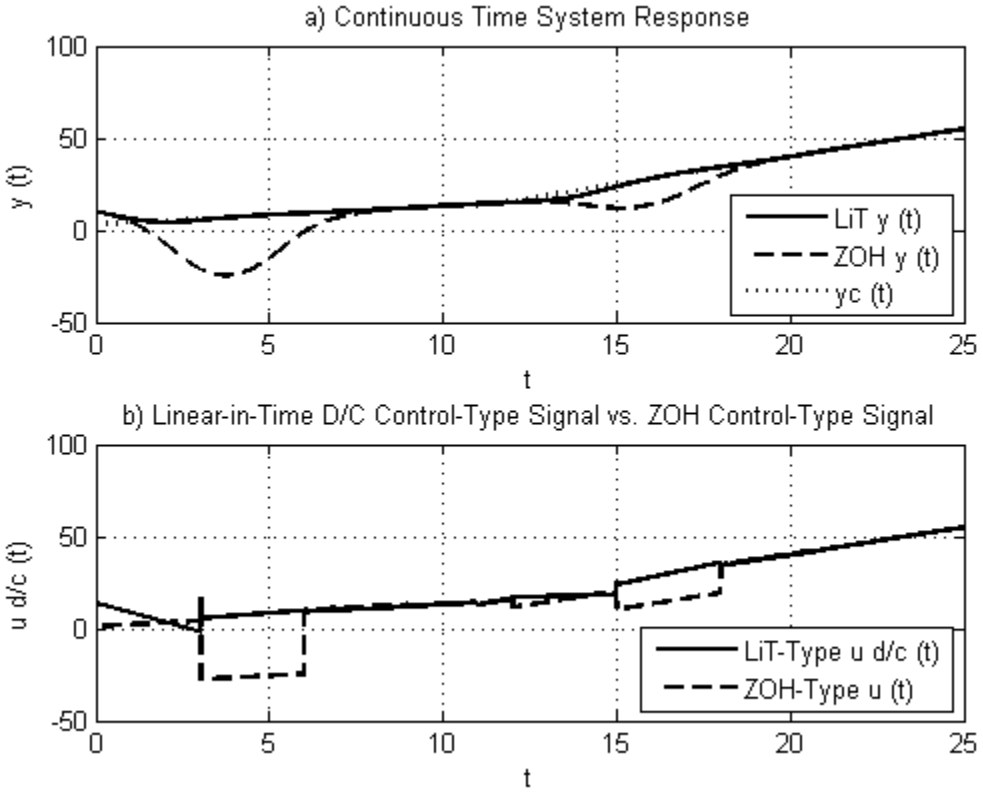

Figure 4.45 Command Signal-Tracking for the Third-Order Plant Model with LiT-Type D/C Control

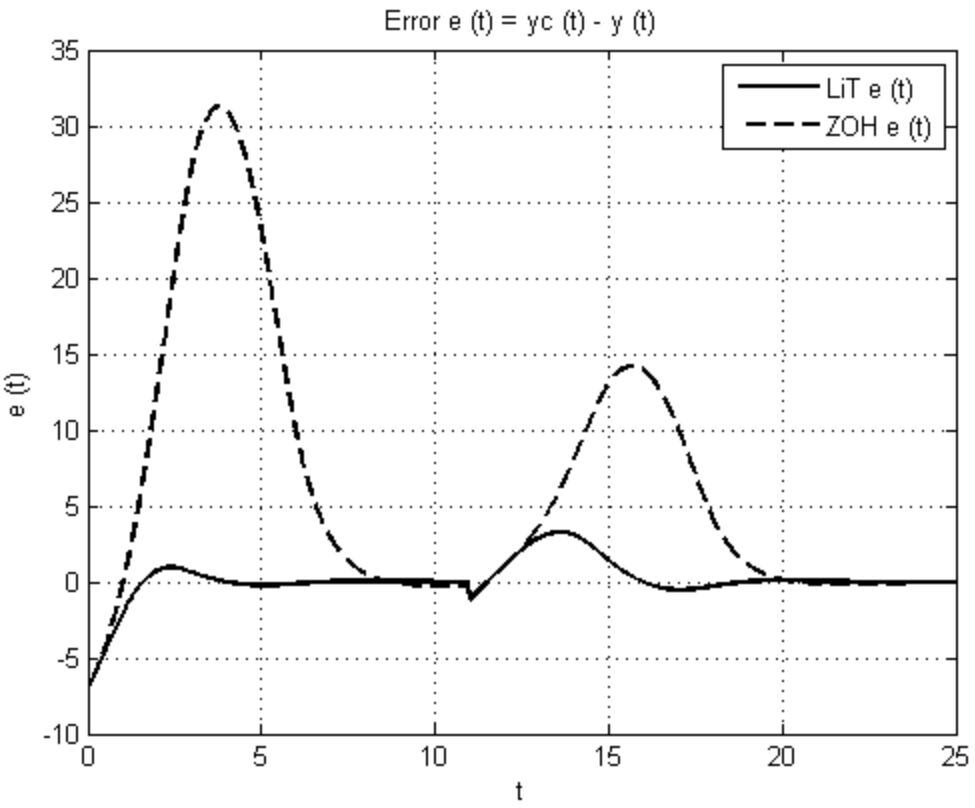

Figure 4.46 Command Signal Error for the Third-Order Plant Model with LiT-Type D/C Control

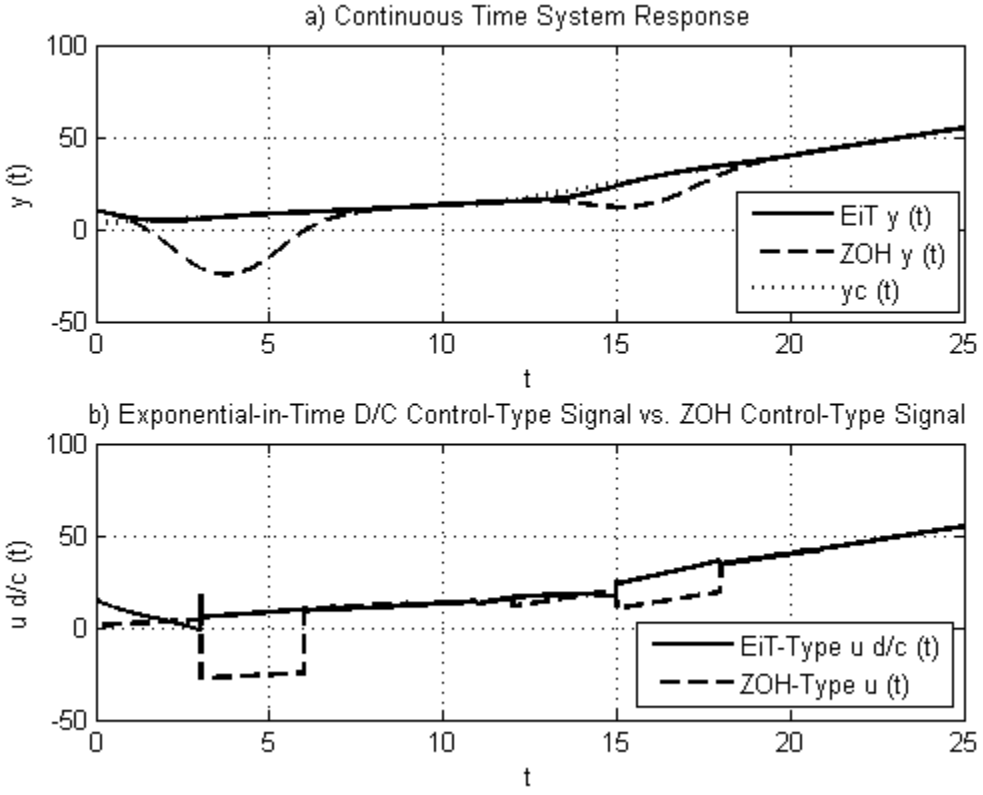

Figure 4.47 Command Signal-Tracking for the Third-Order Plant Model with EiT-Type D/C Control

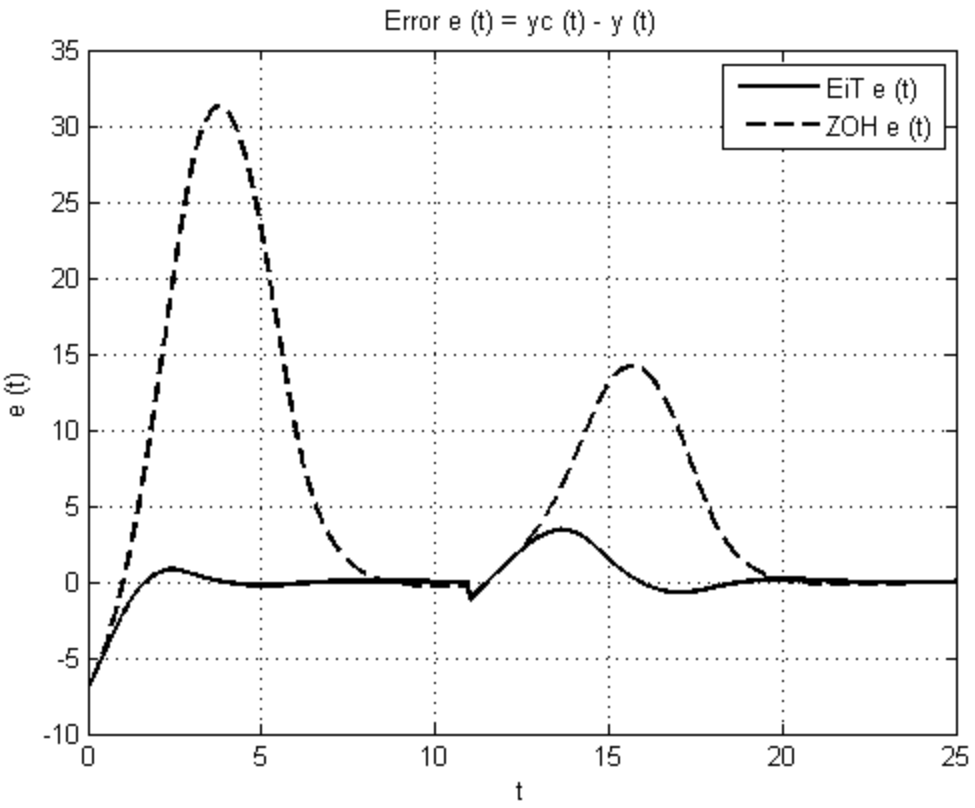

Figure 4.48 Command Signal Error for the Third-Order Plant Model with EiT-Type D/C Control

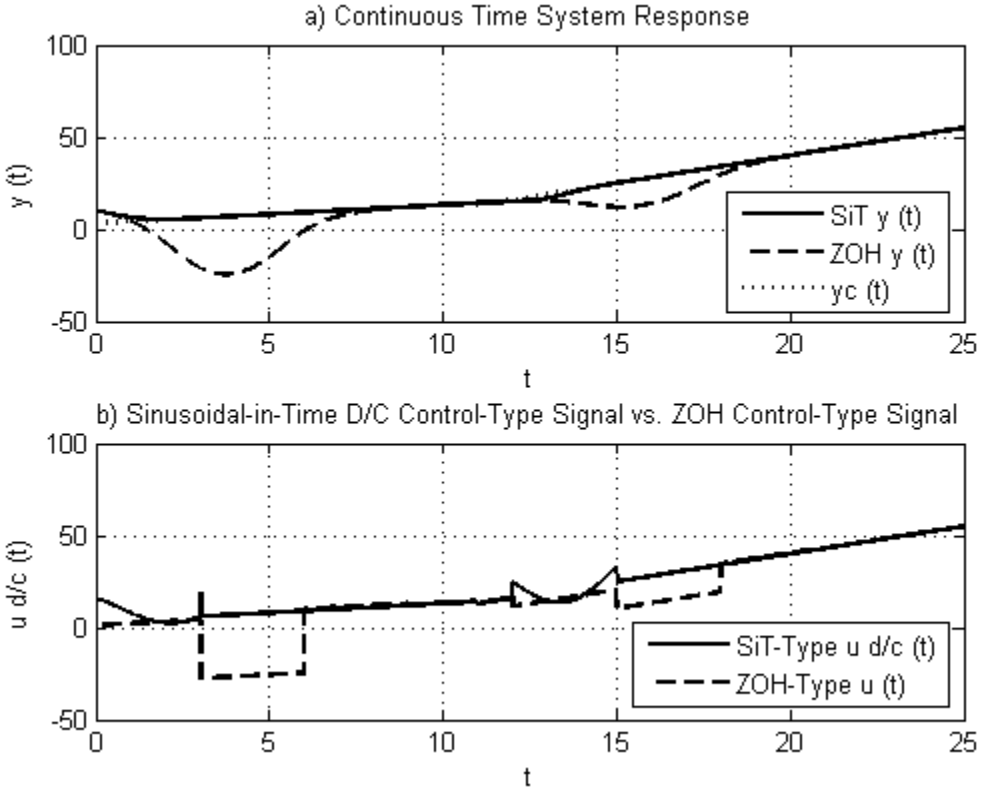

Figure 4.49 Command Signal-Tracking for the Third-Order Plant Model with SiT-Type D/C Control

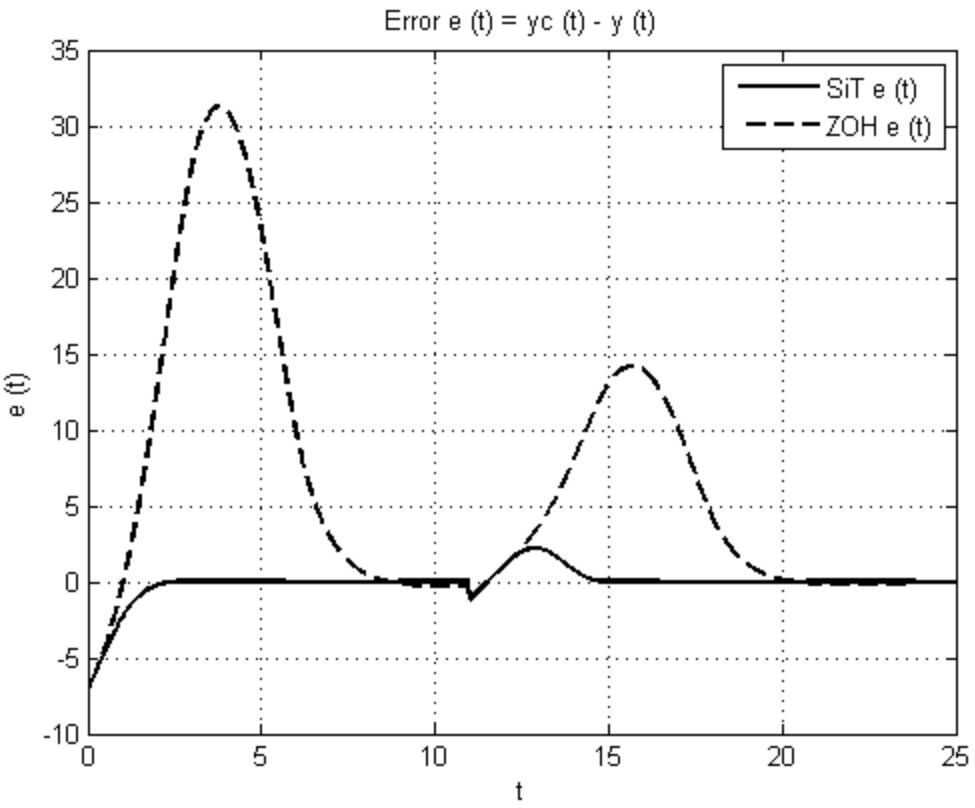

Figure 4.50 Command Signal Error for the Third-Order Plant Model with SiT-Type D/C Control

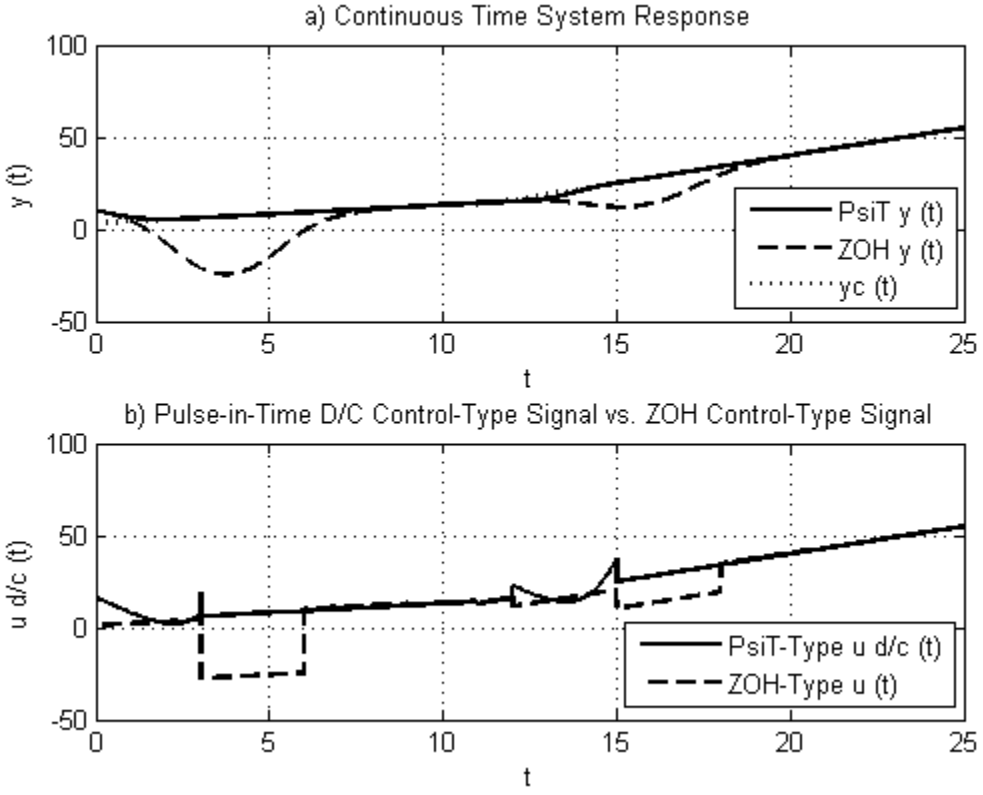

Figure 4.51 Command Signal-Tracking for the Third-Order Plant Model with PsiT-Type D/C Control

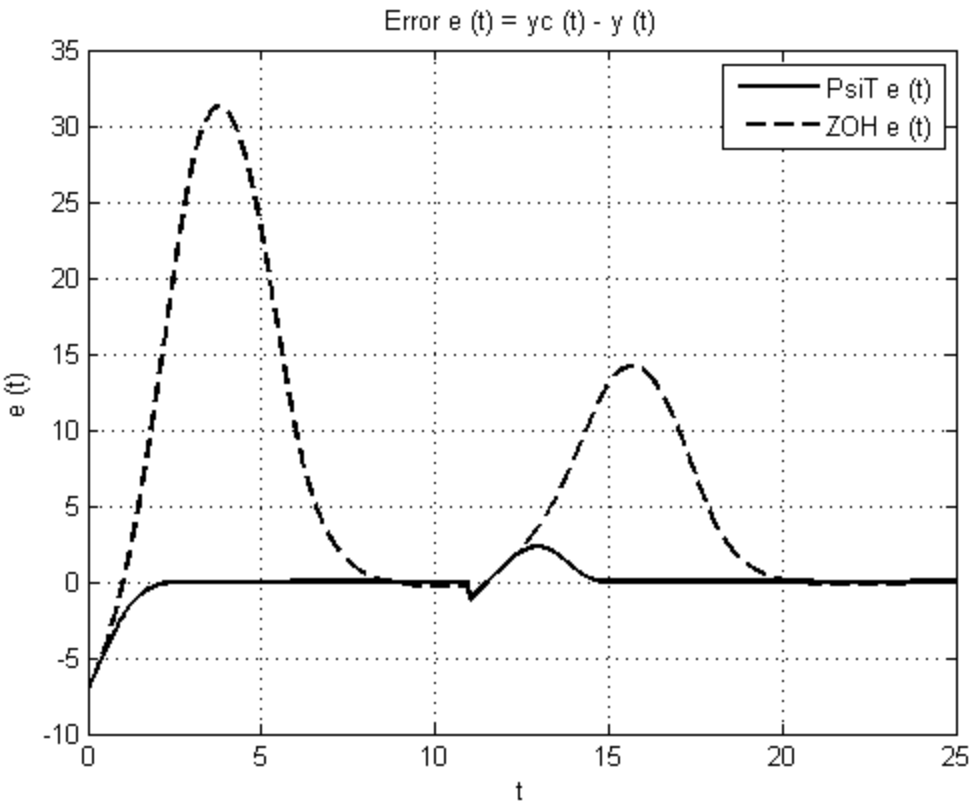

Figure 4.52 Command Signal Error for the Third-Order Plant Model with PsiT-Type D/C Control

4.3.4 Example 4: Observer Design and Disturbance Accommodation

The final control task to be studied in this chapter is Disturbance Accommodation. Systems are rarely free from unwanted noise, parasitic effects, or outside interference. For this reason, Disturbance Accommodating Control has evolved [20],[22],[23].

Considering the continuous-time system of

$$\dot{x}(t) = A(t)x(t) + B(t)u(t) + F(t)w(t) \tag{4.65}$$

$$y(t) = C(t)x(t), \tag{4.66}$$

control $u(t)$ is designed in a composite form (4.47) to include $u_d(t)$, which minimizes, cancels, or utilizes system disturbance $w(t)$. It is often necessary to compute "estimates" of any signals which cannot be measured, which may include any "unknowable" system states as well as disturbances. In this case, a full or reduced-order observer may be used [20],[22]. By choice of estimate state variable, $z(t)$, a matrix H is determined. The relationship between the disturbance and disturbance state estimate is [22],[25]

$$w(t) = H(t)z(t). \tag{4.67}$$

The three main types of Disturbance Accommodating Control (DAC) are (i) Disturbance Minimization, (ii) Disturbance Utilization, and (iii) Disturbance Rejection (Cancellation), [20]. Disturbance Minimization, developed by Johnson, [26], produces $u(t)$ control effort to reduce system disturbance effects by providing the "best" choice that achieves [27],[28]

$$\min_{u_d} \left\| Bu_d + FHz \right\|. \tag{4.68}$$

Disturbance Rejection (Cancelation), [20] uses control effort designed as

$$Bu_d = -F\hat{w}, \tag{4.69}$$

provided that

$$\operatorname{rank}\left([B \mid FH]\right) = \operatorname{rank}(B) \tag{4.70}$$

to directly negate system disturbance $w(t)$. Disturbance Utilization (DUC), [20] accesses useful effects of w(t) to help accomplish the control task, which in the LQR form, is [27],[29]

$$J[u] = \tilde{x}^T(t_f)\bar{S}\tilde{x}(t_f) + \int_0^{t_f}\left[\tilde{x}^T(t)\bar{Q}\tilde{x}(t) + u^T(t)Ru(t)\right]dt. \quad (4.71)$$

For the research conducted in this section, disturbance rejection (cancellation) was evaluated using both ZOH-type discrete-time control and D/C-type discrete-time control signals.

The Full-Order D/C Observer model is presented in detail in [4],[30]. For the discrete-time system model

$$Ex(kT) = \tilde{A}(kT)x(kT) + \overline{BH}v(kT) + \widetilde{FH}z(kT), \quad (4.72)$$

(where E represents the forward shift operator) the D/C-type Discrete-Time Observer equations are, [4]

$$E\hat{x}(kT) = \tilde{A}(kT)\hat{x}(kT) + \widetilde{FH}\hat{z}(kT) + \overline{BH}\hat{v}(kT) - K_{ox}\left[y(kT) - C\hat{x}(kT)\right] \quad (4.73)$$

$$E\hat{z}(kT) = \tilde{D}(kT)\hat{z} - K_{oz}\left[y(kT) - C\hat{x}(kT)\right] \quad (4.74)$$

$$E\hat{v}(kT) = \bar{\tilde{D}}(kT)\hat{v}(kT) - K_v\left[u(kT) - \bar{H}(kT)\hat{v}(kT)\right], \quad (4.75)$$

where $\widetilde{FH}(kT)$ is calculated from (1.17) and $\bar{\tilde{D}}(kT)$ and $\tilde{D}(kT)$ are computed, respectively,

$$\bar{\tilde{D}}(kT) = \Phi_{\bar{D}}\left[(k+1)T, kT\right], \quad (4.76)$$

$$\tilde{D}(kT) = \Phi_D\left[(k+1)T, kT\right]. \quad (4.77)$$

For the case of time-invariant $\bar{D}$ and D, (4.76) and (4.77) respectively reduce-to

$$\bar{\tilde{D}} = e^{\bar{D}T}, \quad (4.78)$$

$$\tilde{D} = e^{DT}. \quad (4.79)$$

Matrices K_{ox}, K_{oz}, and K_v are designed to minimize the respective signal error measurements, [4]

$$\varepsilon_x(kT) = x(kT) - \hat{x}(kT), \tag{4.80}$$

$$\varepsilon_z(kT) = z(kT) - \hat{z}(kT), \tag{4.81}$$

$$\varepsilon_v(kT) = v(kT) - \hat{v}(kT). \tag{4.82}$$

Matrix $H(t)$ is determined by the choice of disturbance estimate state-variable, $z(t)$, as in (4.67). $D(t)$ is also determined by choice of disturbance estimate state-variable,

$$\dot{z} = D(t)z. \tag{4.83}$$

For the research conducted in this thesis, $\hat{v}(kT)$ was not produced, as $v(kT)$ was directly computed and available.

The dynamics of the composite estimation error of (4.80) and (4.81) are represented as, [4]

$$E\bar{\varepsilon}(kT) = \left[\overline{A} + \left[\frac{K_{ox}}{K_{oz}}\right]\left[C\middle|O\right]\right]\bar{\varepsilon}(kT); \bar{\varepsilon} = \begin{pmatrix} x - \hat{x} \\ z - \hat{z} \end{pmatrix}, \tag{4.84}$$

where the composite system matrix is

$$\overline{A} = \left[\begin{array}{c|c} \widetilde{A} & \widetilde{FH} \\ \hline O & \widetilde{D} \end{array}\right]. \tag{4.85}$$

In this example, the disturbance signal is assumed to be of the structure

$$w(t) = c_{w_1} + c_{w_2}(t) + \sigma_i(t) \tag{4.86}$$

where $\sigma_i(t)$ is a possible series of sparse, unknowable Dirac impulses, as described in [20],[23] and (1.14). As a result of the state estimate variable choices (phase-variable),

$$H = \begin{bmatrix} 1 & 0 \end{bmatrix}, \tag{4.87}$$

$$D = \begin{bmatrix} 0 & 1 \\ 0 & 0 \end{bmatrix}, \tag{4.88}$$

in (4.67) and (4.83).

In the first-order and second-order cases that follow, disturbance $w(t) = 1 + 3t$ for $0 \le t < 13,$ and $w(t) = -4 - 4t$ for $13 \le t < 30.$ In the third-order case, disturbance $w(t) = 1 + 3t$ for $0 \le t < 30.$ The initial conditions of the system states are $x_1(0) = 10,$ $x_2(0) = -4,$ $x_3(0) = -1.$ As in the previous examples, control decision period/sample period $T = 3,$ D/C control parameters $\alpha = 0.5,$ and $\omega = 1.0.$

The simulation results produced for this section were completed with MatLab Simulink ® software. As the interface of this software allows for discrete-time and continuous signals to be simulated, the possibility is not excluded that the D/C observers of (4.73)-(4.75) can be implemented, interfacing both discrete-time and continuous signals. However, no method could be found which properly interfaces the discrete-time and continuous signals for the D/C observer research applications here (including rate-transistions offered by Simulink ®). To illustrate the disturbance-accommodation examples, a continuous-time full-order observer was utilized with sampled output estimates of system states $x(t).$

4.3.4.1 Disturbance Rejection (Cancellation) For a Representative First-Order Plant Model

Considering the first-order plant model

$$\dot{y}(t) + y(t) = w(t) + u_{d/c}(t), \tag{4.89}$$

the value of $\widetilde{A}$ in the exact discretization of (4.72) is computed to be

$$\widetilde{A} = [0.0498]. \tag{4.90}$$

$\widetilde{FH}$ is computed from (1.17), with H as in (4.87), and D as in (4.88), to be

$$\widetilde{FH} = [0.9502 \quad 2.0498]. \tag{4.91}$$

$\widetilde{D}$ is computed from (4.79) to be

$$\widetilde{D} = \begin{bmatrix} 1 & 3 \\ 0 & 1 \end{bmatrix}, \tag{4.92}$$

and the composite form observer gain values are computed from (4.84) to be

$$\begin{bmatrix} K_{ox} \\ \hline K_{oz} \end{bmatrix} = \begin{bmatrix} -2.0498 \\ -2.4004 \\ -0.3508 \end{bmatrix}. \tag{4.93}$$

With the choice of ZOH-type control,

$$\overline{BH} = \widetilde{B} = [0.9502]. \tag{4.94}$$

Control $u_p(t)$ is designed with $\widetilde{K}_{d/c}$ as calculated in (4.7). The results of this simulation can be seen in Figure 4.53-Figure 4.56, compared to each D/C-type control.

With the choice of LiT-type D/C control,

$$\overline{BH} = [0.9502 \quad 2.0498]. \tag{4.95}$$

Control $u_p(t)$ is designed with $\widetilde{K}_{d/c}$ as calculated in (4.8). The simulated results of this controller can be seen compared to ZOH in Figure 4.53.

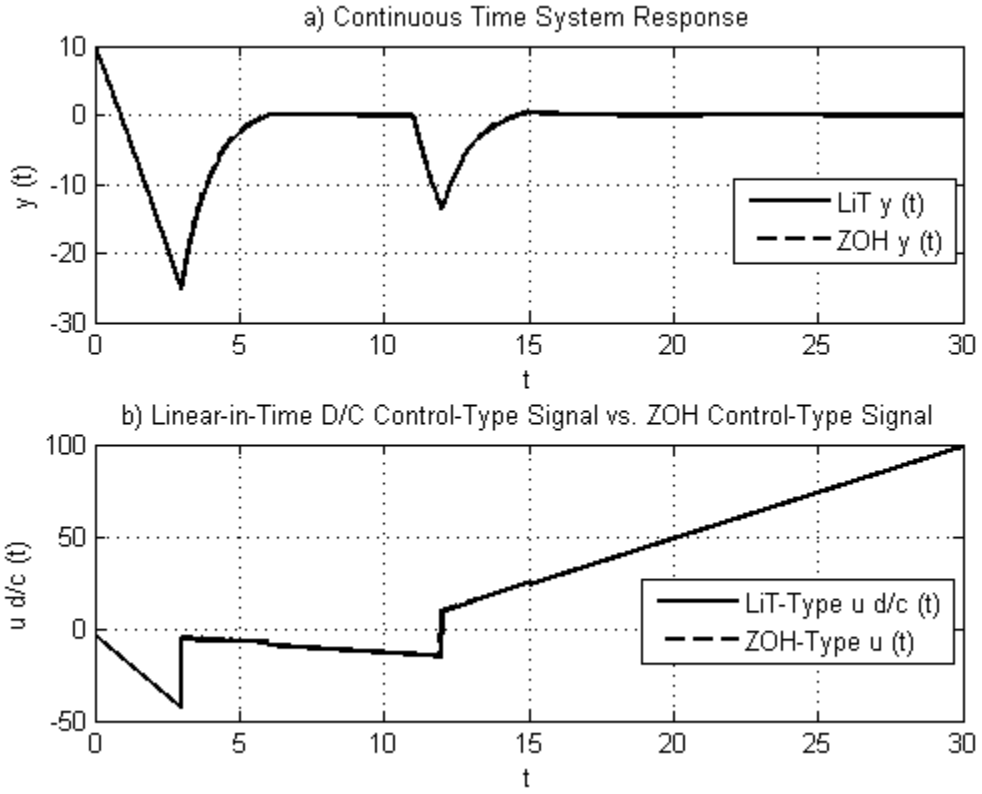

Figure 4.53 Disturbance Rejection (Cancellation) System Response for the First-Order System with LiT-Type D/C Control

With the choice of EiT-type D/C control,

$$\overline{BH} = \begin{bmatrix} 2.5484 & 3.2656 \end{bmatrix}. \tag{4.96}$$

Control $u_p(t)$ is designed with $\widetilde{K}_{d/c}$ as calculated in (4.9). The simulated results can be seen in Figure 4.54, compared to the ZOH results.

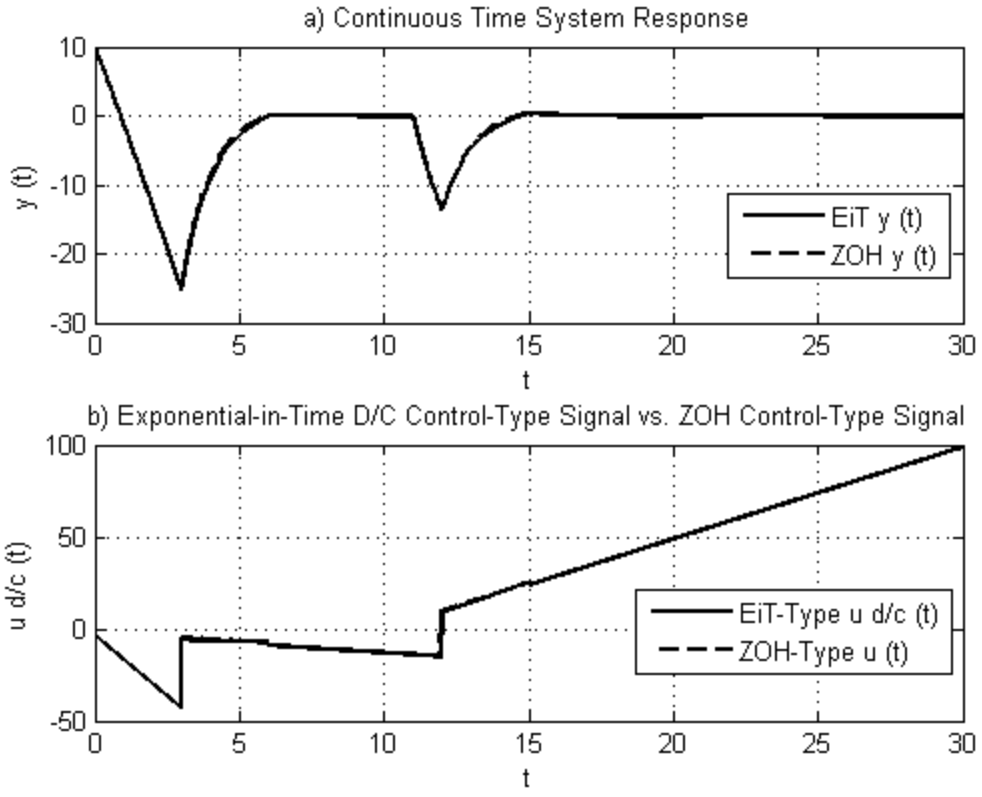

Figure 4.54 Disturbance Rejection (Cancellation) System Response for the First-Order System with EiT-Type D/C Control

With the choice of SiT-type D/C control,

$$\overline{\mathrm{BH}} = \begin{bmatrix} 0.9502 & 0.5904 & 1.3995 \end{bmatrix}. \tag{4.97}$$

Control $u_p(t)$ is designed with $\widetilde{K}_{d/c}$ as calculated in (4.10). The simulated results can be seen in Figure 4.55.

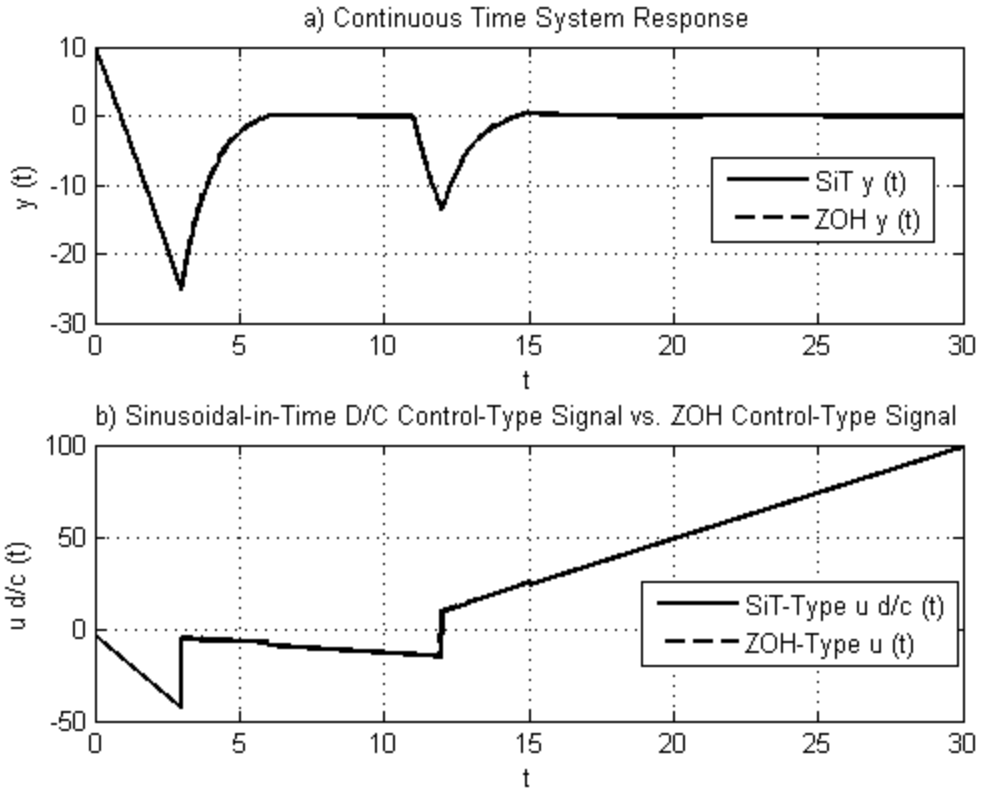

Figure 4.55 Disturbance Rejection (Cancellation) System Response for the First-Order System with SiT-Type D/C Control

With the choice of PsiT-type D/C control,

$$\overline{\mathrm{BH}} = \begin{bmatrix} 0.9502 & 1.0239 & 5.9697 \end{bmatrix}. \tag{4.98}$$

Control $u_p(t)$ is designed with $\widetilde{K}_{d/c}$ as calculated in (4.11). The simulated results can be seen in Figure 4.56.

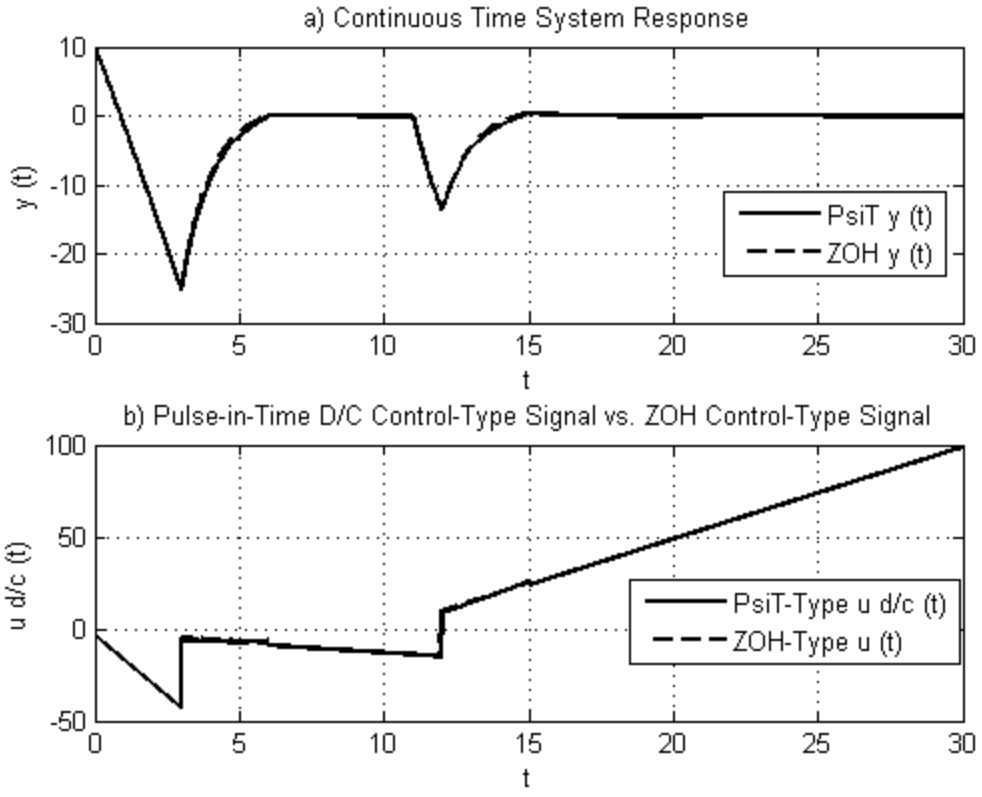

Figure 4.56 Disturbance Rejection (Cancellation) System Response for the First-Order System with PsiT-Type D/C Control

For all first-order cases, the D/C-type controllers performed equivalently to the ZOH-type controller. No significant difference in the number of control-decisions/sample-times needed to accomplish the control task or in magnitude of the system response during the control transient was observed.

4.3.4.2 Disturbance Rejection (Cancellation) For a Representative Second-Order Plant Model

For the second-order plant model,

$$\ddot{y}(t) + a_2\dot{y}(t) + a_1 y(t) = w(t) + u(t), \tag{4.99}$$

where $a_1 = 1,$ and $a_2 = 3,$ as in Table 4.1 with disturbance $w(t)$, the discretized system matrix is computed as

$$\widetilde{A} = e^{AT} = \begin{bmatrix} 0.3722 & 0.1420 \\ -0.1420 & -0.5386 \end{bmatrix}. \tag{4.100}$$

$\widetilde{FH}$ is computed from (1.17), with H as in (4.87), and D as in (4.88), to be

$$\widetilde{FH} = \begin{bmatrix} 0.6278 & 0.9745 \\ 0.1420 & 0.6278 \end{bmatrix}. \tag{4.101}$$

For the D/C observer of (4.73)-(4.76), $\widetilde{D}$ is computed from (4.79) and (4.88) to be

$$\widetilde{D} = \begin{bmatrix} 1 & 3 \\ 0 & 1 \end{bmatrix}. \tag{4.102}$$

The composite form observer gain values are computed from (4.84) to be

$$\begin{bmatrix} K_{ox} \\ \hline K_{oz} \end{bmatrix} = \begin{bmatrix} -2.3183 \\ \underline{-0.4625} \\ -3.7159 \\ -0.4889 \end{bmatrix}, \tag{4.103}$$

to ensure rapid minimization of the error of (4.80) and (4.81).

With the choice of ZOH-type control,

$$\overline{BH} = \widetilde{B} = \begin{bmatrix} 0.6278 \\ 0.1420 \end{bmatrix}. \tag{4.104}$$

Control $u_p(t)$ is designed with $\widetilde{K}_{d/c}$ as calculated in (4.12). The simulated results of this controller can be seen compared to D/C-type control in Figure 4.57-Figure 4.60.

With the choice of LiT-type D/C control,

$$\overline{\overline{BH}} = \begin{bmatrix} 0.6278 & 0.9745 \\ 0.1420 & 0.6278 \end{bmatrix}. \tag{4.105}$$

Control $u_p(t)$ is designed with $\widetilde{K}_{d/c}$ as calculated in (4.13). The simulated results can be seen, compared to the ZOH results in Figure 4.57.

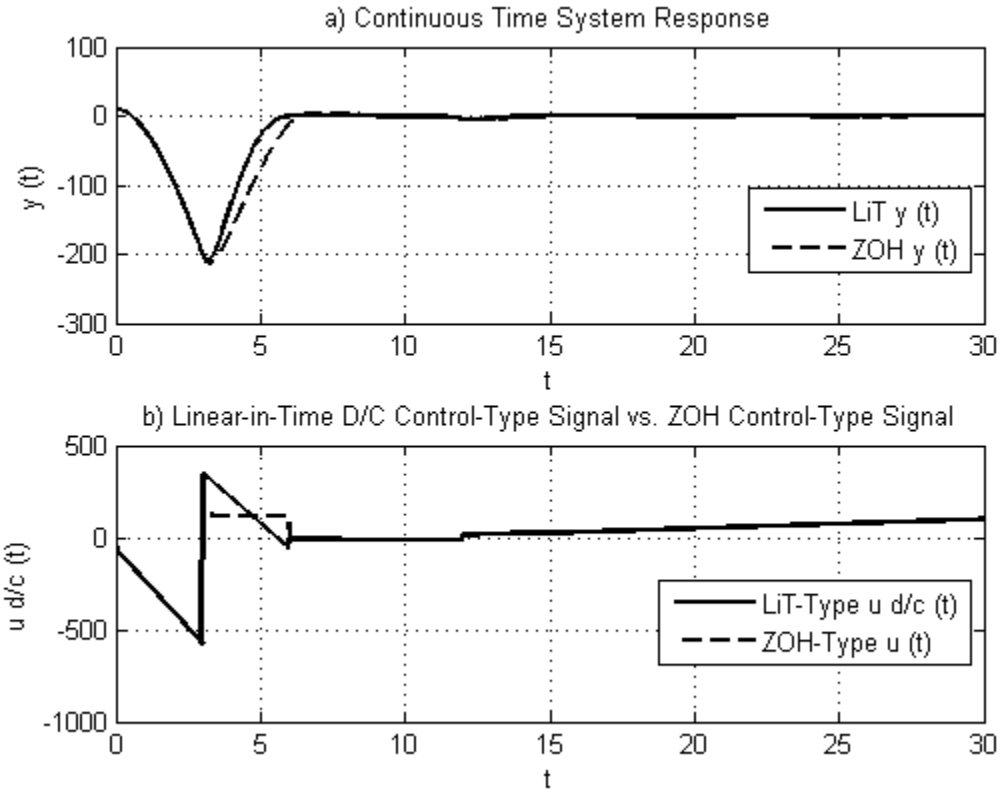

Figure 4.57 Disturbance Rejection (Cancellation) System Response for the Second-Order System with LiT-Type D/C Control

With the choice of EiT-type D/C control,

$$\overline{\overline{BH}} = \begin{bmatrix} 1.2088 & 1.3638 \\ 0.8239 & 1.2088 \end{bmatrix}. \tag{4.106}$$

Control $u_p(t)$ is designed with $\widetilde{K}_{d/c}$ as calculated in (4.14). The simulated results can be seen, compared to the ZOH results in Figure 4.58.

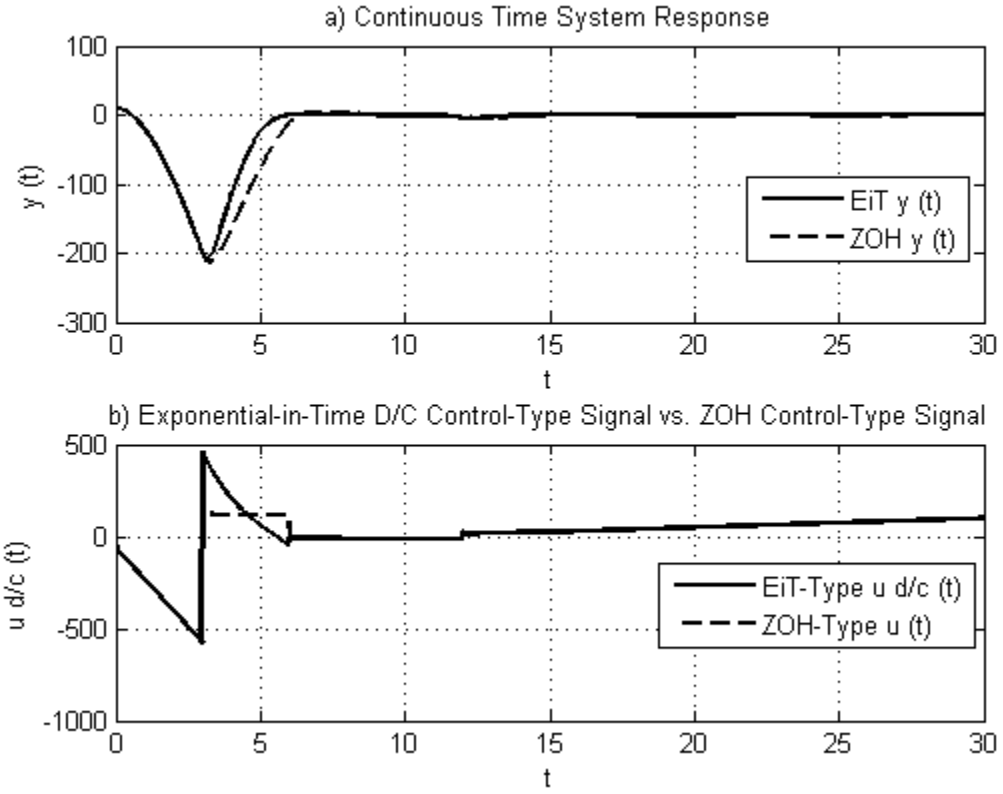

Figure 4.58 Disturbance Rejection (Cancellation) System Response for the Second-Order System with EiT-Type D/C Control

With the choice of SiT-type D/C control,

$$\overline{\mathrm{BH}} = \begin{bmatrix} 0.6278 & 0.4541 & 0.6281 \\ 0.1420 & -0.0003 & 0.4541 \end{bmatrix}. \tag{4.107}$$

Control $u_p(t)$ is designed with $\widetilde{K}_{d/c}$ as calculated in (4.15). The simulated results can be seen, compared to the ZOH results in Figure 4.59.

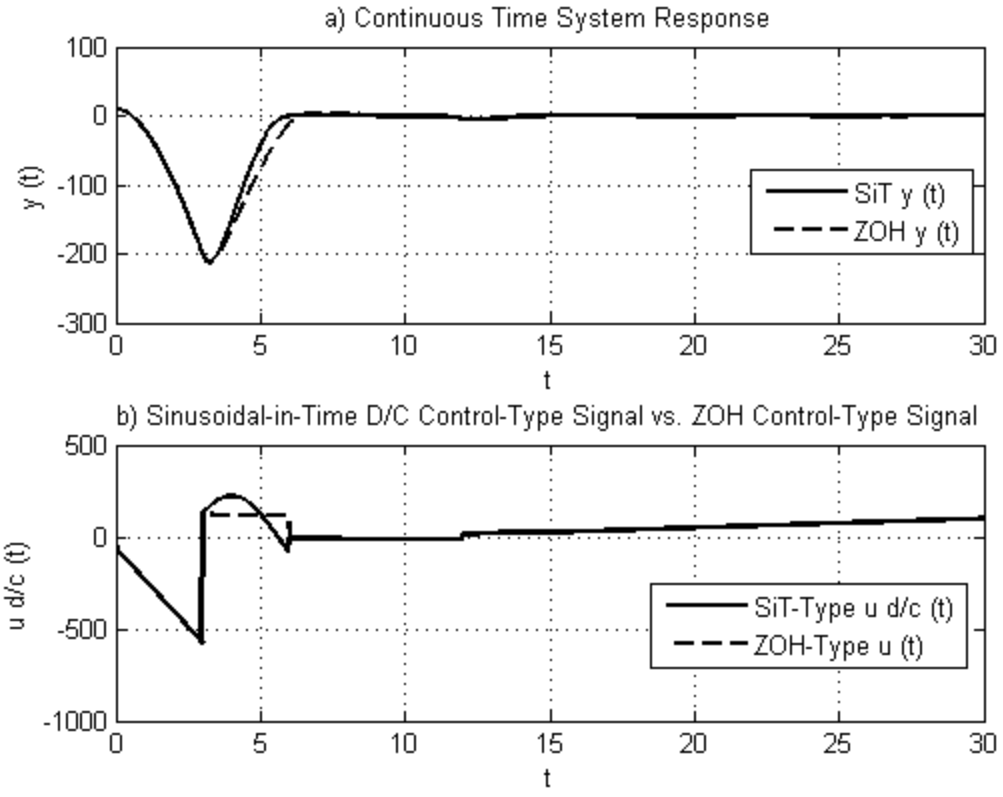

Figure 4.59 Disturbance Rejection (Cancellation) System Response for the Second-Order System with SiT-Type D/C Control

With the choice of PsiT-type D/C control,

$$\overline{\mathrm{BH}} = \begin{bmatrix} 0.6278 & 0.6615 & 2.0399 \\ 0.1420 & 0.1178 & 2.7014 \end{bmatrix}. \tag{4.108}$$

Control $u_p(t)$ is designed with $\widetilde{K}_{d/c}$ as calculated in (4.16). The simulated results can be seen, compared to the ZOH results in Figure 4.60.

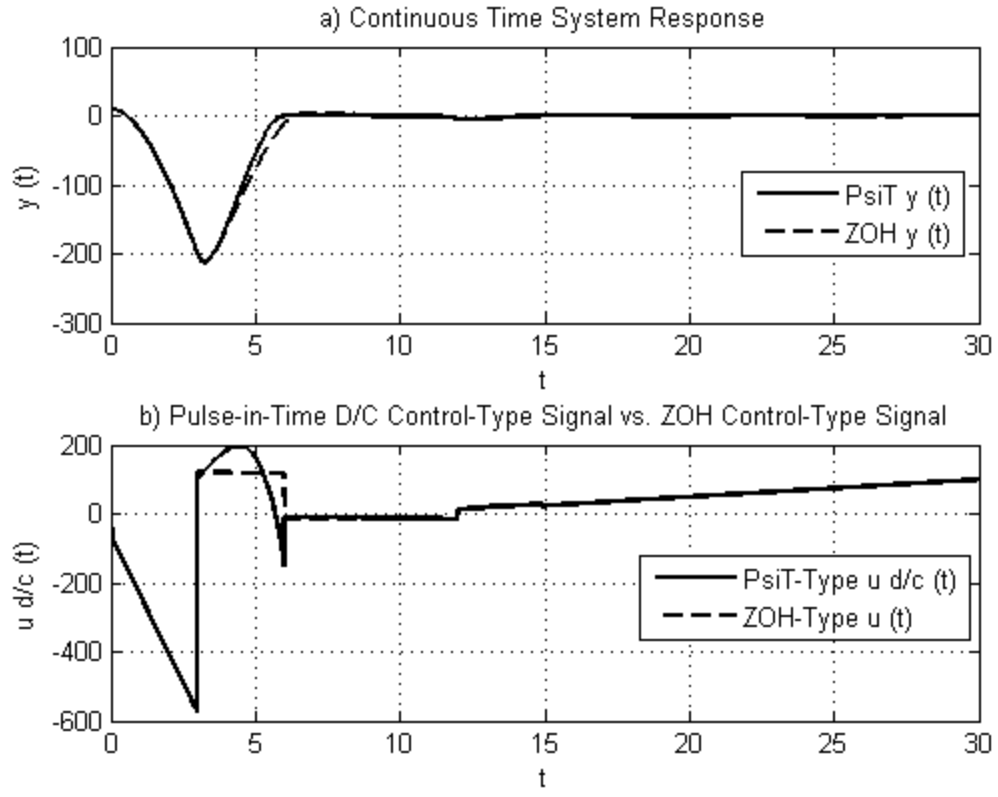

Figure 4.60 Disturbance Rejection (Cancellation) System Response for the Second-Order System with PsiT-Type D/C Control

In the second-order case, the LiT and EiT-type D/C controller performances resulted in slightly decreased magnitude of the system response during the control transient, as compared to the ZOH-type controller. No significant difference in number of control-decisions/sample-times needed to accomplish the control task was observed.

4.3.4.3 Disturbance Rejection (Cancellation) For a Representative Third-Order Plant Model

For the third-order plant model,

$$\dddot{y}(t) + a\ddot{y}(t) = w(t) + u_{d/c}(t), \tag{4.109}$$

where $a = 1,$ as in Table 4.1, the discretized system matrix is computed as

$$\widetilde{A} = \begin{bmatrix} -2.5406 & 0.0429 & 2.6333 \\ -2.6333 & -2.5406 & 0.0429 \\ -0.0429 & -2.6333 & -2.5406 \end{bmatrix}. \tag{4.110}$$

$\widetilde{FH}$ is computed from (1.17), with H as in (4.87), and D as in (4.88), to be

$$\widetilde{FH} = \begin{bmatrix} 3.5406 & 2.9571 \\ 2.6333 & 3.5406 \\ 0.0429 & 2.6333 \end{bmatrix}, \tag{4.111}$$

and the composite form observer gain values are computed from (4.84) to be

$$\begin{bmatrix} K_{ox} \\ \overline{K_{oz}} \end{bmatrix} = \begin{bmatrix} 5.6219 \\ 1.4054 \\ -4.3364 \\ -0.1322 \\ -0.0122 \end{bmatrix}. \tag{4.112}$$

For the third-order ZOH-type observer of (4.109),

$$\overline{BH} = \widetilde{B} = \begin{bmatrix} 3.5406 \\ 2.6333 \\ 0.0429 \end{bmatrix}. \tag{4.113}$$

Control $u_p(t)$ is designed with $\widetilde{K}_{d/c}$ as calculated in (4.18). The simulated results for this design can be seen compared to the D/C-type controls in Figure 4.61-Figure 4.64.

For the third-order LiT-type D/C observer of (4.109),

$$\overline{BH} = \begin{bmatrix} 3.5406 & 2.9571 \\ 2.6333 & 3.5406 \\ 0.04291 & 2.6333 \end{bmatrix}. \tag{4.114}$$

Control $u_p(t)$ is designed with $\widetilde{K}_{d/c}$ as calculated in (4.19). The simulated results for this design can be seen compared to the ZOH results in Figure 4.61.

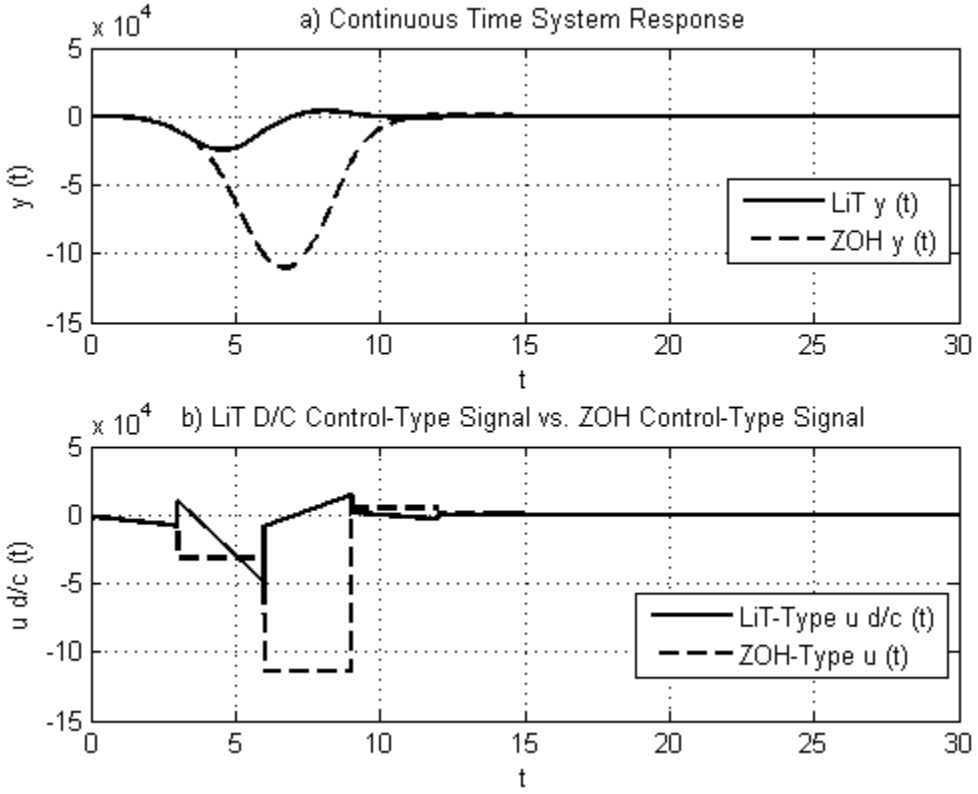

Figure 4.61 Disturbance Rejection (Cancellation) System Response for the Third-Order System with LiT-Type D/C Control

For the third-order EiT-type D/C observer of (4.109),

$$\overline{BH} = \begin{bmatrix} 4.5854 & 3.4784 \\ 4.3726 & 4.5854 \\ 2.3356 & 4.3726 \end{bmatrix}. \tag{4.115}$$

Control $u_p(t)$ is designed with $\widetilde{K}_{d/c}$ as calculated in (4.20). The simulated results for this design can be seen compared to the ZOH results in Figure 4.62.

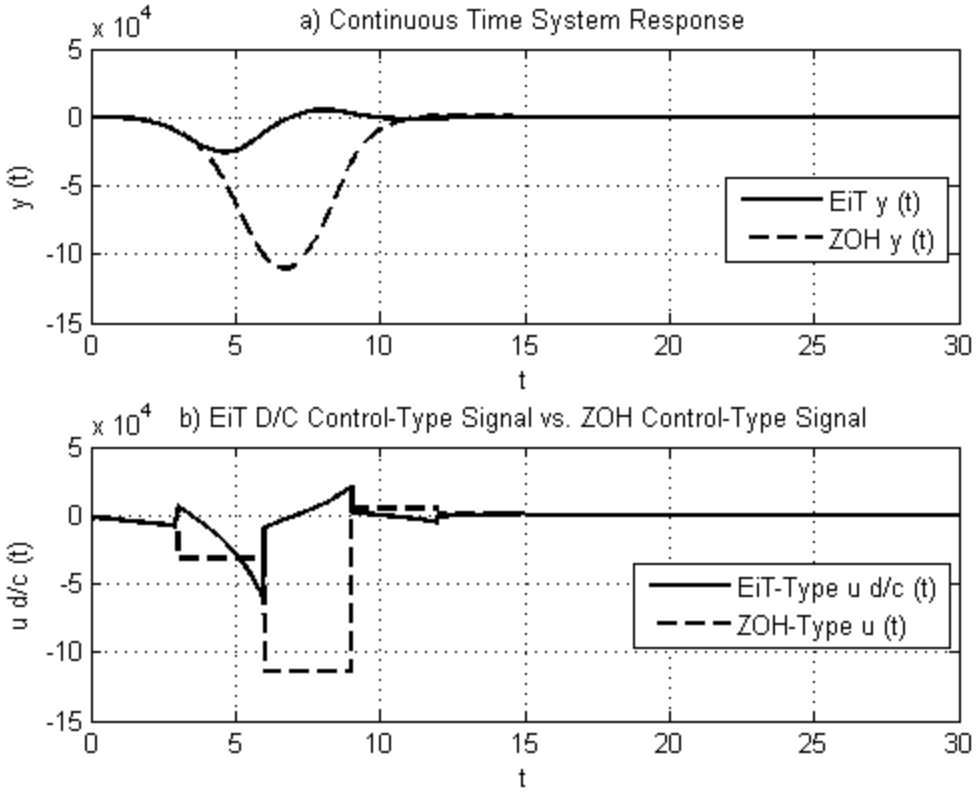

Figure 4.62 Disturbance Rejection (Cancellation) System Response for the Third-Order System with EiT-Type D/C Control

For the third-order SiT-type D/C observer of (4.109),

$$\overline{\mathrm{BH}} = \begin{bmatrix} 3.5406 & 2.1411 & 1.4978 \\ 2.6333 & 2.0429 & 2.1411 \\ 0.0429 & 0.4922 & 2.0429 \end{bmatrix}. \tag{4.116}$$

Control $u_p(t)$ is designed with $\widetilde{K}_{d/c}$ as calculated in (4.21). The simulated results for this design can be seen compared to the ZOH results in Figure 4.63.

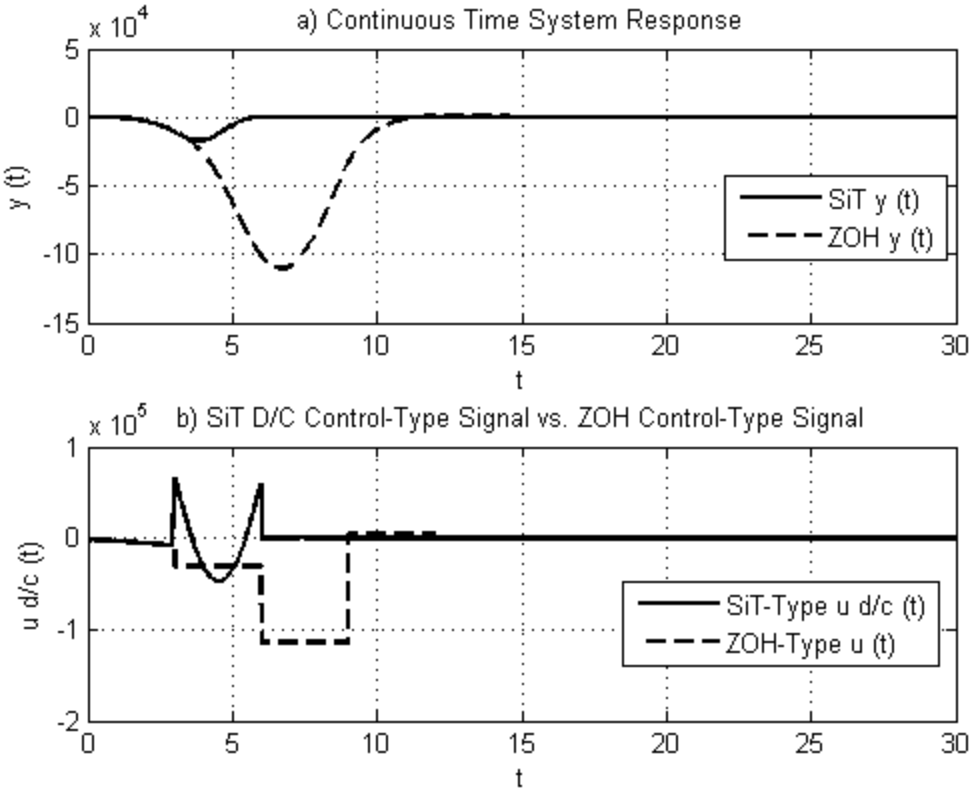

Figure 4.63 Disturbance Rejection (Cancellation) System Response for the Third-Order System with SiT-Type D/C Control

For the third-order PsiT-type D/C observer of (4.109),

$$\overline{\mathrm{BH}} = \begin{bmatrix} 3.5406 & 2.5749 & 3.2388 \\ 2.6333 & 2.7309 & 5.8137 \\ 0.0429 & 1.1799 & 8.5447 \end{bmatrix}. \tag{4.117}$$

Control $u_p(t)$ is designed with $\widetilde{K}_{d/c}$ as calculated in (4.22). The simulated results for this design can be seen compared to the ZOH results in Figure 4.64.

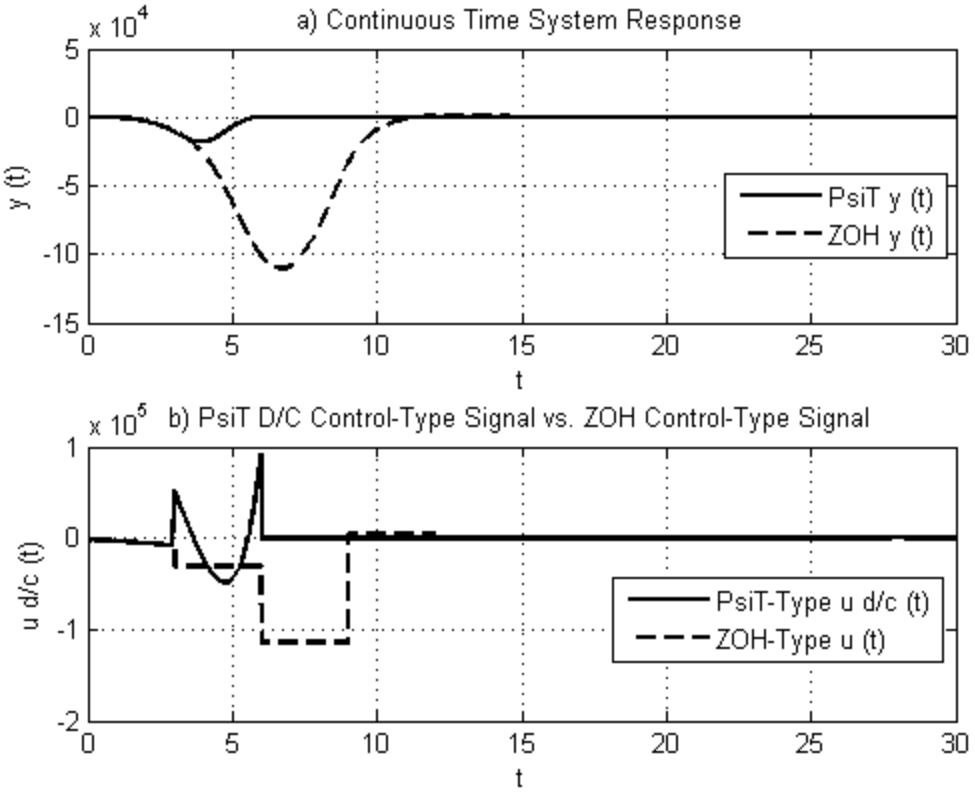

Figure 4.64 Disturbance Rejection (Cancellation) System Response for the Third-Order System with PsiT-Type D/C Control

In the third-order case, the LiT and EiT-type D/C controller performances resulted in greatly decreased magnitude of the system response during the control transient, as well as required one less control-decision/sample period than the ZOH-type controller to completely cancel the disturbance and stabilize the system. The SiT and PsiT-type D/C controller performances resulted in greatly decreased magnitude of the system response compared to both that of the ZOH-type controller and slightly decreased magnitude compared to the LiT and EiT-type D/C controllers. The SiT and PsiT-type D/C controllers required two less control decisions/sample periods to completely cancel the disturbance and stabilize the system, compared to the ZOH-type controller.

4.4 Summary of Performance Capabilities Demonstrated by the Examples

In consideration of control design, an array of plant models were considered, shown in Table 4.1. These choices were made for two reasons: (i) limitations in symbolic computing software exist in cases above third-order (where numerical integration techniques may be utilized [18]) when applying the pole assignment methods used in this research and (ii) specialized cases exist in the state space in some second-order plants control designs, which may lead to simplistic characteristics, masking behavior which would be exhibited fully in higher order cases. For this reason, it was necessary to include first, second, and third-order examples.

D/C-type Discrete-Time control was applied to the three cases for the variety of plants listed in Table 4.1, and compared to the ZOH case. Considerations include: overshoot / undershoot, stabilization time in terms of "deadbeat" response capability and "ultimate deadbeat" response capability, and quality of "complete-cancellation" of disturbances. It was found that in cases of first-order plants, the performance of D/C control and ZOH is similar. In these first-order models, differences between the undershoot and differences between the overshoot using D/C-type and ZOH-type discrete-time control are negligible. Both D/C-type and ZOH-type control provided "ultimate deadbeat" responses (since for all control-tasks in this case "ultimate deadbeat" and "deadbeat" response are equal for the first-order case). Complete disturbance cancellation through disturbance-observer design provided similar results for both D/C-type and ZOH-type discrete-time control for the first-order case, and the disturbance was able to be completely accommodated by the observer disturbance-observer state estimations.

However, in second-order plant models, the difference between the capability of D/C-type and ZOH-type discrete-time control becomes apparent. Each tested D/C control-type successfully accomplished the control task with only one control decision (one sample period $(T = 3)$). This was not true of the ZOH-type control design, and two control decisions (two sample periods $(T = 6)$) were needed to accomplish the control task with ZOH-type control. These results were consistent for each control task in the cases of closed-loop system pole assignment, system output driven to a designer-chosen set-point, and the system output driven to a command-signal. The magnitudes of the overshoot and undershoot were consistently higher for that of the ZOH-controlled system response than that of the D/C-controlled system responses and of disturbance state estimations (and therefore, disturbance-cancellation effectiveness).

In the third-order system examples, differences in the closed-loop performance between the D/C-controlled systems and the ZOH-controlled systems were more noticable. The SiT-type and PsiT-type D/C controls successfully accomplished the control tasks of i) stabilization, ii) set-point regulation, iii) signal-tracking, with only one sample-period decision (one sample period), providing "ultimate deadbeat" performance. The LiT-type and EiT-type D/C controls successfully accomplished the control tasks with two sample periods $(T = 6)$. While the LiT and EiT-type D/C control results were not "ultimate deadbeat" in the third-order cases due to the design of these particular D/C control algorithms, the response time was improved from the "deadbeat" performance of the ZOH-type control in terms of number of sample periods required for control-task achievement. The ZOH-type control required three sample periods, $(T = 9)$ to accomplish the control tasks. This was consistent for each control task considered.

While "deadbeat" performance of ZOH can yield favorable results, the "ultimate deadbeat" capability and reduced "settling-time" error of the ZOH-inclusive D/C-type controller could provide substantial reward. As system order is increased, the accommodation of a spline model which includes more basis functions could provide "ultimate deadbeat" performance for high-order systems. It should be noted that the basis functions and spline models employed here are only a few of many possibilities which exist with D/C-type generalized discrete-time control. For instance, other possibilities include special cases of Polynomial-in-time, such as Cubic-in-time functions, assemblages of Bessel functions, and others.

CHAPTER 5

SUMMARY, CONCLUSIONS, AND RECOMMENTATIONS FOR FURTHER WORK

5.1 Conclusions of the New "Discrete-Continuous" Generalization Control Performance and Practicality

The performance of D/C Generalized Discrete-Time Control was studied in this research. Three main areas of interest were investigated: (i) the form of $\overline{\mathrm{BH}}$ and structure of the matrix for differing plants and D/C control types, (ii) the study of values of T where $\overline{\mathrm{BH}}(\mathrm{T})$ has full-rank, which permits never-before possible discrete-time control design with remarkable capabilities to achieve the control task in one sample-period, (iii) a comparison to ZOH in control task accomplishment. The structure of $\overline{\mathrm{BH}}$ has been explored and further examples may be found in Appendix A.

5.2 New "Discrete-Continuous" –Type Discrete-Time Control as Compared to Modern ZOH-Type Control

While the goal of this paper is not to show the inferiority of ZOH-type discrete-time (which is still the most widely used type of discrete-time control throughout the

world), the comparison in the performance between ZOH and D/C control types considered here is revealing and useful. It has been shown by the results in Chapter 3 that D/C Control presents a superior alternative to the traditional ZOH. Due to the difference of inter-sample control-variation allowed by D/C control as compared to ZOH, several new performance capabilities arise.

Undershoot and Overshoot were generally reduced when employing D/C control, as compared to ZOH-type control. In the second-order case, all D/C-type controls performed equivalently. It was observed that the "best" performing D/C controls among those considered for the factors of reducing overshoot/undershoot in the third-order cases, were the SiT and PsiT control types.

Disturbance Accommodation (disturbance cancellation) was accomplished in all cases. This was accomplished with lower overshoot/undershoot and in the third-order case, shorter response-time when using D/C control. For the third-order plant, the best case of SiT and PsiT-type D/C controls were able to directly cancel the disturbance and stabilize the system with three less control decisions than the best case of ZOH-type control.

An important question in the research of this paper is, "Was ZOH ever chosen over D/C Generalized Control when the D/C spline included the ZOH basis-function $f_i(t) = 1$?" While the possibility exists that such a case could arise, the answer to such a question in the scope of this work is that, no, in fact ZOH was never preferred as the "better" choice over the ZOH-inclusive D/C control. This discovery was made possible by including ZOH in every D/C control type used within the scope of this paper as mentioned in Chapter 1.

5.3 Applicability to Different Plant Types

D/C-type control is applicable to a wide variety of plants, including high-order plants and those with time-varying system matrices, providing numerical integration methods such as [18] are utilized, and adequate computation ability and memory is available. There is an advantage to using ZOH control through the simplicity of the control design techniques. While D/C was symbolically difficult above a 3rd order case (in particular, calculation of the counterflow dual-kernal integration), ZOH calculation of $\tilde{B}$ is significantly less difficult for high-order cases.

5.4 Possible Applications

It is suggested, due to the rigorous calculations necessary for higher-order systems, that a D/C-type control is to be selected within the computational budget of the control designer. While it is not outside the scope of calculation to include higher order D/C control types (such as higher order polynomial terms and such terms as Bessel functions, etc.), the use of LiT-type D/C control is most practical, given the performance preference it offers over ZOH-type control and the degree of calculation necessary.

A possible application is with FPAAs (Field Programmable Analog Arrays) in the control of missile guidance and other aircraft and military-oriented fields. Such devices contain configurable analog component networks and are currently manufactured by companies such as Anadigm®, Altera, and Xilinx, Inc. These devices contain the capability to program gain values in the structure of the D/C control matrix $\widetilde{K}_{d/c}$ utilized in this paper.

Applications are extended to any control task which currently uses ZOH control. By even extending such a control to LiT-type D/C (so that intersample behavior is

allowed both a constant and a slope, determined at the decision / sample times), it has been shown that control can be significantly improved for cases above first-order.

APPENDICES

APPENDIX A

Continuation of Chapter 3: Exact, Symbolic Computations of the D/C Convolution-Matrix $\overline{\mathbf{BH}}$ for Some Common Plant Models and Types of D/C Control

This appendix is a continuation of the symbolic expressions for the D/C convolution matrix $\overline{\mathrm{BH}}$ in Chapter 3 using the following types of scalar D/C control.

Table A.1 D/C Spline Models and Related Control Matrices

Control Type	D/C Spline Model $u_{d/c}(t)$	$\bar{\mathbf{D}}$ (Phase Variables)	$\bar{\mathbf{H}}$ (Phase Variables)
LiT	$c_1 + c_2 t$	$\begin{bmatrix} 0 & 1 \\ 0 & 0 \end{bmatrix}$	$\begin{bmatrix} 1 & 0 \end{bmatrix}$
SiT	$c_1 + c_2 \sin(\omega t) + c_3 \cos(\omega t)$	$\begin{bmatrix} 0 & 1 & 0 \\ 0 & 0 & 1 \\ 0 & -\omega^2 & 0 \end{bmatrix}$	$\begin{bmatrix} 1 & 0 & 0 \end{bmatrix}$
EiT	$c_1 + c_2 e^{\alpha t}$	$\begin{bmatrix} 0 & 1 \\ \alpha & 0 \end{bmatrix}$	$\begin{bmatrix} 1 & 0 \end{bmatrix}$
PsiT	$c_1 + c_2 t e^{\alpha t}$	$\begin{bmatrix} 0 & 1 & 0 \\ 0 & 0 & 1 \\ 0 & -\alpha^2 & 2\alpha \end{bmatrix}$	$\begin{bmatrix} 1 & 0 & 0 \end{bmatrix}$

In each individual example, the elements of the associated $\overline{BH}$ matrix are denoted by bh_{ij} or $bh_{ij,k}$, in order to simplify the presentation-format.

A.1 Second-Order Plant Models (Phase-Variables) $\dot{\mathbf{x}} = \mathbf{Ax} + \mathbf{Bu}_{d/c}(t)$; n = 2, r = 1

Table A.2 Second-Order Plant Models (Phase-Variables)

Case Number	Plant Model	**A**	**B**
1	$\ddot{y} = u$	$\mathbf{A} = \begin{bmatrix} 0 & 1 \\ 0 & 0 \end{bmatrix}$	$B = \begin{bmatrix} 0 \\ 1 \end{bmatrix}$
2	$\ddot{y} - y = u$	$A = \begin{bmatrix} 0 & 1 \\ 1 & 0 \end{bmatrix}$	$B = \begin{bmatrix} 0 \\ 1 \end{bmatrix}$
3	$\ddot{y} - ay = u$	$A = \begin{bmatrix} 0 & 1 \\ a & 0 \end{bmatrix}$	$B = \begin{bmatrix} 0 \\ 1 \end{bmatrix}$
4	$\ddot{y} + \omega_n^2 y = u$	$A = \begin{bmatrix} 0 & 1 \\ -\omega_n{}^2 & 0 \end{bmatrix}$	$B = \begin{bmatrix} 0 \\ 1 \end{bmatrix}$
5	$\ddot{y} + \dot{y} + y = u$	$A = \begin{bmatrix} 0 & 1 \\ -1 & -1 \end{bmatrix}$	$B = \begin{bmatrix} 0 \\ 1 \end{bmatrix}$
6	$\ddot{y} + a_2\dot{y} + a_1 y = u$	$A = \begin{bmatrix} 0 & 1 \\ -a_1 & -a_2 \end{bmatrix}$	$B = \begin{bmatrix} 0 \\ 1 \end{bmatrix}$

A.1.1 Second-Order Plant Model; Case 1

For the LiT-type D/C control, $\overline{BH}$ is

$$\overline{BH} = \begin{bmatrix} bh_{11} & bh_{12} \\ bh_{21} & bh_{22} \end{bmatrix}_{2\times 2} \tag{A.1}$$

$$bh_{11} \triangleq \left(\frac{1}{2}T^2\right) \tag{A.2}$$

$$bh_{12} \triangleq \left(\frac{1}{6}T^3\right) \tag{A.3}$$

$$bh_{21} \triangleq \left(T\right) \tag{A.4}$$

$$bh_{22} \triangleq \left(\frac{1}{2}T^2\right) \tag{A.5}$$

For the SiT-type D/C control, $\overline{BH}$ is

$$\overline{BH} = \begin{bmatrix} bh_{11} & bh_{12} & bh_{13} \\ bh_{21} & bh_{22} & bh_{23} \end{bmatrix}_{2\times 3} \tag{A.6}$$

$$bh_{11} \triangleq \left(\frac{1}{2}T^2\right) \tag{A.7}$$

$$bh_{12} \triangleq \left[\frac{1}{\omega^3}\left(\omega T - \sin\left(\omega T\right)\right)\right] \tag{A.8}$$

$$bh_{13} \triangleq \left[\frac{1}{2\omega^4}\left(\omega^2T^2 - 2 + 2\cos\left(\omega T\right)\right)\right] \tag{A.9}$$

$$bh_{21} \triangleq \left(T\right) \tag{A.10}$$

$$bh_{22} \triangleq \left[\frac{1}{\omega^2}\left(1 - \cos\left(\omega T\right)\right)\right] \tag{A.11}$$

$$bh_{23} \triangleq \left[\frac{1}{\omega^3}\left(\omega T - \sin\left(\omega T\right)\right)\right] \tag{A.12}$$

For the EiT-type D/C control, $\overline{BH}$ is

$$\overline{BH} = \begin{bmatrix} bh_{11} & bh_{12} \\ bh_{21} & bh_{22} \end{bmatrix}_{2\times 2} \tag{A.13}$$

$$bh_{11} \triangleq \left[\frac{1}{2\alpha}\left(e^{(\sqrt{\alpha}T)} + e^{-(\sqrt{\alpha}T)} - 2 \right) \right] \tag{A.14}$$

$$bh_{12} \triangleq \left[\frac{1}{2\alpha^{\frac{3}{2}}}\left(e^{(\sqrt{\alpha}T)} - e^{-(\sqrt{\alpha}T)} - 2\sqrt{\alpha}T \right) \right] \tag{A.15}$$

$$bh_{21} \triangleq \left[\frac{1}{2\sqrt{\alpha}}\left(e^{(\sqrt{\alpha}T)} - e^{-(\sqrt{\alpha}T)} \right) \right] \tag{A.16}$$

$$bh_{22} \triangleq \left[\frac{1}{2\alpha}\left(e^{(\sqrt{\alpha}T)} + e^{-(\sqrt{\alpha}T)} - 2 \right) \right] \tag{A.17}$$

For the PsiT-type D/C control, $\overline{BH}$ is

$$\overline{BH} = \begin{bmatrix} bh_{11} & bh_{12} & bh_{13} \\ bh_{21} & bh_{22} & bh_{23} \end{bmatrix}_{2\times 3} \tag{A.18}$$

$$bh_{11} \triangleq \left(\frac{1}{2}T^2 \right) \tag{A.19}$$

$$bh_{12} \triangleq \left[\frac{1}{\alpha^3}\left((4-\alpha T)e^{(\alpha T)} - \left(4 + 3\alpha T + \alpha^2 T^2 \right) \right) \right] \tag{A.20}$$

$$bh_{13} \triangleq \left[\frac{1}{2\alpha^4}\left((2\alpha T - 6)e^{(\alpha T)} + \left(6 + 4\alpha T + \alpha^2 T^2 \right) \right) \right] \tag{A.21}$$

$$bh_{21} \triangleq (T) \tag{A.22}$$

$$bh_{22} \triangleq \left[\frac{1}{\alpha^2}\left((3-\alpha T)e^{(\alpha T)} - (3 + 2\alpha T) \right) \right] \tag{A.23}$$

$$bh_{23} \triangleq \left[\frac{1}{\alpha^3}\left((\alpha T - 2)e^{(\alpha T)} + (2 + T\alpha) \right) \right] \tag{A.24}$$

A.1.2 Second-Order Plant Model; Case 2

For the LiT-type D/C control $\overline{BH}$ is

$$\overline{BH} = \begin{bmatrix} bh_{11} & bh_{12} \\ bh_{21} & bh_{22} \end{bmatrix}_{2\times 2} \tag{A.25}$$

$$bh_{11} \triangleq \left[\frac{1}{2}\left(e^{T} + e^{-T} - 2\right)\right] \tag{A.26}$$

$$bh_{12} \triangleq \left[\frac{1}{2}\left(e^{T} - e^{-T} - 2T\right)\right] \tag{A.27}$$

$$bh_{21} \triangleq \left[\frac{1}{2}\left(e^{T} - e^{-T}\right)\right] \tag{A.28}$$

$$bh_{22} \triangleq \left[\frac{1}{2}\left(e^{T} + e^{-T} - 2\right)\right] \tag{A.29}$$

For the SiT-type D/C control, $\overline{BH}$ is

$$\overline{BH} = \begin{bmatrix} bh_{11} & bh_{12} & bh_{13} \\ bh_{21} & bh_{22} & bh_{23} \end{bmatrix}_{2\times 3} \tag{A.30}$$

$$bh_{11} \triangleq \left[\frac{1}{2}\left(e^{T} + e^{(-T)} - 2\right)\right] \tag{A.31}$$

$$bh_{12} \triangleq \left[\frac{1}{2\omega\left(1+\omega^{2}\right)}\left(\omega\left(e^{T} - e^{-T}\right) - 2\sin\left(\omega T\right)\right)\right] \tag{A.32}$$

$$bh_{13} \triangleq \left[\frac{1}{2\omega^{2}\left(1+\omega^{2}\right)}\left(\omega^{2}\left(e^{T} + e^{-T}\right) + 2\cos\left(\omega T\right) - 2\left(1+\omega^{2}\right)\right)\right] \tag{A.33}$$

$$bh_{21} \triangleq \left[\frac{1}{2}\left(e^{T} - e^{-T}\right)\right] \tag{A.34}$$

$$bh_{22} \triangleq \left[\frac{1}{2\left(1+\omega^{2}\right)}\left(e^{T} + e^{-T} - 2\cos\left(\omega T\right)\right)\right] \tag{A.35}$$

$$bh_{23} \triangleq \left[\frac{1}{2\omega\left(1+\omega^2\right)} \left(\omega\left(e^{T} - e^{-T}\right) - 2\sin\left(\omega T\right) \right) \right] \tag{A.36}$$

For the EiT-type D/C control, $\overline{BH}$ is

$$\overline{BH} = \begin{bmatrix} bh_{11} & bh_{12} \\ bh_{21} & bh_{22} \end{bmatrix}_{2\times 2} \tag{A.37}$$

$$bh_{11} \triangleq \left[\frac{1}{2\left(\alpha-1\right)} \left(-\left(e^{T} + e^{-T}\right) + e^{\left(\sqrt{\alpha}T\right)} + e^{-\left(\sqrt{\alpha}T\right)} \right) \right] \tag{A.38}$$

$$bh_{12} \triangleq \left[\frac{1}{2\sqrt{\alpha}\left(\alpha-1\right)} \left(\sqrt{\alpha}\left(-e^{T} + e^{-T}\right) + e^{\left(\sqrt{\alpha}T\right)} - e^{-\left(\sqrt{\alpha}T\right)} \right) \right] \tag{A.39}$$

$$bh_{21} \triangleq \left[\frac{1}{2\left(\alpha-1\right)} \left(-e^{T} + e^{-T} + \sqrt{\alpha}\left(e^{\left(\sqrt{\alpha}T\right)} - e^{-\left(\sqrt{\alpha}T\right)} \right) \right) \right] \tag{A.40}$$

$$bh_{22} \triangleq \left[\frac{1}{2\left(\alpha-1\right)} \left(-\left(e^{T} + e^{-T}\right) + e^{\left(\sqrt{\alpha}T\right)} + e^{-\left(\sqrt{\alpha}T\right)} \right) \right] \tag{A.41}$$

For the PsiT-type D/C control, $\overline{BH}$ is

$$\overline{BH} = \begin{bmatrix} bh_{11} & \left(bh_{12,1} + bh_{12,2}\right) & \left(bh_{13,1} + bh_{13,2}\right) \\ bh_{21} & \left(bh_{22,1} + bh_{22,2}\right) & bh_{23} \end{bmatrix}_{2\times 3} \tag{A.42}$$

$$d \triangleq \left[\left(\alpha-1\right)^2 \left(1+\alpha\right)^2 \right] \tag{A.43}$$

$$bh_{11} \triangleq \left[\frac{1}{2} \left(e^{T} + e^{-T} - 2 \right) \right] \tag{A.44}$$

$$bh_{12,1} \triangleq \left[\frac{1}{2\alpha d} \left(\left(-2\alpha^4 - 3\alpha^3 + \alpha\right) e^{T} + \left(3\alpha^3 - \alpha - 2\alpha^4\right) e^{-T} \right) \right] \tag{A.45}$$

$$bh_{12,2} \triangleq \left[\frac{1}{2\alpha d} \left(\left(2\alpha T\left(1-\alpha^2\right) + 8\alpha^2 - 4\right) e^{(\alpha T)} + 4\left(\alpha^4 - 2\alpha^2 + 1\right) \right) \right] \tag{A.46}$$

$$bh_{13,1} \triangleq \left[\frac{1}{2\alpha^2 d}\left(\left(2\alpha^3+\alpha^2+\alpha^4\right)e^{T}+\left(-2\alpha^3+\alpha^2+\alpha^4\right)e^{-T}\right)\right] \tag{A.47}$$

$$bh_{13,2} \triangleq \left[\frac{1}{2\alpha^2 d}\left(\left(2T\alpha\left(\alpha^2-1\right)-6\alpha^2+2\right)e^{(T\alpha)}-2\alpha^4+4\alpha^2-2\right)\right] \tag{A.48}$$

$$bh_{21} \triangleq \left[\frac{1}{2}\left(e^{T}-e^{-T}\right)\right] \tag{A.49}$$

$$bh_{22,1} \triangleq \left[\frac{1}{2d}\left(\left(-2\alpha^3-3\alpha^2+1\right)e^{T}+\left(-3\alpha^2+1+2\alpha^3\right)e^{-T}\right)\right] \tag{A.50}$$

$$bh_{22,2} \triangleq \left[\frac{1}{2d}\left(-2T\alpha^3-2+6\alpha^2+2T\alpha\right)e^{(T\alpha)}\right] \tag{A.51}$$

$$bh_{23} \triangleq \left[\frac{1}{2d}\left(\left(2\alpha+\alpha^2+1\right)e^{T}+\left(-4\alpha-2T+2T\alpha^2\right)e^{(T\alpha)}+\left(-1-\alpha^2+2\alpha\right)e^{-T}\right)\right] \tag{A.52}$$

A.1.3 Second-Order Plant Model; Case 3

For the LiT-type D/C control, $\overline{BH}$ is

$$\overline{BH} = \begin{bmatrix} bh_{11} & bh_{12} \\ bh_{21} & bh_{22} \end{bmatrix}_{2\times 2} \tag{A.53}$$

$$bh_{11} \triangleq \left[\frac{1}{2a}\left(e^{\left(\sqrt{a}T\right)}+e^{-\left(\sqrt{a}T\right)}-2\right)\right] \tag{A.54}$$

$$bh_{12} \triangleq \left[\frac{1}{2a^{\frac{3}{2}}}\left(e^{\left(\sqrt{a}T\right)}-e^{-\left(\sqrt{a}T\right)}-2\sqrt{a}T\right)\right] \tag{A.55}$$

$$bh_{21} \triangleq \left[\frac{1}{2\sqrt{a}}\left(e^{\left(\sqrt{a}T\right)}-e^{-\left(\sqrt{a}T\right)}\right)\right] \tag{A.56}$$

$$bh_{22} \triangleq \left[\frac{1}{2a}\left(e^{\left(\sqrt{a}T\right)}+e^{-\left(\sqrt{a}T\right)}-2\right)\right] \tag{A.57}$$

For the SiT-type D/C control, $\overline{BH}$ is

$$\overline{BH} = \begin{bmatrix} bh_{11} & bh_{12} & bh_{13} \\ bh_{21} & bh_{22} & bh_{23} \end{bmatrix}_{2\times 3} \tag{A.58}$$

$$bh_{11} \triangleq \left[\frac{1}{2a}\left(e^{\left(\sqrt{a}T\right)} + e^{-\left(\sqrt{a}T\right)} - 2 \right) \right] \tag{A.59}$$

$$bh_{12} \triangleq \left[\frac{1}{2\sqrt{a}\omega\left(a+\omega^2\right)}\left(\omega e^{\left(\sqrt{a}T\right)} - \omega e^{-\left(\sqrt{a}T\right)} - 2\sqrt{a}\sin\left(\omega T\right) \right) \right] \tag{A.60}$$

$$bh_{13} \triangleq \left[\frac{1}{2a\omega^2\left(a+\omega^2\right)}\left(\omega^2\left(e^{\left(\sqrt{a}T\right)} + e^{-\left(\sqrt{a}T\right)} \right) + 2a\cos\left(\omega T\right) - 2a - 2\omega^2 \right) \right] \tag{A.61}$$

$$bh_{21} \triangleq \left[\frac{1}{2\sqrt{a}}\left(e^{\left(\sqrt{a}T\right)} - e^{-\left(\sqrt{a}T\right)} \right) \right] \tag{A.62}$$

$$bh_{22} \triangleq \left[\frac{1}{2\left(a+\omega^2\right)}\left(e^{\left(\sqrt{a}T\right)} + e^{-\left(\sqrt{a}T\right)} - 2\cos\left(\omega T\right) \right) \right] \tag{A.63}$$

$$bh_{23} \triangleq \left[\frac{1}{2\sqrt{a}\omega\left(a+\omega^2\right)}\left(\omega\left(e^{\left(\sqrt{a}T\right)} - e^{-\left(\sqrt{a}T\right)} \right) - 2\sqrt{a}\sin\left(\omega T\right) \right) \right] \tag{A.64}$$

For the EiT-type D/C control, $\overline{BH}$ is

$$\overline{BH} = \begin{bmatrix} bh_{11} & bh_{12} \\ bh_{21} & bh_{22} \end{bmatrix}_{2\times 2} \tag{A.65}$$

$$bh_{11} \triangleq \left[\frac{1}{2\left(a-\alpha\right)}\left(e^{\left(\sqrt{a}T\right)} + e^{-\left(\sqrt{a}T\right)} - e^{\left(\sqrt{\alpha}T\right)} - e^{-\left(\sqrt{\alpha}T\right)} \right) \right] \tag{A.66}$$

$$bh_{12} \triangleq \left[\frac{1}{2\sqrt{a}\sqrt{\alpha}\left(a-\alpha\right)}\sqrt{\alpha}\left(e^{\left(\sqrt{a}T\right)} - e^{-\left(\sqrt{a}T\right)} \right) - \sqrt{a}\left(e^{\left(\sqrt{\alpha}T\right)} - e^{-\left(\sqrt{\alpha}T\right)} \right) \right] \tag{A.67}$$

$$bh_{21} \triangleq \left[\frac{1}{2(a-\alpha)} \left(\sqrt{a} \left(e^{(\sqrt{a}T)} - e^{-(\sqrt{a}T)} \right) - \sqrt{\alpha} \left(e^{(\sqrt{\alpha}T)} - e^{-(\sqrt{\alpha}T)} \right) \right) \right] \tag{A.68}$$

$$bh_{22} \triangleq \left[\frac{1}{2(a-\alpha)} \left(e^{(\sqrt{a}T)} + e^{-(\sqrt{a}T)} - e^{(\sqrt{\alpha}T)} - e^{-(\sqrt{\alpha}T)} \right) \right] \tag{A.69}$$

For the PsiT-type D/C control, $\overline{BH}$ is

$$\overline{BH} = \begin{bmatrix} bh_{11} & \left(bh_{12,1} + bh_{12,2}\right) & \left(bh_{13,1} + bh_{13,2}\right) \\ bh_{21} & \left(bh_{22,1} + bh_{22,2}\right) & \left(bh_{23,1} + bh_{23,2}\right) \end{bmatrix}_{2\times 3} \tag{A.70}$$

$$q \triangleq \left(\sqrt{a}\right) \tag{A.71}$$

$$d \triangleq \left[(q-\alpha)^2 (q+\alpha)^2 \right] \tag{A.72}$$

$$bh_{11} \triangleq \left[\frac{1}{2q^2} \left(e^{(qT)} + e^{-(qT)} - 2 \right) \right] \tag{A.73}$$

$$bh_{12,1} \triangleq \left[\frac{1}{2\alpha q^2 d} \left(\left(q^3\alpha - 3q\alpha^3 - 2\alpha^4 \right) e^{(qT)} + \left(-q^3\alpha + 3q\alpha^3 - 2\alpha^4 \right) e^{-(qT)} \right) \right] \tag{A.74}$$

$$bh_{12,2} \triangleq \left[\frac{1}{\alpha q^2 d} \left(q^2 \left(q^2\alpha T - \alpha^3 T - 2q^2 + 4\alpha^2 \right) e^{(\alpha T)} + 2\left(\alpha^2 - q^2 \right)^2 \right) \right] \tag{A.75}$$

$$bh_{13,1} \triangleq \left[\frac{1}{2q^2\alpha^2 d} \left(\left(2q\alpha^3 + \alpha^2 q^2 + \alpha^4 \right) e^{(qT)} + \left(-2q\alpha^3 + \alpha^2 q^2 + \alpha^4 \right) e^{-(qT)} \right) \right] \tag{A.76}$$

$$bh_{13,2} \triangleq \left[\frac{1}{q^2\alpha^2 d} \left(q^2 \left(\alpha^3 T - q^2\alpha T - 3\alpha^2 + q^2 \right) e^{(\alpha T)} - (\alpha - q)^2 \right) \right] \tag{A.77}$$

$$bh_{21} \triangleq \left[\frac{1}{2q} \left(e^{(qT)} - e^{-(qT)} \right) \right] \tag{A.78}$$

$$bh_{22,1} \triangleq \left[\frac{1}{2qd} \left(\left(q^3 - 3q\alpha^2 - 2\alpha^3 \right) e^{(qT)} + \left(q^3 - 3q\alpha^2 + 2\alpha^3 \right) e^{-(qT)} \right) \right] \tag{A.79}$$

$$bh_{22,2} \triangleq \left[\frac{1}{d} \left(q^2 \left(\alpha T - 1 \right) + \alpha^2 \left(3 - \alpha T \right) \right) e^{(\alpha T)} \right] \tag{A.80}$$

$$bh_{23,1} \triangleq \left[\frac{1}{2qd} \left(\left(q + \alpha \right)^2 e^{(qT)} - \left(q - \alpha \right)^2 e^{-(qT)} \right) \right] \tag{A.81}$$

$$bh_{23,2} \triangleq \left[\frac{1}{d} \left(\left(\alpha^2 - q^2 \right) T - 2\alpha \right) e^{(\alpha T)} \right] \tag{A.82}$$

A.1.4 Second-Order Plant Model; Case 4

For the LiT-type D/C control, $\overline{BH}$ is

$$\overline{BH} = \begin{bmatrix} bh_{11} & bh_{12} \\ bh_{21} & bh_{22} \end{bmatrix}_{2\times 2} \tag{A.83}$$

$$bh_{11} \triangleq \left[\frac{1}{\omega_n^2} \left(1 - \cos\left(\omega_n T \right) \right) \right] \tag{A.84}$$

$$bh_{12} \triangleq \left[\frac{1}{\omega_n^3} \left(\omega_n T - \sin\left(\omega_n T \right) \right) \right] \tag{A.85}$$

$$bh_{21} \triangleq \left[\frac{1}{\omega_n} \sin\left(\omega_n T \right) \right] \tag{A.86}$$

$$bh_{22} \triangleq \left[\frac{1}{\omega_n^2} \left(1 - \cos\left(\omega_n T \right) \right) \right] \tag{A.87}$$

For the SiT-type D/C control, $\overline{BH}$ is

$$\overline{BH} = \begin{bmatrix} bh_{11} & bh_{12} & bh_{13} \\ bh_{21} & bh_{22} & bh_{23} \end{bmatrix}_{2\times 3} \tag{A.88}$$

$$bh_{11} \triangleq \left[\frac{1}{\omega_n{}^2} \left(1 - \cos\left(\omega_n T \right) \right) \right] \tag{A.89}$$

$$bh_{12} \triangleq \left[\frac{1}{\omega_n \omega \left(\omega^2 - {\omega_n}^2 \right)} \left(\omega \sin\left(\omega_n T \right) - \omega_n \sin\left(\omega T \right) \right) \right] \tag{A.90}$$

$$bh_{13} \triangleq \left[\frac{1}{{\omega_n}^2 \omega^2 \left(\omega^2 - {\omega_n}^2 \right)} \left({\omega_n}^2 \cos\left(\omega T \right) - \omega^2 \cos\left(\omega_n T \right) + \omega^2 - {\omega_n}^2 \right) \right] \tag{A.91}$$

$$bh_{21} \triangleq \left[\frac{1}{\omega_n} \sin\left(\omega_n T \right) \right] \tag{A.92}$$

$$bh_{22} \triangleq \left[\frac{1}{\omega^2 - {\omega_n}^2} \left(\cos\left(\omega_n T \right) - \cos\left(\omega T \right) \right) \right] \tag{A.93}$$

$$bh_{23} \triangleq \left[\frac{1}{\omega_n \omega \left(\omega^2 - {\omega_n}^2 \right)} \left(\omega \sin\left(\omega_n T \right) - \omega_n \sin\left(\omega T \right) \right) \right] \tag{A.94}$$

For the EiT-type D/C control, $\overline{BH}$ is

$$\overline{BH} = \begin{bmatrix} bh_{11} & bh_{12} \\ bh_{21} & bh_{22} \end{bmatrix}_{2\times 2} \tag{A.95}$$

$$bh_{11} \triangleq \left[\frac{1}{2\left(\alpha + \omega_n^2 \right)} \left(-2\cos\left(\omega_n T \right) + e^{\left(\sqrt{\alpha} T \right)} + e^{-\left(\sqrt{\alpha} T \right)} \right) \right] \tag{A.96}$$

$$bh_{12} \triangleq \left[\frac{1}{2\sqrt{\alpha}\omega_n \left(\alpha + \omega_n^2 \right)} \left(-2\sqrt{\alpha} \sin\left(\omega_n T \right) + \omega_n \left(e^{\left(\sqrt{\alpha} T \right)} - e^{-\left(\sqrt{\alpha} T \right)} \right) \right) \right] \tag{A.97}$$

$$bh_{21} \triangleq \left[\frac{1}{2\left(\alpha + \omega_n^2 \right)} \left(2\omega_n \sin\left(\omega_n T \right) + \sqrt{\alpha} \left(e^{\left(\sqrt{\alpha} T \right)} - e^{-\left(\sqrt{\alpha} T \right)} \right) \right) \right] \tag{A.98}$$

$$bh_{22} \triangleq \left[\frac{1}{2\left(\alpha + \omega_n^2 \right)} \left(-2\cos\left(\omega_n T \right) + e^{\left(\sqrt{\alpha} T \right)} + e^{-\left(\sqrt{\alpha} T \right)} \right) \right] \tag{A.99}$$

For the PsiT-type D/C control, $\overline{\mathrm{BH}}$ is

$$\overline{\mathrm{BH}} = \begin{bmatrix} \mathrm{bh}_{11} & \left(\mathrm{bh}_{12,1} + \mathrm{bh}_{12,2}\right) & \left(\mathrm{bh}_{13,1} + \mathrm{bh}_{13,2}\right) \\ \mathrm{bh}_{21} & \left(\mathrm{bh}_{22,1} + \mathrm{bh}_{22,2}\right) & \left(\mathrm{bh}_{23,1} + \mathrm{bh}_{23,2}\right) \end{bmatrix}_{2\times 3} \tag{A.100}$$

$$\mathrm{bh}_{11} = \left[\frac{1}{\omega_n^2}\left(1-\cos\left(\omega_n \mathrm{T}\right)\right)\right] \tag{A.101}$$

$$\mathrm{bh}_{12,1} \triangleq \left[\frac{1}{\omega_n^2\left(\alpha^2+\omega_n^2\right)^2}\left(2\alpha^3\cos\left(\omega_n \mathrm{T}\right) - \omega_n\left(\omega_n^2+3\alpha^2\right)\sin\left(\omega_n \mathrm{T}\right)\right)\right] \tag{A.102}$$

$$\mathrm{bh}_{12,2} \triangleq \left[\frac{1}{\alpha\omega_n^2\left(\alpha^2+\omega_n^2\right)^2}\left(\omega_n^2\left(2\omega_n^2+4\alpha^2-\alpha^3\mathrm{T}-\alpha\omega_n^2\mathrm{T}\right)\mathrm{e}^{(\alpha \mathrm{T})} - 2\left(\alpha^2+\omega_n^2\right)^2\right)\right] \tag{A.103}$$

$$\mathrm{bh}_{13,1} \triangleq \left[\frac{1}{\omega_n^2\left(\alpha^2+\omega_n^2\right)^2}\left(\left(\omega_n^2-\alpha^2\right)\cos\left(\omega_n \mathrm{T}\right) + 2\alpha\omega_n\sin\left(\omega_n \mathrm{T}\right)\right)\right] \tag{A.104}$$

$$\mathrm{bh}_{13,2} \triangleq \left[\frac{1}{\alpha^2\omega_n^2\left(\alpha^2+\omega_n^2\right)^2}\left(\omega_n^2\left(\alpha^3\mathrm{T}+\alpha\omega_n^2\mathrm{T}-3\alpha^2-\omega_n^2\right)\mathrm{e}^{(\alpha \mathrm{T})} + \left(\alpha^2+\omega_n^2\right)^2\right)\right] \tag{A.105}$$

$$\mathrm{bh}_{21} \triangleq \left[\frac{1}{\omega_n}\sin\left(\omega_n \mathrm{T}\right)\right] \tag{A.106}$$

$$\mathrm{bh}_{22,1} \triangleq \left[\frac{1}{\left(\alpha^2+\omega_n^2\right)^2}\left(3\alpha^2+\omega_n^2-\alpha^3\mathrm{T}-\omega_n^2\alpha\mathrm{T}\right)\mathrm{e}^{(\alpha \mathrm{T})}\right] \tag{A.107}$$

$$\mathrm{bh}_{22,2} \triangleq \left[\frac{-1}{\omega_n\left(\alpha^2+\omega_n^2\right)^2}\left(\omega_n\left(3\alpha^2+\omega_n^2\right)\cos\left(\omega_n \mathrm{T}\right) + 2\alpha^3\sin\left(\omega_n \mathrm{T}\right)\right)\right] \tag{A.108}$$

$$\mathrm{bh}_{23,1} \triangleq \left[\frac{1}{\left(\alpha^2+\omega_n^2\right)^2}\left(\alpha^2\mathrm{T}+\omega_n^2\mathrm{T}-2\alpha\right)\mathrm{e}^{(\alpha \mathrm{T})}\right] \tag{A.109}$$

$$bh_{23} \triangleq \left[\frac{1}{\omega_n \left(\alpha^2 + \omega_n^2\right)^2} \left(2\alpha\omega_n \cos\left(\omega_n T\right) + \left(\alpha^2 - \omega_n^2\right)\sin\left(\omega_n T\right)\right) \right] \tag{A.110}$$

A.1.5 Second-Order Plant Model; Case 5

For the LiT-type D/C control, $\overline{BH}$ is

$$\overline{BH} = \begin{bmatrix} bh_{11} & bh_{12} \\ bh_{21} & bh_{22} \end{bmatrix}_{2\times 2} \tag{A.111}$$

$$\theta \triangleq \left(\frac{\sqrt{3}}{2} T \right) \tag{A.112}$$

$$bh_{11} \triangleq \left[1 - \left(\cos\left(\theta\right) + \frac{1}{3}\sqrt{3}\sin\left(\theta\right) \right) e^{\left(\frac{-T}{2}\right)} \right] \tag{A.113}$$

$$bh_{12} \triangleq \left[\left(\cos\left(\theta\right) - \frac{1}{3}\sqrt{3}\sin\left(\theta\right) \right) e^{\left(\frac{-T}{2}\right)} + T - 1 \right] \tag{A.114}$$

$$bh_{21} \triangleq \left[\frac{2}{3}\sqrt{3}\sin\left(\theta\right) e^{\left(\frac{-T}{2}\right)} \right] \tag{A.115}$$

$$bh_{22} \triangleq \left[1 - \left(\cos\left(\theta\right) + \frac{1}{3}\sqrt{3}\sin\left(\theta\right) \right) e^{\left(\frac{-T}{2}\right)} \right] \tag{A.116}$$

For the SiT-type D/C control, $\overline{BH}$ is

$$\overline{BH} = \begin{bmatrix} bh_{11} & \left(bh_{12,1} + bh_{12,2}\right) & \left(bh_{13,1} + bh_{13,2}\right) \\ bh_{21} & \left(bh_{22,1} + bh_{22,2}\right) & \left(bh_{23,1} + bh_{23,2}\right) \end{bmatrix}_{2\times 3} \tag{A.117}$$

$$\theta \triangleq \left(\frac{\sqrt{3}}{2} T \right) \tag{A.118}$$

$$d \triangleq \left(1 - \omega^2 + \omega^4\right) \tag{A.119}$$

$$bh_{11} \triangleq \left[1-\frac{1}{3}\left(3\cos(\theta)+\sqrt{3}\sin(\theta)\right)e^{\left(\frac{-T}{2}\right)}\right] \tag{A.120}$$

$$bh_{12,1} \triangleq \left[\frac{1}{3d}\left(3\cos(\theta)+\sqrt{3}\left(2\omega^2-1\right)\sin(\theta)\right)e^{\left(\frac{-T}{2}\right)}\right] \tag{A.121}$$

$$bh_{12,2} \triangleq \left[\frac{1}{\omega d}\left(-\omega\cos(\omega T)+\left(1-\omega^2\right)\sin(\omega T)\right)\right] \tag{A.122}$$

$$bh_{13,1} \triangleq \left[\frac{1}{3d}\left(-3\omega^2\cos(\theta)+\sqrt{3}\left(2-\omega^2\right)\sin(\theta)\right)e^{\left(\frac{-T}{2}\right)}\right] \tag{A.123}$$

$$bh_{13,2} \triangleq \left[\frac{1}{\omega^2 d}\left(\left(\omega^2-1\right)\cos(\omega T)-\omega\sin(\omega T)+\omega^4-\omega^2+1\right)\right] \tag{A.124}$$

$$bh_{21} \triangleq \left[\frac{2}{3}\sqrt{3}e^{\left(\frac{-T}{2}\right)}\sin(\theta)\right] \tag{A.125}$$

$$bh_{22,1} \triangleq \left[\frac{1}{3d}\left(3\left(\omega^2-1\right)\cos(\theta)-\sqrt{3}\left(\omega^2+1\right)\sin(\theta)\right)e^{\left(\frac{-T}{2}\right)}\right] \tag{A.126}$$

$$bh_{22,2} \triangleq \left[\frac{1}{d}\left(\left(1-\omega^2\right)\cos(\omega T)+\omega\sin(\omega T)\right)\right] \tag{A.127}$$

$$bh_{23,1} \triangleq \left[\frac{1}{3d}\left(3\cos(\theta)+\sqrt{3}\left(2\omega^2-1\right)\sin(\theta)\right)e^{\left(\frac{-T}{2}\right)}\right] \tag{A.128}$$

$$bh_{23,2} \triangleq \left[\frac{-1}{\omega d}\left(\omega\cos(\omega T)+\left(\omega^2-1\right)\sin(\omega T)\right)\right] \tag{A.129}$$

For the EiT-type D/C control, $\overline{BH}$ is

$$\overline{BH} = \begin{bmatrix} \left(bh_{11,1}+bh_{11,2}\right) & \left(bh_{12,1}+bh_{12,2}\right) \\ \left(bh_{21,1}+bh_{21,2}\right) & \left(bh_{22,1}+bh_{22,2}\right) \end{bmatrix}_{2\times 2} \tag{A.130}$$

$$\theta \triangleq \left(\frac{\sqrt{3}}{2}T\right) \tag{A.131}$$

$$d \triangleq \left(1+\alpha+\alpha^2\right) \tag{A.132}$$

$$bh_{11,1} \triangleq \left[\frac{1}{3d}\left(-3(\alpha+1)\cos(\theta)+\sqrt{3}(\alpha-1)\sin(\theta)\right)e^{\left(\frac{-T}{2}\right)}\right] \tag{A.133}$$

$$bh_{11,2} \triangleq \left[\frac{1}{2d}\left(\left(\alpha-\sqrt{\alpha}+1\right)e^{(\sqrt{\alpha}T)}+\left(\alpha+\sqrt{\alpha}+1\right)e^{-(\sqrt{\alpha}T)}\right)\right] \tag{A.134}$$

$$bh_{12,1} \triangleq \left[\frac{1}{3d}\left(3\cos(\theta)-\sqrt{3}(2\alpha+1)\sin(\theta)\right)e^{\left(\frac{-T}{2}\right)}\right] \tag{A.135}$$

$$bh_{12,2} \triangleq \left[\frac{1}{2\sqrt{\alpha}d}\left(\left(\alpha-\sqrt{\alpha}+1\right)e^{(\sqrt{\alpha}T)}-\left(\alpha+\sqrt{\alpha}+1\right)e^{-(\sqrt{\alpha}T)}\right)\right] \tag{A.136}$$

$$bh_{21,1} \triangleq \left[\frac{1}{3d}\left(3\alpha\cos(\theta)+\sqrt{3}(2+\alpha)\sin(\theta)\right)e^{\left(\frac{-T}{2}\right)}\right] \tag{A.137}$$

$$bh_{21,2} \triangleq \left[\frac{\sqrt{\alpha}}{2d}\left(\left(\alpha-\sqrt{\alpha}+1\right)e^{(\sqrt{\alpha}T)}-\left(\alpha+\sqrt{\alpha}+1\right)e^{-(\sqrt{\alpha}T)}\right)\right] \tag{A.138}$$

$$bh_{22,1} \triangleq \left[\frac{1}{3d}\left(-3(\alpha+1)\cos(\theta)+\sqrt{3}(\alpha-1)\sin(\theta)\right)e^{\left(\frac{-T}{2}\right)}\right] \tag{A.139}$$

$$bh_{22,2} \triangleq \left[\frac{1}{2d}\left(\left(\alpha-\sqrt{\alpha}+1\right)e^{(\sqrt{\alpha}T)}+\left(\alpha+\sqrt{\alpha}+1\right)e^{-(\sqrt{\alpha}T)}\right)\right] \tag{A.140}$$

For the PsiT-type D/C control, $\overline{BH}$ is

$$\overline{BH} = \begin{bmatrix} bh_{11} & \left(bh_{12,1}+bh_{12,2}+bh_{12,3}+bh_{12,4}\right) & \left(bh_{13,1}+bh_{13,2}+bh_{13,3}\right) \\ bh_{21} & \left(bh_{22,1}+bh_{22,2}+bh_{22,3}\right) & \left(bh_{23,1}+bh_{23,2}\right) \end{bmatrix}_{2\times 3} \tag{A.141}$$

$$\theta \triangleq \left(\frac{\sqrt{3}}{2}T\right) \tag{A.142}$$

$$d \triangleq \left[\left(1+\alpha+\alpha^2\right)^2 \right] \tag{A.143}$$

$$bh_{11} \triangleq \left[-\cos(\theta) e^{\left(\frac{-T}{2}\right)} - \frac{1}{3}\sqrt{3}\sin(\theta) e^{\left(\frac{-T}{2}\right)} + 1 \right] \tag{A.144}$$

$$bh_{12,1} \triangleq \left[\frac{1}{\alpha d}\left(-\alpha^3 T + (4-T)\alpha^2 + (3-T)\alpha + 2\right) e^{(\alpha T)} \right] \tag{A.145}$$

$$bh_{12,2} \triangleq \left[\frac{1}{d}\left(2\alpha^3 + 4\alpha^2 + 2\alpha + 1\right)\cos(\theta) e^{\left(\frac{-T}{2}\right)} \right] \tag{A.146}$$

$$bh_{12,3} \triangleq \left[\frac{\sqrt{3}}{3d}\left(2\alpha^3 - 2\alpha^2 - 2\alpha - 1\right)\sin(\theta) e^{\left(\frac{-T}{2}\right)} \right] \tag{A.147}$$

$$bh_{12,4} \triangleq \left[\frac{-2}{\alpha d}\left(\alpha^4 + 2\alpha^3 + 3\alpha^2 + 2\alpha + 1\right) \right] \tag{A.148}$$

$$bh_{13,1} \triangleq \left[\frac{1}{3\alpha^2 d}\left(3T\alpha^3 + (3T-9)\alpha^2 + (3T-6)\alpha - 3\right) e^{(\alpha T)} \right] \tag{A.149}$$

$$bh_{13,2} \triangleq \left[\frac{1}{3\alpha^2 d}\left(-3\alpha^3(\alpha+2)\cos(\theta) + \sqrt{3}\alpha^2\left(-\alpha^2 + 2\alpha + 2\right)\sin(\theta)\right) e^{\left(\frac{-T}{2}\right)} \right] \tag{A.150}$$

$$bh_{13,3} \triangleq \left[\frac{1}{\alpha^2 d}\left(\alpha^4 + 2\alpha^3 + 3\alpha^2 + 2\alpha + 1\right) \right] \tag{A.151}$$

$$bh_{21} \triangleq \left[\frac{2}{3}\sqrt{3}\sin(\theta) e^{\left(\frac{-T}{2}\right)} \right] \tag{A.152}$$

$$bh_{22,1} \triangleq \left[\frac{1}{d}\left(-T\alpha^3 + (3-T)\alpha^2 + (2-T)\alpha + 1\right) e^{(T\alpha)} \right] \tag{A.153}$$

$$bh_{22,2} \triangleq \left[\frac{-1}{d}\left(3\alpha^2 + 2\alpha + 1\right)\cos(\theta) e^{\left(\frac{-T}{2}\right)} \right] \tag{A.154}$$

$$bh_{22,3} \triangleq \left[\frac{-\sqrt{3}}{3d}\left(4\alpha^3 + 5\alpha^2 + 2\alpha + 1\right)\sin(\theta)e^{\left(\frac{-T}{2}\right)} \right] \tag{A.155}$$

$$bh_{23,1} \triangleq \left[\frac{1}{d}\left(T\alpha^2 + (T-2)\alpha - 1 + T\right)e^{(T\alpha)} \right] \tag{A.156}$$

$$bh_{23,2} \triangleq \left[\frac{1}{3d}\left(3(2\alpha+1)\cos(\theta) + \sqrt{3}\left(2\alpha^2 + 2\alpha - 1\right)\sin(\theta)\right)e^{\left(\frac{-T}{2}\right)} \right] \tag{A.157}$$

A.1.6 Second-Order Plant Model; Case 6

For the LiT-type D/C control, $\overline{BH}$ is

$$\overline{BH} = \begin{bmatrix} bh_{11} & bh_{12} \\ bh_{21} & bh_{22} \end{bmatrix}_{2\times 2} \tag{A.158}$$

$$q \triangleq \left[\left(a_2^2 - 4a_1\right)^{1/2} \right] \tag{A.159}$$

$$\delta_p \triangleq e^{\left(\frac{(q-a_2)T}{2}\right)} \tag{A.160}$$

$$\delta_m \triangleq e^{\left(\frac{-(q+a_2)T}{2}\right)} \tag{A.161}$$

$$bh_{11} \triangleq \left[\frac{1}{2qa_1}\left((-a_2 - q)\delta_p + (a_2 - q)\delta_m + 2q\right) \right] \tag{A.162}$$

$$bh_{12} \triangleq \left[\frac{1}{2qa_1^{\,2}}\left(\left(a_2 q - 2a_1 + a_2^{\,2}\right)\delta_p + \left(2a_1 - a_2^{\,2} + a_2 q\right)\delta_m + 2q\left(a_1 T - a_2\right)\right) \right] \tag{A.163}$$

$$bh_{21} \triangleq \left[\frac{1}{q}\left(\delta_p - \delta_m\right) \right] \tag{A.164}$$

$$bh_{22} \triangleq \left[\frac{1}{2qa_1}\left((-a_2 - q)\delta_p + (a_2 - q)\delta_m + 2q\right) \right] \tag{A.165}$$

For the SiT-type D/C control, $\overline{BH}$ is

$$\overline{BH} = \begin{bmatrix} bh_{11} & \left(bh_{12,1} + bh_{12,2}\right) & \left(bh_{13,1} + bh_{13,2}\right) \\ bh_{21} & \left(bh_{22,1} + bh_{22,2}\right) & \left(bh_{23,1} + bh_{23,2}\right) \end{bmatrix}_{2\times 3} \tag{A.166}$$

$$q \triangleq \left(a_2^2 - 4a_1\right)^{1/2} \tag{A.167}$$

$$d \triangleq \left[a_2{}^2\omega^2 - 2a_1\omega^2 + a_1{}^2 + \omega^4\right] \tag{A.168}$$

$$\delta_p \triangleq e^{\left(\frac{(q-a_2)T}{2}\right)} \tag{A.169}$$

$$\delta_m \triangleq e^{\left(\frac{-(q+a_2)T}{2}\right)} \tag{A.170}$$

$$bh_{11} \triangleq \left[\frac{-1}{2a_1 q}\left(a_2\left(\delta_p - \delta_m\right) + q\left(\delta_p + \delta_m\right) - 2q\right)\right] \tag{A.171}$$

$$bh_{12,1} \triangleq \left[\frac{1}{2q\omega d}\left(a_2 q\omega\left(\delta_p + \delta_m\right) + \omega\left(a_2{}^2 - 2a_1 + 2\omega^2\right)\left(\delta_p - \delta_m\right)\right)\right] \tag{A.172}$$

$$bh_{12,2} \triangleq \left[\frac{1}{2q\omega d}\left(-2a_2 q\omega\cos\left(\omega T\right) + 2q\left(a_1 - \omega^2\right)\sin\left(\omega T\right)\right)\right] \tag{A.173}$$

$$bh_{13,1} \triangleq \left[\frac{q\left(a_1 - a_2{}^2 - \omega^2\right)\left(\delta_p + \delta_m\right) + a_2\left(3a_1 - a_2{}^2 - \omega^2\right)\left(\delta_p - \delta_m\right)}{2a_1 qd}\right] \tag{A.174}$$

$$bh_{13,2} \triangleq \left[\frac{2a_1\left(\omega^2 - a_1\right)\cos\left(\omega T\right) - 2a_1 a_2\omega\sin\left(\omega T\right) + 2d}{2a_1\omega^2 d}\right] \tag{A.175}$$

$$bh_{21} \triangleq \left(\frac{\delta_p - \delta_m}{q}\right) \tag{A.176}$$

$$bh_{22,1} \triangleq \left[\frac{1}{2qd}\left(q\left(-a_1 + \omega^2\right)\left(\delta_p + \delta_m\right) - a_2\left(\omega^2 + a_1\right)\left(\delta_p - \delta_m\right)\right)\right] \tag{A.177}$$

$$bh_{22,2} \triangleq \left[\frac{1}{2qd}\left(2q\left(a_1-\omega^2\right)\cos\left(\omega T\right)+2a_2q\omega\sin\left(\omega T\right)\right)\right] \tag{A.178}$$

$$bh_{23,1} \triangleq \left[\frac{1}{2qd}\left(a_2q\left(\delta_p+\delta_m\right)+\left(a_2{}^2+2\omega^2-2a_1\right)\left(\delta_p-\delta_m\right)\right)\right] \tag{A.179}$$

$$bh_{23,2} \triangleq \left[\frac{1}{2qd}\left(-2a_2q\cos\left(\omega T\right)+2q\left(a_1-\omega^2\right)\sin\left(\omega T\right)\right)\right] \tag{A.180}$$

For the EiT-type D/C control, $\overline{BH}$ is

$$\overline{BH} = \begin{bmatrix} \left(bh_{11,1}+bh_{11,2}\right) & \left(bh_{12,1}+bh_{12,2}\right) \\ \left(bh_{21,1}+bh_{21,2}\right) & \left(bh_{22,1}+bh_{22,2}\right) \end{bmatrix}_{2\times 2} \tag{A.181}$$

$$q \triangleq \left(a_2^2-4a_1\right)^{1/2} \tag{A.182}$$

$$d \triangleq \left[\alpha^2+\left(2a_1-a_2{}^2\right)\alpha+a_1{}^2\right] \tag{A.183}$$

$$\delta_p \triangleq e^{\left(\frac{\left(q-a_2+\sqrt{\alpha}\right)T}{2}\right)} \tag{A.184}$$

$$\delta_m \triangleq e^{\left(\frac{\left(-q-a_2+\sqrt{\alpha}\right)T}{2}\right)} \tag{A.185}$$

$$\gamma_p \triangleq \left[e^{\left(\sqrt{\alpha}T\right)}+e^{\left(-\sqrt{\alpha}T\right)}\right] \tag{A.186}$$

$$\gamma_m \triangleq \left[e^{\left(\sqrt{\alpha}T\right)}-e^{\left(-\sqrt{\alpha}T\right)}\right] \tag{A.187}$$

$$bh_{11,1} \triangleq \left[\frac{1}{2qd}\left(-q\left(\alpha+a_1\right)\left(\delta_p+\delta_m\right)+a_2\left(\alpha-a_1\right)\left(\delta_p-\delta_m\right)\right)\right] \tag{A.188}$$

$$bh_{11,2} \triangleq \left[\frac{1}{2qd}\left(\left(a_1q+\alpha q\right)\gamma_p-a_2q\sqrt{\alpha}\gamma_m\right)\right] \tag{A.189}$$

$$bh_{12,1} \triangleq \left[\frac{1}{2qd}\left(a_2q\left(\delta_p+\delta_m\right)-\left(2a_1-a_2^2+2\alpha\right)\left(\delta_p-\delta_m\right)\right)\right] \tag{A.190}$$

$$bh_{12,2} \triangleq \left[\frac{1}{2\sqrt{\alpha}qd} \left(-qa_2\sqrt{\alpha}\gamma_p + q\left(a_1+\alpha\right)\gamma_m \right) \right] \tag{A.191}$$

$$bh_{21,1} \triangleq \left[\frac{1}{2qd} \left(qa_2\alpha\left(\delta_p+\delta_m\right) + \left(2a_1{}^2 + 2a_1\alpha - a_2{}^2\alpha\right)\left(\delta_p-\delta_m\right) \right) \right] \tag{A.192}$$

$$bh_{21,2} \triangleq \left[\frac{1}{2qd} \left(-q\alpha a_2\gamma_p + \sqrt{\alpha}q\left(a_1+\alpha\right)\gamma_m \right) \right] \tag{A.193}$$

$$bh_{22,1} \triangleq \left[\frac{1}{2qd} \left(\left(-\alpha q - a_1 q\right)\left(\delta_p+\delta_m\right) + \left(-a_1a_2 + a_2\alpha\right)\left(\delta_p-\delta_m\right) \right) \right] \tag{A.194}$$

$$bh_{22,2} \triangleq \left[\frac{1}{2qd} \left(q\left(a_1+\alpha\right)\gamma_m - a_2q\sqrt{\alpha}\gamma_p \right) \right] \tag{A.195}$$

For the PsiT-type D/C control, $\overline{BH}$ is

$$\overline{BH} = \begin{bmatrix} bh_{11} & \left(bh_{12,1}+bh_{12,2}+bh_{12,3}+bh_{12,4}\right) & \left(bh_{13,1}+bh_{13,2}+bh_{13,3}+bh_{13,4}\right) \\ bh_{21} & \left(bh_{22,1}+bh_{22,2}+bh_{22,3}\right) & \left(bh_{23,1}+bh_{23,2}\right) \end{bmatrix}_{2\times 3} \tag{A.196}$$

$$q \triangleq \left(a_2^2 - 4a_1\right)^{1/2} \tag{A.197}$$

$$d \triangleq \left(a_1 + a_2\alpha + \alpha^2\right)^2 \tag{A.198}$$

$$\delta_p \triangleq e^{\left(\frac{(q-a_2)T}{2}\right)} \tag{A.199}$$

$$\delta_m \triangleq e^{\left(\frac{-(q+a_2)T}{2}\right)} \tag{A.200}$$

$$bh_{11} \triangleq \left[\frac{-1}{2a_1q} \left(q\left(\delta_p+\delta_m\right) + a_2\left(\delta_p-\delta_m\right) - 2q \right) \right] \tag{A.201}$$

$$bh_{12,1} \triangleq \left[\frac{1}{2a_1d} \left(2\alpha^3 + 4a_2\alpha^2 + 2a_2{}^2\alpha + a_2a_1 \right)\left(\delta_p+\delta_m\right) \right] \tag{A.202}$$

$$bh_{12,2} \triangleq \left[\frac{1}{2a_1 qd} \left(-2a_1^{\,2} + \left(-6\alpha^2 - 4\alpha a_2 + a_2^{\,2} \right) a_1 + 2\alpha a_2^{\,3} + 2\alpha^3 a_2 + 4\alpha^2 a_2^{\,2} \right) \left(\delta_p - \delta_m \right) \right] \tag{A.203}$$

$$bh_{12,3} \triangleq \left[\frac{1}{2\alpha d} \left(\left(-2\alpha T + 4 \right) a_1 + \alpha \left(\left(-2\alpha T + 6 \right) a_2 - 2\alpha^2 T + 8\alpha \right) \right) e^{(\alpha T)} \right] \tag{A.204}$$

$$bh_{12,4} \triangleq \left[\frac{-2}{a_1 \alpha d} \left(a_1^{\,2} + 2\left(\alpha^2 + a_2 \alpha \right) a_1 + \alpha^4 + a_2^{\,2} \alpha^2 + 2\alpha^3 a_2 \right) \right] \tag{A.205}$$

$$bh_{13,1} \triangleq \left[\frac{-1}{2a_1 \alpha^2 d} \left(2a_2 \alpha^3 + a_2^{\,2} \alpha^2 + \alpha^4 - a_1 \alpha^2 \right) \left(\delta_p + \delta_m \right) \right] \tag{A.206}$$

$$bh_{13,2} \triangleq \left[\frac{1}{2a_1 qd} \left(\left(4\alpha + 3a_2 \right) a_1 - \alpha^2 a_2 - a_2^{\,3} - 2\alpha a_2^{\,2} \right) \left(\delta_p - \delta_m \right) \right] \tag{A.207}$$

$$bh_{13,3} \triangleq \left[\frac{1}{\alpha^2 d} \left(\left(\alpha T - 1 \right) a_1 + \left(\left(\alpha^2 T - 2\alpha \right) a_2 - 3\alpha^2 + \alpha^3 T \right) \right) e^{(\alpha T)} \right] \tag{A.208}$$

$$bh_{13,4} \triangleq \left[\frac{1}{a_1 \alpha^2 d} \left(a_1^{\,2} + 2\left(\alpha^2 + a_2 \alpha \right) a_1 + 2\alpha^3 a_2 + a_2^{\,2} \alpha^2 + \alpha^4 \right) \right] \tag{A.209}$$

$$bh_{21} \triangleq \left[\frac{1}{q} \left(\delta_p - \delta_m \right) \right] \tag{A.210}$$

$$bh_{22,1} \triangleq \left[\frac{-1}{2d} \left(a_1 + 2a_2 \alpha + 3\alpha^2 \right) \left(\delta_p + \delta_m \right) \right] \tag{A.211}$$

$$bh_{22,2} \triangleq \left[\frac{-1}{2qd} \left(5\alpha^2 a_2 + 2\alpha a_2^{\,2} + a_2 a_1 + 4\alpha^3 \right) \left(\delta_p - \delta_m \right) \right] \tag{A.212}$$

$$bh_{22,3} \triangleq \left[\frac{1}{d} \left(\left(1 - \alpha T \right) a_1 + \left(2\alpha - \alpha^2 T \right) a_2 + 3\alpha^2 - \alpha^3 T \right) e^{(\alpha T)} \right] \tag{A.213}$$

$$bh_{23,1} \triangleq \left[\frac{1}{2qd} \left(\left(a_2 q + 2\alpha q \right) \left(\delta_p + \delta_m \right) + \left(-2a_1 + a_2^{\,2} + 2a_2 \alpha + 2\alpha^2 \right) \left(\delta_p - \delta_m \right) \right) \right] \tag{A.214}$$

$$bh_{23,2} \triangleq \left[\frac{1}{d}\left(a_1 T + (\alpha T - 1)a_2 - 2\alpha + \alpha^2 T\right)e^{(\alpha T)}\right] \tag{A.215}$$

A.2 Third-Order Plant Models (Phase-Variables); $\dot{x} = Ax + Bu_{d/c}(t)$; n = 3; r = 1

Table A.3 Third-Order Plant Models (Phase-Variables)

Case Number	Plant	**A**	**B**
1	$\dddot{y} = u$	$A = \begin{bmatrix} 0 & 1 & 0 \\ 0 & 0 & 1 \\ 0 & 0 & 0 \end{bmatrix}$	$B = \begin{bmatrix} 0 \\ 0 \\ 1 \end{bmatrix}$
2	$\dddot{y} + a\dot{y} = u$	$A = \begin{bmatrix} 0 & 1 & 0 \\ 0 & 0 & 1 \\ -a & 0 & 0 \end{bmatrix}$	$B = \begin{bmatrix} 0 \\ 0 \\ 1 \end{bmatrix}$

A.2.1 Third-Order Plant Model; Case 1

For the LiT-type D/C control $\overline{BH}$ is

$$\overline{BH} = \begin{bmatrix} bh_{11} & bh_{12} \\ bh_{21} & bh_{22} \\ bh_{31} & bh_{32} \end{bmatrix}_{2\times 3} \tag{A.216}$$

$$bh_{11} \triangleq \left(\frac{1}{6}T^3\right) \tag{A.217}$$

$$bh_{12} \triangleq \left(\frac{1}{24}T^4\right) \tag{A.218}$$

$$bh_{21} \triangleq \left(\frac{1}{2}T^2\right) \tag{A.219}$$

$$bh_{22} \triangleq \left(\frac{1}{6}T^3\right) \tag{A.220}$$

$$bh_{31} \triangleq (T) \tag{A.221}$$

$$bh_{32} \triangleq \left(\frac{1}{2}T^2\right) \tag{A.222}$$

For the SiT-type D/C control, $\overline{BH}$ is

$$\overline{BH} = \begin{bmatrix} bh_{11} & bh_{12} & bh_{13} \\ bh_{21} & bh_{22} & bh_{23} \\ bh_{31} & bh_{32} & bh_{33} \end{bmatrix}_{3\times 3} \tag{A.223}$$

$$bh_{11} \triangleq \left(\frac{1}{6}T^3\right) \tag{A.224}$$

$$bh_{12} \triangleq \left[\frac{1}{2\omega^4}\left(-2+\omega^2T^2+2\cos\left(\omega T\right)\right)\right] \tag{A.225}$$

$$bh_{13} \triangleq \left[\frac{1}{6\omega^5}\left(-6\omega T+\omega^3T^3+6\sin\left(\omega T\right)\right)\right] \tag{A.226}$$

$$bh_{21} \triangleq \left(\frac{1}{2}T^2\right) \tag{A.227}$$

$$bh_{22} \triangleq \left[\frac{1}{\omega^3}\left(\omega T-\sin\left(\omega T\right)\right)\right] \tag{A.228}$$

$$bh_{23} \triangleq \left[\frac{1}{2\omega^4}\left(-2+\omega^2T^2+2\cos\left(\omega T\right)\right)\right] \tag{A.229}$$

$$bh_{31} \triangleq \left(T\right) \tag{A.230}$$

$$bh_{32} \triangleq \left[\frac{1}{\omega^2}\left(1-\cos\left(\omega T\right)\right)\right] \tag{A.231}$$

$$bh_{33} \triangleq \left[\frac{1}{\omega^3}\left(\omega T-\sin\left(\omega T\right)\right)\right] \tag{A.232}$$

For the EiT-type D/C control, $\overline{BH}$ is

$$\overline{BH} = \begin{bmatrix} bh_{11} & bh_{12} \\ bh_{21} & bh_{22} \\ bh_{31} & bh_{32} \end{bmatrix}_{3\times 2} \tag{A.233}$$

$$bh_{11} \triangleq \left[\frac{1}{2\alpha^{\frac{3}{2}}} \left(e^{(\sqrt{\alpha}T)} - e^{(-\sqrt{\alpha}T)} - 2\sqrt{\alpha}T \right) \right] \tag{A.234}$$

$$bh_{12} \triangleq \left[\frac{1}{2\alpha^{2}} \left(e^{(-\sqrt{\alpha}T)} + e^{(\sqrt{\alpha}T)} - \alpha T^{2} - 2 \right) \right] \tag{A.235}$$

$$bh_{21} \triangleq \left[\frac{1}{2\alpha} \left(e^{(-\sqrt{\alpha}T)} + e^{(\sqrt{\alpha}T)} - 2 \right) \right] \tag{A.236}$$

$$bh_{22} \triangleq \left[\frac{1}{2\alpha^{\frac{3}{2}}} \left(e^{(\sqrt{\alpha}T)} - e^{(-\sqrt{\alpha}T)} - 2\sqrt{\alpha}T \right) \right] \tag{A.237}$$

$$bh_{31} \triangleq \left[\frac{1}{2\sqrt{\alpha}} \left(e^{(\sqrt{\alpha}T)} - e^{(-\sqrt{\alpha}T)} \right) \right] \tag{A.238}$$

$$bh_{32} \triangleq \left[\frac{1}{2\alpha} \left(e^{(-\sqrt{\alpha}T)} + e^{(\sqrt{\alpha}T)} - 2 \right) \right] \tag{A.239}$$

For the PsiT-type D/C control, $\overline{BH}$ is

$$\overline{BH} = \begin{bmatrix} bh_{11} & bh_{12} & bh_{13} \\ bh_{21} & bh_{22} & bh_{23} \\ bh_{31} & bh_{32} & bh_{33} \end{bmatrix}_{3\times 3} \tag{A.240}$$

$$bh_{11} \triangleq \left(\frac{1}{6} T^{3} \right) \tag{A.241}$$

$$bh_{12} \triangleq \left[\frac{1}{6\alpha^{4}} \left((30 - 6\alpha T) e^{(\alpha T)} - 9\alpha^{2}T^{2} - 30 - 24\alpha T - 2\alpha^{3}T^{3} \right) \right] \tag{A.242}$$

$$bh_{13} \triangleq \left[\frac{1}{6\alpha^{5}} \left((6\alpha T - 24) e^{(\alpha T)} + 24 + 6\alpha^{2}T^{2} + 18\alpha T + \alpha^{3}T^{3} \right) \right] \tag{A.243}$$

$$bh_{21} \triangleq \left(\frac{1}{2}T^2\right) \tag{A.244}$$

$$bh_{22} \triangleq \left[\frac{1}{\alpha^3}\left(\left(-\alpha T+4\right)e^{(\alpha T)}-3\alpha T-4-\alpha^2T^2\right)\right] \tag{A.245}$$

$$bh_{23} \triangleq \left[\frac{1}{2\alpha^4}\left(\left(2\alpha T-6\right)e^{(\alpha T)}+6+4\alpha T+\alpha^2T^2\right)\right] \tag{A.246}$$

$$bh_{31} \triangleq \left(T\right) \tag{A.247}$$

$$bh_{32} \triangleq \left[\frac{1}{\alpha^2}\left(\left(3-\alpha T\right)e^{(\alpha T)}-3-2\alpha T\right)\right] \tag{A.248}$$

$$bh_{33} \triangleq \left[\frac{1}{\alpha^3}\left(\left(\alpha T-2\right)e^{(\alpha T)}+2+\alpha T\right)\right] \tag{A.249}$$

A.2.2 Third-Order Plant Model; Case 2

For the LiT-type D/C control, $\overline{BH}$ is

$$\overline{BH} = \begin{bmatrix} bh_{11} & bh_{12} \\ bh_{21} & bh_{22} \\ bh_{31} & bh_{32} \end{bmatrix}_{3\times 2} \tag{A.250}$$

$$q \triangleq \left(\frac{\left(-a\right)^{(1/3)}T}{2}\right) \tag{A.251}$$

$$bh_{11} \triangleq \left[\frac{1}{3a}\left(3-e^{(2q)}-2e^{(-q)}\cos\left(\sqrt{3}q\right)\right)\right] \tag{A.252}$$

$$bh_{12} \triangleq \left[\frac{1}{3\left(-a\right)^{\frac{4}{3}}}\left(e^{(2q)}-6q-e^{(-q)}\left(\cos\left(\sqrt{3}q\right)-\sqrt{3}\sin\left(\sqrt{3}q\right)\right)\right)\right] \tag{A.253}$$

$$bh_{21} \triangleq \left[\frac{1}{3\left(-a\right)^{\frac{2}{3}}}\left(e^{(2q)}-e^{(-q)}\left(\cos\left(\sqrt{3}q\right)+\sqrt{3}\sin\left(\sqrt{3}q\right)\right)\right)\right] \tag{A.254}$$

$$bh_{22} \triangleq \left[\frac{1}{3a}\left(3 - e^{(2q)} - 2e^{(-q)}\cos\left(\sqrt{3}q\right)\right)\right] \tag{A.255}$$

$$bh_{31} \triangleq \left[\frac{1}{3(-a)^{(1/3)}}\left(e^{(2q)} + e^{(-q)}\left(-\cos\left(\sqrt{3}q\right) + \sqrt{3}\sin\left(\sqrt{3}q\right)\right)\right)\right] \tag{A.256}$$

$$bh_{32} \triangleq \left[\frac{1}{3(-a)^{\frac{2}{3}}}\left(e^{(2q)} - e^{(-q)}\left(\cos\left(\sqrt{3}q\right) - \sqrt{3}\sin\left(\sqrt{3}q\right)\right)\right)\right] \tag{A.257}$$

For the SiT-type D/C control, $\overline{BH}$ is

$$\overline{BH} = \begin{bmatrix} bh_{11} & \left(bh_{12,1} + bh_{12,2}\right) & \left(bh_{13,1} + bh_{13,2}\right) \\ bh_{21} & \left(bh_{22,1} + bh_{22,2}\right) & \left(bh_{23,1} + bh_{23,2}\right) \\ bh_{31} & \left(bh_{32,1} + bh_{32,2}\right) & \left(bh_{33,1} + bh_{33,2}\right) \end{bmatrix}_{3\times 3} \tag{A.258}$$

$$q \triangleq \left(\frac{(-a)^{(1/3)}\,T}{2}\right) \tag{A.259}$$

$$d \triangleq \left(a^2 + \omega^6\right) \tag{A.260}$$

$$bh_{11} \triangleq \left[\frac{1}{-3a}\left(e^{(2q)} - 3 + 2e^{(-q)}\cos\left(\sqrt{3}q\right)\right)\right] \tag{A.261}$$

$$bh_{12,1} \triangleq \left[\frac{1}{3a^{\frac{2}{3}}d}\left(a^{\frac{2}{3}} + \omega^2\right)\left(-\left(a^{\frac{2}{3}} + \omega^2\right)\cos\left(\sqrt{3}q\right) + \left(\sqrt[3]{a} - \omega\right)\left(\sqrt[3]{a} + \omega\right)\sqrt{3}\sin\left(\sqrt{3}q\right)\right)e^{(-q)}\right] \tag{A.262}$$

$$bh_{12,2} \triangleq \left[\frac{1}{3\omega d}\left(3\omega^3\cos(T\omega) + 3a\sin(T\omega) + \omega\left(a^{\frac{2}{3}} - \omega^2 + a^{\frac{-2}{3}}\omega^4\right)e^{(2q)}\right)\right] \tag{A.263}$$

$$bh_{13,1} \triangleq \left[\frac{1}{3a\left(a^2 + \omega^6\right)}\left(a^{\frac{2}{3}} + \omega^2\right)\left(\left(a^{\frac{2}{3}} - 2\omega^2\right)\cos\left(\sqrt{3}q\right) + a^{\frac{2}{3}}\sqrt{3}\sin\left(\sqrt{3}q\right)\right)e^{(-q)}\right] \tag{A.264}$$

$$bh_{13,2} \triangleq \left[\frac{1}{3\omega^2 ad} \left(3a\left(a - a\cos\left(\omega T\right) + \omega^3 \sin\left(\omega T\right)\right) - e^{(2q)}\omega^6 + 3\omega^6 + a^{\frac{2}{3}} e^{(2q)}\omega^4 - a^{\frac{4}{3}} e^{(2q)}\omega^2 \right) \right] \tag{A.265}$$

$$bh_{21} \triangleq \left[\frac{1}{-3a^{\frac{2}{3}}} \left(-e^{(3q)} + \cos\left(\sqrt{3}q\right) + \sqrt{3}\sin\left(\sqrt{3}q\right)\right) e^{(-q)} \right] \tag{A.266}$$

$$bh_{22,1} \triangleq \left[\frac{1}{3\sqrt[3]{a}d} \left(a^{\frac{2}{3}} + \omega^2 \right) \left(\left(\omega^2 - 2a^{\frac{2}{3}} \right) \cos\left(\sqrt{3}q\right) + \sqrt{3}\omega^2 \sin\left(\sqrt{3}q\right) \right) e^{(-q)} \right] \tag{A.267}$$

$$bh_{22,2} \triangleq \left[\frac{1}{3\sqrt[3]{a}d} \left(3a^{\frac{4}{3}} \cos\left(\omega T\right) - 3\sqrt[3]{a}\omega^3 \sin\left(\omega T\right) - e^{(2q)} \left(a^{\frac{4}{3}} - a^{\frac{2}{3}}\omega^2 + \omega^4 \right) \right) \right] \tag{A.268}$$

$$bh_{23,1} \triangleq \left[\frac{1}{3a^{\frac{2}{3}}d} \left(a^{\frac{2}{3}} + \omega^2 \right) \left(-\left(a^{\frac{2}{3}} + \omega^2 \right) \cos\left(\sqrt{3}q\right) + \sqrt{3}\left(\sqrt[3]{a} - \omega\right)\left(\sqrt[3]{a} + \omega\right) \sin\left(\sqrt{3}q\right) \right) e^{(-q)} \right] \tag{A.269}$$

$$bh_{23,2} \triangleq \left[\frac{1}{3a^{\frac{2}{3}}\omega d} \left(3a^{\frac{2}{3}}\omega^3 \cos\left(\omega T\right) + 3a^{\frac{5}{3}} \sin\left(\omega T\right) + \omega\left(a^{\frac{4}{3}} - a^{\frac{2}{3}}\omega^2 + \omega^4 \right) e^{(2q)} \right) \right] \tag{A.270}$$

$$bh_{31} \triangleq \left[\frac{1}{3\sqrt[3]{a}} \left(e^{(-q)} \left(\cos\left(\sqrt{3}q\right) - \sqrt{3}\sin\left(\sqrt{3}q\right)\right) - e^{(2q)} \right) \right] \tag{A.271}$$

$$bh_{32,1} \triangleq \left[\frac{1}{3d} \left(a^{\frac{2}{3}} + \omega^2 \right) \left(\left(2\omega^2 - a^{\frac{2}{3}} \right) \cos\left(\sqrt{3}q\right) - \sqrt{3}a^{\frac{2}{3}} \sin\left(\sqrt{3}q\right) \right) e^{(-q)} \right] \tag{A.272}$$

$$bh_{32,2} \triangleq \left[\frac{1}{3d} \left(-3\omega^4 \cos\left(\omega T\right) - 3a\omega \sin\left(\omega T\right) + e^{(2q)} \left(a^{\frac{4}{3}} - a^{\frac{2}{3}}\omega^2 + \omega^4 \right) \right) \right] \tag{A.273}$$

$$bh_{33,1} \triangleq \left[\frac{1}{3\sqrt[3]{a}d} \left(a^{\frac{2}{3}} + \omega^2 \right) \left(\left(\omega^2 - 2a^{\frac{2}{3}} \right) \cos\left(\sqrt{3}q\right) - \sqrt{3}\omega^2 \sin\left(\sqrt{3}q\right) \right) e^{(-q)} \right] \tag{A.274}$$

$$bh_{33,2} \triangleq \left[\frac{1}{3\sqrt[3]{a}d} \left(3\sqrt[3]{a} \left(a\cos(\omega T) - 3\omega^3 \sin(\omega T) \right) - e^{(2q)} \left(a^{\frac{4}{3}} - a^{\frac{2}{3}}\omega^2 + \omega^4 \right) \right) \right] \tag{A.275}$$

For the EiT-type D/C control, $\overline{BH}$ is

$$\overline{BH} = \begin{bmatrix} \left(bh_{11,1} + bh_{11,2}\right) & \left(bh_{12,1} + bh_{12,2} + bh_{12,3}\right) \\ \left(bh_{21,1} + bh_{21,2}\right) & \left(bh_{22,1} + bh_{22,2}\right) \\ \left(bh_{31,1} + bh_{31,2}\right) & \left(bh_{32,1} + bh_{32,2}\right) \end{bmatrix}_{3\times 2} \tag{A.276}$$

$$q \triangleq \left((-a)^{(1/3)} \right) \tag{A.277}$$

$$d \triangleq \left(q^6 - \alpha^3 \right) \tag{A.278}$$

$$\theta \triangleq \left(\frac{\sqrt{3}}{2} qT \right) \tag{A.279}$$

$$\delta_p \triangleq \left(e^{\left(\sqrt{\alpha}T\right)} + e^{\left(-\sqrt{\alpha}T\right)} \right) \tag{A.280}$$

$$\delta_m \triangleq \left(e^{\left(\sqrt{\alpha}T\right)} - e^{\left(-\sqrt{\alpha}T\right)} \right) \tag{A.281}$$

$$bh_{11,1} \triangleq \left[\frac{1}{3qd} \left(-\alpha + q^2\right) \left(\left(\alpha + 2q^2\right)\cos(\theta) - \sqrt{3}\alpha \sin(\theta) \right) e^{\left(\frac{-qT}{2}\right)} \right] \tag{A.282}$$

$$bh_{11,2} \triangleq \left[\frac{1}{6qd} \left(2\left(q^4 + \alpha q^2 + \alpha^2\right) e^{(qT)} - 3q \left(\alpha^{\frac{3}{2}}\delta_m + q^3\delta_p \right) \right) \right] \tag{A.283}$$

$$bh_{12,1} \triangleq \left[\frac{-1}{3q^2 d} \left(\sqrt{\alpha} - q\right)^2 \left(q + \sqrt{\alpha}\right)^2 \cos(\theta) e^{\left(\frac{-qT}{2}\right)} \right] \tag{A.284}$$

$$bh_{12,2} \triangleq \left[\frac{-\sqrt{3}}{3q^2 d} \left(\sqrt{\alpha} - q\right) \left(\sqrt{\alpha} + q\right) \left(\alpha + q^2\right) \sin(\theta) e^{\left(\frac{-qT}{2}\right)} \right] \tag{A.285}$$

$$bh_{12,3} \triangleq \left[\frac{1}{6\sqrt{\alpha}q^2 d} \left(2\sqrt{\alpha}\left(\alpha + q\sqrt{\alpha} + q^2\right)\left(q^2 - q\sqrt{\alpha} + \alpha\right)e^{(Tq)} - 3q^2\left(q^3\delta_m + \alpha^{\frac{3}{2}}\delta_p \right) \right) \right] \tag{A.286}$$

$$bh_{21,1} \triangleq \left[\frac{1}{3d}\left(\alpha - q^2\right)\left(\left(2\alpha + q^2\right)\cos(\theta) + \sqrt{3}q^2\sin(\theta)\right)e^{\left(\frac{-qT}{2}\right)} \right] \tag{A.287}$$

$$bh_{21,2} \triangleq \left[\frac{1}{6d}\left(2\left(q^4 + \alpha q^2 + \alpha^2\right)e^{(qT)} - 3\left(\sqrt{\alpha}q^3\delta_m + \alpha^2\delta_p\right)\right) \right] \tag{A.288}$$

$$bh_{22,1} \triangleq \left[\frac{1}{3qd}\left(-\alpha + q^2\right)\left(\left(\alpha + 2q^2\right)\cos(\theta) - \sqrt{3}\alpha\sin(\theta)\right)e^{\left(\frac{-qT}{2}\right)} \right] \tag{A.289}$$

$$bh_{22,2} \triangleq \left[\frac{1}{6qd}\left(\left(2q^4 + 2\alpha q^2 + 2\alpha^2\right)e^{(qT)} - 3q\alpha^{\frac{3}{2}}\delta_m - 3q^4\delta_p \right) \right] \tag{A.290}$$

$$bh_{31,1} \triangleq \left[\frac{q}{3d}\left(-\alpha + q^2\right)\left(\left(\alpha - q^2\right)\cos(\theta) + \sqrt{3}q\left(\alpha + q^2\right)\sin(\theta)\right)e^{\left(\frac{-qT}{2}\right)} \right] \tag{A.291}$$

$$bh_{31,2} \triangleq \left[\frac{1}{6d}\left(2q\left(q^4 + \alpha q^2 + \alpha^2\right)e^{(qT)} - 3\alpha\left(\alpha^{\frac{3}{2}}\delta_m + q^3\delta_p \right) \right) \right] \tag{A.292}$$

$$bh_{32,1} \triangleq \left[\frac{1}{3d}\left(\alpha - q^2\right)\left(\left(2\alpha + q^2\right)\cos(\theta) + \sqrt{3}q^2\sin(\theta)\right)e^{\left(\frac{-qT}{2}\right)} \right] \tag{A.293}$$

$$bh_{32,2} \triangleq \left[\frac{1}{6d}\left(\left(2q^4 + 2\alpha q^2 + 2\alpha^2\right)e^{(qT)} - 3\left(\sqrt{\alpha}q^3\delta_m + \alpha^2\delta_p\right)\right) \right] \tag{A.294}$$

For the PsiT-type D/C control, $\overline{BH}$ is

$$\overline{BH} = \begin{bmatrix} bh_{11} & \left(bh_{12,1} + bh_{12,2} + bh_{12,3} + bh_{12,4}\right) & \left(bh_{13,1} + bh_{13,2} + bh_{13,3} + bh_{13,4}\right) \\ bh_{21} & \left(bh_{22,1} + bh_{22,2} + bh_{22,3}\right) & \left(bh_{23,1} + bh_{23,2} + bh_{23,3}\right) \\ \left(bh_{31,1} + bh_{31,2}\right) & \left(bh_{32,1} + bh_{32,2} + bh_{32,3}\right) & \left(bh_{33,1} + bh_{33,2} + bh_{33,3}\right) \end{bmatrix}_{3\times 3} \tag{A.295}$$

$$q \triangleq \left((-a)^{(1/3)} \right) \tag{A.296}$$

$$d \triangleq \left[(q-\alpha)^2 \left(\alpha^2 + q\alpha + q^2 \right)^2 \right] \tag{A.297}$$

$$\theta \triangleq \left(\frac{\sqrt{3} qT}{2} \right) \tag{A.298}$$

$$bh_{11} \triangleq \left[\frac{1}{3a} \left(-2e^{\left(\frac{-qT}{2}\right)} \cos(\theta) - e^{(qT)} + 3 \right) \right] \tag{A.299}$$

$$bh_{12,1} \triangleq \left[\frac{1}{3\alpha ad} \left(\alpha(\alpha+q)\left(4\alpha^2 + q\alpha + q^2\right)(-\alpha+q)^2 e^{\left(\frac{-qT}{2}\right)} \cos(\theta) \right) \right] \tag{A.300}$$

$$bh_{12,2} \triangleq \left[\frac{-\sqrt{3}}{3\alpha ad} \left(\left(q^2 + 2q\alpha + 3\alpha^2\right) q\alpha (-\alpha+q)^2 e^{\left(\frac{-qT}{2}\right)} \sin(\theta) \right) \right] \tag{A.301}$$

$$bh_{12,3} \triangleq \left[\frac{-1}{3\alpha ad} \left(\alpha(q-2\alpha)\left(\alpha^2 + q\alpha + q^2\right)^2 e^{(qT)} + 6(-\alpha+q)^2 \left(\alpha^2 + q\alpha + q^2\right)^2 \right) \right] \tag{A.302}$$

$$bh_{12,4} \triangleq \left[\frac{-1}{3\alpha ad} \left(3q^3 \left(-2q^3 + q^3 T\alpha + 5\alpha^3 - \alpha^4 T \right) e^{(T\alpha)} \right) \right] \tag{A.303}$$

$$bh_{13,1} \triangleq \left[\frac{1}{3\alpha^2 ad} \left(\alpha^2 \left(q^2 - 2q\alpha - 2\alpha^2\right)(-\alpha+q)^2 e^{\left(\frac{-qT}{2}\right)} \cos(\theta) \right) \right] \tag{A.304}$$

$$bh_{13,2} \triangleq \left[\frac{\sqrt{3}}{3\alpha^2 ad} \left((2\alpha+q) q (-\alpha+q)^2 \alpha^2 e^{\left(\frac{-qT}{2}\right)} \sin(\theta) \right) \right] \tag{A.305}$$

$$bh_{13,3} \triangleq \left[\frac{-1}{3\alpha^2 ad} \left(\alpha^2 \left(\alpha^2 + q\alpha + q^2\right)^2 e^{(qT)} + 3q^3 \left(-q^3 + q^3 T\alpha - \alpha^4 T + 4\alpha^3 \right) e^{(T\alpha)} \right) \right] \tag{A.306}$$

$$bh_{13,4} \triangleq \left[\frac{3}{3\alpha^2 ad} \left((-\alpha+q)^2 \left(\alpha^2 + q\alpha + q^2\right)^2 \right) \right] \tag{A.307}$$

$$bh_{21} \triangleq \left[\frac{1}{3q^2}\left(-e^{\left(\frac{-qT}{2}\right)}\cos(\theta)+e^{(qT)}-\sqrt{3}e^{\left(\frac{-qT}{2}\right)}\sin(\theta)\right)\right] \tag{A.308}$$

$$bh_{22,1} \triangleq \left[\frac{1}{3q^2d}\left(2q^3+4q^2\alpha+7q\alpha^2+2\alpha^3\right)(-\alpha+q)^2 e^{\left(\frac{-qT}{2}\right)}\cos(\theta)\right] \tag{A.309}$$

$$bh_{22,2} \triangleq \left[\frac{1}{3q^2d}\left(\sqrt{3}(2\alpha+q)(-\alpha+q)^2\alpha^2 e^{\left(\frac{-qT}{2}\right)}\sin(\theta)\right)\right] \tag{A.310}$$

$$bh_{22,3} \triangleq \left[\frac{1}{3q^2d}(q-2\alpha)\left(\alpha^2+q\alpha+q^2\right)^2 e^{(qT)}+3q^2\left(-q^3+q^3T\alpha-\alpha^4T+4\alpha^3\right)e^{(T\alpha)}\right] \tag{A.311}$$

$$bh_{23,1} \triangleq \left[\frac{-1}{3q^2d}\left(\left(q^2+4q\alpha+\alpha^2\right)(-\alpha+q)^2 e^{\left(\frac{-qT}{2}\right)}\cos(\theta)\right)\right] \tag{A.312}$$

$$bh_{23,2} \triangleq \left[\frac{\sqrt{3}}{3q^2d}\left((\alpha+q)(-\alpha+q)^3 e^{\left(\frac{-qT}{2}\right)}\sin(\theta)\right)\right] \tag{A.313}$$

$$bh_{23,3} \triangleq \left[\frac{1}{3q^2d}\left(\left(\alpha^2+q\alpha+q^2\right)^2 e^{(qT)}-3q^2\left(Tq^3+3\alpha^2-\alpha^3T\right)e^{(T\alpha)}\right)\right] \tag{A.314}$$

$$bh_{31} \triangleq \left[\frac{1}{3q}\left(e^{(qT)}-e^{\left(\frac{-qT}{2}\right)}\cos(\theta)+\sqrt{3}e^{\left(\frac{-qT}{2}\right)}\sin(\theta)\right)\right] \tag{A.315}$$

$$bh_{32,1} \triangleq \left[\frac{-1}{3qd}\left(\left(q^3+2q^2\alpha+2q\alpha^2-2\alpha^3\right)(-\alpha+q)^2 e^{\left(\frac{-qT}{2}\right)}\cos(\theta)\right)\right] \tag{A.316}$$

$$bh_{32,2} \triangleq \left[\frac{-\sqrt{3}}{3qd}\left(\left(q^3+2q^2\alpha+4q\alpha^2+2\alpha^3\right)(-\alpha+q)^2 e^{\left(\frac{-qT}{2}\right)}\sin(\theta)\right)\right] \tag{A.317}$$

$$bh_{32,3} \triangleq \left[\frac{1}{3qd}\left((q-2\alpha)\left(\alpha^2+q\alpha+q^2\right)^2 e^{(qT)}+3q\alpha^2\left(Tq^3+3\alpha^2-\alpha^3T\right)e^{(T\alpha)}\right)\right] \tag{A.318}$$

$$bh_{33,1} \triangleq \left[\frac{1}{3qd} \left(\left(2q^2 + 2q\alpha - \alpha^2 \right) \left(-\alpha + q \right)^2 e^{\left(\frac{-qT}{2} \right)} \cos\left(\theta \right) \right) \right] \tag{A.319}$$

$$bh_{33,2} \triangleq \left[\frac{\sqrt{3}}{3qd} \left(\left(2q + \alpha \right) \alpha \left(-\alpha + q \right)^2 e^{\left(\frac{-qT}{2} \right)} \sin\left(\theta \right) \right) \right] \tag{A.320}$$

$$bh_{33,3} \triangleq \left[\frac{1}{3qd} \left(\left(\alpha^2 + q\alpha + q^2 \right)^2 e^{(qT)} - 3q \left(q^3 + q^3 T\alpha + 2\alpha^3 - \alpha^4 T \right) e^{(T\alpha)} \right) \right] \tag{A.321}$$

APPENDIX B

Example Maple Listing for $\overline{BH}$ Computation

The mathematical program Maple, Version 12 was used to help compute the $\overline{BH}$ matrix. The following is an example listing of the A.2.2 Third-Order Plant Model; Case 2 with PsiT-type D/C Control.

```
restart;

with(linalg):

with(LinearAlgebra):

A:=Matrix([[0,1,0],[0,0,1],[-a,0,0]]);

AT:=exponential(A*T);

B:=Matrix([[0],[0],[1]]);

Dm:=Matrix([[0,1,0],[0,0,1],[0,-alpha^2,2*alpha]]);

H:=Matrix([[1,0,0]]);
```

```
BH:=evalm(int(exponential(A*(T-tau))
     &*B&*H&*exponential(Dm*tau),tau=0..T));
```

Some other Maple commands that were helpful in simplifying the resulting equations are

```
with(MTM);

BH1 := simplify(algsubs(a[2]^2-4*a[1] = q*q,
     expand(BH), exact), radical, symbolic);

scell2 := proc (x) options operator, arrow;
     collect(numer(x), [cos((1/2)*T*sqrt(3)*q),
     sin((1/2)*T*sqrt(3)*q), exp(-(1/2)*q*T),
     exp(q*T), exp(T*alpha)], factor)/factor(denom(x))
     end proc;

scell2(BH1[1, 1]);
```

APPENDIX C

Rank Preservation Property of the Gram Matrix

For a rectangular matrix A with entries a_{ij}, the Gram matrix, denoted as G, is the Hermitian matrix of inner products, where entries are given as $G_{ij} = \langle a_j, a_i \rangle$, [24]. The Gram matrix has the property

$$\operatorname{rank}\left[G\left(a_{ij}\right)\right] = \operatorname{rank}\left[AA^{*} \right] = \operatorname{rank}\left[A \right], \tag{C.1}$$

where A^{*} denotes the Hermitian transpose of A, [1]. Since $\overline{BH}(T)$ has only real-valued elements, $\overline{BH}(T)^{*} = \overline{BH}(T)^{T}$; therefore, by the structure of $M(T)$, as defined in (2.12) the rank of $\overline{BH}(T)$ is preserved in $M(T)$.

APPENDIX D

Existence and Calculation of $\widetilde{K}_{d/c}$

For the fundamental matric equation

$$AX = B, \tag{D.1}$$

where A is an $n \times s$ matrix, $s \times n$ matrix, and B is an $n \times n$ matrix, it is well-known that B exists if, and only if [24],

$$R_c[B] \subseteq R_c[A]. \tag{D.2}$$

Similarly, the form of (2.16) can be rearranged-to

$$\overline{BH}\widetilde{K}_{d/c} = \widetilde{A}_{CL} - \widetilde{A}, \tag{D.3}$$

where $\widetilde{A}_{CL} = \widetilde{A}_m$, a desired closed-loop system matrix. The existence of matrix $\widetilde{K}_{d/c}$ is then given by (2.19), [9].

The set of all solutions, X which solve (D.1) is given by

$$X = A^{\dagger}B + \left[I - A^{\dagger}A\right]Q, \tag{D.4}$$

where Q is completely arbitrary. Similarly, the set of all solutions, $\widetilde{K}_{d/c}$ which solve (D.3) is given by [9]

$$\widetilde{K}_{d/c} = \overline{BH}\left[\widetilde{A}_{CL} - \widetilde{A}\right] + \left[I - \overline{BH}^{\dagger}\overline{BH}\right]Q, \tag{D.5}$$

which reduces-to

$$\widetilde{K}_{d/c} = \overline{BH}^{\dagger}\left[\widetilde{A}_{CL} - \widetilde{A}\right] \tag{D.6}$$

when a unique solution exists.

APPENDIX E

Calculations for $\widetilde{K}_{d/c}$ in the Simulation Examples of Chapter 4

E.1 First-Order Plant Model

The first-order plant model used in the simulation examples of Chapter 4 is

$$\dot{y} + ay = u, \tag{E.1}$$

where $a = 1$. For this first-order example, the system matrix A, control distribution matrix B, and output matrix C are respectively,

$$A = [-1], \tag{E.2}$$

$$B = [1], \tag{E.3}$$

$$C = [1]. \tag{E.4}$$

Since A is time invariant, (2.1) is used to calculate $\widetilde{A}$ to be

$$\widetilde{A} = [0.0498]. \tag{E.5}$$

Control state variable v, is chosen as in Chapter 1, Section 1.2.6.1, which determines the values of matrices $\overline{D}$ and $\overline{H}$ for the calculation of $\overline{BH}$ from (1.20). Sample period $T = 3,$ and D/C control parameters $\alpha = 0.5,\ \omega = 1.0.$

The necessary and sufficient conditions for the existence of $\widetilde{K}_{d/c}$ is given by (2.18) for the ZOH case and (2.19) for D/C-type discrete-time control. Matrix $\widetilde{K}_{d/c}$ is calculated from (4.5), as detailed in Appendix C, where $\left[\widetilde{A}_{CL}\right]=\left[\widetilde{A}_{m}\right]=[0]$.

E.1.1 ZOH

With phase-variable choices for D/C control-state v, so that $v=u_{d/c}$, the resulting $\overline{D}$ and $\overline{H}$ are, respectively

$$\overline{D}=[0], \tag{E.6}$$

$$\overline{H}=[1]. \tag{E.7}$$

Matrix $\overline{BH}$ is computed from (1.20) to be

$$\overline{BH}=\widetilde{B}=[0.9502]. \tag{E.8}$$

The Moore-Penrose Generalized Inverse of $\overline{BH}$ is computed to be

$$\overline{BH}^{\dagger}=\widetilde{B}^{\dagger}=[1.0524]. \tag{E.9}$$

The resulting $\widetilde{K}_{d/c}=\widetilde{K}_{zoh}$ is computed in (4.7).

E.1.2 LiT

With phase-variable choices for D/C control-state v, so that $v_1=u_{d/c}$, $v_2=\dot{u}_{d/c}$, the resulting $\overline{D}$ and $\overline{H}$ are, respectively

$$\overline{D}=\begin{bmatrix}0 & 1\\ 0 & 0\end{bmatrix}, \tag{E.10}$$

$$\overline{H}=\begin{bmatrix}1 & 0\end{bmatrix}. \tag{E.11}$$

Matrix $\overline{BH}$ is computed from (1.20) to be

$$\overline{BH} = \begin{bmatrix} 0.9502 & 2.0498 \end{bmatrix}. \tag{E.12}$$

The Moore-Penrose Generalized Inverse of $\overline{BH}$ is computed to be

$$\overline{BH}^{\dagger} = \begin{bmatrix} 0.1862 \\ 0.4016 \end{bmatrix}. \tag{E.13}$$

The resulting $\widetilde{K}_{d/c}$ is computed in (4.8).

E.1.3 EiT

With phase-variable choices for D/C control-state v, so that $v_1 = u_{d/c}$, $v_2 = \dot{u}_{d/c}$, the resulting $\overline{D}$ and $\overline{H}$ are, respectively

$$\overline{D} = \begin{bmatrix} 0 & 1 \\ \alpha & 0 \end{bmatrix}, \tag{E.14}$$

$$\overline{H} = \begin{bmatrix} 1 & 0 \end{bmatrix}. \tag{E.15}$$

Matrix $\overline{BH}$ is computed from (1.20) to be

$$\overline{BH} = \begin{bmatrix} 2.5484 & 3.2656 \end{bmatrix}. \tag{E.16}$$

The Moore-Penrose Generalized Inverse of $\overline{BH}$ is computed to be

$$\overline{BH}^{\dagger} = \begin{bmatrix} 0.1485 \\ 0.1903 \end{bmatrix}. \tag{E.17}$$

The resulting $\widetilde{K}_{d/c}$ is computed in (4.9).

E.1.4 SiT

With phase-variable choices for D/C control-state v, so that $v_1 = u_{d/c}$, $v_2 = \dot{u}_{d/c}$, $v_3 = \ddot{u}_{d/c}$, the resulting $\overline{D}$ and $\overline{H}$ are, respectively

$$\overline{D} = \begin{bmatrix} 0 & 1 & 0 \\ 0 & 0 & 1 \\ 0 & -\omega^2 & 0 \end{bmatrix}, \tag{E.18}$$

$$\overline{H} = \begin{bmatrix} 1 & 0 & 0 \end{bmatrix}. \tag{E.19}$$

Matrix $\overline{BH}$ is computed from (1.20) to be

$$\overline{BH} = \begin{bmatrix} 0.9502 & 0.5904 & 1.3995 \end{bmatrix}. \tag{E.20}$$

The Moore-Penrose Generalized Inverse of $\overline{BH}$ is computed to be

$$\overline{BH}^{\dagger} = \begin{bmatrix} 0.2960 \\ 0.1839 \\ 0.4360 \end{bmatrix}. \tag{E.21}$$

The resulting $\widetilde{K}_{d/c}$ is computed in (4.10).

E.1.5 PsiT

With phase-variable choices for D/C control-state v, so that $v_1 = u_{d/c}$, $v_2 = \dot{u}_{d/c}$, $v_3 = \ddot{u}_{d/c}$, the resulting $\overline{D}$ and $\overline{H}$ are, respectively

$$\overline{D} = \begin{bmatrix} 0 & 1 & 0 \\ 0 & 0 & 1 \\ 0 & -\alpha^2 & 2\alpha \end{bmatrix}, \tag{E.22}$$

$$\overline{H} = \begin{bmatrix} 1 & 0 & 0 \end{bmatrix}. \tag{E.23}$$

Matrix $\overline{BH}$ is computed from (1.20) to be

$$\overline{BH} = \begin{bmatrix} 0.9502 & 1.0239 & 5.9697 \end{bmatrix}. \tag{E.24}$$

The Moore-Penrose Generalized Inverse of $\overline{BH}$ is computed to be

$$\overline{BH}^{\dagger} = \begin{bmatrix} 0.0253 \\ 0.0272 \\ 0.1588 \end{bmatrix}. \tag{E.25}$$

The resulting $\widetilde{K}_{d/c}$ is computed in (4.11).

E.2 Second-Order Plant Model

The second-order plant model used in the simulation examples of Chapter 4 is

$$\ddot{y} + a_2\dot{y} + a_1 y = u, \tag{E.26}$$

where $a_1 = 1,\ a_2 = 3$. For this second-order example, the system matrix A, control distribution matrix B, and output matrix C are respectively,

$$A = \begin{bmatrix} 0 & 1 \\ -1 & -3 \end{bmatrix}, \tag{E.27}$$

$$B = \begin{bmatrix} 0 \\ 1 \end{bmatrix}, \tag{E.28}$$

$$C = \begin{bmatrix} 1 & 0 \end{bmatrix}. \tag{E.29}$$

Since A is time invariant, (2.1) is used to calculate $\widetilde{A}$ to be

$$\widetilde{A} = \begin{bmatrix} 0.3722 & 0.1420 \\ -0.1420 & -0.0539 \end{bmatrix}. \tag{E.30}$$

E.2.1 ZOH

With phase-variable choices for D/C control-state v, so that $v = u_{d/c}$, the resulting $\overline{D}$ and $\overline{H}$ expressions are given by (E.6) and (E.7), respectively. For the second-order plant model of (E.26), matrix $\overline{BH}$ and its Moore-Penrose Generalized Inverse are computed respectively, to be

$$\overline{BH} = \widetilde{B} = \begin{bmatrix} 0.6278 \\ 0.1420 \end{bmatrix}, \tag{E.31}$$

$$\overline{BH}^{\dagger} = \widetilde{B}^{\dagger} = \begin{bmatrix} 1.5153 & 0.3428 \end{bmatrix}. \tag{E.32}$$

The resulting $\widetilde{K}_{d/c} = \widetilde{K}_{zoh}$ is computed in (4.12).

E.2.2 LiT

With phase-variable choices for D/C control-state v, so that $v_1 = u_{d/c},\ v_2 = \dot{u}_{d/c}$ the resulting $\overline{D}$ and $\overline{H}$ expressions are given by (E.10) and (E.11), respectively. Matrix $\overline{BH}$ and $\overline{BH}^{\dagger}$ are computed respectively, to be

$$\overline{BH} = \begin{bmatrix} 0.6278 & 0.9745 \\ 0.1420 & 0.6278 \end{bmatrix}, \tag{E.33}$$

$$\overline{BH}^{\dagger} = \begin{bmatrix} 2.4547 & -3.8104 \\ -0.5553 & 2.4547 \end{bmatrix}. \tag{E.34}$$

The resulting $\widetilde{K}_{d/c}$ is computed in (4.13).

E.2.3 EiT

With phase-variable choices for D/C control-state v, so that $v_1 = u_{d/c},\ v_2 = \dot{u}_{d/c}$ the resulting $\overline{D}$ and $\overline{H}$ expressions are given by (E.14) and (E.15), respectively. Matrix $\overline{BH}$ and $\overline{BH}^{\dagger}$ are computed respectively, to be

$$\overline{BH} = \begin{bmatrix} 1.2088 & 1.3638 \\ 0.8239 & 1.2088 \end{bmatrix}, \tag{E.35}$$

$$\overline{BH}^{\dagger} = \begin{bmatrix} 3.5808 & -4.0398 \\ -2.4406 & 3.5808 \end{bmatrix}. \tag{E.36}$$

The resulting $\widetilde{K}_{d/c}$ is computed in (4.14).

E.2.4 SiT

With phase-variable choices for D/C control-state v, so $v_1 = u_{d/c}$, $v_2 = \dot{u}_{d/c}$, $v_3 = \ddot{u}_{d/c}$, the resulting $\overline{D}$ and $\overline{H}$ expressions are given by (E.18) and (E.19), respectively. Matrix $\overline{BH}$ and $\overline{BH}^{\dagger}$ are computed respectively, to be

$$\overline{BH} = \begin{bmatrix} 0.6278 & 0.4541 & 0.6281 \\ 0.1420 & -0.0003 & 0.4541 \end{bmatrix}, \tag{E.37}$$

$$\overline{BH}^{\dagger} = \begin{bmatrix} 1.0449 & -1.1003 \\ 1.2085 & -1.9995 \\ -0.3260 & 2.5452 \end{bmatrix}. \tag{E.38}$$

The resulting $\widetilde{K}_{d/c}$ is computed in (4.15).

E.2.5 PsiT

With phase-variable choices for D/C control-state v, so that $v_1 = u_{d/c}$, $v_2 = \dot{u}_{d/c}$, $v_3 = \ddot{u}_{d/c}$, the resulting $\overline{D}$ and $\overline{H}$ expressions are given by (E.22) and (E.23), respectively. Matrix $\overline{BH}$ and $\overline{BH}^{\dagger}$ are computed respectively, to be

$$\overline{BH} = \begin{bmatrix} 0.6278 & 0.6615 & 2.0399 \\ 0.1420 & 0.1178 & 2.7014 \end{bmatrix}, \tag{E.39}$$

$$\overline{BH}^{\dagger} = \begin{bmatrix} 0.8688 & -0.6534 \\ 0.9567 & -0.7248 \\ -0.0874 & 0.4361 \end{bmatrix}. \tag{E.40}$$

The resulting $\widetilde{K}_{d/c}$ is computed in (4.16).

E.3 Third-Order Plant Model

The third-order plant model used in the simulation examples of Chapter 4 is

$$\dddot{y} + a\ddot{y} = u, \tag{E.41}$$

where $a = 1$. For this third-order example, the system matrix A, control distribution matrix B, and output matrix C are respectively,

$$A = \begin{bmatrix} 0 & 1 & 0 \\ 0 & 0 & 1 \\ -1 & 0 & 0 \end{bmatrix}, \tag{E.42}$$

$$B = \begin{bmatrix} 0 \\ 0 \\ 1 \end{bmatrix}, \tag{E.43}$$

$$C = \begin{bmatrix} 1 & 0 & 0 \end{bmatrix}. \tag{E.44}$$

Since A is time invariant, (2.1) is used to calculate $\widetilde{A}$ to be

$$\widetilde{A} = \begin{bmatrix} -2.5406 & 0.0429 & 2.6333 \\ -2.6333 & -2.5406 & 0.0429 \\ -0.0429 & -2.6333 & -2.5406 \end{bmatrix}. \tag{E.45}$$

E.3.1 ZOH

With phase-variable choices for D/C control-state v, so that $v = u_{d/c}$, the resulting $\overline{D}$ and $\overline{H}$ expressions are given by (E.6) and (E.7). Matrix $\overline{BH}$ and $\overline{BH}^{\dagger}$ are computed respectively, to be

$$\overline{BH} = \widetilde{B} = \begin{bmatrix} 3.5406 \\ 2.6333 \\ 0.0429 \end{bmatrix}, \tag{E.46}$$

$$\overline{BH}^{\dagger} = \widetilde{B}^{\dagger} = \begin{bmatrix} 0.1818 & 0.1352 & 0.0022 \end{bmatrix}. \tag{E.47}$$

Since $R_c\left[-\widetilde{A}\right] \not\subset R_c\left[\overline{BH}\right]$, the existence condition of $\widetilde{K}_{d/c} = \widetilde{K}_{zoh}$ for ZOH-type discrete-time control is not satisfied for the "ultimate deadbeat" case. Since calculation of $\widetilde{K}_{zoh}$ by (4.5) results in closed-loop λ_i outside the unit circle (unstable) in this case, $\widetilde{K}_{zoh}$ is computed from (4.4) to obtain the form (4.18).

E.3.2 LiT

With phase-variable choices for D/C control-state v, so that $v_1 = u_{d/c}$, $v_2 = \dot{u}_{d/c}$ the resulting $\overline{D}$ and $\overline{H}$ expressions are given by (E.10) and (E.11), respectively. Matrix $\overline{BH}$ and $\overline{BH}^{\dagger}$ are computed respectively, to be

$$\overline{BH} = \begin{bmatrix} 3.5406 & 2.9571 \\ 2.6333 & 3.5406 \\ 0.0429 & 2.6333 \end{bmatrix}, \tag{E.48}$$

$$\overline{BH}^{\dagger} = \begin{bmatrix} 0.2679 & 0.0249 & -0.3344 \\ -0.0842 & 0.1079 & 0.3293 \end{bmatrix}. \tag{E.49}$$

The resulting $\widetilde{K}_{d/c}$ is computed in (4.19).

E.3.3 EiT

With phase-variable choices for D/C control-state v, so that $v_1 = u_{d/c}$, $v_2 = \dot{u}_{d/c}$ the resulting $\overline{D}$ and $\overline{H}$ expressions are given by (E.14) and (E.15), respectively. Matrix $\overline{BH}$ and $\overline{BH}^{\dagger}$ are computed respectively, to be

$$\overline{BH} = \begin{bmatrix} 4.5854 & 3.4784 \\ 4.3726 & 4.5854 \\ 2.3356 & 4.3726 \end{bmatrix}, \tag{E.50}$$

$$\overline{\mathrm{BH}}^{\dagger} = \begin{bmatrix} 0.3194 & 0.0670 & -0.3244 \\ -0.2159 & 0.0285 & 0.3706 \end{bmatrix}. \tag{E.51}$$

The resulting $\widetilde{\mathrm{K}}_{d/c}$ is computed in (4.20).

E.3.4 SiT

With phase-variable choices for D/C control-state v, so that $v_1 = u_{d/c}$, $v_2 = \dot{u}_{d/c}$, $v_3 = \ddot{u}_{d/c}$, the resulting $\overline{\mathrm{D}}$ and $\overline{\mathrm{H}}$ expressions are given by (E.18) and (E.19), respectively. Matrix $\overline{\mathrm{BH}}$ and $\overline{\mathrm{BH}}^{\dagger}$ are computed respectively, to be

$$\overline{\mathrm{BH}} = \begin{bmatrix} 3.5406 & 2.1411 & 1.4978 \\ 2.6333 & 2.0429 & 2.1411 \\ 0.0429 & 0.4922 & 2.0429 \end{bmatrix}, \tag{E.52}$$

$$\overline{\mathrm{BH}}^{\dagger} = \begin{bmatrix} 2.0343 & -2.3716 & 0.9942 \\ -3.4483 & 4.6750 & -2.3716 \\ 0.7881 & -1.0766 & 1.0401 \end{bmatrix}. \tag{E.53}$$

The resulting $\widetilde{\mathrm{K}}_{d/c}$ is computed in (4.21).

E.3.5 PsiT

With phase-variable choices for D/C control-state v, so that $v_1 = u_{d/c}$, $v_2 = \dot{u}_{d/c}$, $v_3 = \ddot{u}_{d/c}$, the resulting $\overline{\mathrm{D}}$ and $\overline{\mathrm{H}}$ expressions are given by (E.22) and (E.23), respectively. Matrix $\overline{\mathrm{BH}}$ and $\overline{\mathrm{BH}}^{\dagger}$ are computed respectively, to be

$$\overline{\mathrm{BH}} = \begin{bmatrix} 3.5406 & 2.5749 & 3.2388 \\ 2.6333 & 2.7309 & 5.8137 \\ 0.0429 & 1.1799 & 8.5447 \end{bmatrix}, \tag{E.54}$$

$$\overline{\mathrm{BH}}^{\dagger} = \begin{bmatrix} 1.5368 & -1.6959 & 0.5713 \\ -2.0756 & 2.8091 & -1.1245 \\ 0.2789 & -0.3794 & 0.2694 \end{bmatrix}. \qquad \text{(E.55)}$$

The resulting $\widetilde{\mathrm{K}}_{\mathrm{d/c}}$ is computed in (4.22).

APPENDIX F

Examples of Simulink Simulation Math Models Used in This Research

F.1 Closed-Loop System Overview

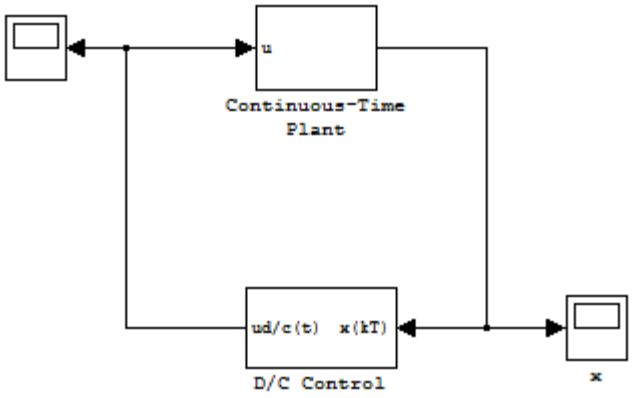

Figure F.1 D/C-Controlled Closed-Loop System Overview

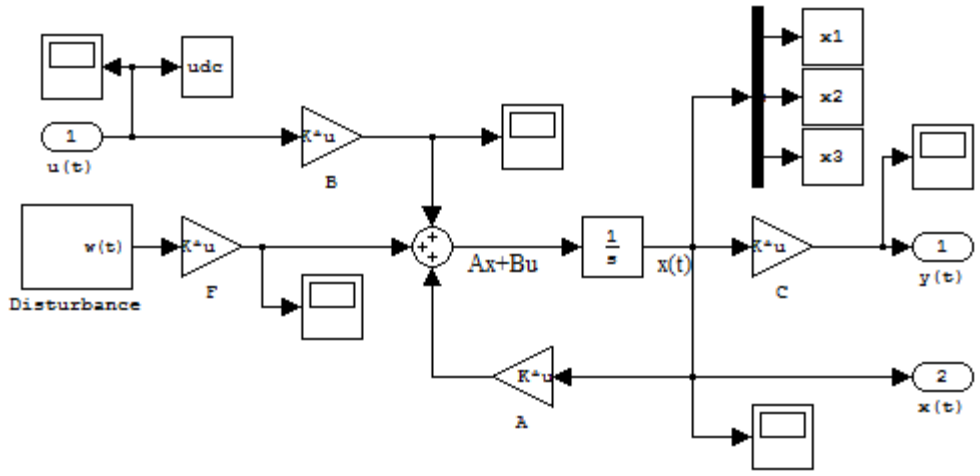

Figure F.2 Example of a Continuous-Time Plant Block

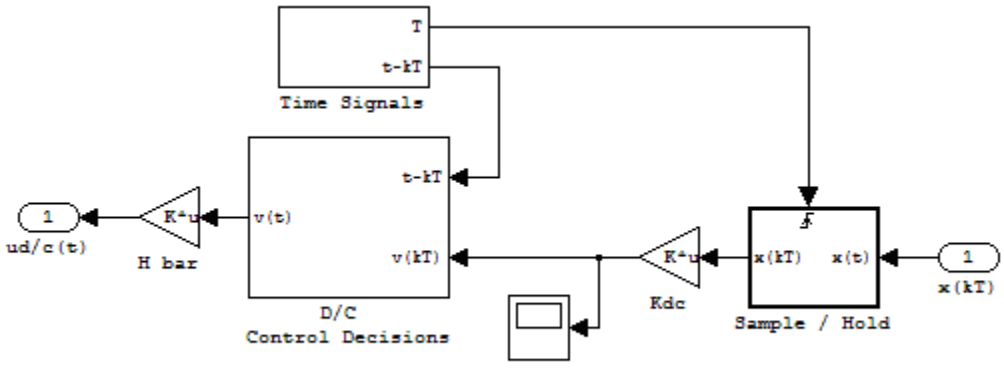

Figure F.3 D/C Control Block

F.2 D/C Control-Type Implementation

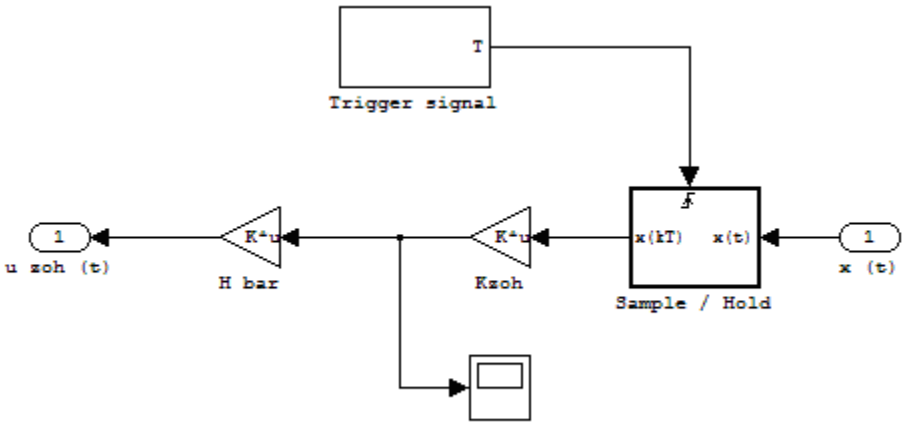

Figure F.4 ZOH Control Block

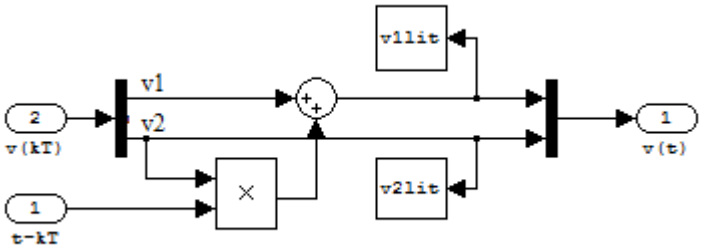

Figure F.5 LiT-Type D/C Control Decisions Block

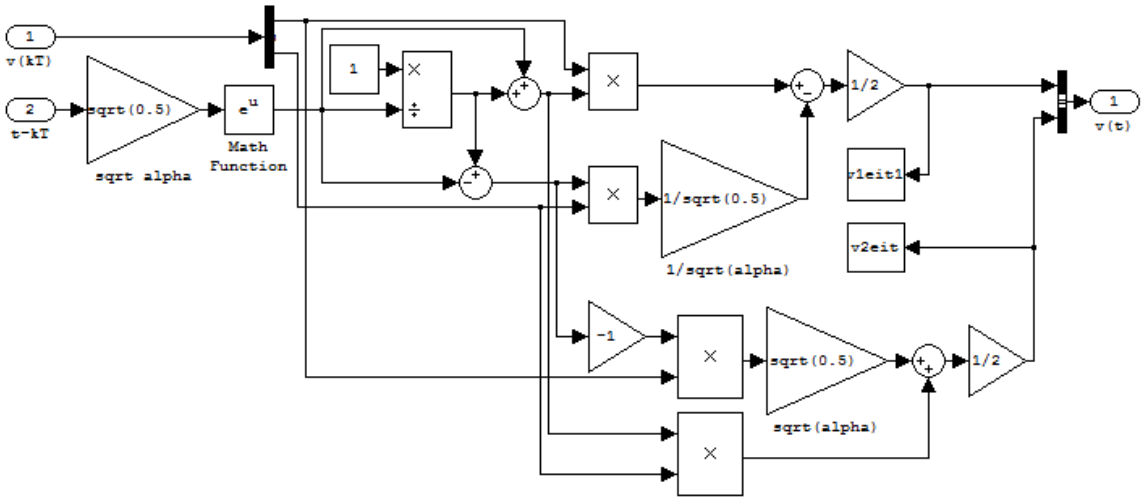

Figure F.6 EiT-Type D/C Control Decisions Block

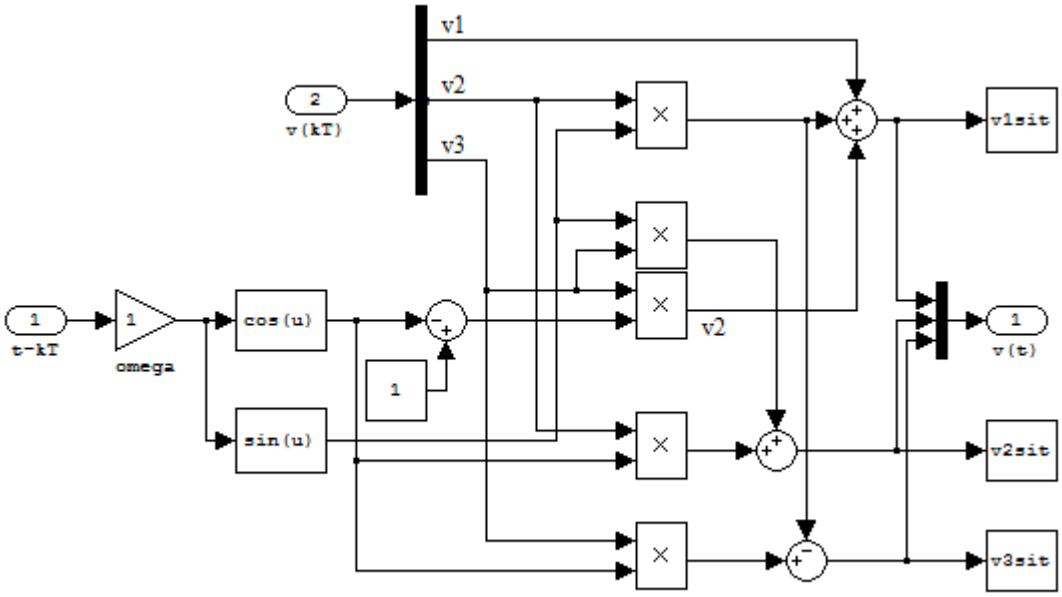

Figure F.7 SiT-Type D/C Control Decisions Block

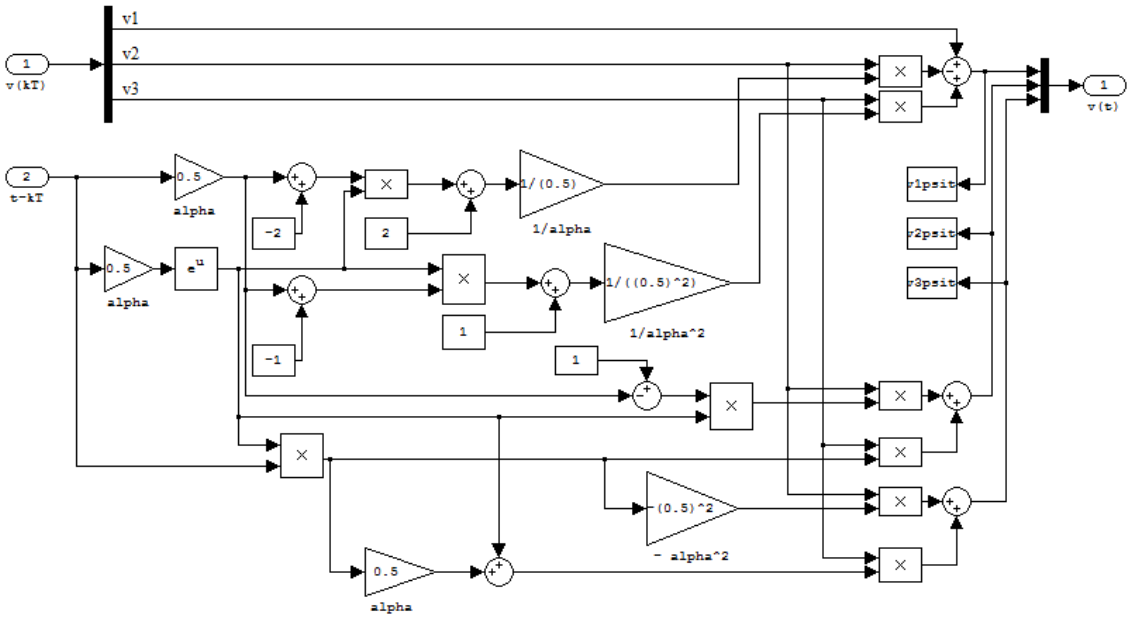

Figure F.8 PsiT-Type D/C Control Decisions Block

REFERENCES

[1] Dorf, Richard C. Modern Control Systems 5th Ed. Addison Wesley, 1989.

[2] Brogan, William L. Modern Control Theory, 3rd Ed. Prentice-Hall. Englewood Cliffs, New Jersey, 1990.

[3] Ogata, K. Discrete-Time Control Systems, 2nd Ed. Prentice-Hall. Englewood Cliffs, New Jersey, 1994.

[4] Johnson, C.D. "A New Discrete-Time State Model for Linear Dynamical Systems with Continuously-Varying Control/Disturbance Inputs," Proceedings of the 26th Southeastern Symposium on System Theory (SSST), 1994, pp. 523-527.

[5] Abdel-Haleem, Mohamed Hafez. "Optimal Discrete Continuous Control for the Linear Quadratic Regulator Problem". Ph.D. Dissertation, University of Alabama in Huntsville, 1996.

[6] Abdel-Haleem, M. and C.D. Johnson. "Superiority of LiT Discrete/Continuous Control Compared to ZOH Control in the DT LQR Problem". Proceedings of the 29th Southeastern Symposium on System Theory (SSST), 1997, pp. 2-6.

[7] Johnson, C.D. "A General Theory of "Discrete/Continuous" Type Discrete-Time Control for Linear Dynamical Systems," Proceedings of the 30th Southeastern Symposium on System Theory (SSST), 1998, pp. 56-61.

[8] Abdel-Haleem, M. and C.D. Johnson. "Optimal Discrete/Continuous Control with LQR Performance Criterion and a General Class of 3rd-Order Linear Dynamic Control Variations with One Zero Eigenvalue," Proceedings of the 33rd Southeastern Symposium on System Theory (SSST), 2001, pp. 233-239.

[9] Johnson, C.D. "Improved Discrete-Time Controller Performance Using the "Control-Dimension Multiplier Effect" of Discrete/Continuous Control Theory," Proceedings of the 34th Southeastern Symposium on System Theory (SSST), 2002, pp. 484-490.

[10] Johnson, C.D. "On the Theory of Discrete-Time Signals of the Discrete/Continuous Type," Proceedings of the 35th Southeastern Symposium on System Theory (SSST), 2003, pp. 113-121.

[11] Johnson, C.D. "Improved Discrete-Time, Disturbance-Accommodating Control Performance Using Discrete/Continuous Control Theory. Part I. Complete Disturbance-Cancellation (Rejection)," Proceedings of the 35th Southeastern Symposium on System Theory (SSST), 2003, pp. 127-133.

[12] Johnson, C.D. "Application of Discrete/Continuous Signal-Theory to Discrete-Time State-Estimation Problems for Linear Dynamical Systems with Intersample Variations of Inputs," Proceedings of the 35th Southeastern Symposium on System Theory (SSST), 2003, pp. 122-126.

[13] Mehmeti, B. and C.D. Johnson. "Analysis and Design of 'Discrete/Continuous'-Type Discrete-Time Controllers by Transfer-Function Methods; Some Examples," Proceedings of the 36th Southeastern Symposium on System Theory (SSST), 2004, pp. 74-78.

[14] Johnson, C.D. "An Exact Discrete-Time Transfer-Function Representation for the Analysis and Design of Discrete/Continuous Control Systems," Proceedings of the 36th Southeastern Symposium on System Theory (SSST), 2004, pp. 64-68.

[15] Mehmeti, B. "Transfer-Function Formulation of Analysis and Design Problems for Discrete/Continuous Control Theory". Master's Thesis, University of Alabama in Huntsville, 2004.

[16] Johnson, C.D. "A MIMO Transfer-Function Approach to the Design of "Bumpless" Type and "Smooth-Bumpless" Type Discrete/Continuous (D/C) Controllers." Proceedings of the 40th Southeastern Symposium on System Theory (SSST), 2008, pp. 1-6.

[17] Johnson, C.D. "Computation of a Matric Convolution-Integral that Arises in Discrete-Time DAC Theory, and Similarly in Discrete/Continuous (D/C) Control Theory," Proceedings of the 41st Southeastern Symposium on System Theory (SSST), 2009, pp. 291-294.

[18] Nixon, D.D. and C.D. Johnson. "Numerical Evaluation of the "Dual-Kernel, Counter-Flow Matric Convolution Integral that Arises in Discrete/Continuous (D/C) Control Theory," Proceedings of the 41st Southeastern Symposium on System Theory (SSST), 2009, pp. 285-290.

[19] Hunt, A. and C.D. Johnson. "On the Dual-Kernel, Matric Convolution Integral in Discrete/Continuous Control Theory; Exact, Explicit, Closed-Form Expressions for Some Simple Cases," Proceedings of the 41st Southeastern Symposium on System Theory (SSST), 2009, pp. 295-299.

[20] Johnson, C.D. "Accommodation of External Disturbances in Linear Regulator and Servomechanism Problems," IEEE Transactions on Automatic Control, 1971, Vol. 16, No. 6, pp. 635-644.

[21] Johnson, C.D. "A Discrete-Time Disturbance-Accommodating Control Theory for Digital Control of Dynamical Systems," Control and Dynamic Systems. Academic Press, Inc. Vol. 18, 1982.

[22] Johnson, C.D. "Theory of Disturbance Accommodating Controllers," Chapter 7 in the book: Advances in Control and Dynamic Systems, Vol. 12, Academic Press, 1976.

[23] Johnson, C.D. "Disturbance-Accommodating Control; An Overview," American Control Conference, 1986, pp. 526-536.

[24] Lancaster, Peter and Miron Tismenetsky. The Theory of Matrices with Applications, 2nd Ed. Academic Press, 1985, pp. 432-438.

[25] Johnson, C.D. "Real-Time Disturbance-Observers; Origin and Evolution of the Idea Part 1: The Early Years," Proceedings of the 40th Southeastern Symposium on System Theory (SSST), 2008, pp. 88-91.
[26] Johnson, C.D. "Disturbance-Accommodating Control: An Overview of the Subject," Journal of Interdisciplinary Model and Simulation, 1980, Vol. 3, pp. 1-29.
[27] Parker, Glenn and C.D. Johnson. "Improved Speed Regulation and Mitigation of Drive-Train Torsion Fatigue in Flexible Wind Turbines, Using Disturbance Utilization Control: Part One," Proceedings of the 41st Southeastern Symposium on System Theory (SSST), 2009, pp. 171-176.
[28] Parker, Glenn and C.D. Johnson. "Improved Speed Regulation and Mitigation of Drive-Train Torsion Fatigue in Flexible Wind Turbines, Using Disturbance Utilization Control: Part Two," Proceedings of the 41st Southeastern Symposium on System Theory (SSST), 2009, pp. 177-183.
[29] Johnson, C.D. "Utility of Disturbances in Disturbance-Accommodating Control Problems," Proceedings of the 50th Annual Meeting of the Society of Engineering Science, Gainesville, Florida, December 1978, pp. 347-352.
[30] Johnson, C.D. "Improved Discrete-Time, Disturbance-Accommodating Control Performance Using Discrete/Continuous Control Theory; Part I: Complete Disturbance-Cancellation (Rejection)," Proceedings of the 35th Southeastern Symposium on System Theory (SSST), 2003, pp. 127-133.